SUSTAINABLE BIOREMEDIATION OF SHRIMP AQUACULTURE WASTEWATER USING *Chlorella sp.* MICROALGAE

By

NURFARAHANA BINTI MOHD NASIR

Thesis Submitted to the School of Graduate Studies, Universiti Putra Malaysia, in Fulfilment of the Requirements for the Degree of Doctor of Philosophy

August 2024

FK 2024 40

Abstract of thesis presented to the Senate of Universiti Putra Malaysia in fulfilment of the requirement for the degree of Doctor of Philosophy

SUSTAINABLE BIOREMEDIATION OF SHRIMP AQUACULTURE WASTEWATER USING *Chlorella sp.* MICROALGAE

By

NURFARAHANA BINTI MOHD NASIR

August 2024

Chairman : Professor Ir.Wan Azlina binti Wan Abdul Karim Ghani, PhD
Faculty : Engineering

Shrimp farming is a rapidly expanding sector within aquaculture and has dramatically increased global production. This growth has brought challenges in the management of wastewater. The wastewater from shrimp aquaculture effluents contains harmful organic and inorganic contaminants, including nitrogenous chemicals such as ammonium and nitrate, which result from excessive feed and high stocking density. These contaminants pose serious threats to ecosystems, human health, and the growth and survival of aquatic animals. Green microalgae have gained attention as an effective alternative treatment in shrimp wastewater management strategies. However, the potential of microalgae to become an extensive application will require continuous monitoring to overcome current limitations regarding harvesting for future applications. Therefore, the first objective was to determine the bioremediation capabilities of green microalgae, *Chlorella* sp., isolated from shrimp farms across varying microalgae concentrations of 0% (v/v) to 60% (v/v). Findings revealed that the optimum dosages were 30% (v/v) and 40%

(v/v) for Marine water (MW) and Freshwater (FW), respectively. On Day 10, microalgae achieved significant nutrient removal for ammonia, nitrite, and orthophosphate, with efficiencies of 96.77%, 82.07%, 75.96% for MW and 90.10%, 87.09%, 95.60% for FW. Furthermore, microalgae cell density increased by over tenfold, leading to specific growth rates of 0.18 day^{-1} and 0.15 day^{-1}.

The second objective was to evaluate the harvesting efficiency of the excess microalgae by focusing on the dosage that achieved the highest nutrient removal efficiency. In this study, a bio-flocculant fungus, *Aspergillus niger,* and Response Surface Methodology (RSM) with a central composite design was used to assess the effects of fungus dosage, pH, and mixing rate. The optimized conditions yielded harvesting efficiencies exceeding 90% at a dosage of 30 g L^{-1}, pH of 7, and mixing rate of RPM 125. The third objective involved using machine learning using Waikato Environment for Knowledge Analysis (WEKA) to develop models for bioremediation and bio-harvesting processes. In this study, various algorithms were used to analyze the dataset involving computational methods to create predictive models that enhance the efficiency of the processes. The analysis using WEKA software identified the M5P algorithm as the most effective for nutrient removal and microalgae harvesting due to its high correlation coefficient (*>0.9*) and low error rates (*<0.1*). The M5P decision tree analysis results can identify the optimal conditions for bioremediation and harvesting. This can help save time when designing new experiments for large-scale wastewater treatment. A user-friendly interface was developed to facilitate practical applications that

integrate the predictive model. This interface makes it easy for future research and simplifies the process of large-scale wastewater treatment. The findings of this study highlight that *Chlorella* sp. effectively removes pollutants, *Aspergillus niger* is helpful for aggregating microalgae, and the application of the M5P algorithm enhances both bioremediation and harvesting processes. These findings contribute to sustainable bioremediation and biomass harvesting while promoting sustainable environmental practices and renewable energy production.

Keywords: Bioremediation, Filamentous fungus, Microalgae, Machine Learning, WEKA

SDG: GOAL 6: Clean Water and Sanitation, GOAL 12: Responsible Consumption and Production, GOAL 14: Life below Water

Abstrak tesis yang dikemukakan kepada Senat Universiti Putra Malaysia sebagai memenuhi keperluan untuk ijazah Doktor Falsafah

BIOREMIDIASI LESTARI AIR SISA AKUAKULTUR UDANG MENGGUNAKAN MIKROALGA *Chlorella sp.*

Oleh

NURFARAHANA BINTI MOHD NASIR

Ogos 2024

Pengerusi : Profesor Ir.Wan Azlina binti Wan Abdul Karim Ghani, PhD
Fakulti : Kejuruteraan

Penternakan udang merupakan sektor yang berkembang pesat dalam akuakultur dan telah meningkatkan pengeluaran global dengan ketara. Pertumbuhan ini membawa cabaran dalam pengurusan air sisa buangan. Air sisa dari buangan akuakultur udang mengandungi bahan pencemar organik dan bukan organik yang berbahaya, termasuk bahan kimia nitrogen seperti amonium dan nitrat, yang dihasilkan daripada pemberian makanan yang berlebihan dan kepadatan stok yang tinggi. Bahan pencemar ini menimbulkan ancaman serius kepada ekosistem, kesihatan manusia, serta pertumbuhan dan kelangsungan hidup haiwan akuatik. Mikroalga hijau telah mendapat perhatian sebagai rawatan alternatif yang berkesan dalam strategi pengurusan air sisa buangan. Walau bagaimanapun, potensi mikroalga untuk aplikasi yang meluas memerlukan pemantauan berterusan untuk mengatasi masalah semasa berkenaan proses penuaian untuk aplikasi masa depan. Oleh itu, objektif pertama adalah untuk menentukan keupayaan bioremediasi mikroalga hijau, *Chlorella* sp., yang diasingkan dari ladang udang dengan

kepekatan mikroalga dari 0% (v/v) hingga 60% (v/v). Penemuan menunjukkan dos optimum adalah 30% (v/v) dan 40% (v/v) untuk air laut (MW) dan air tawar (FW), masing-masing. Pada Hari ke-10, mikroalga mencapai penyingkiran nutrien yang ketara, terutamanya ammonia, nitrit, dan ortofosfat, dengan kecekapan 96.77%, 82.07%, 75.96% untuk MW dan 90.10%, 87.09%, 95.60% untuk FW. Selain itu, ketumpatan sel mikroalga meningkat lebih dari sepuluh kali ganda, menyebabkan kadar pertumbuhan spesifik sebanyak 0.18 $hari^{-1}$ dan 0.15 $hari^{-1}$.

Objektif kedua adalah untuk menilai kecekapan penuaian mikroalga yang berlebihan dengan memberi tumpuan kepada dos yang mencapai kecekapan penyingkiran nutrien tertinggi. Dalam kajian ini, kulat bio-flokulan, *Aspergillus niger* dan Kaedah Permukaan Respon (RSM) dengan reka bentuk komposit pusat digunakan untuk menilai kesan dos kulat, pH, dan kadar pencampuran. Keadaan yang dioptimumkan menghasilkan kecekapan penuaian melebihi 90%, dengan dos 30 g L^{-1}, pH 7, dan kadar pencampuran RPM 125. Objektif ketiga melibatkan penggunaan pembelajaran mesin menggunakan Waikato Environment for Knowledge Analysis (WEKA) untuk membangunkan model bagi proses bioremediasi dan bio-penuaian. Dalam kajian ini, pelbagai algoritma digunakan untuk menganalisis set data yang melibatkan kaedah pengiraan untuk mencipta model ramalan yang meningkatkan kecekapan proses. Analisis menggunakan perisian WEKA mengenal pasti algoritma M5P sebagai yang paling berkesan untuk penyingkiran nutrien dan penuaian mikroalga, disebabkan oleh pekali korelasi yang tinggi (>*0.9*) dan kadar ralat yang rendah (<*0.1*). Keputusan yang diperoleh melalui analisis pokok

keputusan M5P boleh mengenal pasti keadaan optimum untuk bioremediasi dan penuaian. Ini dapat membantu menjimatkan masa dalam merancang eksperimen baru untuk rawatan air buangan berskala besar. Untuk memudahkan aplikasi praktikal, antaramuka mesra pengguna telah dibangunkan untuk mengintegrasikan model ramalan. Antaramuka ini memudahkan penyelidikan masa depan dan mempermudah proses rawatan air buangan berskala besar. Penemuan kajian ini menekankan bahawa *Chlorella* sp. berkesan dalam menghapuskan pencemar, *Aspergillus niger* berguna untuk mengagregatkan mikroalga dan penggunaan algoritma M5P meningkatkan kedua-dua proses bioremediasi dan penuaian. Penemuan ini menyumbang kepada amalan lestari dalam bioremediasi dan penuaian biomas, dengan mempromosikan amalan alam sekitar yang mampan dan pengeluaran tenaga boleh diperbaharui

Kata Kunci: Bioremediasi, Kulat Berfilamen, Mikroalga, Pembelajaran Mesin, WEKA

SDG: MATLAMAT 6: Air Bersih dan Sanitasi, MATLAMAT 12: Penggunaan dan Pengeluaran yang Bertanggungjawab, MATLAMAT 14: Kehidupan di dalam Air

ACKNOWLEDGEMENTS

First, I would like to express my deepest gratitude to Almighty Allah S.W.T. for giving me the strength and composure to complete my study and prepare this thesis within the scheduled time. I am especially grateful to *Prof. Ir. Dr. Wan Azlina binti Ab Karim Ghani* for her guidance, support and constant supervision, which contributed immensely to my research project and thesis report. Not to forget her encouragement to upgrade my studies. I deeply appreciate and thank my supervisory committee, *Dr. Nik Nor Liyana binti Nik Ibrahim* and *Prof Madya. Dr. Razif Bin Harun* from Universiti Putra Malaysia and *Prof Emeritus Ir. Dr. Ahmad bin Jusoh* from Universiti Malaysia Terengganu for their continuous assistance throughout this study.

I want to express my heartfelt appreciation to my beloved parents, *Mohd Nasir bin Che Deraman* and *Rogayah binti Mat Jusoh*, whose unwavering love and support have been my pillar of strength throughout this academic journey. My deepest gratitude goes to my husband, *Ahmad Hafizuddin bin Omar*, for his constant encouragement and understanding. I am truly blessed to have a supportive family who have provided endless love and encouragement during this challenging yet rewarding pursuit of my PhD. I thank the Ministry of Higher Education (MoHE) and the Universiti Malaysia Terengganu (UMT) for their support and financial assistance during my studies. I appreciate the UMT, especially the AKUATROP staff, for providing me with a lab for conducting experiments. Thanks to my fellow PhD friends, lecturers, and lab staff for their contributions, ideas, and technical support in completing my research.

This thesis was submitted to the Senate of the Universiti Putra Malaysia and has been accepted as fulfilment of the requirement for the degree of Doctor of Philosophy. The members of the Supervisory Committee were as follows:

Wan Azlina binti Wan Abdul Karim Ghani, PhD
Professor Ir.
Faculty of Engineering
Universiti Putra Malaysia
(Chairman)

Nik Nor Liyana binti Nik, PhD
Senior Lecturer
Faculty of Engineering
Universiti Putra Malaysia
(Member)

Razif bin Harun, PhD
Associate Professor Ts.
Faculty of Engineering
Universiti Putra Malaysia
(Member)

ZALILAH MOHD SHARIFF, PhD
Professor and Dean
School of Graduate Studies
Universiti Putra Malaysia

Date: 12 December 2024

TABLE OF CONTENTS

		Page
ABSTRACT		i
ABSTRAK		iv
ACKNOWLEDGEMENTS		vii
APPROVAL		viii
DECLARATION		x
LIST OF TABLES		xvi
LIST OF FIGURES		xviii
LIST OF ABBREVIATIONS		xxii
CHAPTER		
1	**INTRODUCTION**	1
1.1	Background of Study	1
1.2	Problem Statement	7
1.3	Objectives of Study	9
1.4	Scope of Study	9
1.5	Significance of Study	10
1.6	Thesis Layout	11
2	**LITERATURE REVIEW**	12
2.1	Development of Aquaculture Industry	12
2.1.1	Aquaculture Industry in Malaysia	13
2.1.2	Shrimp Aquaculture Industry in Malaysia	13
2.2	Shrimp Aquaculture Wastewater	15
2.2.1	Shrimp Aquaculture Wastewater Characteristics	15
2.2.2	Shrimp Aquaculture Wastewater Treatment	18
2.3	Green Microalgae	21
2.3.1	Application of Green Microalgae in Wastewater Treatment	21
2.3.2	Mechanism of Microalgae Bioremediation	27
2.3.3	First-Order Kinetics in Nutrient Removal by Microalgae	28
2.3.4	Composition of Microalgae Biomass by Physicochemical Analysis	31
2.3.5	Algal Bloom in Aquaculture	33
2.4	Harvesting Technique of Microalgae Biomass	35
2.4.1	Centrifugation	35
2.4.2	Flotation	36
2.4.3	Filtration	37
2.4.4	Coagulation Flocculation	37
2.5	Filamentous Fungus	41
2.5.1	Application of Filamentous Fungus in Harvesting Process	41
2.5.2	Mechanism of Microalgae Harvesting Using	

Fungus 44
2.6 Response Surface Methodology (RSM) 46
2.7 Machine Learning 49
2.7.1 Machine Learning Techniques 49
2.7.2 Machine Learning Process 51
2.7.3 Waikato Environmental Knowledge Analysis (WEKA) 57
2.7.4 Algorithms in WEKA 59
2.8 Summary 60

3 GENERAL METHODOLOGY 62
3.1 Introduction 62
3.2 Microalgae Cultivation 64
3.2.1 Microalgae Collection 64
3.2.2 Microalgae Biomass Determination 65
3.3 Bioremediation Process Using Green Microalgae 66
3.3.1 Aquaculture Wastewater Collection 67
3.3.2 Experimental Design for Bioremediation Process 68
3.3.3 Kinetic Model of Wastewater Treatment 69
3.3.4 Water Quality Analysis for Nutrient Removal 70
3.4 Harvesting Process Using Filamentous Fungus 71
3.4.1 Filamentous Fungus Collection and Identification 71
3.4.2 Bio-Flocculant Production 73
3.4.3 Experimental Design for Harvesting Process 74
3.5 Profiling Process Using WEKA 75
3.5.1 Dataset Collection 76
3.5.2 Monte Carlo Simulation (MCS) 76
3.5.3 Machine Learning of WEKA 77
3.6 Statistical Analysis 82

4 UTILIZATION OF GREEN MICROALGAE, *Chlorella* sp. IN AQUACULTURE WASTEWATER BIOREMEDIATION 84
4.1 Introduction 84
4.2 Methodology 88
4.2.1 Microalgae Isolation and Identification 88
4.2.2 Microalgae Cultivation for Bioremediation Process 93
4.2.3 Experimental Set-Up for Bioremediation Process 93
4.2.4 Water Quality Analysis of Bioremediation Process for Nutrient Removal 94
4.2.5 Microalgae Biomass Cultivation and Model Development for Kinetic Study 94
4.2.6 Microalgae Biomass Preparation for Characterization Analysis (FTIR and SEM/EDS) 95
4.3 Statistical Analysis and Modelling 96
4.4 Results and Discussion 97

4.4.1 Molecular Identification of Green Microalgae, *Chlorella* sp. 97
4.4.2 Characteristics of Aquaculture Wastewater and Water Quality Standard 99
4.4.3 Bioremediation Process of Aquaculture Wastewater Using Microalgae 101
4.4.4 Microalgae Characterization FTIR Analysis and SEM/EDX Analysis 114
4.4.5 First-Order Kinetic Model of Nutrient Removal during Bioremediation 126
4.5 Conclusion 141

5 OPTIMIZATION OF MICROALGAE BIO-HARVESTING USING BIO-FLOCCULANT FILAMENTOUS FUNGUS 143
5.1 Introduction 143
5.2 Methodology 146
5.2.1 Experimental Design of Microalgae Harvesting 146
5.2.2 Collection and Preparation of Water Sample for Harvesting Process 148
5.2.3 Cultivation of Filamentous Fungus and Pelletization 148
5.3 Data Analysis of Microalgae Harvesting 149
5.4 Results and Discussion 149
5.4.1 Optimization Using Response Surface Methodology (RSM) of Bio-Flocculation of Microalgae 150
5.4.2 Fitting of Quadratic Model 153
5.4.3 Efficiency of Harvesting Microalgae Using Central Composite Design 157
5.4.4 Validation of the Experimental Model 162
5.5 Conclusion 164

6 DEVELOPMENT OF DATA PROFILING FOR BIOREMEDIATION AND BIO-HARVESTING PROCESS USING WAIKATO ENVIRONMENT OF KNOWLEDGE ANALYSIS (WEKA) 167
6.1 Introduction 167
6.2 Green Microalgae-Based Bioremediation Profiling 170
6.2.1 Model Selection 170
6.2.2 Model Development 172
6.2.3 Model Validation 177
6.3 Filamentous Fungus-Based Bioharvesting 181
6.3.1 Model Selection 181
6.3.2 Model Development 183
6.3.3 Model Validation 185
6.4 Development of User-Friendly Interface 187
6.4.1 Interface Development 188
6.4.2 Interface Testing and Validation 192
6.5 Development of New Framework 193

6.6 Conclusion 195

7 SUMMARY, GENERAL CONCLUSION AND RECOMMENDATIONS FOR FUTURE RESEARCH 198
7.1 Summary and General Conclusion 198
7.2 Recommendations for Future Research 199

REFERENCES 200
APPENDICES 221
BIODATA OF STUDENT 238
LIST OF PUBLICATIONS 239

LIST OF TABLES

Table		Page
2.1	Shrimp Aquaculture Wastewater Characteristics from Various Shrimp Culture	17
2.2	Applications of Microalgae in Wastewater Treatment	24
2.3	Advantages and Disadvantages of Microalgae Harvesting Techniques	40
2.4	Applications of *Aspergillus* sp. in Microalgae Harvesting	43
2.5	Applications of Machine Learning in Water Quality Monitoring and Wastewater Treatment	54
2.6	Applications of Machine Learning in Flocculation/Harvesting	56
4.1	Physicochemical Characteristics of the Shrimp Aquaculture Wastewater	101
4.2	The Removal Efficiency (%) of Ammonia, Nitrite, and Orthophosphate for MW and FW on Day 10	107
4.3	Functional Group /Assignment of *Chlorella* sp. of Marine Water (MW). References	117
4.4	Functional Group /Assignment of *Chlorella* sp. of Fresh Water (FW). References	117
4.5	Elemental Identification by EDX	124
4.6	First-Order Kinetic Equation of Ammonia, NH_3^- Removal Efficiency at Different Microalgae Concentrations for Two Types of Wastewaters	130
4.7	First-Order Kinetic Equation of Nitrite, NO_2^- Removal Efficiency at Different Microalgae Concentrations for Two Types of Wastewaters	134
4.8	First-Order Kinetic Equation of Orthophosphate, PO_4^{-3} Removal Efficiency at Different Microalgae Concentrations for Two Types of Wastewaters	138
5.1	Experimental Result from Bioremediation Process for Marine Wastewater and Freshwater Wastewater	147
5.2	Comparison of Actual and Predicted Harvesting Efficiency of Microalgae Concentrations	151

5.3	Comparison of RSM Model Accuracy in Predicting Harvesting Efficiency for Marine and Fresh Water Microalgae	164
6.1	Correlation Coefficient of Cross-Validation Results for Different Days (Day 10, Day 12, and Day 14) and Parameters of MW Using Various Function Algorithms	171
6.2	Linear Equation for Ammonia on Day 10 (MW)	174
6.3	Inverted Equation Model of M5P Day 10 Marine Wastewater (MW) Treatment	175
6.4	Inverted Equation Model of M5P Day 10 Fresh Wastewater (FW) Treatment	176
6.5	Comparison Value between WEKA Predictions with the Actual Dataset for Validation Analysis MW	179
6.6	Comparison of Algorithm Models for Cross-Validation: Harvesting Performance between Dosage and Day for Marine Water Treatment (MW)	182
6.7	M5P Linear Equation of Cross-Validation for Determination of Cell Density vs Dosage for Marine Water Harvesting on Day 1	184
6.8	Inverted M5P Linear Equation of Cross-Validation for Determination of Cell Density vs Dosage for Marine Water Harvesting on Day 1	185
6.9	M5P Model Performance in Predicting Harvesting Efficiency (Average Difference): Dosage (a) and Mixing Rate (b)	186
6.10	Validation of Experimental and Predicted Values Using Interface with Percentage Error	192

LIST OF FIGURES

Figure		Page
2.1	World Capture Fisheries and Aquaculture Production	12
2.2	Microalgae in Treating Various Sources of Wastewater	22
2.3	First Order Kinetic Graph	30
2.4	Illustration of Microalgae Entrapped in Hyphae of Filamentous Fungus	45
2.5	Types of Algorithms in Machine Learning	50
3.1	Detailed Flowchart for Overall Study	63
3.2	General Steps in Microalgae Cultivation and Isolation	65
3.3	An Erlenmeyer Flask Containing Aquaculture Wastewater at Day 0 Bioremediation Process	69
3.4	Microscopic Image under the Magnification (400x), *Aspergillus niger*	72
3.5	Cultivation of Fungus Pellet	74
3.6	Machine Learning Framework of the Study	76
3.7	Procedure of Monte Carlo Simulation	77
3.8	WEKA: GUI Chooser	78
3.9	Visual Representation of the Steps in Accessing the Interface Explorer in WEKA	79
3.10	Preprocess Procedure in WEKA	80
3.11	Algorithms Used to Train the Dataset	81
4.1	Flowchart of an Experiment Conducted for Bioremediation Process Using *Chlorella* sp. for Shrimp Wastewater Treatment	88
4.2	Microalgae Culture on Petri Dish	90
4.3	Microalgae Biomass Coating with Gold (AU)	96
4.4	Phylogenetic Analysis of Freshwater and Marine Water *Chlorella* sp. (UMT LF1 and UMT LF2) Based on 18S rDNA Sequences and Neighbor-Joining Tree Construction	99

4.5 Bioremediation Process at Different Dosages, 0, 10, 20, 30, 40, 50, and 60 % (v/v) (a) Day 0 (b) Day 7 102

4.6 Microalgae Growth throughout the 14-day Treatment Period (A) Marine Water Bioremediation (B) Freshwater Bioremediation 104

4.7 Specific Growth Rate of *Chlorella* sp. during the Bioremediation Process 106

4.8 Bioremediation Performance at (A) 10, (B) 20, (C) 30, (D) 40, (E) 50, and (F) 60% (v/v) Microalgae *Chlorella* sp. Inoculation Dosages throughout 14-day Treatment Period for Marine Water Treatment (MW) 111

4.9 Bioremediation Performance at Different Microalgae, *Chlorella* sp. Inoculations Dosage; (a) 10, (b) 20, (c) 30, (d) 40, (e) 50, and (f) 60% (v/v) throughout 14-Day Treatment Period for Freshwater Treatment (FW) 112

4.10 FTIR Spectra: *Chlorella* sp. LF2 Culture in the Medium, F/2 (red), *Chlorella* sp. LF2 Culture in Aquaculture Wastewater (Blue) 116

4.11 FTIR Spectra: *Chlorella* sp. LF1 Culture in the Medium, BBM (red), *Chlorella* sp. LF1 Culture in Aquaculture Wastewater (Blue) 116

4.12 SEM Images of Microalgae at Magnifications (x1000, x5000, x10,000). Images (a-b-c) Represented *Chlorella* sp. Culture in Guillard's F/2 Media, and İmages (d-e-f) Represented *Chlorella* sp. Culture in MW 120

4.13 SEM Images of Microalgae at Magnifications (x1000, x5000, x10,000). Images (g-h-i) Represented *Chlorella* sp. Culture in BBM, and İmages (j-k-l) Represented the *Chlorella* sp. Culture in FW 122

4.14 EDS Image of Spectra Element in Microalgae, *Chlorella* sp. a) *Chlorella* sp. UMT LF2 in Media b) *Chlorella* sp. UMT LF2 in MW c) *Chlorella* sp. UMT LF1 in Media d) *Chlorella* sp.UMT LF1 in FW 123

4.15 Graph of ln NH_3 Versus Treatment Period (Day) at Different Microalgae Concentrations of Marine Water Treatment 128

4.16 Graph of ln NH_3 Versus Treatment Period (Day) at Different Microalgae Concentrations of Freshwater Treatment 129

4.17 Correlation between Predicted Data (Dash Line) and Experimental Data (Solid Line Symbol) of NH_3 Removal in

Marine Aquaculture Wastewater at Different Microalgae Concentrations 131

4.18 Correlation between Predicted Data (Dash Line) and Experimental Data (Solid Line Symbol) of NH_3 Removal in Freshwater (FW) Aquaculture Wastewater at Different Microalgae Concentrations 132

4.19 Graph of ln NO_2^- Versus Treatment Period (Day) at Different Microalgae Concentrations of Marine Water Treatment 133

4.20 Graph of ln NO_2^- versus Treatment Period (Day) at Different Microalgae Concentrations of Freshwater Treatment 134

4.21 Correlation between Predicted Data (Dash Line) and Experimental Data (Solid Line Symbol) of Removal NO_2^- in Marine Aquaculture Wastewater at Different Microalgae Concentrations 135

4.22 Correlation between Predicted Data (Dash Line) and Experimental Data (Solid Line Symbol) of Reduction NO_2^- in Freshwater Aquaculture Wastewater at Different Microalgae Concentrations 136

4.23 Graph of ln PO_4^{-3} Versus Treatment Period (Day) at Different Microalgae Concentrations of Marine Water Treatment 137

4.24 Graph of ln PO_4^{-3} Versus Treatment Period (Day) at Different Microalgae Concentrations of Freshwater Treatment 137

4.25 Correlation between Predicted Data (Dash Line) and Experimental Data (Solid Line Symbol) of Removal PO_4^{-3} in Marine Aquaculture Wastewater at Different Microalgae Concentrations 140

4.26 Correlation between Predicted Data (Dash Line) and Experimental Data (Solid Line Symbol) of Removal PO_4^{-3} in Freshwater Aquaculture Wastewater at Different Microalgae Concentrations 141

5.1 Flow Chart of Experiments Conducted for the Optimization of Bioflocculant, *Aspergillus niger* in Harvesting Green Microalgae 146

5.2 Harvesting Process of Microalgae Using Bio Flocculant Fungus 150

5.3 Three–Dimensional Response Surface Plots Depicting the Effects of Three Independent Variables on Harvesting Efficiency for Marine Water Species (A) Effect of Dosage and pH (B) Effect of Dosage and Mixing Rate (C) Effect of pH and

	Mixing Rate	160
5.4	Three–Dimensional Response Surface Plots Depicting the Effects of Three Independent Variables on Harvesting Efficiency for Freshwater Species (A) Effect of Dosage and pH (B) Effect of Dosage and Mixing Rate (C) Effect of pH and Mixing Rate	161
6.1	Flowchart of Sequence for Developing Data Profiling in Bioremediation and Microalgae Harvesting Using WEKA	169
6.2	M5P Tree Output for Ammonia on Day 10 (MW)	173
6.3	Validation Graph for Ammonia Day 10	179
6.4	Interface without User Input	190
6.5	Interface with User Input	191
6.6	Flow of the Proposed Framework	194

LIST OF ABBREVIATIONS

APHA	American Public Health Association
BOD	Biochemical Oxygen Demand
BLAST	Basic Local Alignment Search Tool
CC	Correlation coefficient
DNA	Deoxyribonucleic acid
DOF	Department of Fisheries
FAO	Food and Agriculture Organization
FTIR	Fourier transform infrared
MAE	Mean absolute error
NCBI	National Centre for Biotechnology Information
PCR	Polymerase Chain Reaction
RMSE	Root means square error
RSM	Response Surface Methodology
STD	Standard deviation
SEM	Scanning Electron Microscopy
TAN	Total Ammonia Nitrogen
UMT	Universiti Malaysia Terengganu
UPM	Universiti Putra Malaysia
USD	United State Dollar
cm	Centimeter
°C	Degree Celsius
et al.	*et alia*
G	Gram
g ind^{-1}	Gram per individual
g DW L^{-1}	Gram dry weight per liter
g L^{-1}	Gram per liter
%	Percentage

h	Hour
mL	millilitre
rRNA	Ribosomal RNA
L	Liter
mM	Millimolar
M	Meter
mg	Milligram
min	Minute
M	Molar
mg L^{-1}	Milligram per liter
Mm	Millimeter
nm	Nanometers
s	Second
sp.	Species
Ppt	Parts per thousand
rpm	Revolution per minute
V	Volt
v/v	Volume per volume
±	Plus minus
µg	Micro gram
µM	Micro molar
µmol m^{-2} s^{-1}	Micromole per square meter per second
µm	Micron
µL	Micro litre
μ	Specific growth rate

CHAPTER 1

INTRODUCTION

1.1 Background of Study

The rapid growth of the global population has contributed to the expansion of the aquaculture industry. As the demand for food, nutrition, income, and livelihood continues to increase, aquaculture has emerged as a critical sector to meet these needs. Aquaculture raises aquatic species in ponds, tanks, and cages, including fish, crustaceans, molluscs, and algae. According to the FAO (2020) and Bush et al. (2019), the aquaculture industry contributes significantly to global food supplies, which increase rapidly by more than 10% annually, making it the fastest-growing sector of the world food economy and reaching new record high of 178 million tons in 2022. Throughout the world aquaculture industries, Asia accounted for a significant portion of the world's aquaculture output, contributing around 23 million tons of aquaculture products in the year 2020. Nevertheless, the aquaculture industry greatly depends on water resources as one of their primary inputs for development.

The aquaculture industry in Malaysia has experienced significant growth over the past few decades and is expected to continue to grow in the coming years. According to the Department of Fisheries Malaysia data, the industry's production value increased from RM 1.7 billion in 2010 to RM 3.8 billion in 2019. Several factors have contributed to the growth of the aquaculture industry in Malaysia. These include the favorable climate, abundant water resources, and increasing demand for seafood, both domestically and

internationally. In Malaysia, the aquaculture industry includes edible products, such as seaweed, marine fish, freshwater fish, brackish water fish, and inedible products, including aquatic plants and ornamental fish. In 2021, seaweeds led the cultured species at 42.88%, followed by freshwater fish (25.32%), shrimp (13.55%), marine fish (13.72%), cockles (4.46%), and black tiger shrimp (*Penaeus monodon*) (0.07%).

Despite the growth in the industry, there are still challenges that need to be addressed. These include the need for better infrastructure, improved access to finance, and the development of sustainable farming practices that minimize environmental impact. The aquaculture industry also generates a substantial amount of wastewater, and the release of this waste has significantly increased. Before being released into natural water bodies, aquaculture wastewater requires thorough treatment due to considerable amounts of chemical and microbiological pollutants. Releasing aquaculture wastewater into natural water bodies causes problems due to high levels of organic matter, nutrients (phosphate), and nitrogenous wastes (such as ammonia, nitrite, nitrate, and dissolved organic carbon) (Kurniawan et al., 2021; Lananan et al., 2014). Improper disposal of this wastewater can have severe environmental consequences, including eutrophication and damage to the natural coastal ecosystem (Wurtsbaugh et al., 2019).

Eutrophication is an excessive enrichment of nutrients in water bodies, which leads to algal blooms and poor water quality. Since the mid-20th century, eutrophication has become a significant and widespread environmental issue

by affecting about 48% of lakes and reservoirs in North America, 54% in Asia and the Pacific, 53% in Europe, 41% in South America, and 28% in Africa (Abdel-Raouf et al., 2012). According to statistics from Kurniawan et al. (2021), Malaysia currently generates 20.15 m^3 of aquaculture wastewater per kilogram of production each year, averaged across intensive ponds, extensive ponds, and flow-through systems. This wastewater generation is expected to increase significantly as the aquaculture sector continues to expand, with predictions estimating a total of 7.519 km^3 of wastewater by 2030 due to the rising demand for inland aquaculture systems.

Therefore, effective wastewater treatment processes are required to maintain the growth of the aquaculture industry while reducing uncontrolled pollution and environmental impacts. Hence, the bioremediation process was suggested since it was an environment-friendly alternative to overcome this problem on a small scale. Bioremediation is an emerging method that uses green plants to convert and remove different kinds of toxins from wastewater in a non-intrusive, cost-effective, and environmentally safe (Do et al., 2022; Kassim et al., 2022). Compared to conventional approaches, bioremediation can treat wastewater more efficiently and affordably without chemical addition or further mixing. Terrestrial plants have historically been utilized in bioremediation, but due to their slow growth, other microbes, such as eukaryotic algae and cyanobacteria, can decrease contaminants 10 to 50 times faster (Iasimone et al., 2017). Hence, it has been continuously replaced by unicellular plants such as microalgae.

Microalgae have many applications and potential, especially in bioremediation (Olguín, 2003; Phu et al., 2021; Zhao et al., 2012). Their ability to absorb nutrients, remove contaminants, and produce biomass makes them an effective tool for sustainable bioremediation in aquaculture systems (Lananan et al., 2014). Furthermore, microalgae biomass is increasingly recognized as a source of sustainable biofuels, offering renewable and eco-friendly alternatives to fossil fuels, including biodiesel, bioethanol, and biogas (Hossain et al., 2020; Khan et al., 2018). However, the cost of microalgae cultivation remains a challenge. Traditional cultivation methods often rely on expensive chemicals and fertilizers to provide the necessary nutrients for microalgae growth (Hossain et al., 2020; Santos et al., 2019). Researchers have explored alternative nutrient sources to address this challenge, and wastewater has emerged as a viable option. Wastewater contains various nutrients that can serve as a nutrient-rich medium for microalgae cultivation. Utilizing wastewater as a substitute for traditional culture media can reduce reliance on expensive chemicals and lower production costs (Hossain et al., 2020).

An algal bloom is a potential issue when using microalgae as bioremediation agents. An algal bloom rapidly increases algae populations in freshwater and marine aquatic habitats (Mohyedin et al., 2019). According to earlier research, the *Chlorella* sp. biomass in a declining growth phase releases the absorbed nutrients to the surrounding water (Nasir et al., 2015). Therefore, sustainable harvesting techniques are required to avoid recycling nutrients in receiving waters and control the microalgae's biomass density. This is one of the important technological and financial challenges that must be addressed.

Harvesting methods are promising as they can remove excess microalgae from water bodies, thereby preventing adverse environmental impacts. Traditional bio-harvesting methods include centrifugation, flocculation, filtration, and sedimentation (Xu et al., 2021). Each of these methods has its advantages and limitations. For instance, centrifugation is highly efficient but energy-intensive and costly, while flocculation often relies on chemical additives, which can introduce contaminants and are not environmentally sustainable.

Recent advancements have focused on exploring more sustainable bio-harvesting methods using flocculation to address these challenges. A promising approach is the use of filamentous fungi *Aspergillus niger,* which can be isolated from environments such as aquaculture wastewater. The morphology of filamentous fungi, mainly their sticky hyphae are allowing them to attach to microalgal cells and helping the removal of these cells from aquatic environments (Wang et al., 2023). This method offers several advantages over traditional techniques, including reduced energy consumption and eliminating chemical additives. The successful application of *Aspergillus niger* in microalgae harvesting represents a significant advancement in the development of sustainable bio-harvesting techniques. This approach addresses the technological and financial challenges associated with traditional methods and contributes to the broader goal of minimizing the environmental impact of microalgae cultivation and harvesting processes.

The treatment and harvesting parameters must be optimized to reduce costs while increasing efficiency. Several wastewater and effluent treatment process optimization methods are available in the literature (Singh & Mishra, 2021; Xu et al., 2021). This includes applying analytical techniques, response surface methodology (RSM), and machine learning (ML) algorithms. Artificial intelligence (AI) and machine learning algorithms (MLAs) can rapidly analyze large datasets and identify optimal combinations of predictor variables as needed, leading to effective efficiency optimization (Xu et al., 2021). The conventional approach of optimizing multiple experimental parameters one at a time while other variables are constant is very complicated. Besides, this study focuses on developing a new strategy for the decision-making framework by integrating process networks using machine learning (ML). Waikato Environment for Knowledge Analysis (WEKA) was introduced to select the best algorithm to access big data, automatically learn and handle new future situations through analysis.

WEKA focuses on correlating the parameters of nutrient uptake, treatment periods, and removal of water quality. This is important since the quality of water management determines whether aquaculture production is a success or failure. Moreover, the approach employed by ML in this study is to develop a model that optimizes parameters for best performance for application in the harvesting process using internal cross-validation. Response surface methodology (RSM) is also employed in this study to analyze the interactions between multiple independent factors and determine the optimal parameters for achieving the highest harvesting efficiency.

1.2 Problem Statement

Aquaculture is an important source of food and income, and it is growing rapidly as captured seafood alone could not meet increasing demand (Jegatheesan et al., 2011). However, this expansion leads to significant environmental concerns due to the discharge of untreated wastewater rich in organic matter, nitrogen, phosphorus, and chemicals used to prevent aquatic diseases. This wastewater contributes to eutrophication, resulting in oxygen depletion and mass mortality of aquatic species (Prepas & Charette, 2003; Serediak et al., 2013). To address these issues, green microalgae *Chlorella* sp. has shown promise in treating nutrient-rich wastewater and preventing eutrophication (Alazaiza et al., 2023; Yousif et al., 2022). *Chlorella* sp. can also limit the growth of harmful algae, reducing ecological damage such as algal blooms, which cause hypoxia and affect water quality (Amorim & Moura, 2021).

Moreover, studies indicate that *Chlorella* sp. can release absorbed nutrients into the water during the declining growth phase, highlighting the importance of effective harvesting techniques. Various methods such as centrifugation, filtration, flotation, and coagulation-flocculation have been used, but they are often costly and energy-intensive (Granados et al., 2012; Yang et al., 2018). Hence, the flocculation process utilizing inorganic and organic synthetic flocculants is commonly used in industrial fields because of their cost-effectiveness and efficiency (Liu et al., 2021). However, the major components of both flocculants may cause some environmental health problems towards aquatic life. Therefore, using alternative natural substances known as bio-

flocculants is important in implementing sustainable bio-harvesting techniques and moving toward more environment-friendly practices.

Numerous studies have focused on the conventional 'one-factor-at-a-time' (OFAT) approach in the harvesting process (OFAT) approach in the harvesting process (Nasir et al., 2015). However, the OFAT approach has two significant limitations: an extensive number of experimental runs and a limited capacity to analyze interactions among multiple factors (Desai et al., 2008). To address these drawbacks, Response Surface Methodology (RSM) offers a more efficient alternative for optimizing multiple variables and constructing models that explain factor-response relationships. Several studies have implemented RSM for harvesting microalgae using flocculants (Ghosh & Hallenbeck, 2010; Zheng et al., 2012). Nevertheless, limited research has explored RSM for optimizing bio-flocculant-producing fungi.

Machine learning (ML) has emerged as an efficient alternative to RSM for handling large datasets and building predictive models (Ugonabo et al., 2022; Wang et al., 2021). Despite this, RSM remains useful for studies that benefit from its structured approach and statistical techniques. However, RSM is more easily interpretable than machine learning models, making understanding the relationships between input variables and output responses easier. ML and RSM are useful techniques for modeling and optimizing complex systems but differ in their underlying principles, application areas, and optimization methods.

1.3 Objectives of Study

The primary goal of this study is to provide a systematic data-driven approach to model and optimize the aquaculture wastewater treatment using bioremediation and the harvesting process using bio-flocculants. The goal can be achieved with the following objectives:

1. To evaluate the performance of green microalgae, *Chlorella* sp., in removing nutrients during bioremediation of shrimp aquaculture wastewater.
2. To optimize the parameters (dosage, pH and mixing rate) of bioflocculant filamentous fungus, *Aspergillus niger* in harvesting green microalgae biomass.
3. To predict the efficiency of bioremediation (nutrient removal) and bio-harvesting (microalgae removal) using Machine Learning with Waikato Environment of Knowledge Analysis (WEKA) software.

1.4 Scope of Study

This study aims to evaluate the performance of the green microalgae *Chlorella* sp. in removing pollutants from shrimp aquaculture wastewater. It addresses the removal of nutrients that contribute to eutrophication, such as ammonia, nitrite, and phosphorus. The investigation involves assessing various microalgae biomass concentrations (0 – 60 % (v/v)) and their impact on the removal efficiency of these nutrients in two types of shrimp aquaculture wastewater: marine (*Litopenaeus vannamei*) and freshwater (*Macrobrachium rosenbergii*). The study also focuses on the harvesting efficiency of excess microalgae using the bio-flocculant fungus *Aspergillus niger* and optimizing the process through Response Surface Methodology (RSM) with a Central

Composite Design (CCD), utilizing three parameters, dosage (25 – 35 g L^{-1}), pH (6 – 7), and mixing rate (100 – 150 RPM). Additionally, the study incorporates machine learning techniques via Waikato Environment for Knowledge Analysis (WEKA) software to analyze bioremediation and harvesting efficiency data.

1.5 Significance of Study

This study is significant as it addresses critical environmental issues by suggesting a practical solution for managing wastewater from shrimp farming using *Chlorella* sp. for practical bioremediation. This approach reduces harmful contaminants such as ammonia, nitrite, and orthophosphate and mitigates their impacts on aquatic ecosystems and human health. Additionally, it improves the efficiency of microalgae harvesting by optimizing the use of *Aspergillus niger* as a bio-flocculant. This improvement is crucial for developing effective and large-scale wastewater treatment systems. Incorporating machine learning using WEKA, focusing on the M5P algorithm, represents a major advancement in predicting and optimizing these processes. This approach improves the precision and cost-effectiveness of bioremediation and harvesting. In conclusion, the study reveals effective methods for bioremediation and biomass harvesting, advancing sustainable aquaculture practices and reducing the environmental impact of shrimp farming while supporting renewable energy production. It significantly contributes to environmental management and resource optimization, providing a model that integrates biological and technological solutions to address current aquaculture challenges.

1.6 Thesis Layout

This thesis consists of seven chapters. Chapter 1 gives an overview of the study, including the introduction, problem statement, objectives, scope, significance, and layout. Chapter 2 reviews advancements in bioremediation using microalgae for treating aquaculture wastewater, discussing their benefits, growth factors, and nutrient removal. It also covers the use of filamentous fungi in harvesting and machine learning techniques with WEKA for bioremediation and harvesting. Chapter 3 details the methodology, including experimental procedures and kinetic formulas. Chapter 4 presents and discusses the results of microalgae growth and nutrient removal. Chapter 5 focuses on harvesting green microalgae using filamentous fungi. Chapter 6 explores machine learning applications for data profiling and validation, particularly WEKA. Chapter 7 concludes the study by summarizing the objectives and outcomes and suggesting future research.

CHAPTER 2

LITERATURE REVIEW

2.1 Development of Aquaculture Industry

The aquaculture industry has experienced significant growth over the past decade and is the fastest-growing food production technology in the world. According to the Food and Agriculture Organization of the United Nations (FAO), global farmed fish production has increased nearly 50% of global food production (FAO, 2018, 2020). The global aquaculture industry has experienced significant growth since the 1950s, with an average annual growth rate of 10%. In 2020, global aquaculture production, excluding aquatic plants, reached 178 million metric tons (MMT), valued at USD 406 billion (Figure 2.1). This production value includes USD 141 billion, attributed to capture fisheries, and USD 265 billion to aquaculture.

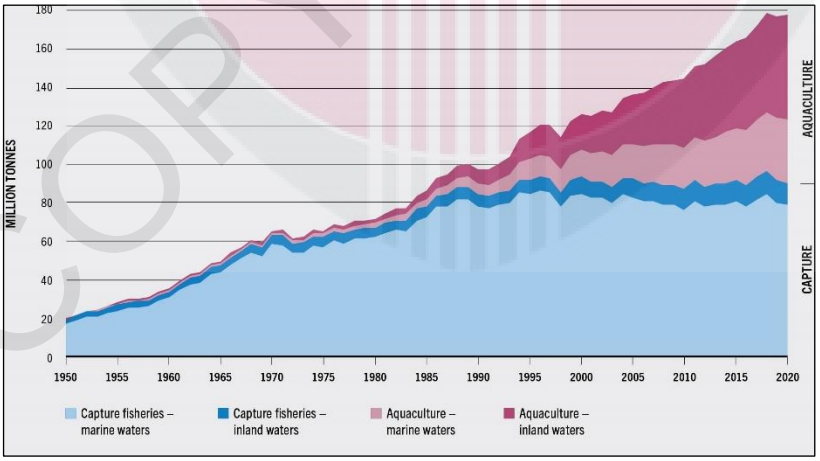

Figure 2.1 : World Capture Fisheries and Aquaculture Production
(Source: FAO, 2020)

2.1.1 Aquaculture Industry in Malaysia

Malaysia has experienced rapid growth in its aquaculture industry in recent years. Aquaculture in Malaysia has become one of the top 15 producers in the world, and the country's aquaculture production has increased more than tenfold since 1990 (Ahmad et al., 2021; Fathi et al., 2018). The aquaculture industry in Malaysia is diverse and includes farming various aquatic species, including fish, shrimp, and other aquatic products. In 2018, aquaculture and fisheries production in Malaysia was worth more than US$2.3 billion, contributing significantly to the country's economy. The Malaysian government has identified aquaculture as a priority sector for generating economic growth and employment opportunities (Isa et al., 2021). In 2019, the industry produced approximately 411,781 tons of aquaculture products and had an estimated economic value of USD 700 million, highlighting its continued importance to the national economy (Tan et al., 2024).

2.1.2 Shrimp Aquaculture Industry in Malaysia

Malaysia is one of the main producers of high-value aquaculture products such as shrimp, prawns and ornamental fish (Kurniawan et al., 2021). Shrimp aquaculture is a growing industry in Malaysia, with the country being the ninth-largest shrimp exporter in the world (Hing, 2022). Based on annual fisheries statistics from the Department of Fisheries Malaysia (DOF), more than 53 million tons of marine shrimp worth 1.3 billion ringgits were produced by the aquaculture industry in 2019 (Department of Fisheries Malaysia, 2020). The Department of Fisheries Malaysia (2023) reported that sixteen hatcheries for

marine shrimp culture and only one hatchery for freshwater shrimp culture were registered under Malaysia Good Agricultural Practices (MyGAP). Hence, marine shrimp species were the main species in capture production, contributing 98.7% of the total captured shrimp production. The remaining capture production came from freshwater shrimp species. In Malaysia, the aquaculture industry is primarily based on three shrimp species: giant freshwater prawn (*Macrobrachium rosenbergii*), giant tiger prawn (*Penaeus monodon*), and whiteleg shrimp (*Litopenaeus vannamei).* Whiteleg shrimp accounts for most production, contributing 89% of the total farmed shrimp output, followed by giant tiger prawn at 10% and giant freshwater prawn at 1% (Chowdhury et al., 2013).

The Malaysian government is committed to supporting its growth and development because shrimp aquaculture is an important industry in Malaysia (Ghee-Thean et al., 2016). With the appropriate policies and incentives, the Malaysian government has implemented various measures to ensure the industry's sustainability, including water quality regulations and food safety standards. The country has also encouraged the development of organic aquaculture practices. Aquaponics is a food production system that combines traditional aquaculture practices with hydroponics, which involves growing plants in water for raising aquatic animals such as snails, fish, crayfish, or prawns in tanks (Turcios & Papenbrock, 2014).

However, the growth of the aquaculture industry has been driven by several factors. These include the rising demand for seafood, advancements in

farming technologies, increased investment and funding, and the creation of job opportunities and rural development. In addition, the expansion of aquaculture into new areas has contributed to the risk associated with handling environmental issues. One of the biggest challenges in handling aquaculture wastewater is its potential environmental impact. Aquaculture wastewater can contain a variety of pollutants, including nutrients, organic matter, and pathogens, which can harm aquatic ecosystems if released untreated. Aquaculture operations can significantly impact the environment, including water pollution, habitat destruction, and the introduction of non-native species. Developing and implementing sustainable aquaculture practices is essential to minimize negative environmental impacts (Ismail, 2021).

2.2 Shrimp Aquaculture Wastewater

2.2.1 Shrimp Aquaculture Wastewater Characteristics

Shrimp aquaculture wastewater has varying characteristics depending on the type of aquaculture environment (freshwater, marine, and brackish) and the species being cultured (Khatoon et al., 2016). Table 2.1 comprehensively summarizes shrimp aquaculture wastewater characteristics from various countries to compare shrimp culture practices. The wastewaters from various countries exhibit pH values that are nearly neutral to slightly alkaline. This pH range is commonly associated with aquaculture practices and can be influenced by regional farming practices and water sources used in these systems. For salinity levels marine aquaculture typically has higher salinity

levels than freshwater systems, as it aims to replicate the natural conditions in the ocean. The specific values for freshwater in the table are not provided since the salinity levels are generally very low, typically close to 0 parts per thousand (ppt) or practical salinity units (PSU). Freshwater bodies, such as rivers, lakes, and ponds, have relatively low salt concentrations compared to marine environments. Salinity values for freshwater can vary slightly depending on the specific location and environmental factors, but they are far lower than the salinity levels found in marine or saltwater environments.

Apart from that, the common wastewater characteristic is the high concentration of organic substances, primarily from uneaten feed, faeces, and the decomposition of organic matter. This organic content contributes significantly to the chemical oxygen demand (COD), indicating the presence of readily biodegradable organic compounds that impact water quality. Furthermore, the presence of nitrogen compounds, including ammonia (NH_3/NH_4^+), nitrate (NO_3^-), and nitrite (NO_2^-), is a common feature in aquaculture wastewater. These compounds stem from the metabolic processes of aquatic animals, the presence of uneaten feed, and the natural decomposition of organic matter. The study by Roy et al. (2010) shows that the sequencing batch reactor system produces wastewater with high levels of ammonia, nitrite, and nitrate, which are much higher than what is considered safe for aquatic environments. These elevated levels can harm shrimp, affecting their health and growth. Specifically, nitrate and nitrite levels above 25 ppm are toxic. The high levels are linked to feeding shrimp on a 40% protein diet and stocking them at a high density of 1,000 shrimp per square meter.

Table 2.1 : Shrimp Aquaculture Wastewater Characteristics from Various Shrimp Culture

Country	Culture type	Parameters pH	Salinity (ppt)	COD (mg L^{-1})	DO (mg L^{-1})	Total Phosphorus (mg L^{-1})	Total Nitrogen (mg L^{-1})	Ammonia Nitrogen (mg L^{-1})	Nitrite (mg L^{-1})	Nitrate (mg L^{-1})	References
China	Shrimp, *Penaeus vannamei*	7.78	-	8.5	-	0.42		4.24	2	-	(Gao et al., 2016)
	Shrimp, *Lito-penaeus vannamei*	7.12 ± 0.01	15 ± 0.03	12.41 ± 0.44	-	-	97.92 ± 0.96	1.62 ± 0.02	0.44 ± 0.01	14.94 ± 0.07	(Xu et al., 2021)
	Mixed culture pond, shrimp and fish	8.1	-	2.25	-	1.21	14.5	-	-	-	(Han et al., 2020)
United States	Shrimp	8.1 ± 0.1	28.6 ± 0.4	-	-	-	-	103.7 ± 6.1	176 ± 22.7	-	(Roy et al., 2010)
Malaysia	Shrimp, *Penaeus vannamei*	-	20 – 37		4.8 – 7.0	-	-	-	-	-	(Kasan et al., 2018)
	Shrimp	8.05 ± 0.01	24.17 ± 0.03		5.20 ± 0.02	3.47 ± 0.02		6.12 ± 0.01	3.80 ± 0.03	3.47 ± 0.02	(Khatoon et al., 2016)

* Sign (-) salinity = freshwater, (-) other parameters = data not available

In summary, the characteristics of aquaculture wastewater differ depending on the environment and the species cultured. Effective treatment of wastewater with high nutrient levels is crucial before it is released. The necessity for treatment depends on the specific aquaculture system, with some requiring more intensive treatment than others. Proper wastewater management is vital to reduce the environmental impact of aquaculture practices and ensure compliance with regulations regarding acceptable nutrient levels before discharge into water bodies.

2.2.2 Shrimp Aquaculture Wastewater Treatment

Shrimp aquaculture has become a significant sector in global food production, driven by the increasing demand for seafood. However, this growth has led to substantial challenges related to wastewater management, which poses environmental and public health risks. The wastewater generated during shrimp farming results from a combination of excess feed, shrimp faeces, dead organisms, and metabolite excretion, particularly ammonia, nitrite, and nitrate. These compounds degrade water quality and make it unsuitable for reuse or discharge into the environment without proper treatment. In addition, poor farm management practices, such as the overuse of fertilizers, chemicals, and antibiotics can worsen pollution levels, contributing to nutrient buildup and chemical contamination (Iber & Kasan, 2021)

To mitigate these impacts, various wastewater treatment technologies have been developed, both traditional and modern. Traditional methods include coagulation, membrane filtration, adsorption, and advanced oxidation

processes, all of which aim to remove toxic substances from wastewater (Bhatt et al., 2023). However, these conventional approaches often have limitations, such as high operational costs, energy demands, and secondary pollution from chemical treatments. Therefore, recent technological advances have focused on more sustainable and efficient methods.

One of the innovations in technology in shrimp wastewater treatment is cavitation which uses the physical process of creating and collapsing microbubbles to destroy contaminants in water (Nguyen et al., 2024). This method is highly effective at breaking down organic pollutants and eliminating pathogenic microorganisms. Another promising approach is the nanotechnology. This method has also made significant advancements in wastewater treatment through the development of nanomaterials such as nano adsorbents (Manyangadze et al., 2020), polymeric nano adsorbents (Nguyen et al., 2024), and nanomaterial-based membranes (Thamer et al., 2021) which are highly effective at removing contaminants. Nanoadsorbents, for example, offer a large surface area for pollutant binding, allowing for more efficient removal of organic and inorganic contaminants, including heavy metals. Nanomaterial-based membranes have been used to enhance filtration processes, improving permeability and fouling resistance while removing viruses, pathogens, and suspended solids from shrimp wastewater. Although still an emerging field, nanotechnology holds great promise for improving the sustainability and efficiency of shrimp aquaculture wastewater treatment (Iber & Kasan, 2021).

Biofloc technology (BFT) is another innovative solution gaining popularity in shrimp aquaculture wastewater management (Wan Mahari et al., 2024). BFT involves the cultivation of beneficial bacteria and microorganisms in the shrimp pond, which consume waste products such as ammonia and convert them into protein-rich bioflocs. These bioflocs can then be consumed by the shrimp, reducing the need for additional feed and enhancing water quality. BFT has been particularly successful in maintaining good water quality without the need for frequent water exchanges while supporting shrimp growth. However, BFT requires continuous aeration and careful management of the carbon-to-nitrogen ratio to ensure optimal bacterial activity.

In addition to these technologies, biological wastewater has shown the potential to improve wastewater quality in shrimp farming. This process uses microorganisms, such as bacteria and other biological agents, to break down and remove organic pollutants and contaminants from wastewater. Biological wastewater treatment typically involves two main processes such as aerobic treatment and anaerobic treatment. Aerobic methods, such as bioreactors, activated sludge, and biofiltration, are effective at breaking down organic matter and pollutants but require significant energy for aeration and produce substantial sludge (Rajasulochana & Preethy, 2016). Anaerobic treatment, which operates in oxygen-free conditions, generates biogas and treats sludge with lower energy needs but can be less effective and slower. On top of that, microalgae cultivation in aquaculture wastewater has been proposed as a technique for the circular economy (Bhatt et al., 2023). This innovative approach not only utilizes the nutrient-rich wastewater from shrimp

farming but also contributes to the sustainable production of biomass. The biomass generated from microalgae can be used for various applications, including biofuels, animal feed, and fertilizers (Wan Mahari et al., 2024).

Several advantages and disadvantages exist for both traditional and modern methods of shrimp wastewater treatment. Furthermore, biological treatment using microalgae offers a sustainable alternative with several benefits: they can effectively remove nutrients and heavy metals, produce valuable byproducts such as biofuels and require less energy than traditional methods. Additionally, microalgae can integrate into existing wastewater treatment systems, potentially enhancing overall efficiency. However, there are challenges associated with using microalgae. For instance, large-scale cultivation and harvesting can be costly, and pollutant removal efficiency can vary depending on the microalgae species and environmental conditions (Yaakob et al., 2021). Moreover, integrating microalgae in conventional treatment systems may require modifications to existing infrastructure to accommodate the specific needs of microalgae-based processes.

2.3 Green Microalgae

2.3.1 Application of Green Microalgae in Wastewater Treatment

Green microalgae have been widely recognized as an effective biological tool for treating wastewater generated from various sources, including municipal wastewater, industrial wastewater, agricultural runoff, and aquaculture effluent (Alishah Aratboni et al., 2019; Zerrouki et al., 2019). Green microalgae are also known for their high growth rates and ability to remove nitrogen,

phosphorus, and other pollutants from water, which makes them an ideal candidate for wastewater treatment (Abdel-Raouf et al., 2012; Aditya et al., 2022). Microalgae are photosynthetic organisms that use nutrients and organic matter in wastewater as a food source for their growth and metabolism. They are converting the food source with the help of carbon dioxide to biomass during photosynthesis (Aditya et al., 2022; Do et al., 2022; Yaakob et al., 2021). Their photosynthetic activity also enriches aquatic ecosystems by releasing oxygen during daylight time and improving dissolved oxygen levels in water (Zhou et al., 2012). Figure 2.2 shows how microalgae-based wastewater treatment effectively manages various types of wastewater and produces cleaner water.

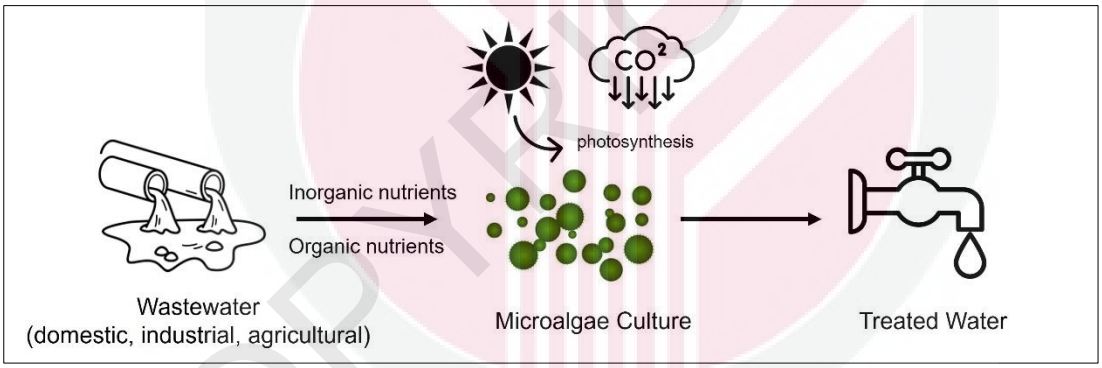

Figure 2.2 : Microalgae in Treating Various Sources of Wastewater
(Source: Zerrouki & Henni, 2019)

Furthermore, microalgae can also remove nutrients such as nitrogen and phosphorus from wastewater by incorporating them into their biomass. This reduces the nutrient contents in the water bodies, preventing eutrophication and algal blooms (Wang et al., 2014). In addition, microalgae also can remove organic matter from feces and uneaten feed of aquaculture wastewater. This can reduce the amount of BOD and TSS, which improves water quality and

reduces the risk of oxygen depletion. Green microalgae that are cultivated in wastewater enhances their biomass production. This biomass can be harvested for various applications, including biofuel production, animal feed, and bioplastics (Khan et al., 2018). Besides biomass production, green microalgae can produce valuable compounds such as lipids, pigments, and proteins (Alishah Aratboni et al., 2019). These compounds can be extracted and used in various industries, especially food, cosmetic and pharmaceutical industries, creating additional revenue streams from wastewater treatment as waste to wealth.

Table 2.2 illustrates the nutrient removal efficiency and growth rates of various green microalgae species across different types of wastewater. The data reveal significant variations in performance based on microalgae species and cultivation conditions, with some species achieving up to 99.8% nitrogen and 99.97% phosphorus removal. These differences underscore the influence of both species-specific characteristics and environmental factors on nutrient removal effectiveness. Therefore, algae-based wastewater treatment systems often demonstrate greater cost-effectiveness and sustainability as green technologies than traditional methods due to the rapid growth rate and efficient reproduction of microalgae. The byproduct of microalgae biomass can also serve as a valuable source of protein, thereby reducing the dependency on traditional protein sources such as fishmeal (Han et al., 2019).

Table 2.2 : Applications of Microalgae in Wastewater Treatment

Wastewater Type	Cultivation conditions	Microalgae species	Initial to Final Concentration	Removal Efficiency (%)	Growth Rate (mg L^{-1} d^{-1})	References
Aquaculture wastewater	Batch Culture	Platymonas subcordiformis	N = 47.8 mg L^{-1} to 0.82 mg L^{-1} P = 0.213 mg L^{-1} to 0.005 mg L^{-1}	N = 98 % P = 99 %	N/A	Guo et al., 2013
		Scenedesmus obliquus	Initial (N = 5.32 mg L^{-1}; P = 8.82 mg L^{-1})	N = 77.7 % P = 100 %	89.61	Ansari et al., 2017
			Final (N =1.18 mg L^{-1}; P = 0 mg L^{-1})		160.79	
		Ankistrodesmus falcatus	Final (N = 1.02 mg L^{-1}; P = 0.13 mg L^{-1})	N = 80.85 % P = 98.52 %	107.89	
		Chlorella sorokiniana	Final (N = 1.28 mg L^{-1}; P = 0 mg L^{-1})	N = 75.76 % P = 100 %		
	Batch and semi-continuous culture	Chlorella sp.	N = 6.81 to 1.30 mg L^{-1} P = 0.42 to 0.12 mg L^{-1}	N = 86.1 % P = 82.7 %	42.6	Gao et al., 2016
	Continuous culture	Chlorella sp. GD	N = 60 ± 3.6 mg L^{-1} to 6.0 ± 0.7 mg L^{-1} P = 6.8 ± 0.3 mg L^{-1} to 0.1 ± 0.1 mg L^{-1}	N = 90 % P = 99 %	309	Kuo et al., 2016
	Raceway system	Chlorella vulgaris	N/A	N = 99.8 % P = 99.7%	N/A	(Tejido-Nuñez et al., 2019)
		Tetradesmus obliquus		N = 99.7% P = 99.6%,		
	Continuous culture	Spirulina sp.	N = 1.33 mg L^{-1} to 0.25 mg L^{-1} P = 6.0 ± 0.7 mg L^{-1} to 0.25 mg L^{-1}	N = 81.10 % P = 99.97 %	260	Cardoso et al., 2020

Table 2.2 : Continued

Wastewater Type	Cultivation conditions	Microalgae species	Initial to Final Concentration	Removal Efficiency (%)	Growth Rate (mg L^{-1} d^{-1})	References
	(Raceway system)					
Municipal Wastewater	Batch Culture system	Chlorella sp.	N = 190.7 mg L^{-1} to 30.30 mg L^{-1} P = 19.11 mg L^{-1} to 3.377 mg L^{-1}	N = 84.11 % P = 82.36 %	N/A	Rasoul-Amini et al., 2014
	Semi-continuous system	Auxenochlorella protothecoides	N/A	N = 59.70 % P = 81.52 %	N/A	Zhou et al., 2012
Synthetic Wastewater	Photobioreactor		Initial (N = 41.3 mg L^{-1}; P = 25 mg L^{-1})	Photon flux (900, 1500 and 2000 µmol m^{-2} s^{-1})		(Sacristán de Alva et al., 2018)
		Dunaleilla sp.	Final N = 1.27, 0.113, 1.02 mg L^{-1} Final P = 1.495, 1.44, 1.68 mg L^{-1}		190	
		Nannochloropsis salina	Final N = 2.41, 4.1, 2.38 mg L^{-1} Final P = 0.72, 0.71, 0.7 mg L^{-1}	N = 96.91, 97.26, 97.53 % P = 94.02, 94.25, 93.27 %	200	
		Tetraselmis sp.	Final N = 0.83, 0.81, 0.80 mg L^{-1} Final P = 1.095, 1.015, 1.083 mg L^{-1}		170	
				N = 94.16, 90.07, 94.24 % P = 97.12, 97.16, 97.2 %		

Table 2.2 : Continued

Wastewater Type	Cultivation conditions	Microalgae species	Initial to Final Concentration	Removal Efficiency (%)	Growth Rate (mg L^{-1} d^{-1})	References
				N = 97.99, 98.03, 98.06 % P = 95.62, 95.94,95.67 %		
Hydroponic Wastewater		Chlorella vulgaris	N = 12 mg L^{-1} to 0.18 mg L^{-1} P = 1.8 mg L^{-1} to 0.018 mg L^{-1}	N = 98.5% P = >99%	110.8	(Yousif et al., 2022)

N and P = Values of N and P calculated from given values of $(NH_4)_2SO_4$, $NaNO_2$, KNO_3 and K_3PO, N/A = Data not available

2.3.2 Mechanism of Microalgae Bioremediation

Microalgae play a significant role in removing various types of toxins from the environment through processes such as biosorption, bioaccumulation, and biodegradation (Goh et al., 2023; Sutherland & Ralph, 2019). Biosorption is a passive process where pollutants are removed from water onto the surface of microalgae cells via electrostatic forces, Van der Waals interactions, and other physical and chemical interactions (Abdelfattah et al., 2023; Chia et al., 2020). Studies have demonstrated that biosorption effectively removes heavy metals such as cadmium, lead, mercury, and arsenic from aquatic environments. However, biosorption efficiency can vary significantly among microalgae species, and factors such as pH and ionic strength of the water can influence the process.

Bioaccumulation refers to the process in which microalgae actively accumulate toxins within their cellular structures, typically in the cytoplasm or organelles (Mustafa et al., 2021). This mechanism is vital for removing inorganic pollutants such as sulfates, nitrates, phosphates and organic pollutants such as pesticides. The capacity for bioaccumulation varies across different microalgae species, and research indicates that some species can accumulate higher concentrations of pollutants than others. Biodegradation involves the enzymatic breakdown of pollutants by microorganisms, including microalgae (Sutherland & Ralph, 2019; Xiong et al., 2017). Microalgae can release enzymes that degrade certain organic compounds, converting them into less harmful substances. This process is particularly effective for complex organic pollutants, though the efficiency of biodegradation can be influenced

by factors such as the type of microalgae and the environmental conditions. Recent studies have shown that different microalgae species exhibit varying effectiveness in these mechanisms (Mahlangu et al., 2024). For instance, some species are more efficient in the biosorption of heavy metals, while others are in the biodegradation of organic pollutants. Understanding these variations and the condition under each mechanism operates optimally is essential for improving bioremediation strategies.

2.3.3 First-Order Kinetics in Nutrient Removal by Microalgae

The first-order kinetics model is often applied to study the decay or removal of a substance in various fields such as chemistry, environmental science, and wastewater treatment. The first-order kinetic model can be applied to describe nutrient removal using microalgae. Nutrients, such as nitrogen and phosphorus, are essential for microalgae growth and metabolism. The first-order kinetic model helps to understand the rate at which microalgae consume these nutrients. In this model, the nutrient removal rate is assumed to be directly proportionate to the concentration of the nutrient present. Mathematically, it can be expressed as:

$$\frac{d[A]}{dt} = -k[A] \quad (2.2)$$

Where:

d[A]/dt is the rate of change of nutrient concentration over time,

[A] is the concentration of the nutrient,

k is the rate constant, which determines the reaction rate.

To integrate, rearrange and separate variables:

$$\frac{d[A]}{[A]} = -kdt \tag{2.3}$$

Now, integrate both sides:

$$\int_{[A]_O}^{[A]} \frac{d\,[A]}{[A]} = -\int_{t_o}^{t} k\,dt \tag{2.4}$$

$$\int_{[A]_O}^{[A]} \frac{1}{[A]}\,\mathrm{d}\,[A] = -\int_{t_o}^{t} k\,dt \tag{2.5}$$

This leads to:

$$\ln\,[A] = -kt + C \tag{2.6}$$

Exponentiate both sides to solve for [A]

$$[A] = e^{-kt+C} \tag{2.7}$$

Rewrite by combing the exponentials,

$$[A] = Ce^{-kt} \tag{2.8}$$

Here, C is constant by integration that depends on the initial conditions of the problem.

If assume the initial condition is $[A]_o$ at t=0, then C = $[A_o]$. Substituting this back into the equation and get

$$[A] = [A_O]e^{-kt} \tag{2.9}$$

Taking the natural algorithms of both sides:

$$\ln\,[A] = -kt + \ln[A]_0 \tag{2.10}$$

Integrating gives:

1) ln [A] represents the natural logarithm of the concentration of reactant A at any given time.

2) −kt represents the term derived from integrating the rate equation, characteristic of first-order kinetics.

3) ln [A_0] represents the natural logarithm of the initial concentration of reactant A.

This model suggests that the reaction rate depends on the reactant's concentration, and the rate constant (k) represents the proportionality factor. The negative sign indicates that the concentration decreases over time.

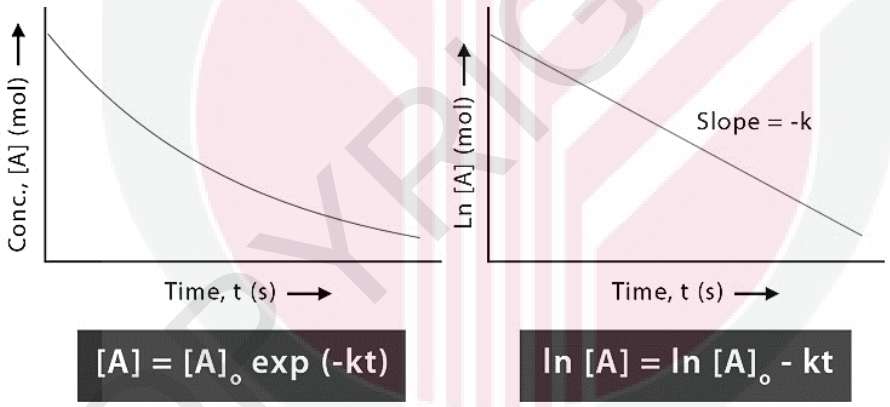

Figure 2.3 : First Order Kinetic Graph

As shown in Figure 2.3, by plotting ln([Nutrient]) against time, the slope of the line (-k) can be determined, which corresponds to the rate constant of the nutrient removal reaction. On the y-axis, plot the concentration of the reactant; on the x-axis, plot the time. The graph will typically show a decreasing curve over time. Since the first-order kinetics model is often associated with exponential decay, the graph will resemble an exponential decay curve. The

shape of the curve signifies that the concentration is decreasing at a rate proportional to its current value. The rate constant (k) determines the steepness of the curve. A higher k value results in a faster decrease in concentration. As time approaches infinity, the concentration will asymptotically approach zero. This behavior signifies that the reaction will never completely stop but will approach an infinitely small concentration. Using the first-order kinetic model provided complementary information about the bioremediation process (Sousa et al., 2021).

2.3.4 Composition of Microalgae Biomass by Physicochemical Analysis

Fourier Transform Infrared (FTIR) spectroscopy and Scanning Electron Microscopy (SEM) coupled with Energy-Dispersive X-ray Spectroscopy (EDS) are commonly used techniques to analyze the chemical composition and structural properties of microalgae biomass. These methods provide detailed information about the relative abundance of components, such as proteins, carbohydrates, and lipids, essential for various applications, including biofuel production and bioremediation. The composition of green microalgae biomass, which varies depending on species, growth conditions, and harvesting methods, plays a significant role in its application potential. For example, *Chlorella vulgaris* has protein contents ranging from 34 – 54% of proteins, with lipids accounting for 13%, and carbohydrates from 46 – 51%, depending on the cultivation conditions (Spain & Funk, 2022). These composition values are essential for evaluating the potential use of microalgae in biofuel production, as higher lipid content is desirable for biodiesel. At the

same time, elevated protein levels are useful for animal feed or biofertilizers.

FTIR spectra often reveal typical regions associated with carbohydrates (960−1180 cm^{-1}), proteins (amide II; 1475−1620 cm^{-1} and amide I; 1620−1710 cm^{-1}), and lipids (around 1740 cm^{-1}), as reported by Dean et al. (2010). The lipid fraction typically shows a weak absorption band, indicating minimal fatty acids in cell walls. However, during nitrogen limitation, an increase in lipid content up to 20 – 30 % has been observed, aligning with the findings from Dean et al. (2010). For example, FTIR analysis has revealed high concentrations of lipids in certain *Chlorella* strains when subjected to nutrient stress conditions (Duygu et al., 2012).

Furthermore, the chemical composition obtained through Energy-Dispersive X-ray Spectroscopy (EDX) has shown the elemental makeup of the microalgae biomass, particularly highlighting the presence of nitrogen, carbon, and oxygen, which are essential for understanding nutrient uptake and metabolic activity (Michalak et al., 2014). For example, a study by Kusumaningrum et al. (2018) reported that the EDX analysis of *Chlorella* sp. revealed the following mass percentages: carbon at 60.92%, nitrogen at 19.7%, oxygen at 5.45%, and sulfur at 1.42%. SEM-EDX analysis complements the data on biomass composition by revealing cell-wall integrity and structural robustness, which are essential for optimizing harvesting and processing methods.

2.3.5 Algal Bloom in Aquaculture

Algal blooms occur frequently in aquaculture and can significantly impact the marine and fresh environment (Wurtsbaugh et al., 2019). In aquaculture systems, nutrient-rich conditions can occur because of various factors, including excessive feeding, inadequate waste management, or the release of nutrients from fish waste. Algal blooms, whether toxic or not, can positively and negatively affect aquaculture systems. On one hand, the algal bloom can have significant consequences, leading to water quality deterioration within aquatic environments. When excessive algal growth occurs, it has a direct impact on the surrounding water. A significant effect is the depletion of dissolved oxygen levels during nighttime hours (Mohyedin et al., 2019). This oxygen depletion is particularly problematic for aquatic organisms, as they rely on oxygen in the water for respiration. When dissolved oxygen levels drop to insufficient levels, it can create a stressful and even life-threatening situation for fish, shellfish, and other aquatic life forms.

Moreover, reducing oxygen availability is not the only challenge aquatic organisms face during algal bloom; dense algal populations can also reduce water transparency. This reduction in water clarity occurs because the algae block sunlight from penetrating the water column. Sunlight is crucial for photosynthesis because, during photosynthesis, plants, algae, and some bacteria use a pigment called chlorophyll to capture the energy from sunlight (Ruban, 2015). When photosynthesis is slowed due to reduced light availability, oxygen depletion will happen as less oxygen is generated through this vital process. Thus, the combined effects of low dissolved oxygen and

reduced water clarity during algal blooms create a harmful environment for aquatic life.

Additionally, algal decay can lead to the release of organic matter and nutrients in the water bodies, which may contribute to eutrophication (Amorim & Moura, 2021). Eutrophication is when water bodies become excessively enriched with nutrients, particularly nitrogen and phosphorus. Besides, Amorim & Moura (2021) also reported that some algal species, particularly certain types of dinoflagellates and cyanobacteria, can form toxic blooms known as harmful algal blooms (HABs). These toxic algae can produce harmful toxins that can be detrimental or deadly to aquaculture species, such as fish, shellfish, and even human health through contaminated seafood consumption.

Nevertheless, not all blooms are detrimental since blooms are referred to as nuisance blooms that can discolor water, smell bad, and cause a bad taste in water or fish. Nuisance blooms are typically not harmful to people, pets, and livestock because they do not release toxins. Algal blooms can provide some aquaculture species with a natural and abundant food source. Certain species of algae are rich in nutrients. They can be a valuable part of the diet for filter-feeding organisms such as mollusks (oysters, clams) and some types of zooplankton, which are essential components of aquaculture systems (Huang et al., 2022; Silva et al., 2022). Besides, during the day, photosynthetic algae produce oxygen as a byproduct. This oxygen production can benefit fish and other aquatic organisms in the aquaculture system.

Proper nutrient inputs and water quality management are essential to prevent algal blooms in aquaculture. This may involve monitoring nutrient levels in the water, reducing feed inputs to the system, and maintaining a healthy balance of aquatic plants and animals. Physical or chemical treatments may sometimes be necessary to control algae growth. Additionally, there have been efforts to promote the use of alternative protein sources for fish and shrimp feed, such as insect meal and algae, which can reduce the need for excessive fertilizer use (Aragão et al., 2022; Ferrer Llagostera et al., 2019). Efforts are also being made to raise public awareness about the importance of maintaining healthy aquatic ecosystems and reducing human activities contributing to algal blooms.

2.4 Harvesting Technique of Microalgae Biomass

The harvesting of microalgae is the most challenging step in their cultivation and use due to their unique characteristics, such as low density, typically 0 – 5 g $L^{-1,}$ and small size, generally 1 – 30 µm in diameter (Molina Grima et al., 2003; Xu et al., 2021). Several techniques have been implemented, including centrifugation, flotation, filtration, and coagulation-flocculation (Abdul Hamid et al., 2014; Granados et al., 2012). Table 2.3 shows the advantages and disadvantages of various techniques for harvesting microalgae.

2.4.1 Centrifugation

Centrifugation is a separation technique that uses centrifugal force to separate materials suspended in a liquid, accelerating particles to settle faster (Najjar & Abu-Shamleh, 2020). It involves high-speed rotation to create forces up to a

million times greater than gravity, effectively separating particles from a solution. Different centrifuges, including multi-chamber, tubular, and decanter models, are used for microalgae separation (Gultom & Hu, 2013). Centrifugation effectively separates microalgae from their growth medium by causing the algae to settle at the bottom of the container. Research by Heasman et al. (2000) and Najjar & Abu-Shamleh (2020) found that higher centrifugation speeds can achieve microalgae recoveries of over 90%. Despite its effectiveness, centrifugation is energy-intensive and generally suited for smaller-scale operations.

2.4.2 Flotation

The flotation method is used for harvesting microalgae by leveraging gravity separation, where fine air bubbles attach to solids, causing them to float to the surface. This float is then skimmed off using a skimmer. Various flotation techniques exist, including dissolved air flotation (DAF), dispersed air flotation (DiAF), and electro-flotation (EF) (Xu et al., 2021). DAF involves dissolving air in water to create small bubbles (10 – 100 µm) that attach to flocculated solids, which then float to the surface for removal. This method is widely used for wastewater treatment and microalgae harvesting (Laamanen et al., 2016). DiAF introduces air via mechanical agitation or diffusers, producing larger bubbles (100 – 1000 µm) and is less energy-intensive than DAF but has limited use due to bubble size. ECF combines electrocoagulation with electro-flotation, generating gas bubbles through electrolysis. This method is energy-intensive and costly, mainly suitable for high-value products.

2.4.3 Filtration

Solid-liquid separation through filtration uses various types of membranes, including microfiltration (M-F), ultrafiltration (U-F), reverse osmosis (R-O), and nanofiltration (N-F) (Morais et al., 2023). These membranes act as filters, with their pore sizes determining their ability to remove dissolved solids, turbidity, and microorganisms. Substances larger than the membrane pores are fully removed, while smaller substances are partially filtered based on the membrane's fouling and construction. Materials used in these membranes include polyvinylidene fluoride (PVDF), polyether sulfone (PES), polyvinyl chloride (PVC), and poly-sulfone (PSF) found that membrane filtration effectively removes debris and microalgae cells, facilitating water recycling (Safarpour et al., 2021). Studies from Kanchanatip et al. (2016) have compared the performance of crossflow M-F and U-F membranes for separating marine microalgae species, *Haslea ostrearia* and *Skeletonema costatum.* Despite its effectiveness, membrane filtration faces challenges such as membrane fouling, which can be mitigated through optimization and developing new membranes. However, this technique remains costly and energy-intensive for large-scale applications.

2.4.4 Coagulation Flocculation

Flocculation is a gentle mixing process used to aggregate fine particles into larger flocs or flakes through natural processes or by adding flocculant agents. This technique often involves chemicals to neutralize the surface charge of microalgae cells, enhancing their size and facilitating sedimentation.

Flocculants are broadly categorised into three types: inorganic coagulants, organic coagulants and natural coagulants (Aljuboori et al., 2016) Inorganic coagulants, such as aluminium sulphate and poly-aluminium chloride (PAC), are commonly used in microalgae harvesting (Yan et al., 2019). These coagulants work by neutralizing the charges on microalgae cells, leading to their aggregation into larger clusters that can be easily separated from the water. Aluminium sulphate (alum) is cost-effective and widely available, though it can produce sludge that requires additional treatment and may leave residual aluminium in the treated water. PAC is a more efficient alternative to alum, requiring lower doses and performing well across a wide pH range, but it is more expensive and still poses concerns regarding aluminium residues. Organic coagulants, including polyacrylamide derivatives and melamine formaldehyde, are polymers that facilitate coagulation by binding microalgae cells together. Polyacrylamide derivatives are highly effective at low doses and produce less sludge, but they can be toxic if they degrade into harmful substances. Melamine formaldehyde is effective in forming stable flocs, though its production involves formaldehyde, raising environmental and health concerns.

Natural coagulants from biological sources offer a more environmentally friendly alternative. Chitosan is a biopolymer from crustacean shells that are biodegradable, non-toxic, and effective at low concentrations (Ahmad et al., 2011). However, it is relatively expensive, and water conditions can influence its performance. For example, Mohd Yunos et al. (2017) reported that chitosan extracted from shrimp successfully demonstrated its effectiveness in

coagulating green microalgae, *Chlorella* sp. Microbial or bio-flocculants, produced by microorganisms, are biodegradable and environmentally friendly, though their production can be inconsistent and challenging to scale. Each type of coagulant has its unique advantages and disadvantages, making them suitable for different applications depending on the specific needs of the microalgae harvesting process. Several studies have shown that bio-flocculants produced from microalgae such as *Ankistrodesmus* sp., and *Scenedesmus* sp. are particularly effective in water and wastewater treatment, as well as in harvesting other microalgae species, such as *Chlorella* sp. (Lananan et al., 2016; Salim et al., 2011).

Table 2.3 : Advantages and Disadvantages of Microalgae Harvesting Techniques

Harvesting Techniques	Advantages	Disadvantages	Reference
Centrifugation	- High efficiency for separating microalgae cells - Can achieve high recovery rates - Suitable for higher solid contents	- High energy consumption - Often limited to small-scale applications - Expensive operational costs - Can cause cell damage due to shear forces.	(Gultom & Hu, 2013; Heasman et al., 2000; Najjar & Abu-Shamleh, 2020)
Flotation	- Effective for large-scale applications - Can handle high-volume flows - Types of flotations; DAF, DiAF, ECF	- Less effective for small particles and high turbidity - High energy costs, especially for small bubbles - Limited information on economic feasibility	(Xu et al., 2021; Zhang & Zhang, 2019)
Filtration	- Simple and effective for larger microalgae. - Low energy consumption. - Effective for recycling water - Types of membranes; MF, UF, RO, NF	- Membrane fouling is a major issue - High cost and energy-intensive for large-scale operations - Limited by membrane pore size and fouling	(Morais et al., 2023)
Coagulation - Flocculation	- Simple and cost-effective - Types of coagulants; inorganic, organic, natural	- Inorganic coagulants can be toxic and cause environmental issues - Natural coagulants are less efficient - Potential for cell lysis and contamination	(Abdul Hamid et al., 2014; Mohd Yunos et al., 2017)

2.5 Filamentous Fungus

2.5.1 Application of Filamentous Fungus in Harvesting Process

Filamentous fungi from various genera are utilized in numerous industrial sectors, including traditional fermentation, pharmaceuticals, and food processing (Pel et al., 2007). In recent years, there has been a growing interest in utilizing *Aspergillus niger* as a flocculant for microalgae harvesting. The research on this field is gaining momentum and shows great promise as an emerging field of study (Jin et al., 2021; Wang et al., 2023). Despite studies exploring the use of *Aspergillus niger* for microalgae harvesting, the mechanisms behind the process and the ideal conditions remain largely unexplored.

Microalgae are unicellular photosynthetic microorganisms that have the potential to produce various valuable products in an environment-friendly manner, such as biofuels, nutraceuticals, and pharmaceuticals, making them a top choice. However, the harvesting of microalgae is often a challenging and costly process. Therefore, the potential of *Aspergillus niger* to flocculate and harvest the microalgae, as well as their flocculation mechanism, should be extensively investigated (Li et al., 2017). Furthermore, combining microalgae with fungi through co-cultivation could potentially enhance the value of microalgae as a source of energy crop (Xu et al., 2022).

Aspergillus sp. can be used to harvest microalgae by forming pellets that can settle down rapidly, leading to the aggregation of microalgae cells (Li et al., 2017). *Aspergillus* sp. is the coagulative type and in submerged culture, it can

develop either in spherical pellets, consisting of compact hyphal aggregation, or in filamentous form where hyphae are uniformly dispersed (Veiter et al., 2018). *Aspergillus* sp. can also produce a variety of extracellular enzymes, including proteases and amylases, which can break down the cell walls of microalgae and release intracellular contents (Hom-Diaz et al., 2016). This process results in microalgae flocculation, making it easier to separate them from the growth medium. Moreover, *Aspergillus niger* can produce polysaccharides, such as chitin and chitosan, which can be used as a natural coagulant to flocculate microalgae (Elieh-Ali-Komi et al., 2016). Chitosan is a biodegradable and non-toxic compound that is effective in harvesting microalgae.

The symbiotic relationship between microalgae and fungi has existed for over 600 million years, and this interaction has gained recent attention due to its potential applications in various biotechnological fields. Particularly, the use of *Aspergillus* sp. in microalgae harvesting has several advantages over conventional methods. This collaboration offers benefits not only in wastewater treatment but also in the creation of diverse compounds valuable to the food, cosmetic, and renewable energy sectors (Laezza et al., 2022).

Table 2.4 : Applications of *Aspergillus* sp. in Microalgae Harvesting

Fungus species	Microalgae species	Experimental Conditions	Findings	References
Aspergillus niger	*Chlorella* sp.	Optimum dosage at 30 mg L^{-1} (dry weight) with 125 rpm	Time: 72 hr Efficiency: 99%	(Nasir et al., 2015)
Aspergillus niger hsn26	*Chlorella* sp.	120 rpm, pH 8.0–9.0 with addition of 5 mM CaCl2 at room temperature	Time: 24hr Efficiency: >90	(Li et al., 2017)
Aspergillus niger	*Synechococcus subsalsus*	28 °C, 100 rpm, pH 6.0 with fungi:algae ratio of 1:5	Time: 48 hr Efficiency: 98%	(Oliveira et al., 2019)
Aspergillus fumigatus	*Chlorella pyrenoidosa*	38 °C, 100 rpm with fungi:algae ratio of 1:5	Time: 3 hr Efficiency: 99	(Bhattacharya et al., 2017)
	Chlorella protothecoides	25 °C, 150 rpm	Time: 24 hr Efficiency: 80%	(Muradov et al., 2015)
	Scenedesmus quadricauda	25 °C, 150 rpm	Time: 48 hr Efficiency: >95%	(Wrede et al., 2014)
Aspergillus oryzae	*Synechocystis* sp. PCC 6803	30 °C, 130 rpm, pH 7.4 with the fungi: algae ratio of 1:4.26	Time: 48 hr Efficiency: 90%	(Choi et al., 2016)
Aspergillus lentulus	*Chroococcus sp.*	30 °C, fungi: algae ratio of 1:3	Time: 6 hr Efficiency: >99%	(Prajapati et al., 2016)

2.5.2 Mechanism of Microalgae Harvesting Using Fungus

Recent research highlights that the microalgae-fungi interaction holds the potential for enhancing various aspects, including wastewater treatment, cultivation management, and the production of valuable compounds (Egede et al., 2016; Wang et al., 2014; Xu et al., 2022; Yang et al., 2019). Particularly, fungi are frequently employed in co-cultures due to their ability to induce the aggregation of microalgae, thereby enhancing their harvest efficiency without resorting to costly chemical flocculants. This symbiotic relationship between microalgae and fungi offers promising avenues for sustainable and economically viable applications. Therefore, it is essential to emphasize the mechanisms of interaction between fungi as bio-flocculant and microalgae since these interactions could offer potential benefits for both industrial and biotechnological applications.

Fungi display the potential to serve as bio-flocculants due to their inherent capacity for self-pelletization across various fungal strains. This characteristic can be utilized to improve the accumulation of algal biomass. The co-pelletization phenomenon arises from the distinct surface characteristics of microalgae and fungi (Laezza et al., 2022). Microalgae surfaces carry negatively charged functional groups such as phosphoric, phosphodiester, amine, hydroxyl, and proton-active carboxylic groups. Similarly, fungi also possess negatively surface-charged polysaccharides on their surfaces (Douglas et al., 1959; Veiter et al., 2018). Consequently, the surface charge cannot fully explain the mechanism of using fungi for microalgae harvesting.

Trapping green microalgae in fungal pellet hyphae during harvesting can be achieved through physical aggregation. The microalgae cells become entrapped within the developing fungal pellets. This can occur as the microalgae cells contact the growing hyphae and lead to the physical entrapment of microalgae within the fungal hyphae (as illustrated in Figure 2.4). The fine, branching structure of the hyphae acts as a physical net that captures and holds the microalgae cells. In this environment, microalgae aggregate and become segregated from the surrounding liquid, facilitating their recovery.

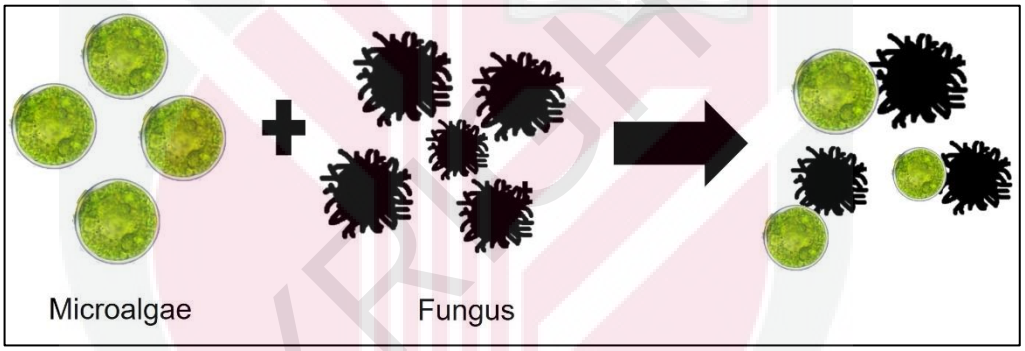

Figure 2.4 : Illustration of Microalgae Entrapped in Hyphae of Filamentous Fungus
(Source: Laezza et al. 2022)

The mechanism for harvesting green microalgae can also be discussed in the biotechnology field. However, ongoing research in the biotechnology field is needed to develop various strategies for harvesting green microalgae using enzymes produced by filamentous fungi or other microorganisms. For instance, lectins, which are proteins capable of binding to specific carbohydrate structures on the surface of microalgae, can be produced by filamentous fungi. These lectins recognize the carbohydrate molecules on the

microalgae's surface, creating a system where the fungi attract the microalgae (Roopashri & Savitha, 2022; Singh et al., 2015).

In a study conducted by Li et al. (2017), it was confirmed that surface protein plays a pivotal role in the flocculation mechanism between mycelial pellets and algal cells. Furthermore, the study demonstrated that adding calcium to algal cultures as coagulants can significantly enhance flocculation efficiency. This mechanism involves calcium binding to the surfaces of both mycelial pellets and algal cells, effectively establishing a bridge that connects this particle. The calcium bridging mechanism is the primary force responsible for the aggregation and flocculation of mycelial pellets onto algal cells. In addition to calcium bridging, hydrophobic interactions also assist in this process, further promoting the adhesion and aggregation of mycelial pellets onto algal cells. Together, these mechanisms create the conditions for effective flocculation, which can have important applications in various fields, including wastewater treatment and biotechnology. In addition, filamentous fungi can facilitate biofilm formation by producing extracellular polymeric substances (EPS) (Nowak et al., 2023). This biofilm formation is a vital substrate for microalgae to attach and thrive, particularly in wastewater treatment and bioremediation applications.

2.6 Response Surface Methodology (RSM)

Response surface methodology (RSM) is a commonly used mathematical and statistical method for modelling and analyzing a process in which a variable affects the response of interest (Braimah et al., 2016). RSM is a statistical

approach to understanding the relationship between various parameters and the desired outcome. It can be applied in various fields, including harvesting. It can be used to optimize the harvesting process by analyzing the effects of multiple independent variables on a single response, such as the biomass yield of microalgae. The use of RSM in microalgae harvesting is a promising and powerful tool for optimizing the process to achieve the highest yield (Kalil et al., 2000). The parameters that affect the process are called dependent variables, while the responses are called dependent (Yolmeh & Jafari, 2017). The RSM approach consists of three steps: design of experiments, analysis of variance (ANOVA), and response surface optimization. The experiment design helps determine the range of values for the independent variables and the number of experiments needed to cover the range adequately. ANOVA determines the effects of each independent variable on the response. Finally, response surface optimization is used to identify the optimal combination of parameters that can be used to achieve the highest yield.

RSM has been widely used to optimize the process of harvesting microalgae and improve flocculation efficiency. Recently, Hadiyanto et al. (2022) reported that *Chlorella* sp. was harvested using chitosan as a bio-coagulant using RSM with a central composite design (CCD). The flocculation efficiency was achieved at 96.12 %, and biomass recovery was 312.5 when the optimum condition was pH 8, chitosan concentration was 100 g/100 mL, and cationic inducer was 50 mg L^{-1}. In another study reported by Kim et al. (2013), optimisation of harvesting conditions by varying concentrations of $FeCl_3$, the bio flocculant, and the slow mixing optimal for flocculation of *Botryococcus*

braunii. The most favourable parameters from the equation were 0.79 mM of $FeCl_3$, 0.58% (v/v) of bio flocculant, and 180 seconds of slow mixing for a concentration of 1.1 g DCW L^{-1} of *B. braunii.* When these conditions were applied, the flocculation efficiency reached 90.6%. This study used response surface methodology (RSM) to achieve optimal flocculation conditions for *B. braunii* more rapidly and effectively.

Furthermore, RSM has optimized process parameters such as pH, temperature, light, agitation, and nutrient levels. The method has been applied to different microalgae species, such as *Chlorella vulgaris* and *Nannochloropsis salina*, to optimise the biomass yield (Bajwa et al., 2019). The results obtained with RSM have been successful in achieving higher yields than those obtained by traditional cultivation techniques. In addition to biomass optimisation, RSM has also been successfully applied using different bio flocculants for optimisation of experimental design of microalgae such as *Bacillus* sp. and chitosan; the application of RSM in harvesting microalgae using filamentous fungus has not yet been reported. To our knowledge, although the application of filamentous fungus in harvesting has been reported by Li et al. (2017) and Nazari et al. (2020), the experiment involves the OFAT. Therefore, this study focuses on applying RSM to optimize microalgae harvesting using filamentous fungus. RSM is crucial for systematically analyzing how various factors, such as bio-flocculant dosage, pH, and mixing rate, can affect harvesting efficiency. RSM identifies optimal conditions that maximize microalgae recovery and minimize resource use. This approach enhances the overall efficiency and sustainability of the bioremediation

process. It offers a more refined method than traditional single-factor approaches and supports the development of a more effective and economical harvesting strategy.

2.7 Machine Learning

Machine learning (ML) is an artificial intelligence (AI) technique that combines computer science, data science, and statistics to enable computers to learn (Witten et al., 2017). Moreover, ML also allows the software to improve the accuracy of predicting outcomes and use historical data as input to predict new output values (Ning et al., 2022). Machine learning allows computers to recognize patterns in data, both expected and unexpected, rather than putting data and algorithms into a computer to produce a specific result.

2.7.1 Machine Learning Techniques

Therefore, ML can potentially revolutionize wastewater treatment in aquaculture by enabling more efficient and effective wastewater management. For example, several studies about machine learning applications for aquaculture systems have included the prediction of water quality parameters, optimal nutrient management, and monitoring and treatment processes (Li et al., 2022; Zhao et al., 2021). Additionally, by leveraging the power of machine learning, the aquaculture industry can improve the efficiency and sustainability of its operations and produce high-quality aquatic products (Sundui et al., 2021).

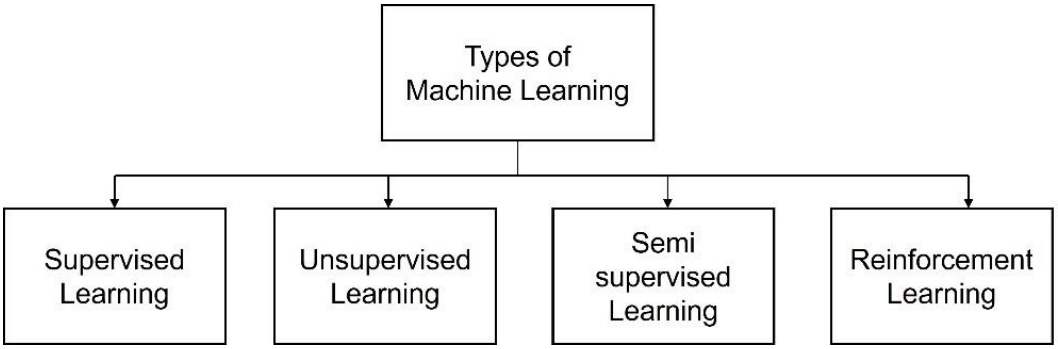

Figure 2.5 : Types of Algorithms in Machine Learning
(Source: Zhao et al., 2021)

Figure 2.5 shows the four main types of techniques in machine learning: supervised learning, unsupervised learning, semi-supervised learning, and reinforced learning (Mahesh, 2018; Ning et al., 2022). Supervised learning is a type of machine learning that involves training a model to make predictions based on labeled data (Ghiassi & Lee, 2018). The data for training the model includes input data and the corresponding output or target data. Supervised learning aims to learn how to map between input and output variables. The algorithm is trained on a dataset where both the features and labels are known, and the goal is to learn a function that can make accurate predictions on new data. In unsupervised learning, the data used for training the model is unlabeled, meaning no corresponding target data (Isaac Abiodun et al., 2018). Unsupervised learning aims to identify patterns and relationships in the data and group similar data points together. Unsupervised learning is often used for clustering, anomaly detection, and dimensionality reduction tasks. Semi-supervised learning is the learning method combining supervised learning with unsupervised learning. This method can combine classification, regression, and clustering.

Unsupervised learning is a machine learning approach where the algorithm learns patterns and structures in the data without any labeled specific target variables. The goal is to discover hidden patterns, relationships, or structures within the data. On the other hand, semi-supervised learning is a combination of supervised and unsupervised learning techniques. In this approach, a small portion of labeled data is used alongside a larger amount of unlabeled data to train the algorithm. Semi-supervised learning can be beneficial when acquiring labeled data is expensive, time-consuming, or impractical. It allows for leveraging the vast amounts of unlabeled data available to guide the learning process and enhance the model's performance. This approach can be applied to various tasks, including classification, regression, and clustering, depending on the problem.

In summary, unsupervised learning identifies patterns and relationships in unlabeled data. In contrast, semi-supervised learning combines labeled and unlabeled data to improve learning accuracy and efficiency in various machine learning tasks. Lastly, reinforcement learning includes teaching a model to make decisions depending on information from the outside world. The model learns by interacting with the environment and receiving rewards or penalties for its actions. The goal of reinforcement learning is to discover a policy or set of actions to maximize the cumulative reward over time.

2.7.2 Machine Learning Process

Each type of machine learning has its strengths and weaknesses, and the choice of algorithm will depend on the specific application and available data.

Machine learning uses algorithms and statistical models to analyze large amounts of data and identify patterns, relationships, and trends. The process involves several steps: data collection, preprocessing, model training, model evaluation, model deployment, and model retraining (Gupta, 2021). Data collection is the first step in machine learning is to collect and prepare the data that will be used to train the algorithm. This may involve gathering data from sensors, databases, or other sources. Data preprocessing is used when the data has been collected, and it needs to be cleaned and pre-processed to remove any noise or errors that may affect the algorithm's accuracy.

A typical complete machine learning process comprises three main phases: training, cross-validation, and testing (Oruganti et al., 2023). The following step in this process is model training, where the machine learning model is trained using pre-processed data. The appropriate algorithm is chosen during this phase, and its parameters are fine-tuned to attain optimal performance. In the cross-validation phase, a separate validation dataset is utilized to fine-tune the model's hyperparameters and identify the best-performing model. Hyperparameter tuning helps explore the best solution efficiently with fewer computational resources and in less time. Once the optimal model is selected, it is tested in the testing phase using a separate dataset to measure its performance. After successful testing, the developed and optimized ML model is ready for prediction and can be used in practical applications (Guo et al., 2021). ML is well-known for its high prediction accuracy and its ability to save time and resources by reducing the need for repeated tests, especially in complex non-linear domains (Singh & Mishra, 2022). Furthermore, machine

learning algorithms enable the quick analysis of large datasets, allowing the identification of optimal predictor variable combinations and significant patterns. This capability empowers researchers to explore and leverage the valuable insights hidden within large and complex datasets.

This review provides a comprehensive perspective on utilizing Machine Learning Algorithms (MLAs) in microalgae research and development. Machine learning techniques have shown potential in diverse areas of wastewater treatment. Specifically, they have proven successful in water quality monitoring, prediction, and process optimization, providing valuable contributions to this field. Table 2.5 offers an overview of machine learning applications related to water quality parameters in wastewater. Furthermore, Table 2.6 summarizes the application of machine learning techniques in the context of flocculation and harvesting processes. While numerous studies have explored water treatment and harvesting, none have successfully presented a mathematical model for algae-fungus interactions. This comprehensive review offers diverse ML applications in wastewater treatment, specifically emphasizing water quality parameters, bioremediation, and the flocculation/harvesting process.

Table 2.5 : Applications of Machine Learning in Water Quality Monitoring and Wastewater Treatment

Machine Learning Software		Classifiers/Algorithms	Application	References
WEKA Software	-	J48, LMT, Random Forest, Hoeffding tree and Decision Stump	Analysis of water quality data from different counties in Kenya and classification/prediction of clean and non-clean water.	(Gakii & Jepkoech, 2019)
MATLAB	-	Back Propagation Neural Network (BPNN), Radial Basis Function Neural Network (RBFNN), Support Vector Machine (SVM), Least Squares Support Vector Machine (LSSVM)	Simulate and predict water quality factors involving dissolved oxygen (DO), pH, ammonium-nitrogen (NH_3-N), nitrate nitrogen (NO_3-N), and nitrite-nitrogen (NO_2-N).	(Li et al., 2022)
	-	Quantile Regression Neural Network	Optimized nutrient removal.	(Icke et al., 2020)
	-	Bayesian Optimization Algorithms (Gaussian Process Regression (GPR)) and Random Forest Algorithms	Predicting the uncertain performance of treatment processes reducing pollution and promoting circular economy.	(Sundui et al., 2021)
	-	Genetic Algorithm (GA)	Predicting the behaviour and optimizing the treatment of sulphate-containing wastewaters with Bromophenol blue dye using an electro-oxidation (EO) process	(Picos-Benítez et al., 2020)
		Support Vector Machine, Genetic Algorithms, Decision Trees and Random Forest Algorithms	Discuss the potential application of ML/AI in integrated microalgal wastewater treatment and resource recovery	(Oruganti et al., 2023)

Table 2.5 : Continued

Machine Learning Software	Classifiers/Algorithms	Application	References
	Decision Tree	Assess the impacts and identify the optimal combination of predictor variables. These variables include microalgae class, pre-cultivation stage deciding factors, and operating variables.	(Singh & Mishra, 2021)
R software (R Studio)	- Multiple Linear Regression	Treatment of fourteen types of wastewater from fruit and vegetable processing (fruit, root vegetables, leafy greens)	(Mundi et al., 2021)
TensorFlow	Deep Learning Technique	Classify the group of microalgae between the same taxonomic group and the image extracted from the particle analyzer.	(Correa et al., 2017)

Table 2.6 : Applications of Machine Learning in Flocculation/Harvesting

Machine Learning Software	Classifiers/Algorithms	Application	References
MATLAB® 2019a software	Bayesian regularization model	Harvest the freshwater microalgae and predict complex processes	(Suparmaniam et al., 2022)
	Deep Neural Network Machine Learning Algorithm	Maximize the biomass production and improve duckweed yields for large-scale applications which incorporate regular harvesting	(Calicioglu et al., 2021)
	Neural network architectures of multilayer perceptron (MLP) and radial basis function	Evaluate and predict the flocculation modelling performance under different affective parameters for harvesting and dewatering microalgae	(Zenooz et al., 2017)
Phyton and NCSS-PASS software version 20.0	Random Forest (RF), Decision Tree (DT), Support Vector Machine (SVM), And Polynomial Regression Model (PM).	Assess the viability of using the machine learning (ML) algorithm and time-evolution kinetics to fulfill the design specifications of the treatment unit.	(Ugonabo et al., 2022)

2.7.3 Waikato Environmental Knowledge Analysis (WEKA)

WEKA stands for Waikato Environment for Knowledge Analysis, named after a bird native to New Zealand. WEKA is a research-based and open-source software developed by the University of Waikato in New Zealand and released in 1997 (Witten et al., 2017). WEKA provides a graphical user interface for working with data, including tools for data preprocessing, classification, regression, clustering, association rules, and visualization. It also supports various file formats for input and output, including *CSV, ARFF, and XML*. Weka is written in Java and is cross-platform, meaning it can be used on Windows, Mac OS X, and Linux. One of the advantages of WEKA is that it is easy to use and does not require extensive programming experience. It is widely used in academic and research settings and in the industry for fraud detection, customer segmentation, and predictive maintenance tasks. This software is used to develop predictive models that can be used to analyze data sets and create models (Merlini & Rossini, 2021).

Using WEKA, researchers can build predictive models that can help identify patterns and relationships in data (Ismail et al., 2013). Potential applications of WEKA for this study can be used to optimize wastewater treatment processes and improve the efficiency and effectiveness of aquaculture operations for various environmental applications, including bioremediation processes. Besides, researchers and practitioners can understand how bioremediation processes work and how they can be applied to different environmental conditions. For example, researchers could use WEKA to analyze data on water quality parameters such as nutrients (ammonia and

nitrite level) and pH and predict how changes in these parameters will impact the health and growth of aquatic species. This information can then be used to optimize wastewater treatment processes, reducing the amounts of harmful compounds in the water and ensuring the health and well-being of the species being raised.

Additionally, WEKA serves as a powerful data mining tool for wastewater treatment by enabling the analysis and interpretation of data to identify patterns and trends. It helps develop models to optimize treatment system performance, focusing on microbe technology and microbial communities. The WEKA tool is open source, easy to use, and works on any platform, improving efficiency and cost savings (Song et al., 2023). The WEKA tool was chosen for this study because it is open source, simple to get off the internet, and written in Java code that works on any platform (Ismail et al., 2013). Another potential application of WEKA for this study is used in microalgae harvesting. This data could include factors such as the concentration and type of bio flocculant and the density of the microalgae culture. WEKA built a predictive model to help optimize the microalgae harvesting process. For example, WEKA could be used to analyze the relationship between the concentration of bio flocculant and the agitation rate to determine the optimal concentration for maximum harvesting efficiency. WEKA can be a valuable tool for optimizing the use of bio flocculants in microalgae harvesting, helping to improve the efficiency and sustainability of this important process.

2.7.4 Algorithms in WEKA

WEKA is an open-source data mining software that offers a variety of machine-learning algorithms for tasks such as data classification, regression, clustering, and association rule mining (Song et al., 2023; Witten et al., 2017). Among the common algorithms available in WEKA are Linear Regression, Decision Trees, M5P, Support Vector Machines (SVM), and Multilayer Perceptron (MLP) (Dou & Meng, 2023). Linear Regression models are the relationship between a dependent variable and one or more independent variables by fitting a linear equation to observed data. It is used for predicting continuous output variables and is valued for its simplicity and interpretability, which helps understand relationships between variables. Decision Trees, including algorithms, M5P, J48, Random Tree, and REPTree, predict the value of a target variable by splitting the data into subsets based on input variables. They are easy to visualize and interpret, effectively handling numerical and categorical data.

M5P is a decision tree algorithm that incorporates linear regression models at the leaves of the tree, making it particularly useful for continuous output variables (Dong et al., 2022). M5P handles large datasets well and generates simple linear models that capture complex relationships in the data. Support Vector Machines (SVM) are supervised learning models for classification and regression tasks. They work by finding the hyperplane that best separates the data into classes. They are powerful for high-dimensional spaces but are computationally expensive and require careful parameter tuning.

Multilayer Perceptron (MLP), a type of artificial neural network (ANN) with input, hidden, and output layers, can model complex non-linear relationships between inputs and outputs (Windarti & Prasetyaninrum, 2020). MLPs are flexible and capable of capturing intricate patterns but demand significant. However, it is computationally intensive and requires careful data preprocessing to avoid overfitting. Random Forest is an ensemble learning method that constructs multiple decision trees during training and outputs the mean prediction for regression tasks or the mode of the classes for classification tasks. It improves prediction accuracy by reducing overfitting, making it robust and reliable for various data types.

In summary, WEKA provides a range of machine-learning algorithms suited for different tasks. For this study, the M5P algorithm was chosen to develop a user-friendly graphical interface (GUI) for algae profiling due to its high accuracy and ability to generate simple yet effective linear models for predicting bio-harvesting outcomes (Song et al., 2023).

2.8 Summary

The rapid development of shrimp aquaculture in Malaysia has led to significant wastewater challenges characterized by high nutrient loads. *Chlorella* sp. is highlighted for its potential in wastewater treatment due to its bioremediation capabilities. Traditional microalgae bio-harvesting methods, such as centrifugation and coagulation-flocculation, are compared to using *Aspergillus niger* for more sustainable harvesting. Optimization techniques such as Response Surface Methodology (RSM) and machine learning (ML) are

explored to improve efficiency. Research gaps include optimizing nutrient removal, assessing the sustainability of fungal bio-harvesting, and integrating ML with RSM for better predictions. This study aims to address these gaps by optimizing shrimp wastewater treatment and enhancing bio-harvesting using *Aspergillus niger* by combining RSM and ML.

CHAPTER 3

GENERAL METHODOLOGY

3.1 Introduction

This chapter aims to discuss the general research design throughout the study, which includes developing a bioremediation process to reduce the excess nutrients in water bodies, harvesting the microalgae biomass using bio-flocculant fungus as a low-cost alternative method, and using machine learning to optimize and improve the performance of the culture system. Figure 3.1 illustrates the flowchart that summarizes the general study design and provides an overview of the steps involved in the study.

This chapter begins by outlining the fundamentals of microalgae collection and cultivation conditions. It was determined how much microalgae would affect bioremediation. Second, this chapter explains the basic procedures for cultivating filamentous fungi, preparation for bio-flocculant production and harvesting techniques. Third, using machine learning tools through data processing and model building, Waikato Environment Knowledge Analysis is investigated to improve the bioremediation and harvesting process. After a model was developed, testing analysis was conducted to optimize the algorithm and validate the model.

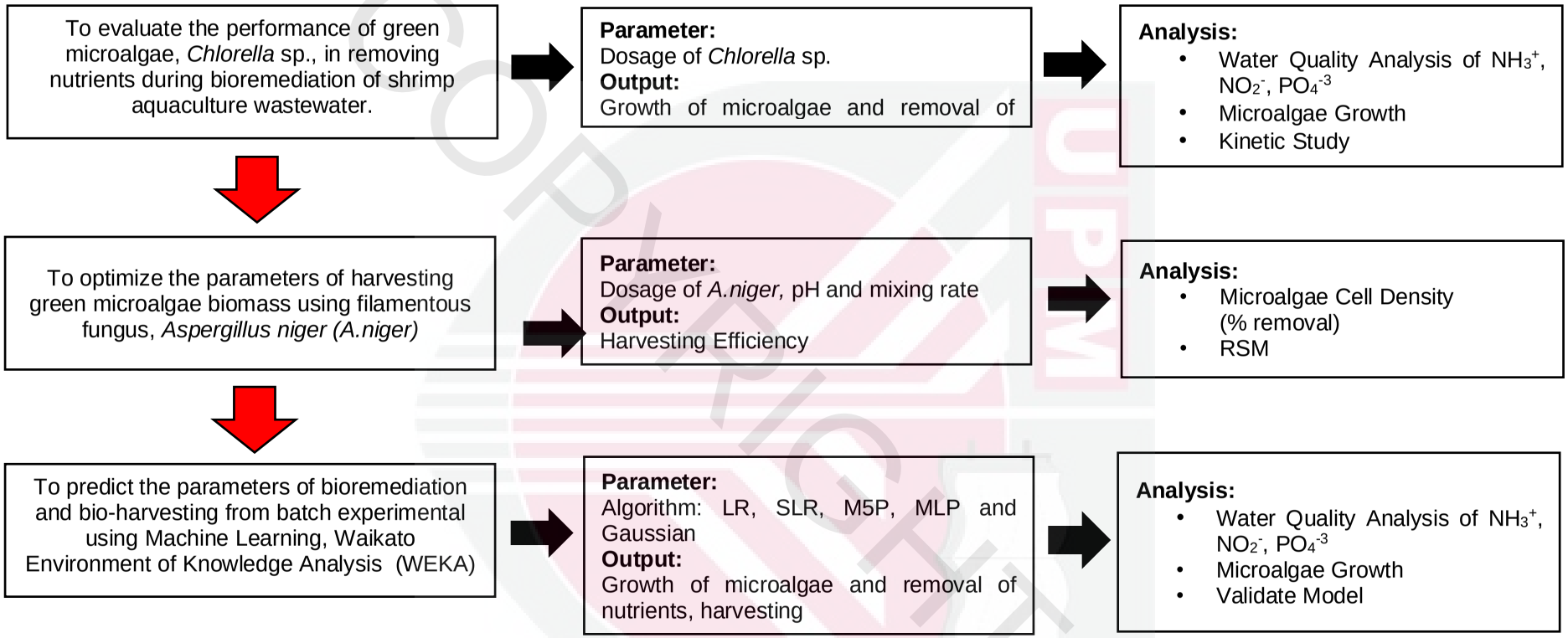

Figure 3.1 : Detailed Flowchart for Overall Study

3.2 Microalgae Cultivation

3.2.1 Microalgae Collection

In this study, microalgae were sampled at the hatchery and in tanks containing two different species: *Litopenaeus vannamei* (*L. vannamei*) for marine water species and *Macrobrachium rosenbergii* (*M. rosenbergii*) for freshwater species. A plankton net with a mesh size of 35 µm, mouth diameter of 25 cm, and a length of approximately 1.5 m was employed to collect the samples. The sampling process involved submerging the net into the water to a depth of 1.5 meters below the surface. In situ, water was sprayed on the net before collecting the water samples, helping to ensure that the samples were representative of the surrounding water. At the end of the net, a sampling bottle was attached to collect the water samples. In addition to collecting microalgae samples, the physicochemical parameters of the water were also measured using a portable instrument, Multiparameter YSI Professional Plus (YSI, Xylem Inc., USA). This instrument can measure various parameters, including pH, dissolved oxygen (DO), temperature (°C), conductivity (µs cm^{-1}), total dissolved solids (TDS), and salinity (ppt). These measurements provide valuable information about the water quality and environmental conditions where the microalgae grew.

Figure 3.2 illustrates the general process of microalgae cultivation and isolation. To promote the growth of the algae, the collected sample is enriched for 7 days using Guillard's F/2 Media for marine microalgae and Bold's Basal Media (BBM) for freshwater microalgae. Following the enrichment phase, 50

mL of the cultured microalgae are centrifuged at 3000 rpm for 15 minutes to concentrate the biomass. The cell pellet is resuspended in a fresh medium, and the supernatant is carefully discarded. This centrifugation process is repeated multiple times to remove a significant proportion of the unwanted microorganisms present in the sample. The concentrated microalgae cells are streaked onto agar plates using a sterile loop, ensuring the maintenance of sterile conditions to prevent contamination. The plates are then incubated for at least 7 days, allowing the microalgae to grow and form visible colonies on the agar surface. Multiple rounds of streak-plating are performed to isolate single species, progressively selecting single colonies from previous streaked plates. The isolated microalgae cultures are incubated under continuous illumination at a constant temperature of 20 ± 2 °C, with sterilized filtered air continuously aerated into the cultures to maintain a stable environment for upscaling.

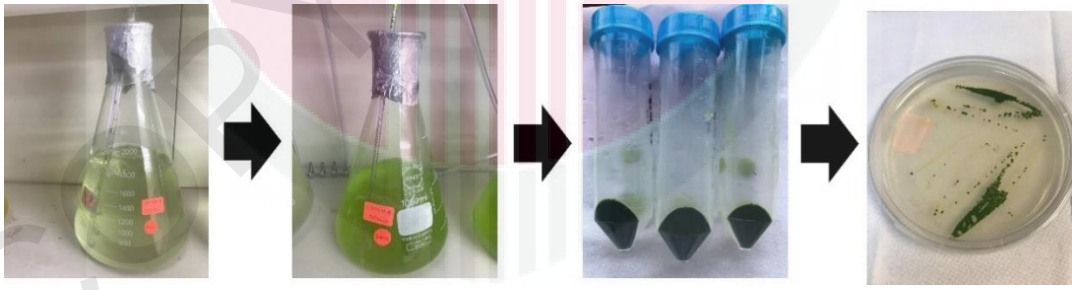

Figure 3.2 : General Steps in Microalgae Cultivation and Isolation

3.2.2 Microalgae Biomass Determination

In this study, three different methods were employed to determine the growth of microalgae cells: cell count analysis, absorbance measurement, and dry weight analysis, as described by Ratomski & Hawrot-Paw (2021), Schagerl et

al. (2022) and Thiviyanathan et al. (2023). A Neubauer hemocytometer was used for cell count analysis. This device allows for the manual counting of microalgae cells under a microscope. A known volume of the microalgae culture was loaded onto the hemocytometer, and the cells were counted within the grid lines of the device. The cell count provides quantitative information about the abundance of microalgae cells in the culture. Absorbance was measured using a UV/VIS spectrophotometer (Shimadzu UV-1800, Japan). The culture was measured at an optical density of 680 nm, corresponding to the absorption peak of microalgae pigments. The absorbance measurement indicates the biomass density in the culture based on the light absorption by the microalgae cells.

Appendix A indicates that the dry weight analysis involved filtering 10 mL of the microalgae culture through Whatman GF/C filter paper (Cellulose nitrate). These filters are known for their ability to retain fine particles. The microalgae biomass filters were then rinsed with 0.5 M ammonium formate to remove excess salts from the culture media. After rinsing, the filters were dried at 95 °C overnight to remove moisture and reweighed. The difference in weight before and after drying represents the dry weight of the microalgae biomass on the filter. This method measures biomass concentration in milligrams per liter (mg L^{-1}).

3.3 Bioremediation Process Using Green Microalgae

Subsequent sections provide details on the experimental setup, data collection methodologies, and the application of the first-order kinetics model to

thoroughly comprehend the microalgae's specific growth rate.

3.3.1 Aquaculture Wastewater Collection

Aquaculture wastewater was collected from the hatchery ponds of two different species: *Litopenaeus vannamei (L. vannamei)* for marine water bioremediation (MW) and *Macrobrachium rosenbergii (M. rosenbergii)* for freshwater bioremediation (FW) at Universiti Malaysia Terengganu (UMT), Malaysia. The wastewater was filtered to remove any suspended solids and microorganisms. The filtered wastewater was then autoclaved for sterilization for 20 minutes at a temperature of 121°C. This sterilization step was essential to eliminate any potential contaminants and ensure that the samples used in the bioremediation process were free from unwanted microorganisms. The main objective was to preserve the vital nutrients in the wastewater from any processes, such as nitrification and denitrification. This ensures a controlled environment in the bioremediation process without interference from unwanted microorganisms.

By preparing filtered sterile wastewater through autoclaving, the researchers aimed to maintain the original nutrient content while preventing any further changes in nutrient composition that could occur through microbial processes such as nitrification. This ensured the stability of the wastewater composition during the bioremediation process and allowed for the accurate evaluation of the effectiveness of microalgae in removing nutrients from the aquaculture wastewater.

3.3.2 Experimental Design for Bioremediation Process

The present study aimed to investigate the uptake of nutrients, including ammonia, nitrite, and orthophosphate, during batch bioremediation of aquaculture wastewater under sterile conditions. The focus was on utilizing aquaculture wastewater as a nutrient source for microalgae cultivation while concurrently reducing nutrient levels in the wastewater (Khatoon et al., 2016). Green microalgae, *Chlorella* sp., was used as a bioremediation agent for the bioremediation process. *Chlorella* sp. was cultured in 2 L until the early exponential growth phase, from Day 4 to Day 6 of the cultivation period. Figure 3.3 illustrates that the batch bioremediation process was carried out with seven different inoculation dosages: 0%, 10%, 20%, 30%, 40%, 50%, and 60% (v/v), as outlined in Nasir et al. (2015).

Before inoculation with *Chlorella* sp., the initial concentrations of NH_3-N (ammonia), NO_2^- (nitrite), and PO_4^{3-} (orthophosphate) in the marine aquaculture wastewater (MW) were approximately 2.80 ± 0.11 mg L^{-1}, 1.53 ± 0.08 mg L^{-1}, and 4.10 ± 0.05 mg L^{-1}, respectively. The initial concentrations for freshwater aquaculture wastewater (FW) were approximately 3.66 ± 0.75 mg L^{-1} for NH_3-N, 1.75 ± 0.04 mg L^{-1} for NO_2^-, and 3.46 ± 0.11 mg L^{-1} for PO_4^{3-}. Each treatment was carried out in triplicates for a 14-day treatment period. Throughout the treatment process, the growth performance of microalgae and water quality analysis were monitored every 2 days. The growth performance was measured by determining cell concentration (cell mL^{-1}) and the water quality analysis by determining nutrient removal (mg L^{-1}).

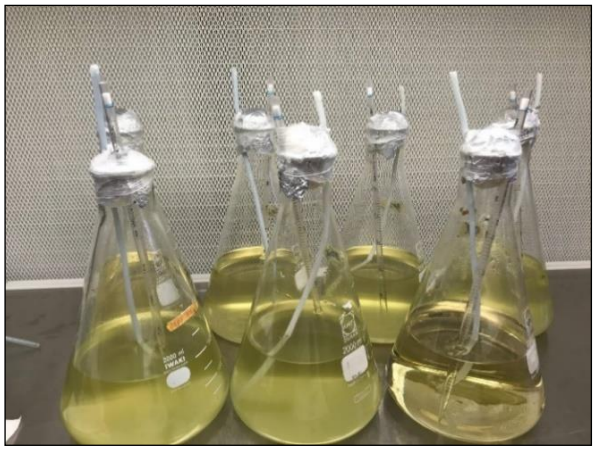

Figure 3.3 : An Erlenmeyer Flask Containing Aquaculture Wastewater at Day 0 Bioremediation Process

3.3.3 Kinetic Model of Wastewater Treatment

The first-order kinetic model describes the nutrient reduction process during the treatment of ammonia, nitrite, and orthophosphate in shrimp aquaculture wastewater using microalgae. The equations derived in Chapter 2 (Equations 2.2 – 2.10) are used to model the reduction of these nutrients based on the assumption that their uptake by microalgae follows first-order kinetic (Wang et al., 2014). Equation 2.2 characterizes the rate at which microalgae dosages remove each nutrient from the wastewater.

In this study, the natural logarithm of the nutrient concentration (ln [A]) was plotted against time (t) using Excel. The resulting linear relationship and a high R^2 value confirmed that the nutrient reduction follows first-order kinetics. In many scientific disciplines, an R^2 value above 0.70 or 0.80 is considered good, indicating that a significant portion of the variance in the dependent variable is explained by the independent variables in the regression model (Ozili, 2022). The best-fit line equation, obtained through Excel's trendline feature,

corresponds to the linearized form of the first-order kinetic equation ($\ln [A] = -kt + \ln [A_0]$). This empirical equation was then exponentiated to match Equation 2.9, ensuring consistency with the theoretical model and accurately representing the bioremediation process.

3.3.4 Water Quality Analysis for Nutrient Removal

The water samples were collected every two days to analyze the selected water quality parameters, namely ammonia (NH_3), nitrite-N (NO_2^-), and orthophosphate-P (PO_4^+) for determining the nutrient removal. The removal efficiency in percentage was determined by using the following Equation 3.3:

$$RE\ (\%) = \frac{C_O\ (mg\ L^{-1}) - C_i (mg\ L^{-1})}{C_O (mg\ L^{-1})} \times 100 \qquad (3.3)$$

Where:

RE is Removal Efficiency (%)

C_O is the Initial Concentration (mg L^{-1})

C_i is the Final Concentration (mg L^{-1})

The concentrations of these parameters were determined using the Standard Methods for the Examination of Water and Wastewater. These methods were adopted from the American Public Health Association (APHA) guidelines published in 2012. The Ammonia nitrogen content (NH_3) was determined using the Phenate Method (Method No. 4500-NH_3-F). This method involves the reaction of ammonia with phenol and hypochlorite, forming a colored compound that can be quantified spectrophotometrically. The concentration of

ammonia in the water samples was measured based on the intensity of the color produced. Nitrite (NO_2-) was determined using the Colorimetric Method (Method No. 4500-NO_2-B). This method relies on the reaction between nitrite and a reagent, such as a sulfanilamide and N-(1-naphthyl) ethylenediamine dihydrochloride, to form a colored azo dye. The nitrite concentration in the water samples was measured by spectrophotometrically analyzing the intensity of the color produced. Orthophosphate (PO_4^{3-}) was determined using the Ascorbic Acid Method (Method No. 4500-P-E). This method involves the reaction of orthophosphate with a mixture of molybdate and ascorbic acid, forming a blue-colored phosphomolybdate complex. The concentration of orthophosphate in the water samples was determined by measuring the intensity of the blue color using a spectrophotometer. To ensure accurate analysis, the water samples were filtered using a 0.45 µm cellulose acetate microfilter before performing the measurements. These filtration steps help remove any particulate matter or larger organisms that may interfere with the water quality analysis.

3.4 Harvesting Process Using Filamentous Fungus

3.4.1 Filamentous Fungus Collection and Identification

The filamentous fungus, *Aspergillus niger* (*A. niger*), was isolated from an aquaculture rearing tank at the shrimp hatchery of Universiti Malaysia Terengganu, Malaysia. Strict aseptic techniques were employed to ensure sterility and prevent contamination during isolation. The work area and all instruments were thoroughly sterilized before use, and samples were

transferred under a laminar flow hood to minimize the risk of airborne contaminants.

The isolation process began by transferring 0.5 mL of the water sample containing *A. niger* to a sterile Petri dish containing potato dextrose agar (PDA). PDA was chosen based on the study by Bahiram et al. (2020), which identified it as an optimal growth medium for fungi. The inoculated plates were then incubated at a controlled temperature of 27 ± 2 °C using a Memmert INE 200 incubator (Germany) to promote fungal growth. Once the fungus had propagated, *A. niger* was isolated from the mother plate to obtain a monospecific colony. The identification of *A. niger* was confirmed through careful observation of its morphological characteristics, including its distinctive black conidia, globose conidiophores, and vesicles, as well as the presence of spores, all of which are consistent with known descriptions of the species (Figure 3.4).

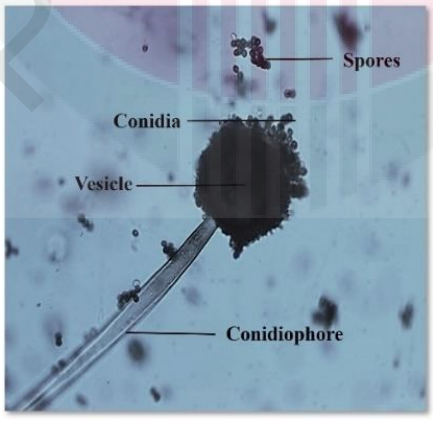

Figure 3.4 : Microscopic Image under the Magnification (400x), *Aspergillus niger*

3.4.2 Bio-Flocculant Production

Bio-flocculant from *Aspergillus niger* was carried out using submerged fermentation purposes (Nazari et al., 2021). Figure 3.5 depicts the steps involved in growing fungus in liquid culture and cultivating it to form fungal pellets. The process begins with preparing fungal cultures on Potato Dextrose Agar (PDA) plates to promote sporulation (Image 1). Once sporulation is achieved, the surface of the PDA plate is flooded with sterile Richard's Broth (RB) medium, and the sporulated aerial mycelium is scraped using a loop to collect the spores (Image 2). The flask is then placed in an incubator shaker (Lab Companion SI-600, Korea) (Image 3) and incubated for 72 hours at 37°C with a constant shaker speed of 125 rpm, ensuring consistent agitation throughout the cultivation period to achieve a sufficient biomass concentration. The spores are then transferred into a 250 mL Erlenmeyer flask containing 150 mL of RB growth medium.

The Richard's Broth is prepared according to the detailed method provided in Appendix C, using distilled water and specific concentrations of nutrients before being sterilized by autoclaving at 121°C for 20 minutes (Image 4). After three days of incubation, uniformly sized soft sphere pellets are formed (Image 5), which can then be harvested using filtration (Image 6). The shaker speed remained constant throughout the cultivation period to ensure a sufficient biomass concentration to facilitate the agglomeration of the suspended microalgae biomass. After a cultivation period of three days, the emergence of uniformly sized soft sphere pellets was observed, as depicted in Figure 3.5. The methodology employed for the pellet formation was derived from a study

conducted by Nasir et al. (2015).

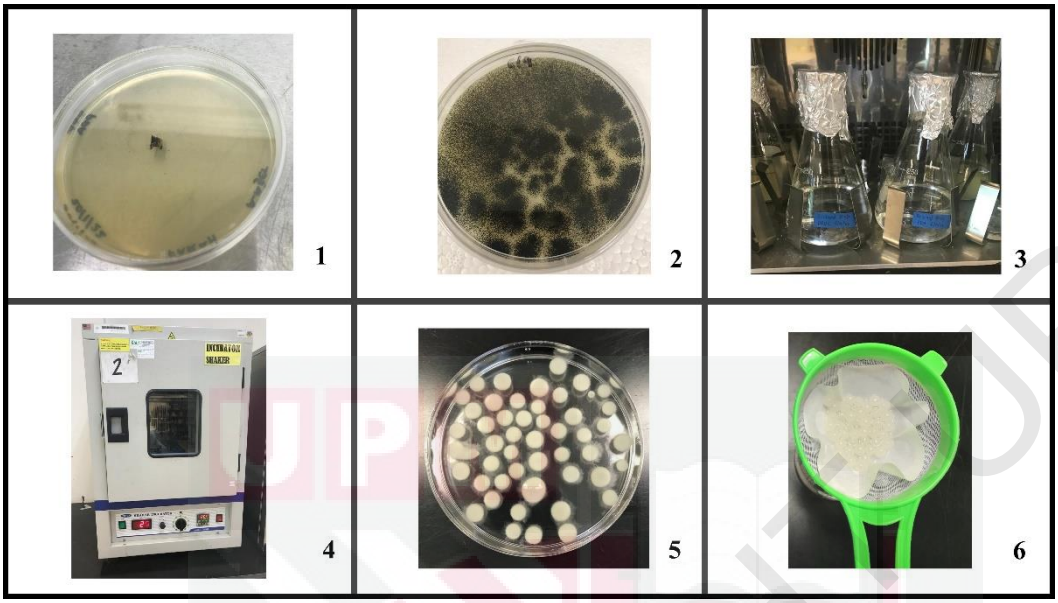

Figure 3.5 : Cultivation of Fungus Pellet

3.4.3 Experimental Design for Harvesting Process

The harvesting process involves a two-step approach. First, fungal pellets are cultured as wet bio-flocculant, then introduced into the microalgae liquid. Response Surface Methodology (RSM) was employed to optimize this process to study the interactions of various factors influencing microalgae biomass harvesting, using data extracted from a previous One-Factor-at-a-Time (OFAT) study. The OFAT study identified the optimal conditions for each factor, which were then used as central points in the Central Composite Design (CCD) for further evaluation. Based on the previous study, the three central points chosen were the dosage of bio-flocculant (25 g L^{-1}, 30 g L^{-1}, and 35 g L^{-1}), pH (pH 6, pH 7, and pH 8) and mixing rate (100 rpm, 125 rpm, and 150 rpm) (Mohd Nasir et al., 2019; Nasir et al., 2015). These experiments were conducted using 150 mL of microalgae culture.

The central points were selected and applied in RSM based on optimal conditions identified in the OFAT study. The pH of the medium was adjusted using 1M HCl and 1M NaOH, and then the wet fungal biomass was added. An incubator shaker (Lab Companion SI-600, Korea) was used to mix at a temperature of 27 °C, with a harvesting period of 3 days. The samples were collected on Day 0 as the initial concentration and Day 3 as the final concentration to determine the *Chlorella* sp. biomass concentration. The performance of the harvesting process was determined through harvesting efficiency by Equation 3.4.

$$HE\ (\%) = \frac{C_O\ (abs) - C_i\ (abs)}{C_O\ (abs)} \times 100 \qquad (3.4)$$

Where:

HE is harvesting efficiency,

C_O is the initial concentration at wavelength 680 nm,

C_i is the final concentration at wavelength 680 nm.

3.5 Profiling Process Using WEKA

WEKA is used in this study to offer an extensive set of machine learning algorithms and tools for pre-processing data that will be useful to researchers in the future. The complete machine learning procedure in this work, which uses WEKA, is depicted in Figure 3.6. The path shown covers the entire experiment from start to finish.

Figure 3.6 : Machine Learning Framework of the Study

3.5.1 Dataset Collection

The study utilized two datasets corresponding to different phases in the bioremediation and bio-harvesting processes. The bioremediation phase focused on optimizing the treatment of aquaculture effluent using microalgae, which served as the foundation, followed by the bio-harvesting phase, where a fungus producing bio flocculant was introduced to enhance the harvesting efficiency of the microalgae. Secondary data from prior experiments and studies focusing on water quality parameters and microalgae cell density during treatment were used throughout both processes. The data preprocessing before feeding it into WEKA involved several critical steps to ensure the datasets were clean, consistent, and ready for analysis.

3.5.2 Monte Carlo Simulation (MCS)

The data generation process in this study utilized the Monte Carlo method (MCM), a statistical technique for generating numerical results. The initial dataset was expanded to enhance its size and diversity before being fed into WEKA for machine-learning tasks. This approach improves model performance by learning robust patterns and making predictions on new data.

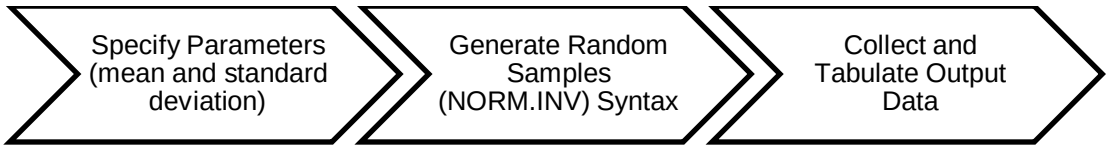

Figure 3.7 : Procedure of Monte Carlo Simulation

Based on Figure 3.7, in the Monte Carlo simulation process, the initial step involves specifying the parameters such as mean and standard deviation for a normal distribution. Subsequently, random samples are generated using syntax tools in Monte Carlo Simulation in Microsoft Excel's RAND() function, and these values are input into the model (Equation 3.5).

=NORM.INV(RAND(), mean, standard deviation) (3.5)

Monte Carlo simulation is particularly advantageous for this study since it relates to bioremediation and bioharvesting, which commonly deal with limited data. Due to the complexity and variability of biological processes, limited data is common. Yi et al. (2019) similarly encounter challenges in numerical modeling, such as the requirements of large amounts of data and time-consuming input construction. Therefore, Monte Carlo simulation allows researchers to generate additional data points, creating a more comprehensive dataset for analysis.

3.5.3 Machine Learning of WEKA

In both studies, WEKA software version 3.8.6 was used. When the software is opened, the graphical user interface (GUI) chooser displays a window that allows the user to choose the type of interface they want to use—Explorer,

Knowledge Flow, Experimenter, Workbench, or Simple CLI (Figure 3.8). The main interface is Explorer, a WEKA data mining software tool that allows users to explore datasets interactively and experiment with different machine learning algorithms.

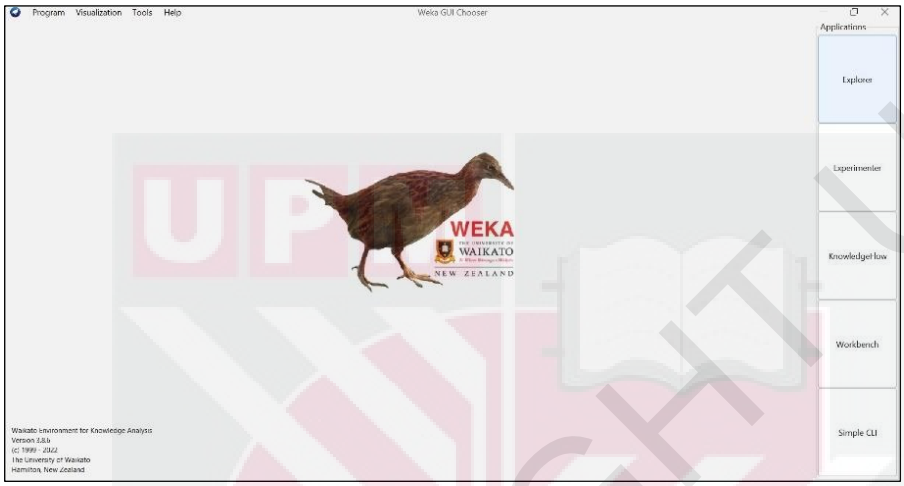

Figure 3.8 : WEKA: GUI Chooser

The flowchart in Figure 3.9 visually represents the steps in accessing the WEKA Interface Explorer. It systematically outlines the process, beginning with the WEKA GUI Chooser's opening, then selecting the "Explorer" option, leading to the subsequent opening of the Interface Explorer. The flowchart then guides the user through loading a dataset by selecting the "Open File" button. Various classification algorithms were employed to analyze the data and create predictive models for these processes. The model was validated by comparing its predictions with actual experimental results. This validation process involved assessing the accuracy and reliability of the model in predicting the outcomes of bioremediation and bio-harvesting. The validation process results demonstrated that the developed model in WEKA could

predict and optimize the bioremediation and bio-harvesting processes. The model's predictions closely matched the experimental results, indicating its reliability and usefulness in these applications.

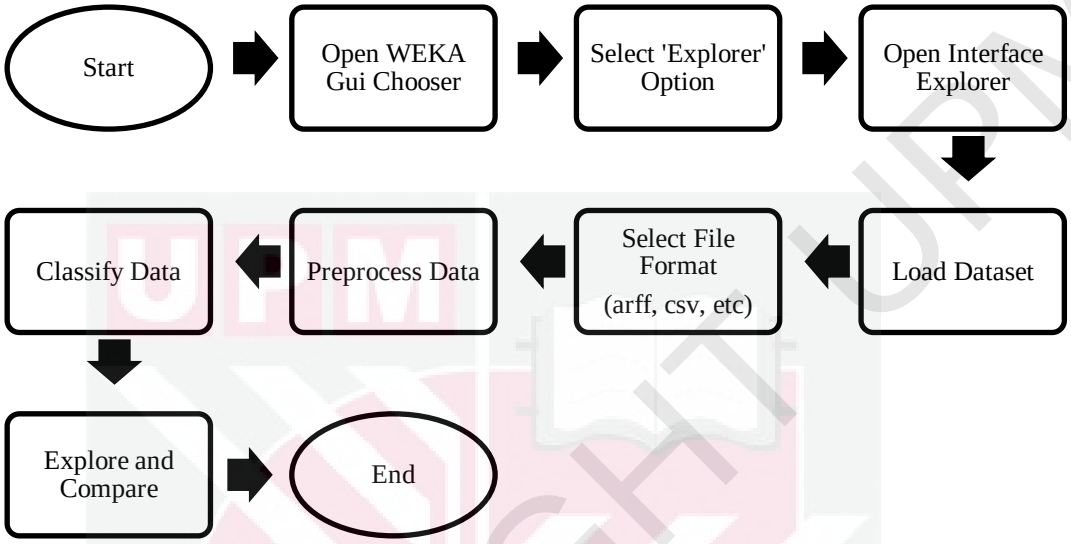

Figure 3.9 : Visual Representation of the Steps in Accessing the Interface Explorer in WEKA

3.5.3.1 Data Preprocessing

The data pre-processing is required to divide the dataset into the training and testing sets. This study split the data into 80% for training and 20% for testing. Figure 3.10 illustrates an example of pre-processed data for bioremediation analysis using the WEKA software. After loading the dataset into WEKA, the software provides a detailed data summary. The dataset includes two attributes: Dosage and ammonia, which represent the dosage applied during treatment and the corresponding ammonia concentration. The dataset comprises 120 instances, indicating 120 data points, each with dosage and ammonia concentration values. On the right side of the figure, WEKA

generates various statistical summaries for each attribute. For example, the Dosage attribute has a minimum value of 10, a maximum of 60, a mean of 35, and a standard deviation of 17.15. Similarly, the Ammonia attribute would have its statistical values, though not shown in this figure.

These statistics are essential as they provide insights into the distribution and variability of the data. For instance, knowing the range (minimum and maximum) helps understand the span of values. At the same time, the mean and standard deviation give a sense of the central tendency and spread of the data, respectively. The histogram at the bottom of the right panel visually represents the distribution of the Ammonia attribute, helping to assess how the data is spread across different values quickly. This preprocessing step ensures that the data is well-understood and prepared for further analysis or modeling within the WEKA environment.

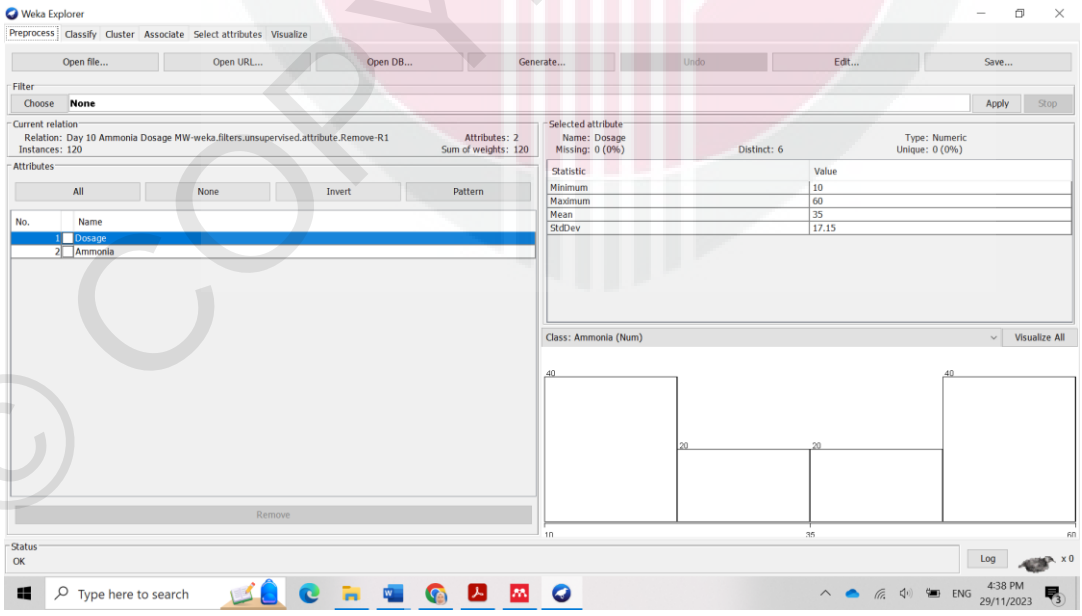

Figure 3.10 : Preprocess Procedure in WEKA

3.5.3.2 Model Training and Evaluation

Figure 3.11 presents a list of algorithms divided into two groups: Functions and Trees. The Functions category includes algorithms such as linear regression, simple linear regression, and SMOReg. On the other hand, the Trees category comprises algorithms such as M5P, Random Forest, and Random Trees.

Figure 3.11 : Algorithms Used to Train the Dataset

These algorithms were used to train the dataset in this study, with the selection of the optimal machine learning model based on key performance metrics such as Correlation Coefficient (CC), Mean Absolute Error (MAE), and Root Mean Squared Error (RMSE). Before choosing the most suitable model, factors such as CC, MAE, and RMSE were carefully considered. MAE measures the average absolute difference between the predicted values and the actual values given by Equation 6.1. To put it differently, the Mean Absolute Error (MAE) and correlation coefficient (R_2) were employed as evaluation metrics to assess the selected data obtained from the machine learning predictions. The MAE represents the average size of the prediction errors, regardless of their positive or negative direction. On the other hand, R_2 quantifies the strength of the linear relationship between the predicted and actual values. These metrics were utilized to gauge the accuracy and performance of the machine learning

predictions on the selected data. RMSE measures the difference between a dataset's predicted and actual values in terms of the square of the difference between them (determined by Equation 6.2).

$$MAE = \frac{1}{n}\sum_{1}^{n}(\text{Actual Output Value - Predicted Output Value}) \quad (6.1)$$

$$RMSE = \sqrt{\frac{1}{n}\sum_{1}^{n}(\text{Actual Output Value - Predicted Output Value})^2} \quad (6.2)$$

Where: n is the number of testing data

The algorithm model will be compared using a 10-fold cross-validation method. Cross-validation is a statistical technique used to assess the performance of a predictive model and select the best model among a set of models (Yates et al., 2023). It helps prevent overfitting by estimating the model's true performance on unseen data. It is particularly useful when the dataset is small and there is a risk of overfitting.

3.6 Statistical Analysis

All the data were recorded in Microsoft Office Excel™, and all the experiments in this study were performed in triplicate. The results were expressed as mean ± deviation. Graphical analyses were performed using OriginLab (OriginPro 2022b™). All statistical analyses were performed using the software SPSS (IBM SPSS Statistics, version 22). The mean values were compared using the Tukey HSD test and correlation with a confidence level of 95% ($p \leq 0.05$). A one-way ANOVA was initially performed to check for significant differences in

microalgae growth and removal efficiency across different dosages in the bioremediation process. Before this, normality was tested using the Kolmogorov-Smirnov test for larger samples (50 or more) and the Shapiro-Wilk test for smaller samples (Mishra et al., 2019).

In the second phase of this study, Response Surface Methodology (RSM) was used to optimize the harvesting process of *Chlorella* sp. The experimental data were analyzed using Design Expert 13.0 software, with a quadratic equation modelling the relationship between variables. Multiple regression analysis and ANOVA were conducted to identify significant variables, which were then used to determine optimal conditions. Three-dimensional analysis helped visualise and interpret the relationships between variables and responses. For the last objective, WEKA software was used to create a data profile, evaluate the model's performance using metrics such as the correlation coefficient (R^2), mean absolute error (MAE), and root mean square error (RMSE), and validate the results obtained from the RSM model.

CHAPTER 4

UTILIZATION OF GREEN MICROALGAE, *Chlorella* sp. IN AQUACULTURE WASTEWATER BIOREMEDIATION

4.1 Introduction

Aquaculture is a significant source of animal protein and contributes to the world's food supply. By 2030, aquaculture production is expected to reach 93 million tons, an increase of 15% from 87 million tons in 2020 (FAO, 2022). According to the forecast, India, Latin America, the Caribbean, and Southeast Asia would grow the most. Therefore, the rapid development and growth of the intensive aquaculture industry requires continuous supervision to avoid deleterious environmental effects. Organic matter and nitrogenous chemicals (ammonia, nitrite, and nitrate), phosphorus, and dissolved organic carbon are typically discharged by the aquaculture industry. The presence of untreated nutrients in wastewater can have significant environmental consequences, including eutrophication and the degradation of natural coastal ecosystems. Several conventional methods for treating aquaculture wastewater, such as chemical coagulation, flocculation, and physical filtration, are unsustainable due to their environmental and health risks, particularly the production of toxic sludge. This sludge contains concentrated pollutants that require costly disposal and can lead to secondary pollution, contaminating soil and water sources. The de-nitrification process, which converts nitrogenous compounds into nitrogen gas, is commonly used among these methods. However, it also generates toxic sludge, contributing to the same environmental and health concerns (Ni et al., 2017). These issues highlight the need for more

environmentally friendly and cost-effective wastewater treatment options, such as bioremediation using microalgae. This offers a sustainable alternative by detoxifying wastewater without generating harmful by-products.

Nevertheless, this approach lacks environmental sustainability as it generates toxic sludge as a by-product that will risk human health. Implementing effective wastewater treatment methods to control pollution and minimize adverse environmental effects is imperative before discharging the wastewater into the water bodies. This study aims to balance maintaining the aquaculture industry's growth and preserving the environment. Bioremediation is a new environment-friendly method that uses green plants to bio-remediate toxins in wastewater. Recent research has identified microalgae as a possible alternative for wastewater bioremediation (Do et al., 2022; Singhal et al., 2021). Bioremediation is the process of removing pollutants from the environment by using plants. In bioremediation treatment, microalgae play a crucial role by effectively removing nitrogen and phosphorus from wastewater. They achieve this by utilizing nutrients in the water for their growth, eliminating the need for chemical additives or additional mixing procedures. This natural approach offers a cost-effective solution for wastewater treatment, as it avoids the expenses associated with chemicals and mechanical mixing requirements (Lananan et al., 2014).

Wastewater from disposable aquaculture produces eutrophication, an overabundance of nutrients in the water body that causes the algae blooms. Treating wastewater with microalgae in optimal conditions can avoid these

negative environmental effects. However, the major challenge is to ensure the optimal design and operation of the system for wastewater treatment, and it is crucial to have an adequate understanding of the kinetics of microalgae development in wastewater. Enhancing and employing the system requires a thorough understanding of the mechanism of algae growth, nutrient usage, and the development of kinetic models to predict biomass growth. Current kinetic models for microalgae-based wastewater treatment have some gaps. They often do not accurately predict how well nutrients are removed or how much biomass is produced under different conditions. This study addresses these gaps by improving model accuracy for various conditions, capturing microalgae responses more accurately, and integrating multiple factors. Understanding kinetic studies is crucial for scaling from small bioreactors to full-scale systems, developing effective photobioreactors, and predicting process performance and optimal operational parameters. Researchers and scientists can use these mathematical models to estimate and forecast algae growth rates under different substrate concentrations. This information is valuable in optimizing culture conditions and understanding the dynamics of algal growth to improve efficiency in various applications, such as wastewater treatment or algae-based biofuel production (Aslan & Kapdan, 2006; Tang et al., 2011; Yao et al., 2011).

Algae need a growth medium, light for photosynthesis, and a water source to grow. The growing media must contain major inorganic elements such as nitrogen, phosphorus, iron and sulphur. Wastewater would fulfil two needs for algae growth and can be used as a water source and a growing medium.

Therefore, this study aims to develop a kinetic model to describe microalgae growth in wastewater when it is limited by more than one substrate, namely inorganic nitrogen (ammonia and nitrite) or phosphorus (orthophosphate). As a result, the model would predict that growing microalgae and treating wastewater would be a combined nutrient-removal process. The model will be calibrated with a satisfactory predictive error and verified using experimental data from microalgae cultivations in aquaculture wastewater. The model development is crucial in predicting the microalgae cultivation performance in aquaculture wastewater (Shoener et al., 2019).

On the other hand, the microalgae strain should also be grown healthy under controlling factors to effectively recover nutrients from wastewater (Madkour et al., 2020). Accordingly, this study also focused on characterizing the effect of bioremediation on both the physical and chemical surface properties of microalgae. Therefore, findings from this study would be meaningful in evaluating the microalgae's growth and capability to remove nutrients from various aquaculture wastewater. Microalgae-based technologies present a possible alternative for treating aquaculture wastewater. Figure 4.1 illustrates the steps in Objective 1 for obtaining the optimum removal of nutrients (ammonia, nitrite and orthophosphate) using microalgae during bioremediation.

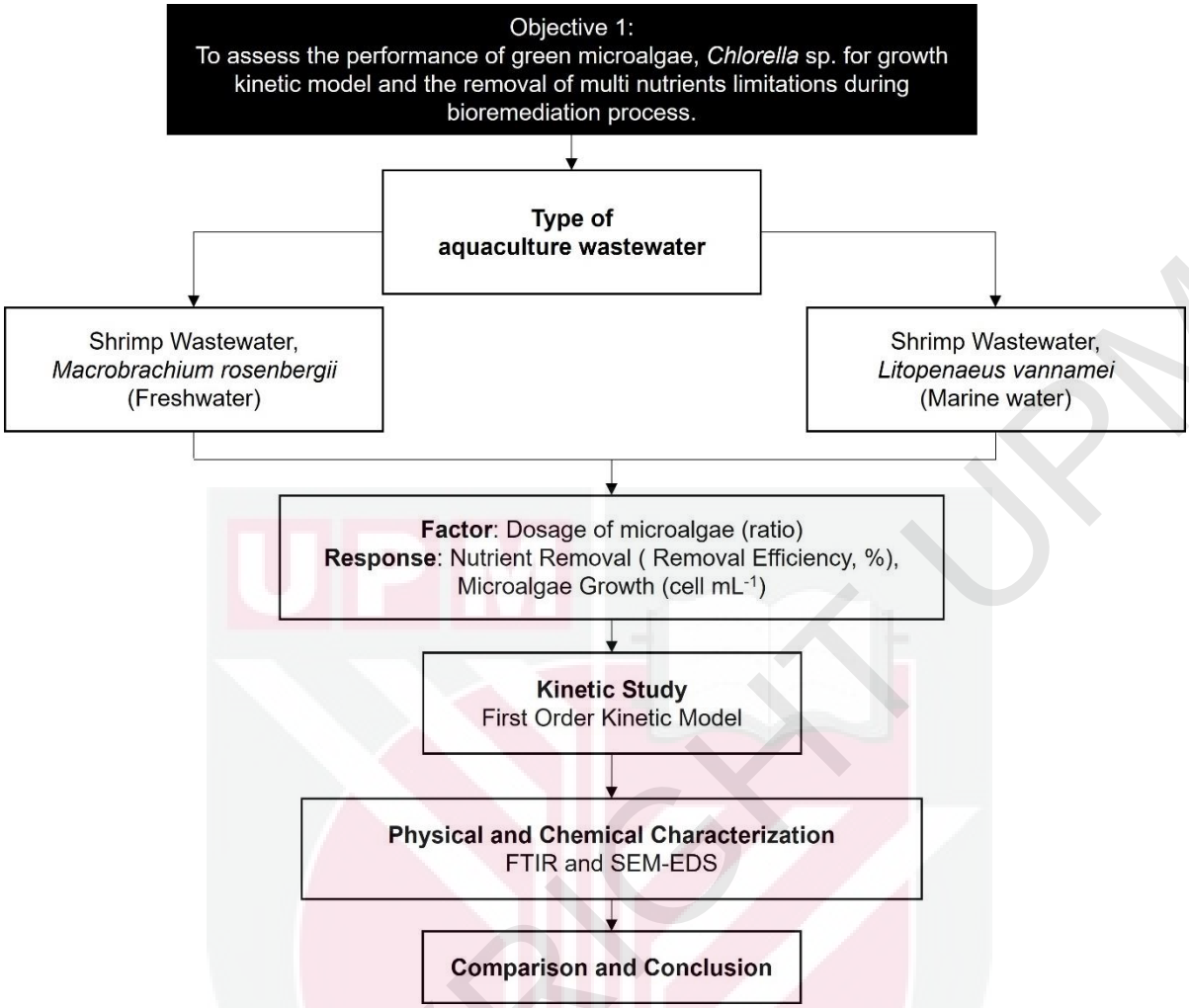

Figure 4.1 : Flowchart of an Experiment Conducted for Bioremediation Process Using *Chlorella* sp. for Shrimp Wastewater Treatment

4.2 Methodology

4.2.1 Microalgae Isolation and Identification

The study focused on isolation techniques for obtaining single-cell microalgae species from water samples collected from the shrimp culture tank, AKUATROP, UMT. Four major techniques were considered: streaking, spraying, serial dilution, and single-cell isolations. For this study, streaking and serial dilution were selected as the methods for isolation. Standard streak plate techniques were used to separate different algal populations, while serial

dilution involved diluting the sample multiple times. The algae were then grown separately in Guillard's F/2 and Bold's Basal Medium (BBM) to ensure successful cultivation. The inoculated plates were sealed, placed under controlled temperature and illumination, and streaked onto additional nutrient media plates for subculture. Isolated algae were collected and maintained as stock cultures, replating onto new nutrient media at least once a month.

The green microalgae, *Chlorella* sp., were successfully isolated and subsequently incubated under specific conditions. The cultures were maintained at a constant temperature of 20 ± 2 °C and kept at a pH of 6.9 ± 2. Continuous illumination was provided to ensure a consistent light source for the algae's growth and metabolic processes. These controlled environmental conditions were crucial for promoting the optimal growth and development of the *Chlorella* sp. microalgae. The microalgae were cultivated in sterile seawater enriched with Guillard's F/2 Media for marine water species and deionized water with Bold's Basal Medium (BBM) for freshwater species. The number of microalgae cells was counted every two days under light microscopy using Neubauer Haemocytomer and measured spectrophotometrically at optical density, OD_{680} nm using a Dual-Beam UV-Vis Spectrophotometer (Shimadzu UV-1800, Japan). The specific growth rates (μ) of microalgae were determined during the exponential growth phase by Equation 4.1 (Kholssi et al., 2023; Miao et al., 2012).

$$\mu=[\frac{\ln N_2 - \ln N_1}{t_2 - t_1}] \quad (4.1)$$

Where:

μ is the specific growth rate, and

N_1 and N_2 are the biomass at time 1 (t_1) and time 2 (t_2)

Two classification methods are used for identification in this study: morphological (based on physical characteristics) and molecular (based on genetic information). These approaches complement each other and accurately identify different species of microalgae (Wang et al., 2016). However, identification through morphology was the general method used in classification. Microalgae cultures were initially separated for identification based on morphological examination of the colonies on an agar nutrient medium. For morphological examination, the single cells were viewed at two magnifications (10x and 40x) using the Nikon Eclipse E800 microscope (Nikon Inc., Tokyo, Japan). Image comparison between the new isolates and the stock cultures was performed regularly to ensure no contamination.

Figure 4.2 : Microalgae Culture on Petri Dish

As shown in Figure 4.2, the single cells were isolated and cultured in media to facilitate molecular identification, promoting microalgae growth. The cultures were harvested using an Eppendorf 5702 Variable Speed Multi-Purpose Centrifuge during the exponential growth phase. The centrifugation involved spinning the samples at 6000 rpm for 10 minutes, which separated microalgae biomass from the culture medium supernatant. The biomass settled at the bottom of the tubes while the supernatant was discarded. To preserve the microalgae biomass for molecular identification, it was treated with 95% ethanol. This preservation step helps maintain the biomass's integrity and facilitates subsequent DNA analysis. The preserved microalgae biomass was then sent to GeneSeq Sdn. Bhd. for Polymerase Chain Reaction (PCR) amplification of Deoxyribonucleic Acid (DNA) sequences.

By amplifying specific regions of the microalgae DNA, PCR allows for comparing obtained sequences with known sequences in databases, aiding in identifying and characterising the microalgae species. The PCR process involves three main steps: denaturation, annealing, and extension. During denaturation, the double-stranded DNA template is heated to a high temperature (typically around 95 °C) to separate the two strands. The PCR was carried out using WizBio HotStart 2x Mastermix (WizBio, Korea) using the PCR condition of 95 °C for 3 minutes followed by 35 cycles of 95 °C for 20s, 50 °C for 20s and 72 °C for 120s. The PCR products were visualized on gel and purified using SPRI Bead, followed by index PCR using the EXP-PBC001 kit (Oxford Nanopore, UK) (Oberacker et al., 2019). The barcoded libraries were pooled based on band intensity and size selected using 0.5X vol SPRI

magnetic beads to remove fragments smaller than 500 bp. Quantifying the pooled barcoded amplicons was performed using Denovix High Sensitivity, and an appropriate amount (~200 fmol) of the amplicons was used as input for LSK110 library preparation (Oxford Nanopore, UK). Sequencing was performed on a Nanopore Flongle Flowcell for 24 hours.

Compare the sequence to a database of known microalgal sequences to identify the species. Basecalling and demultiplexing (assigning reads to their respective samples) of the raw nanopore read was done using Guppy v5.0.7 "super accuracy mode." Primer sequences (non-biological sequences) were cut from the raw reads, followed by read length filtering (1000 bp < N < 2000 bp) using cut adapt v4.0.1 (Martin, 2011). The filtered reads were then processed using NanoClust, which performs clustering of reads based on the K-mer abundance profile and consensus building using Racon v1.4.3 (Vaser et al., 2017) and Medaka v.1.6. It is important to note that the PCR primers used should be specific to the microalgae you are interested in identifying, as different species of microalgae can have genetic variations that require different primers for amplification.

The study utilized Geneseq's DNA sequences to analyze microalgal species. The sequences were analyzed using Bioedit software, the BLASTn program, and the NCBI BLAST website (https://blast.ncbi.nlm.nih.gov/Blast.cgi). Sequence alignment software was used to compare amplified DNA sequences from different samples. MEGA11 software was used for phylogenetic analyses, constructing a tree based on the 18S rDNA gene of microalgae of

the top ten similar results with a similarity of more than 90% in the percentage value. The phylogenetic tree was reconstructed using the maximum-likelihood method and bootstrap analysis (Hall, 2013).

4.2.2 Microalgae Cultivation for Bioremediation Process

The genus *Chlorella*, a type of green microalgae, was employed for the bioremediation of shrimp aquaculture wastewater. *Chlorella* sp. was chosen because it has a simple cell cycle, which makes it easy to grow and maintain (Sánchez-Bayo et al., 2020). It also has a high growth rate, allowing for quick biomass production (Masojídek & Torzillo, 2008). These attributes make *Chlorella* a suitable candidate for utilizing its natural abilities to remediate and improve the quality of shrimp aquaculture wastewater. *Chlorella* sp. was cultured under sterile conditions with an initial concentration of 1.0×10^5 cell mL^{-1} algal cells until the early exponential growth phase, Day 4 to Day 6 of the cultivation period. The microalgae cultivation condition was mentioned in Section 3.2.2.

4.2.3 Experimental Set-Up for Bioremediation Process

The batch bioremediation process for determination of the optimum concentration of *Chlorella* sp. was conducted using seven different inoculation dosages 0 to 60 % (v/v) with a total experiment volume of 1.5 L. Sampling was conducted every two days, and the aeration was closed about 2 mins before collected the sample. This interruption in aeration was implemented to maintain uniformity in the sampling process and allow any dead microalgae biomass to settle at the bottom. Aeration was supplied continuously to ensure

adequate CO_2 for cell growth. The pH was maintained at 7.0 ± 0.5 and monitored regularly. The growth performance and nutrient analysis of microalgae were monitored every 2 days. The initial concentration of NH_3-N (ammonia), NO_2^- (nitrite), and PO_4^{3-} (orthophosphate) was mentioned in Section 3.3.2.

4.2.4 Water Quality Analysis of Bioremediation Process for Nutrient Removal

In this study, water quality testing played a crucial role in monitoring the environmental conditions critical for the success of the aquaculture industry (Lindholm-Lehto, 2023). To assess the impact of the bioremediation, water quality analyses were conducted at regular intervals every 2 days, throughout the 14-day treatment period. Water samples (50 mL) were collected from each treatment flask for analysis. These water samples were centrifugated at 6000 rpm for 10 min using the Eppendorf 5702 Variable Speed Multi-Purpose Centrifuge. This centrifugation allowed for the separation of solid particles, resulting in a clear supernatant utilized for further water quality analysis. The supernatant was processed immediately for water quality analysis to prevent sample degradation. The Dual-Beam UV-Vis Spectrophotometer (Shimadzu UV-1800, Japan) was used to analyze nutrient concentration. The detailed procedure for each method can be found in Section 3.3.4 and Appendix B2.

4.2.5 Microalgae Biomass Cultivation and Model Development for Kinetic Study

Microalgae were cultured in aquaculture wastewater obtained from AKUATROP Hatchery at Universiti Malaysia Terengganu (UMT), Malaysia.

The wastewater was collected in 20 L tanks, filtered using GF/C filter paper to remove suspended solids, and stored at 4 °C. The wastewater had an initial pH range of 7 to 7.5. The detailed procedure for microalgae cultivation was previously stated in Section 3.3.3. Developing a microalgae growth kinetic model includes the utilization rate of ammonia, nitrite, and orthophosphate sources in aquaculture wastewater. Table 4.1 shows some kinetic parameters used to develop the kinetic model.

4.2.6 Microalgae Biomass Preparation for Characterization Analysis (FTIR and SEM/EDS)

The cultures were harvested during the late log phase to analyze the biomass of microalgae cultures. A 100 mL sample of the grown microalgae culture was centrifuged at 10,000 rpm for 10 minutes, and the resulting pellet was dried. The marine microalgae biomass was rinsed with 0.5 M ammonium formate before centrifugation to remove any salt present. The wet microalgae pellets were then freeze-dried using a Freezon 4.5 L, -50 °C Benchtop Freeze Dryer (USA) for 24 hours, forming dried algae powders. The dried samples were analyzed using an FTIR Spectrometer, Thermofisher Scientific NicoletTM iSTM 10 (USA). For this study, the FTIR analysis focused on the transmission region between 4000 and 400 cm^{-1} wave numbers, with a resolution of 4 cm^{-1}. A square aperture of 20 x 20 µm was used for the analysis, and spectra were obtained by taking 64 scans over a clear field (background).

The surface morphology of the microalgae was examined using scanning electron microscopy (SEM) analysis with a TESCAN/VEGA scan-brand Floor

Top Scanning Electron Microscope in the Czech Republic. The SEM was equipped with an EDX BRUKER (Silicon Drift Energy Dispersive Spectrometer model Quantax Compact with XFlash 600Mini) for elemental analysis. Before the SEM analysis, the microalgae biomass underwent the same processing technique mentioned in the FTIR analysis. Figure 4.3 (A) shows that a portion of the microalgae biomass was attached to a stub using black carbon tape. In Figure 4.3 (B), the stub was coated with a thin gold (Au) layer to protect the sample and improve conductivity. This preparation allowed for a detailed examination of the microalgae's surface using SEM.

(A) (B)

Figure 4.3 : Microalgae Biomass Coating with Gold (AU)

4.3 Statistical Analysis and Modelling

This study performed all experiments in triplicate to ensure reliable and reproducible results. A one-factor-at-a-time approach was adopted to evaluate the bioremediation process with two independent variables. The experimental data obtained from these experiments were subjected to a one-way analysis of variance (ANOVA), which is suitable for the design of experiments. The purpose of ANOVA was to determine whether there were statistically significant differences in growth rates and nutrient removal among the tested

parameters, specifically focusing on their consistency with the first-order kinetic. The probability (p) values were calculated to assess the significance level. A 95% confidence level was applied, meaning that a p-value of *≤0.05* was considered statistically significant for all analyses.

4.4 Results and Discussion

In this study, the nutrient removal of *Chlorella* sp. was examined through a batch culture, and the biomass growth yield was measured. The study aimed to assess the ability of *Chlorella* sp. to effectively utilize the nutrients present in shrimp aquaculture wastewater.

4.4.1 Molecular Identification of Green Microalgae, *Chlorella* sp.

Based on molecular identification using 18S rRNA gene sequences and Neighbor-Joining phylogenetic tree (Figure 4.4), the isolated *Chlorella* sp. was found identically with *Chlorella* sp. TNBR1 (Accession number KR869729.1) and *Chlorella* sp. KAS012 (Accession number AB176666.1) with 99.94% of nucleotide similarity. The isolated strain has been deposited in the National Centre of Biotechnology Information (NBCBI) as *Chlorella* sp. UMT LF1 and *Chlorella* sp. UMT LF2 with Accession numbers ON854138.1 and ON854139.1, respectively. Additionally, phylogenetic trees for each *Chlorella* sp. strain are available in Appendix E for reference. The evolutionary history of the analyzed taxa was inferred using the Neighbor-Joining method (Saitou & Nei, 1987). To assess the reliability of the inferred tree, a bootstrap consensus tree was generated from 1000 replicates (Felsenstein J., 1985). The bootstrap consensus tree represents the consensus of the evolutionary

history observed in the replicates. Branches supported by less than 50% of the bootstrap replicates collapsed. The percentage values displayed next to the branches indicate the proportion of replicate trees where the associated taxa clustered together during the bootstrap test (1000 replicates) (Felsenstein J., 1985). These percentages estimate the support for the branching pattern observed in the tree.

The evolutionary distances between taxa were calculated using the Maximum Composite Likelihood method (Tamura et al., 2004). These distances are expressed in units of the number of base substitutions per site, indicating the amount of genetic divergence between sequences. This analysis involved a total of 10 nucleotide sequences. Ambiguous positions were removed for each sequence pair using the pairwise deletion option. After removing ambiguous positions, 1732 positions remained in the final dataset. All the evolutionary analyses were performed using MEGA11 software, which provides a comprehensive platform for conducting various phylogenetic analyses.

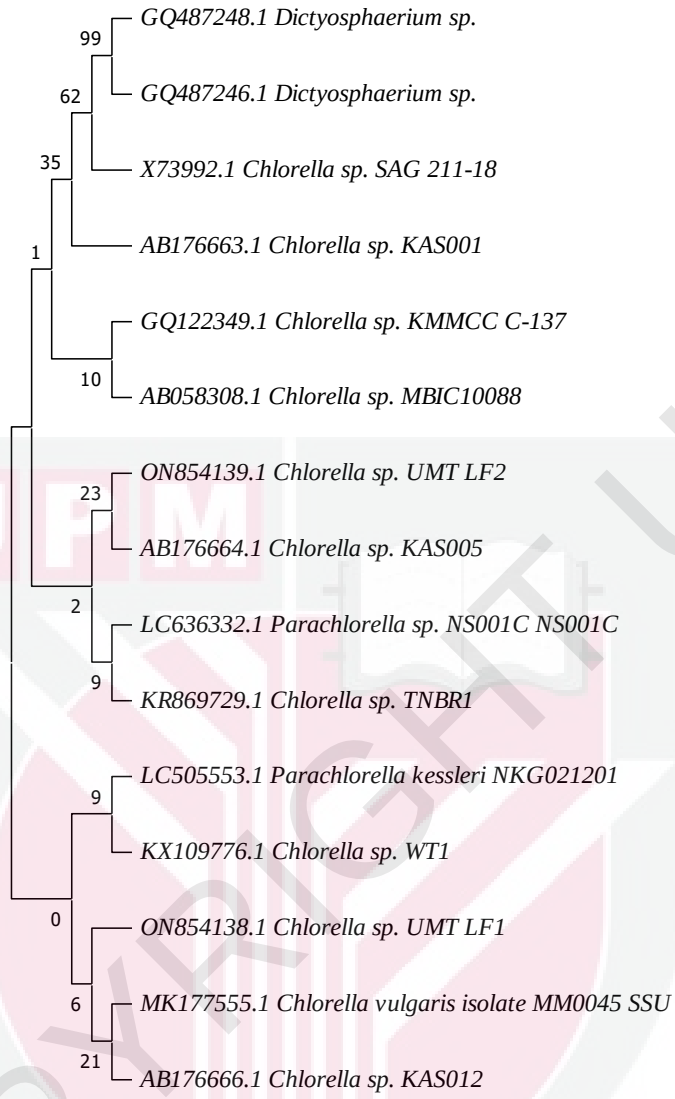

Figure 4.4 : Phylogenetic Analysis of Freshwater and Marine Water *Chlorella* sp. (UMT LF1 and UMT LF2) Based on 18S rDNA Sequences and Neighbor-Joining Tree Construction

4.4.2 Characteristics of Aquaculture Wastewater and Water Quality Standard

The physicochemical analysis of water quality parameters for shrimp marine and freshwater wastewater, shown in Table 4.1, indicates that temperature (27 ± 2 °C for marine, 28 ± 2 °C for fresh), pH (6.5 ± 1.0), and dissolved oxygen (4.17 ± 0.5 mg/L for marine, 4.9 ± 0.5 mg L^{-1} for fresh) were within acceptable ranges (Normal ± 2 °C, pH 6 – 9, and 5 – 7 mg L^{-1}, respectively). However,

other parameters showed significant deviations from Class IIA standards despite being lower than those reported in the study by Khatoon et al. (2016).

Both marine (30 ± 5 mg L^{-1}, 60 ± 5 NTU) and fresh (28 ± 5 mg L^{-1}, 50 ± 5 NTU) exceeded the standard for total suspended solids (TSS) and turbidity, indicating the presence of suspended particles exceeding the recommended limit of 50 mg L^{-1} and 50 NTU. Freshwater additionally displayed a considerably higher biological oxygen demand (BOD) of 32.9 ± 2 mg L^{-1} compared to marine water (40.1 ± 2 mg L^{-1}) and the standard of 3 mg L^{-1}. This suggests a higher concentration of organic matter and potential pollutants in the wastewater, requiring treatment to minimize environmental impact. Similarly, the ammonia content in fresh (3.7 ± 0.12 mg L^{-1}) was significantly higher than marine (2.8 ± 0.11 mg L^{-1}) and surpassed the standard of 0.3 mg L^{-1}, indicating potential toxicity risks to aquatic life. On the other hand, marine water displayed a higher concentration of orthophosphate (4.1 ± 0.5 mg L^{-1}) compared to fresh water (3.46 ± 0.11 mg L^{-1}). Although the standard doesn't specify a limit for orthophosphate, elevated levels can contribute to eutrophication and ecological concerns.

In summary, even though the physicochemical parameters are lower than those reported by Khatoon et al. (2016), this analysis highlights the necessity for effective wastewater treatment to meet environmental standards and safeguard aquatic ecosystems. Addressing these water quality issues is crucial for ensuring sustainable water management and minimizing the environmental impact of wastewater discharge.

Table 4.1 : Physicochemical Characteristics of the Shrimp Aquaculture Wastewater

Water Quality Parameter	units	Concentration		
		Marine water Wastewater	Freshwater Wastewater	Standard Class IIA
Temperature	˚C	27 ± 2	28 ± 2	Normal ± 2
pH	-	6.5 ± 1.0	6.5 ± 1.0	6 – 9
Dissolve Oxygen	mg L^{-1}	4.17 ± 0.5	4.9 ± 0.5	5 – 7
Salinity	ppt	30 ± 2	-	-
Biological Oxygen Demand	mg L^{-1}	40.1 ± 2	32.9 ± 2	3
Total Suspended Solid	mg L^{-1}	30 ± 5	28 ± 5	50
Turbidity	NTU	60 ± 5	50 ± 5	50
Ammonia	mg L^{-1}	2.8 ± 0.11	3.7 ± 0.75	0.3
Nitrite	mg L^{-1}	1.5 ± 0.08	1.8 ± 0.04	-
Orthophosphate	mg L^{-1}	4.1 ± 0.05	3.6 ± 0.11	-

Note: Mean± Standard deviation

4.4.3 Bioremediation Process of Aquaculture Wastewater Using Microalgae

Based on phylogenetic analysis using 18S rDNA sequences in section 4.4.1, identified *Chlorella* sp. UMT LF1 and *Chlorella* sp. UMT LF2 is closely related to known nutrient-removing *Chlorella* species (Ansari et al., 2017; Yousif et al., 2022). Following the strain selection analysis, the study further explored nutrient removal efficiency utilizing *Chlorella* sp. at different concentrations (dosages) in treating shrimp aquaculture wastewater. Microalgae were initially grown in 2 L Erlenmeyer flasks as described in section 3.3.2. Each of the six flasks was filled with 1.5 L of total volume and inoculated with different dosages (Figure 4.5).

(a) (b)

Figure 4.5 : Bioremediation Process at Different Dosages, 0, 10, 20, 30, 40, 50, and 60 % (v/v) (a) Day 0 (b) Day 7

4.4.3.1 Effect of Microalgae Concentration on Growth Performance

The interaction between microalgae concentration and nutrient availability becomes particularly significant when essential nutrients such as nitrogen and phosphorus are limited. This relationship can significantly impact microalgae growth, biomass production, and bioremediation efficiency. The growth performance of microalgae, *Chlorella* sp., is primarily influenced by the availability of nutrients, such as nitrogen and phosphorus, in the growth medium that leads to increased algae yield (Baker et al., 2013; Yaakob et al., 2021). Figure 4.6 depicted the growth patterns of microalgae in marine water (MW) and freshwater (FW) treatment throughout the 14-day treatment period with 7 different concentrations of microalgae to wastewater 0%, 10%, 20%, 30%, 40%, 50%, 60% (v/v). From the graph, the growth dynamics of

microalgae in marine and freshwater environments are influenced by the initial concentration of inoculated microalgae. The growth patterns of *Chlorella* sp. during the bioremediation process align with typical microbial growth kinetics, involving phases of lag, exponential, stationary, and declining growth (Mitchell et al., 2004). This indicates the successful adaptation and proliferation of microalgae under the tested conditions. For both environments, there is a noticeable lag phase in the early days (up to day 4) followed by exponential growth. This is typical as the microalgae acclimatize to the new conditions and nutrient availability. The observed growth patterns were statistically significant, with a *p-value* less than 0.05.

In the marine environment (MW), microalgae growth at 30% and 40% (v/v) concentrations indicates that these levels are optimal for achieving high cell density, as confirmed by statistical significance through a Post Hoc Bonferroni test ($p < 0.05$). In the marine environment (MW), microalgae growth at 30% and 40% (v/v) concentrations suggest that these levels are optimal for achieving high cell density, with statistical significance confirmed by a Post Hoc Bonferroni test ($p < 0.05$). The slower growth observed at 60% (v/v) could be attributed to self-shading, where the dense microalgae culture limits light penetration or to faster nutrient depletion than lower concentrations. The 10% and 20% dosages exhibit a continuous upward trend without any signs of a plateau or decline at the end of the treatment period. In the freshwater environment (FW), the 30% and 40% (v/v) concentrations similarly show the highest growth rates, indicating that these concentrations balance initial cell density and resource availability, thereby promoting optimal growth conditions.

The FW treatments also show no noticeable decline in growth at the end of the treatment period, particularly in the 10%, 20%, 30%, and 40% (v/v) dosages, which maintain a steady increase throughout the experiment.

The lack of a decline in microalgae growth at the end of the treatment period for certain dosages in MW and FW could be due to several factors. Firstly, there might still be sufficient nutrients in the water, allowing the microalgae to grow. Secondly, the environmental conditions, such as light, temperature, and nutrient levels, remained favorable throughout the treatment. Lastly, the microalgae might be entering or are in the stationary phase, where the growth rate slows but does not necessarily decline immediately.

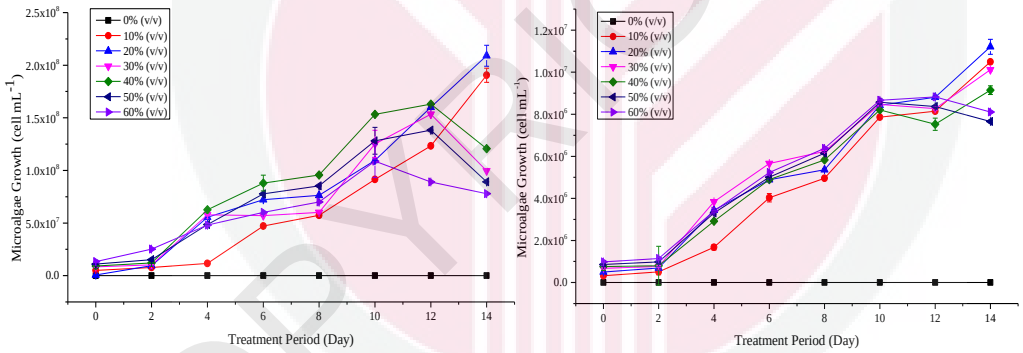

Figure 4.6 : Microalgae Growth throughout the 14-day Treatment Period (A) Marine Water Bioremediation (B) Freshwater Bioremediation

Figure 4.7 illustrates the specific growth rate (SGR) of *Chlorella* sp. during the exponential phase of the bioremediation process across different inoculation concentrations (10% to 60% v/v) in both shrimp wastewater (MW) and freshwater (FW) environments. The SGR values vary significantly with dosage levels, as indicated by the distinct capital letters (A – E) for MW and lowercase

letters (a – e) for FW, which represent statistically significant differences (*p<0.05*).

The SGR follows a relatively stable trend in the MW environment, with a consistent decline as inoculation concentration increases. The highest specific growth rate (SGR) of *Chlorella* sp. is observed at a 10% microalgae concentration, with an SGR of 0.228 day^{-1}. However, as the concentration increases to 60% v/v, the SGR decreases to 0.139 day^{-1}. This decline in growth rate at higher concentrations is due to increased competition for nutrients and light among the densely packed microalgae. The high density can lead to inadequate resources for optimal growth and potential shading, where the dense population blocks sunlight from reaching all cells effectively. These factors contribute to the reduced SGR observed at 60% v/v microalgae concentration. In contrast, the SGR in FW shows a more sinusoidal pattern, with peaks at 10% and 20% concentrations, followed by a drop at 30%, a rise again at 40%, and a final decline at higher concentrations. The highest SGR is recorded at 10% (0.191 day^{-1}), but the fluctuating pattern indicates that *Chlorella* sp. faces more variable conditions in FW, potentially due to inconsistencies in nutrient availability, pH levels, or other environmental factors.

The statistical analysis in Appendix D supports these observations. In FW, the SGR shows significant differences across the concentrations (*F=175.029, p<0.05*), but Post hoc Tukey's HSD and Bonferroni tests indicate no significant difference between the 30% and 60% concentrations (*p>0.05*). In MW, while

the SGR also varies significantly (*F=131.133, p<0.05*), the tests show no significant difference between the 30% and 40% concentrations (*p>0.05*). In conclusion, both environments demonstrate significant growth rate trends influenced by inoculation concentration (Heidari et al., 2016). The relatively stable response in MW suggests a more consistent environment for *Chlorella* sp.. In contrast, the sinusoidal pattern observed in FW points to greater environmental variability. These differences highlight the importance of tailoring bioremediation strategies based on the specific medium to achieve optimal microalgae performance.

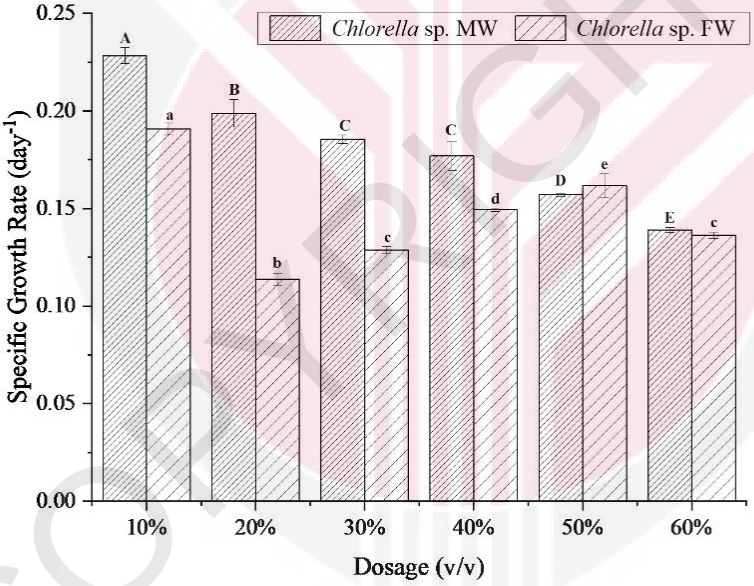

Figure 4.7 : Specific Growth Rate of *Chlorella* sp. during the Bioremediation Process

4.4.3.2 Effect of Microalgae Concentration on Nutrient Removal

The findings of the study demonstrate that microalgae can assimilate nitrogen from various sources, including ammonium, nitrate, nitrite, and urea (Delgadillo-Mirquez et al., 2016). Among these nitrogen sources, ammonia is

the most energy-efficient for microalgae uptake, requiring less energy than others. Table 4.2 shows the effect of microalgae culture dosage (v/v) on the removal efficiency of ammonia, nitrite, and orthophosphate by both marine (MW) and freshwater (FW) cultures on Day 10. The detailed results are provided in Appendix F for a comprehensive overview of the removal efficiency throughout the entire day of treatment (Day 0 to Day 14). Day 10 was chosen as the optimal time since removal efficiency reaches the highest percentage point and middle of the stationary phase. This stage is advantageous for bioremediation processes, allowing for efficient nutrient removal. According to a review from Khoo et al. (2023), microalgae can be highly productive during the stationary phase, making this an ideal stage for processes that rely on stable metabolic activity, such as nutrient removal.

Table 4.2 : The Removal Efficiency (%) of Ammonia, Nitrite, and Orthophosphate for MW and FW on Day 10

Dosage (v/v) / Nutrients	Ammonia (%)		Nitrite (%)		Orthophosphate (%)	
	MW	FW	MW	FW	MW	FW
0%	0.77^{a}	-2.10^{a}	-0.11^{a}	1.72^{a}	-0.01^{a}	4.28^{a}
10%	78.36^{b}	86.14^{b}	61.16^{b}	77.23^{b}	55.19^{b}	56.19^{b}
20%	$90.86^{c,d}$	87.94^{c}	56.72^{b}	77.04^{c}	74.57^{c}	73.49^{c}
30%	95.59^{c}	86.23^{d}	74.80^{b}	73.26^{b}	75.57^{c}	72.47^{c}
40%	93.36^{c}	89.77^{e}	79.13^{c}	82.59^{d}	66.65^{d}	94.73^{d}
50%	92.94^{c}	89.91^{e}	83.10^{c}	78.02^{e}	67.66^{e}	96.08^{d}
60%	87.97^{e}	82.90^{d}	80.63^{c}	72.47^{e}	60.25^{d}	95.97^{d}

Superscript letters (a, b, c, d, e) refer to means for the group in the homogenous subset.

The results indicated that the removal efficiency and removal rate of the control treatment with a dosage of 0% (v/v) were the lowest as it was used as a baseline for the experiment. This control treatment, run without microalgae inoculum, exhibited the lowest removal efficiency and removal rate. There is

no removal of the nutrients being studied as the wastewater has been sterilized, eliminating any biological activity involved in removing contaminants. However, significant differences were observed among the other dosages (10% - 60% v/v) tested for all nutrients ($p < 0.05$) (Appendix D2). This implies that the presence of microalgae inoculum at different dosages significantly impacted the removal efficiency and removal rate of the studied nutrients.

The results indicate that the ammonia concentration was significantly reduced for all dosages, except for the 0% (v/v) dosage, in both MW and FW. However, the bioremediation performance regarding ammonia removal was more effective in MW compared to FW. By Day 10, most dosages exhibited removal efficiencies exceeding 90%, except for the lowest dosage (10% v/v) and the highest dosage (60% v/v). Nevertheless, this is deemed acceptable as the removal efficiency was approximately 80% for the 10% v/v with a remaining concentration of 0.588 mg L^{-1} concentration and close to 90% for the 60% v/v concentration with a remaining concentration of 0.329 mg L^{-1}. Further analyses revealed that the highest removal efficiency was observed in MW, with a dosage of 30% (v/v) achieving a 95.59 ± 0.08% removal and a remaining concentration of 0.092 mg L^{-1}. In contrast, in FW, a dosage of 40% (v/v) achieved an 89.77 ± 0.05% removal with a remaining concentration of 0.294 mg L^{-1}. Both remaining concentrations are within the acceptable range for effluent standard Class IIA (ammonia ≤ 0.3 mg L^{-1}). These findings align with the study conditions and similar results reported by Yousif et al. (2022), demonstrating effective nutrient removal under sterile conditions with TN

removal efficiencies of 98.5%, 96%, and 90% in mixotrophic, heterotrophic, and autotrophic conditions, respectively, as both were conducted under sterile conditions.

It is important to highlight that ammonia and ammonium are typically the dominant nitrogen components in aquaculture. However, this study also found significant amounts of nitrite in the wastewater. During the initial five days of the treatment, the bioremediation process using *Chlorella* sp. showed low removal efficiency for nitrite and orthophosphate. This suggests that *Chlorella* sp. initially exhibited limited capacity to effectively remove these compounds from the wastewater. It is common for microalgae cultures to undergo an acclimation period where they adjust to the new environment and optimize their nutrient uptake mechanisms. Therefore, the lower removal rates observed during the early stages of the treatment period might be attributed to the time needed for *Chlorella* sp. to adapt and reach its maximum efficiency in removing nitrite and orthophosphate. Therefore, subsequent monitoring and analysis could reveal if the removal rates improve over time as the microalgae culture is established and adapts to the wastewater conditions.

During the treatment, nitrite concentration decreased significantly, achieving over 70% removal efficiency with 30% (v/v) dosages for MW and 40% (v/v) for FW. The remaining nitrite concentrations were 1.53 mg L^{-1} and 1.762 mg L^{-1}, respectively. Although no specific acceptable range is mentioned in the standards, these results are still considered acceptable since they represent a more than 70% reduction from the initial concentration. For MW, lower

dosages below 20% (v/v) demonstrated less effective removal, with an efficiency of only 56.72%. This reduced effectiveness is probably due to insufficient microalgae concentration, which may have limited the overall capacity for nitrite absorption and reduced the surface area available for contact with the wastewater. Additionally, lower dosages might result in nutrient imbalances or suboptimal conditions for the microalgae, impacting their ability to remove nitrite efficiently. It is also relevant to note that the nitrification process, which includes the conversion of ammonia to nitrite and nitrite to nitrate, was found to be negligible throughout the treatment (Thakur & Medhi, 2019). This suggests that nitrification did not significantly influence any changes in nitrite levels, reinforcing that the observed removal efficiency issues at lower dosages are probably due to the limitations of microalgae concentration and conditions rather than biological conversion processes.

Furthermore, phosphorus is a crucial component for microalgae growth and is often a major limiting factor (Zheng et al., 2020). Phytoplankton typically assimilates and utilizes orthophosphate for cell development (Eixler et al., 2006). Phosphorus absorbed by microalgae is commonly stored as polyphosphate granules and is a valuable resource during their growth cycle. A study Rawat et al., (2011) mentioned that orthophosphate nutrients are reduced through absorption by *Chlorella* sp. and stored as polyphosphates within the cells. This study observed that phosphorus concentration in orthophosphate (PO_4^{3-}) showed less than 80% removal efficiency in MW with a dosage of 30% (v/v). In comparison, complete removal was achieved with a dosage of 40% (v/v), reaching 95% efficiency. This discrepancy highlights the

importance of optimizing nutrient conditions for effective bioremediation. Nevertheless, all treatments showed higher PO_4^{3-} removal than the control group of 0% (v/v).

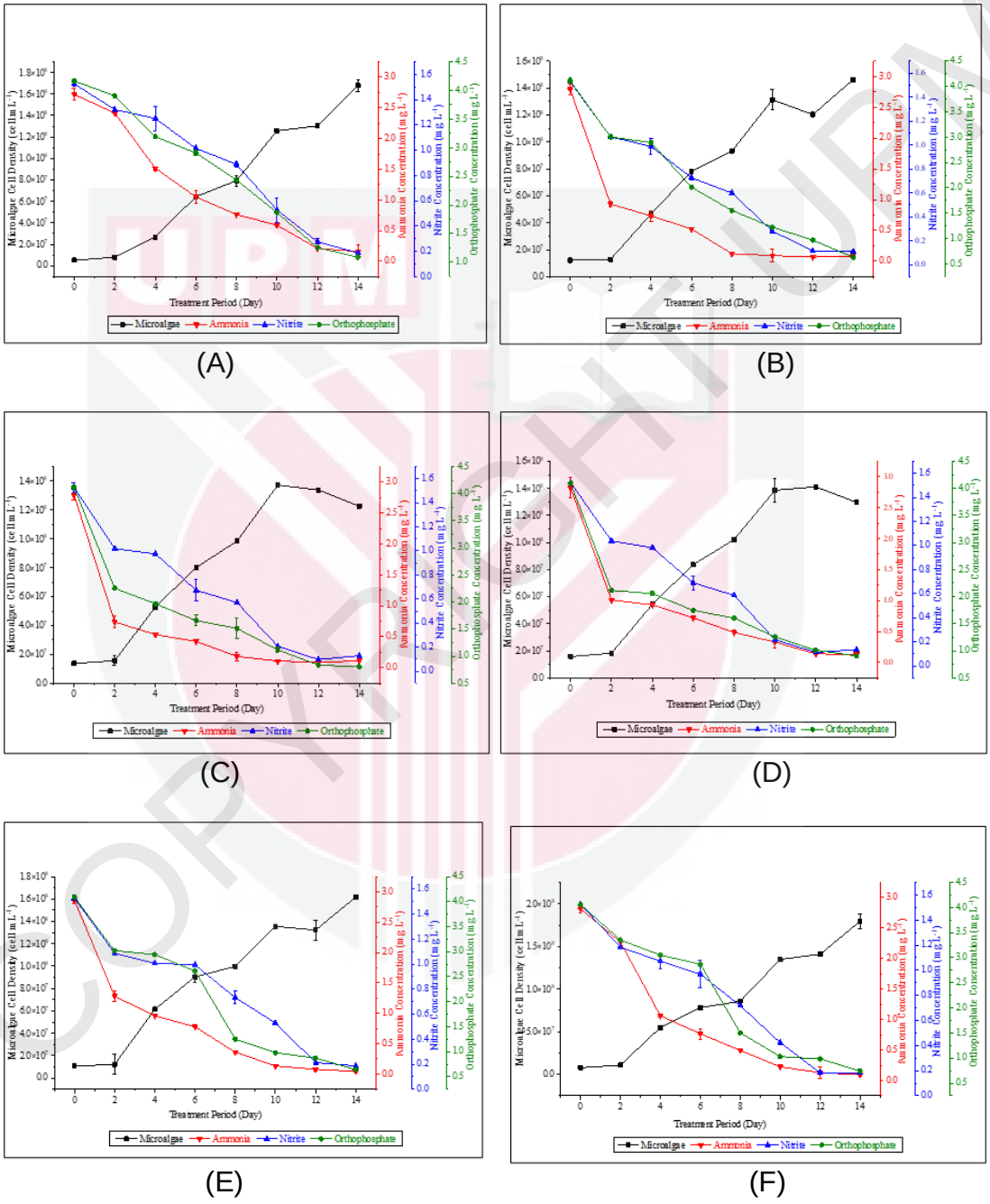

Figure 4.8 : Bioremediation Performance at (A) 10, (B) 20, (C) 30, (D) 40, (E) 50, and (F) 60% (v/v) Microalgae *Chlorella* sp. Inoculation Dosages throughout 14-day Treatment Period for Marine Water Treatment (MW)

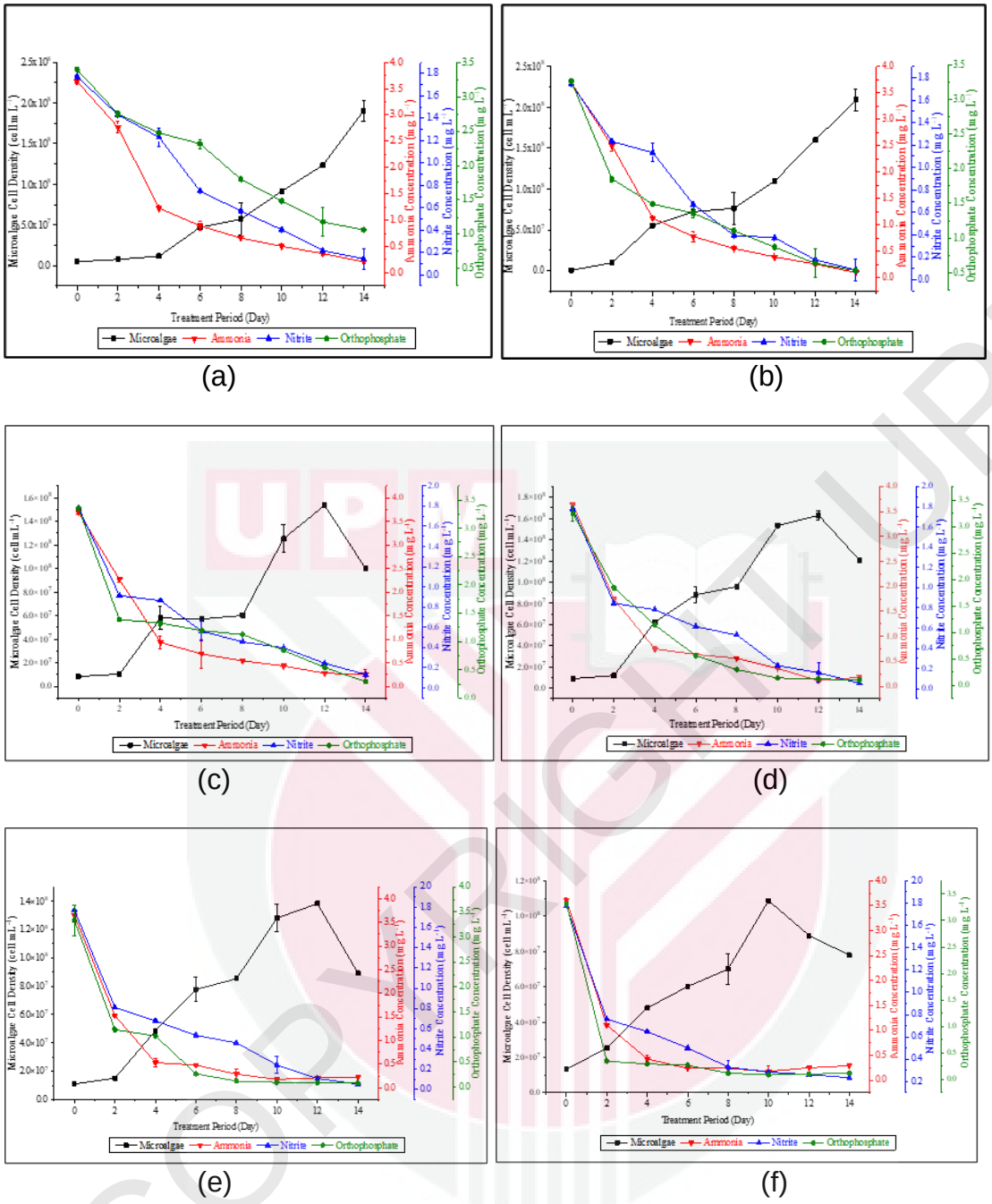

Figure 4.9 : Bioremediation Performance at Different Microalgae, *Chlorella* sp. Inoculations Dosage; (a) 10, (b) 20, (c) 30, (d) 40, (e) 50, and (f) 60% (v/v) throughout 14-Day Treatment Period for Freshwater Treatment (FW)

The graphs shown in Figures 4.8 and 4.9 show the relationship between nutrient levels (ammonia, nitrite, and orthophosphate) and microalgal biomass growth during the treatment of both marine water (MW) and freshwater (FW).

These findings illustrate how decreasing nutrient concentrations correlate with increases in microalgal biomass and highlight the effectiveness of the bioremediation process and the role of nutrient removal in enhancing microalgae growth. The growth pattern of *Chlorella* sp. in different treatments followed a similar trend, with a relatively short lag phase in the first two days, followed by rapid exponential growth from days six to eight. This pattern suggests that *Chlorella* sp. adapted quickly to the treatment conditions and entered a phase of active development and reproduction. The short lag phase indicates that the microalgae efficiently utilized the available nutrients and established their metabolic processes. The death phase was observed starting on Day 12 and continued towards the end of the treatment period. In MW, the death phase was noted only at 50% and 60% concentrations, while in FW, it occurred at all concentrations except for 10% and 20%. This finding suggests that the *Chlorella* sp. is adaptable to different treatment conditions.

These growth and nutrient removal results highlight that *Chlorella* sp. is adaptable and can effectively use nitrogen and phosphorus for growth and accumulating lipids adaptability. *Chlorella* sp. can utilize ammonium and nitrite as nitrogen sources for synthesizing glutamine and glutamate. This process involves the enzymes glutamine synthetase, which helps obtain energy from the breakdown of ammonium, and glutamate synthetase, which facilitates glutamate production using nitrite (Salbitani & Carfagna, 2021). Furthermore, Chu et al. (2019) reported that in addition to nitrogen, phosphorus (P) also plays a beneficial role in increasing the lipid content in *Chlorella* sp. This is accompanied by the accumulation of polyphosphate (poly-P) within the cells.

Additionally, Sacristán de Alva et al. (2018) observed high uptake of ammonia, nitrite, and orthophosphate by *Chlorella* sp., indicating efficient nutrient utilization to support cell growth. According to the graph, the increase in ammonia concentrations observed in MW between Days 12 and 14, especially at the 50% and 60% concentrations, aligns with the microalgae entering the death phase. It is consistent with previous findings on nutrient release during biomass degradation.

4.4.4 Microalgae Characterization FTIR Analysis and SEM/EDX Analysis

According to Wagner et al. (2013), Fourier-transform Infrared spectroscopy (FTIR) has played a vital role in characterizing the biochemical composition of phytoplankton. FTIR analyses the absorption or transmission of infrared radiation, providing information about functional groups and chemical bonds in samples. It uses distinct vibrational frequencies to determine sample composition and molecular functional groups. Analyzing these band positions, widths, and intensities allows determining the sample composition and molecular functional groups. Some common functional groups that FTIR can detect in microalgae include carboxyl groups, hydroxyl groups, and amine groups. These groups can indicate the presence of various biomolecules such as lipids, proteins, and carbohydrates. The FTIR transmittance measurements reveal these groups by providing insights into their composition and potential applications.

Figures 4.10 and 4.11 in the study display the FTIR transmittance spectra of four microalgae biomass samples. The analysis of these spectra revealed the presence of seven distinct bands within specific wavenumber ranges. 3900 - 3800 cm^{-1}, 3700 - 3100 cm^{-1}, 3000 - 2800 cm^{-1}, 1800 - 1700 cm^{-1}, 1700 - 1600 cm^{-1} (MW only), 1600 - 1500 cm^{-1} (MW only) and 1200 - 900 cm^{-1}. These bands indicate the presence of various organic groups in the microalgae biomass. The variances observed in the composition of the microalgae biomass suggest differences in the chemical makeup of the samples despite having comparable organic groups. The FTIR spectrum of *Chlorella* sp. was similar to that reported by Ferreira et al. (2015), indicating consistency in the characteristic infrared absorption patterns of *Chlorella* sp.. This similarity supports the identification and characterisation of microalgae species, confirming the consistent absorption bands and patterns. If the spectra of two samples, in this case, *Chlorella* sp., exhibit similar absorption bands at specific wave numbers, suggest shared functional groups and biomolecular composition. This consistency in the infrared absorption patterns suggests that the microalgae used in both studies will likely be of the same or closely related species.

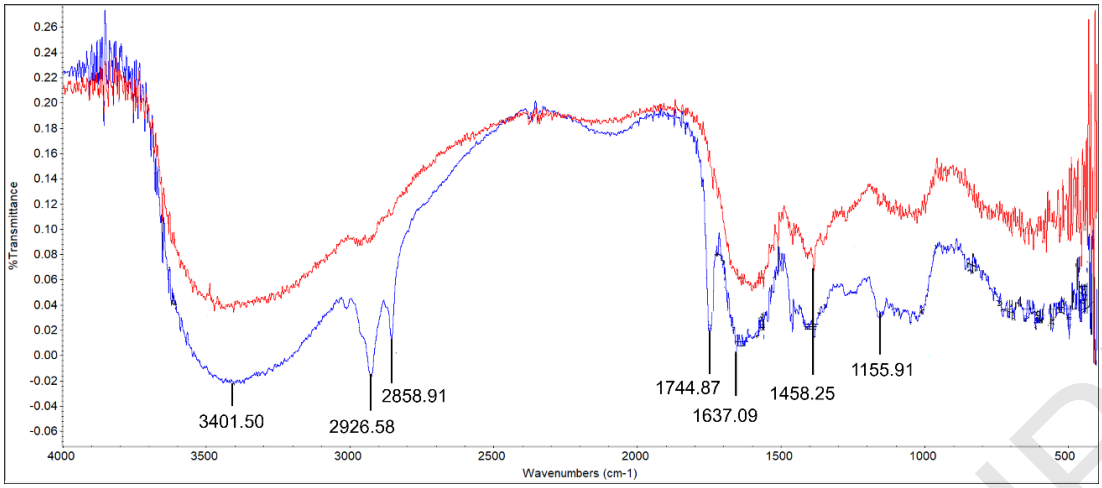

Figure 4.10 : FTIR Spectra: *Chlorella* sp. LF2 Culture in the Medium, F/2 (red), *Chlorella* sp. LF2 Culture in Aquaculture Wastewater (Blue)

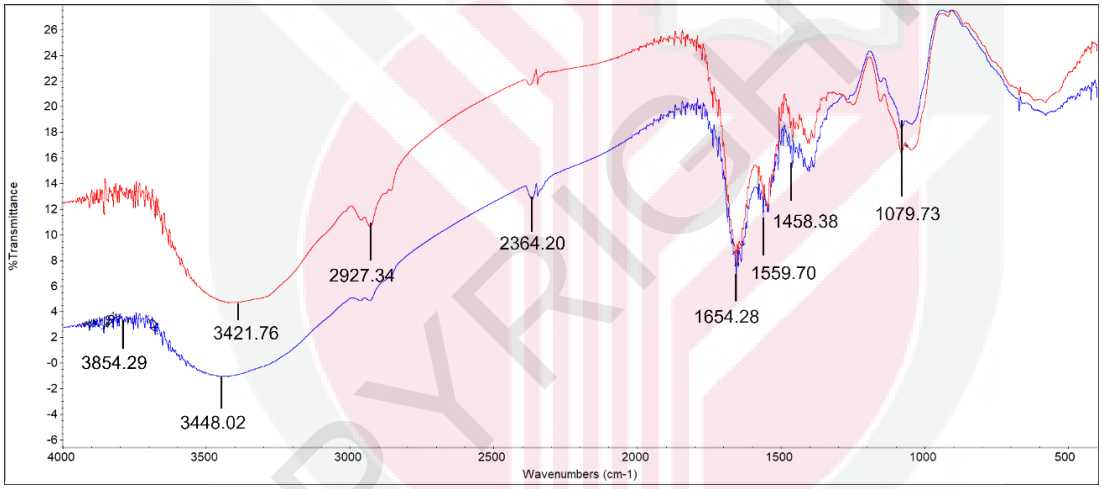

Figure 4.11 : FTIR Spectra: *Chlorella* sp. LF1 Culture in the Medium, BBM (red), *Chlorella* sp. LF1 Culture in Aquaculture Wastewater (Blue)

Table 4.3 : Functional Group /Assignment of *Chlorella* sp. of Marine Water (MW). References

Band	Main peak (cm^{-1})	Wave number range (cm^{-1})	Typical band assignment from literature
1.	3401.50	3700 – 3100	Water v(O-H) stretching Protein v(N-H) stretching (amide A)
2.	2926.58/ 2853.91*	3000 – 2800	Lipid – carbohydrate Mainly vs(CH_2) and vs(CH_2) stretching
3.	1744.87*	1800 – 1700	Cellulose–Fatty Acids v(C=O) stretching of esters
4.	1637.09	1700 – 1600	Protein amide I band Mainly
5.	1458.25	1500 - 1400	Protein $\delta_{as}(CH_2)$ and $\delta_{as}(CH_3)$ bending of methyl, Lipid $\delta_{as}(CH_2)$ bending of methyl
6.	1155.91	1200 – 900	Carbohydrate v(C-O-C) of Polysaccharides

Note: (* sign) Refer to peak present at Bioremediation Process only (adapted from Duygu et al. 2012)

Table 4.4 : Functional Group /Assignment of *Chlorella* sp. of Fresh Water (FW). References

Band	Main peak (cm^{-1})	Wave number range (cm^{-1})	Typical band assignment from literature
1.	3854.31	3900 – 3800	-NH_2 stretching vibration
2.	3448.02	3700 – 3100	Water v(O-H) stretching Protein v(N-H) stretching (amide A)
3.	2927.34*	3000 – 2800	Lipid – carbohydrate Mainly vas(CH_2) and vs(CH_2) stretching
4.	1654.28	1800 – 1600	Protein amide I band Mainly v(C=O) stretching
5.	1559.70	1600-1500	Protein amide II band mainly δ(N-H) bending and v(C-N) stretching
6.	1458.38	1500 - 1400	Protein $\delta_{as}(CH_2)$ and $\delta_{as}(CH_3)$ bending of methyl, Lipid $\delta_{as}(CH_2)$ bending of methyl
7.	1079.73	1200 – 900	Carbohydrate v(C-O-C) of polysaccharides Nucleic Acid (and other phosphate-containing compounds) vs(>P=O) stretching of phosphodiesters

Note: (* sign) Refer to peak present at Bioremediation Process only (adopted from Duygu et al. 2012)

Tables 4.3 and 4.4 summarize the FTIR spectra band assignments observed in the microalgae biomass for both marine water (MW) and freshwater (FW)

environments, where the results align with findings from Duygu et al. (2012) and Ganeson et al. (2024). For marine water (MW), Bands 3 and 4 at 2853.91 cm^{-1} and 1744.87 cm^{-1} only appear in microalgae after bioremediation. This indicates the presence of new constituents related to the treatment conditions, such as increased fatty acids and cellulose-related vibrations, which are components of the microalgal cell wall. In freshwater (FW), Band 3 at 2927.34 cm^{-1} emerges exclusively in the microalgae post-bioremediation. This indicates a significant shift in the microalgae's chemical composition due to the uptake and assimilation of nutrients from the wastewater. The emergence of this band highlights changes in lipid and carbohydrate structures, which are essential components in cellular function and growth.

The FTIR results show how bioremediation changes the biochemical makeup of *Chlorella* sp., demonstrating how the microalgae adapt and grow in treated wastewater with high nutrient levels. The differences between the marine water (MW) and freshwater (FW) spectra highlight the microalgae's flexibility and the specific biochemical processes activated in each water type. Overall, these results confirm the effectiveness of *Chlorella sp.* in bioremediation for both MW and FW, aligning with established mechanisms for nutrient removal and biomass production.

Advanced microscopy techniques, including scanning electron microscopy (SEM), are essential for characterising microalgae, as stated by Nie et al. (2020). In this study, after a 14-day treatment with aquaculture wastewater, the biomass cells of *Chlorella* sp. were visually examined using light

microscopy, SEM, and energy dispersive spectroscopy (EDS) to analyse their elemental composition. After a bioremediation process using microalgae culture in the medium, SEM can be employed to examine the morphological changes in the microalgae. SEM microscopy provides high-resolution images of the sample's surface, allowing for the analysis of microalgae size, shape, and surface features at a magnified scale. Researchers can assess any observable alterations in the microalgae morphology by comparing SEM images before and after the bioremediation process. Changes in size, shape, or surface features can provide valuable information about the effectiveness of the bioremediation process in removing pollutants or contaminants from the environment. For example, if the microalgae appear to have more extensive or irregular shapes or display surface irregularities or damage after the bioremediation process, it may indicate that they have been actively involved in pollutant uptake or adsorption. Conversely, if the microalgae show minimal changes in morphology, it could imply that the bioremediation process had limited effects on pollutant removal. SEM microscopy and other analytical techniques and data can comprehensively assess bioremediation efficiency and provide visual evidence of the microalgae's role in pollutant mitigation.

Based on the SEM images, *Chlorella* sp. grown in commercial media (Guillard's F/2 Media) and shrimp wastewater (bioremediation process) exhibit distinct differences in surface texture and cell arrangement (Figure 4.12). The cells grown in commercial media display a smoother and more uniform surface texture, indicative of a controlled and cleaner growth environment. The distribution of cells in the commercial media is evener, with fewer visible

impurities or debris. In contrast, the cells grown in shrimp wastewater exhibit a rougher, more irregular surface texture and appear more clustered. This is attributed to additional extracellular polymeric substances (EPS) in the wastewater. According to Babiak & Krzemińska (2021), these molecules create a slimy coating around the cells, which acts as a protective barrier against specific environmental stresses. The shrimp wastewater-grown cells exhibit more pronounced surface irregularities and possible contaminants, reflecting the complex composition of the wastewater.

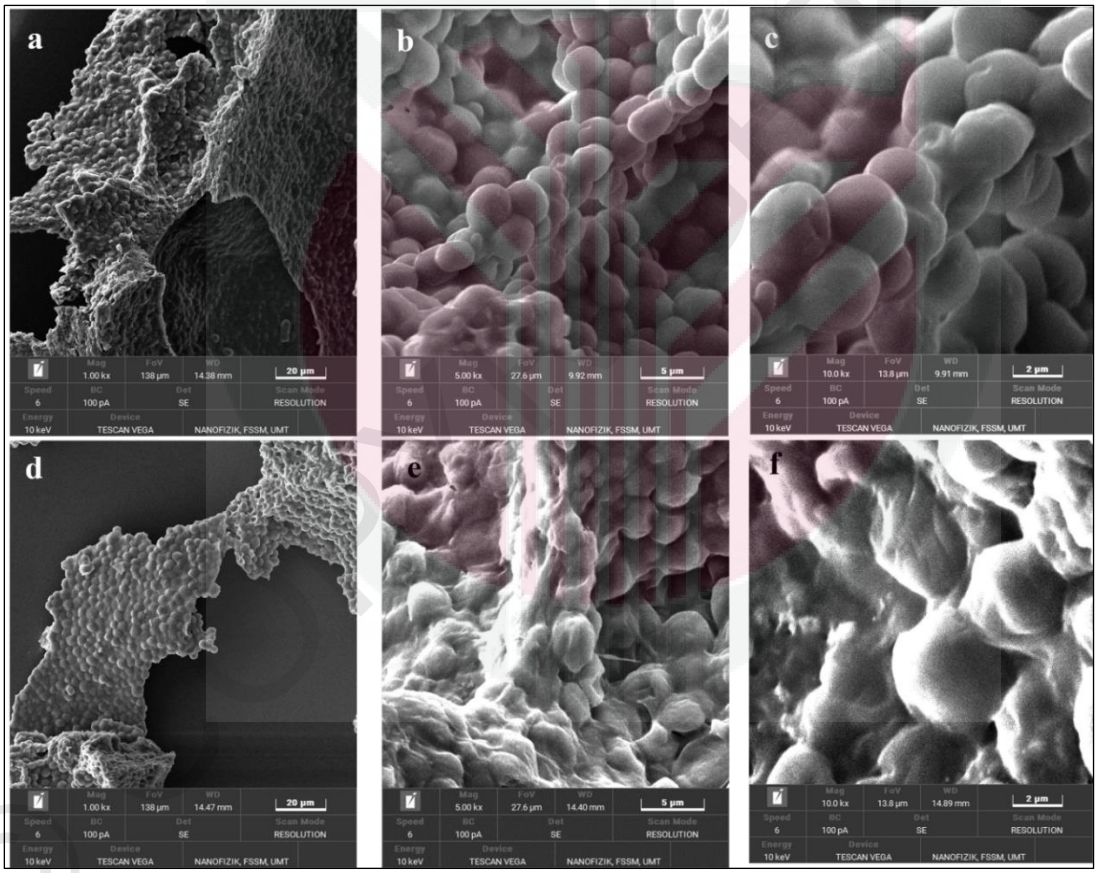

Figure 4.12 : SEM Images of Microalgae at Magnifications (x1000, x5000, x10,000). Images (a-b-c) Represented *Chlorella* sp. Culture in Guillard's F/2 Media, and İmages (d-e-f) Represented *Chlorella* sp. Culture in MW

Figure 4.13 shows the different images of microalgae cells in freshwater (FW) conditions. When microalgae are grown in a culture medium, the composition of the medium is carefully controlled to provide the necessary nutrients for growth. This allows the microalgae to grow under optimal conditions and form uniform colonies. SEM images of microalgae grown in media show consistent morphology with uniform cell sizes and shapes. In contrast, when microalgae is grown in wastewater, the composition of the medium is more variable. It can contain many organic and inorganic compounds, including pollutants and contaminants. These compounds can affect the growth and morphology of the microalgae, leading to more variable and heterogeneous colonies. In addition, other microorganisms in the wastewater can also affect the microalgae morphology. This study aligns with the research by Narayanan et al. (2021), which investigated the morphology of *Chlorella* sp. after phycoremediation in polluted Thirumanimutharu river water. Although this study focuses on aquaculture wastewater rather than river water, it is comparable. Both observed similar morphological changes in *Chlorella* sp. biomass, including asymmetric forms and crenulated textures, as illustrated in Figure 4.13 (l).

As a result, the SEM analysis reveals that the environmental conditions of the growth medium significantly influence the surface characteristics and aggregation behavior of *Chlorella* sp.. The controlled environment of commercial media promotes a cleaner and more consistent cell morphology in both water types. In contrast, the complex composition of shrimp wastewater leads to rougher surfaces, higher cell clustering, and the presence of impurities and extracellular substances, with these effects being more pronounced in

both environments.

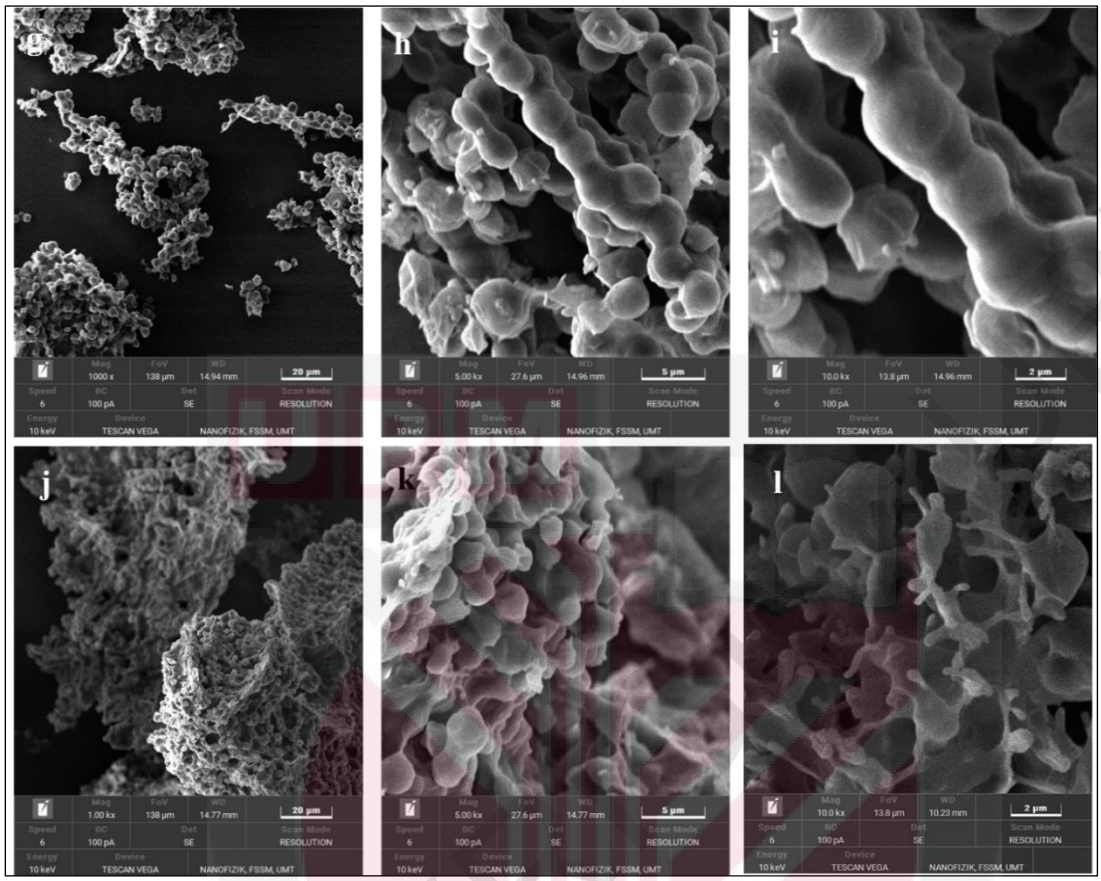

Figure 4.13 : SEM Images of Microalgae at Magnifications (x1000, x5000, x10,000). Images (g-h-i) Represented *Chlorella* sp. Culture in BBM, and İmages (j-k-l) Represented the *Chlorella* sp. Culture in FW

EDX was employed to perform an elemental analysis of the microalgae biomass to characterize the microalgae further. The graph in Figure 4.14 obtained from EDX depicts the elemental composition and reveals a prominent peak corresponding to the expected elemental in the sample. Since nitrogen and phosphorus are crucial for microalgae growth as macronutrients, it is essential to measure them before and after bioremediation (Khan et al., 2018). Analyzing these elements before and after treatment can determine the effectiveness of the treatment process and its impact on the microalgae's

nutrient uptake.

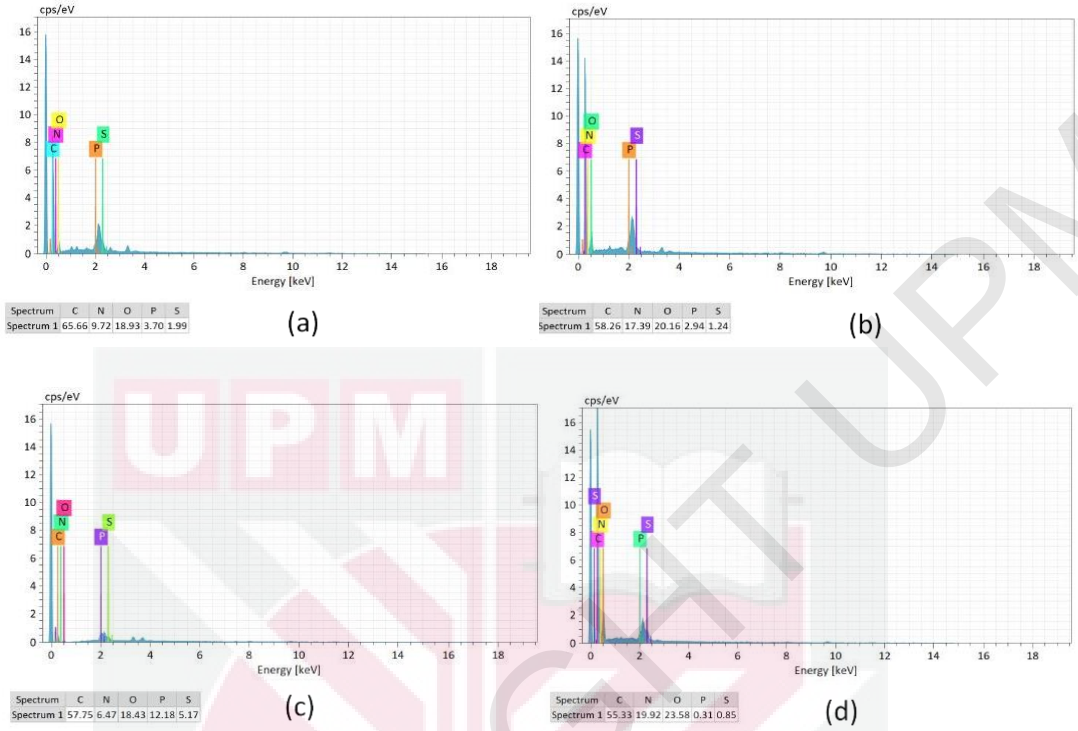

Figure 4.14 : EDS Image of Spectra Element in Microalgae, *Chlorella* sp. a) *Chlorella* sp. UMT LF2 in Media b) *Chlorella* sp. UMT LF2 in MW c) *Chlorella* sp. UMT LF1 in Media d) *Chlorella* sp.UMT LF1 in FW

Table 4.6 presents the weight percentages of various chemical elements, including Carbon (C), Nitrogen (N), Oxygen (O), Phosphorus (P), and Sulphur (S), in different biomass samples of *Chlorella* sp. UMT LF2 (Guillard's F/2), *Chlorella* sp. UMT LF2 (MW), *Chlorella* sp. UMT LF1 (BBM), and *Chlorella* sp. UMT LF1 (FW). The presence of C, N, O, P, and S, which are essential components of cellular macromolecules, play vital roles in the structure and function of microalgae cells (Sultana et al., 2020). From the results obtained, the elemental analysis using EDS yielded different percentages of elements on the microalgae biomass surface.

Table 4.5 : Elemental Identification by EDX

Biomass Sample	Contents of Element by Weight (%)			
	Chlorella sp. LF2 Guillard's F/2	*Chlorella* sp. LF2 MW	*Chlorella* sp. LF1 BBM	*Chlorella* sp. LF1 FW
Carbon, C	65.66	58.26	57.75	55.3
Nitrogen, N	9.72	17.39	6.47	19.91
Oxygen, O	18.93	20.16	18.34	23.58
Phosphorus, P	3.70	2.94	12.18	0.31
Sulphur, S	1.99	1.24	5.17	0.85

The elemental composition of *Chlorella* sp. in marine conditions shows significant differences between cultures grown in F/2 medium and marine wastewater (MW). The carbon content is higher in *Chlorella* sp. cultured in F/2 medium (65.66%) than in MW (58.26%). This increase is likely due to the controlled and nutrient-rich environment of the F/2 medium, which enhances carbon fixation through photosynthesis. In contrast, the variable nutrient levels in MW may limit the carbon fixation process, resulting in lower carbon content. The nitrogen content is much higher in MW (17.39%) than in F/2 medium (9.72%), suggesting that *Chlorella* sp. in natural marine water assimilates more nitrogen. This may be due to different nitrogen sources or higher nitrogen availability in the wastewater, which includes compounds such as ammonia, nitrite, and nitrate that microalgae can readily utilize for growth and protein synthesis (Xu et al., 2001). The slightly higher oxygen levels in MW (20.16%) compared to F/2 medium (18.93%) could reflect variations in oxygenation or oxidative processes, with microalgae in MW potentially experiencing increased photosynthesis or oxidative reactions due to fluctuating light conditions or nutrient availability. Furthermore, the phosphorus content is greater in the F/2 medium (3.70%) than in MW (2.94%), indicating a possible

nutrient limitation in MW that could impact essential metabolic processes like ATP synthesis and nucleic acid formation (Yaakob et al., 2021). Sulphur content is slightly higher in F/2 (1.99%) than in MW (1.24%), reflecting sulphur metabolism or availability differences between the two environments.

In freshwater conditions, the elemental composition of *Chlorella* sp. LF1 is similar to that observed in marine water conditions. *Chlorella* sp. grown in BBM has a higher carbon content (57.75%) compared to FW (55.3%), which can be attributed to the nutrient-rich environment of BBM that supports more carbon fixation. The nitrogen content is significantly higher in FW (19.91%) than in BBM (6.47%). Oxygen content is higher in FW (23.58%) than in BBM (18.34%), suggesting more oxidative processes or higher oxygen availability in FW. Phosphorus content is significantly higher in BBM (12.18%) compared to FW (0.31%) due to the controlled phosphorus levels in BBM, which may not be as available in the freshwater environment. Lastly, sulphur content is higher in BBM (5.17%) than in FW (0.85%), reflecting sulphur metabolism or availability differences between the two environments.

It is essential that the composition of the growth medium or the environment in which microalgae are cultivated can significantly influence their chemical composition and metabolic activities. In summary, the findings of EDX analysis are valuable for understanding the characteristics and properties of microalgae cells, which can further aid in their utilisation and potential applications in various fields such as biofuels, bioremediation, and biotechnology.

4.4.5 First-Order Kinetic Model of Nutrient Removal during Bioremediation

This study focuses on determining the optimal conditions for cultivating *Chlorella* sp. and optimizing nutrient removal to enhance the efficiency and sustainability of wastewater treatment in the aquaculture industry. The results obtained from batch experiments are used to develop kinetic models. A study by Wang et al. (2014) also used a first-order kinetic model to evaluate a nutrient removal model. The model was run for a batch culture mode using growth rate expressions discussed in Section 3.3.3.

However, the first-order kinetic model used in this study has certain limitations and assumptions. It assumes a constant rate of nutrient removal, which may not accurately reflect the variable rates observed in real-world conditions. The model is also based on batch culture data, which could limit its applicability to continuous or semi-continuous systems. This study addresses these limitations by validating the model's predictions against experimental data, which helps assess and improve the model's accuracy and reliability. By closely matching the model's predictions with actual measurements, the research refines the model better to simulate microalgae growth dynamics and nutrient removal processes.

4.4.5.1 Ammonia Removal Efficiency

The first-order kinetic model was employed in the present study to analyze the bioremediation process. To understand the first-order kinetic behavior of nutrient removal, a graph was constructed by plotting the natural logarithm (ln)

of nutrient concentration against the treatment period (in days). This approach, based on the first-order kinetic model, allows for a comprehensive examination of the kinetics involved in the process. Figure 4.15 and Figure 4.16 illustrate the graph of ln NH_3 concentration versus treatment period (day), which was used to determine the first-order kinetic equation, coefficient rate constant, and coefficient of determination (R_2). The steepness of the gradient observed in the graph indicates a higher coefficient rate constant, which in turn implies a higher removal efficiency of NH_3. Referring to Table 4.6, samples with a microalgae concentration of 30% (v/v) in marine water and 20% (v/v) in freshwater exhibited the steepest gradients, measuring 0.2901 and 0.2331, respectively. The predicted NH_3 removal efficiency based on the equation for both samples exceeded 90%, highlighting their effective NH_3 removal capabilities and aligned with the experimental results. A higher R_2 value indicates a better fit, suggesting that the first-order kinetic equation is a suitable data representation.

Among the different samples, the microalgae concentration of 60% (v/v) exhibited the lowest gradient of 0.1678 (MW) and 0.1425 (FW). This indicates that the ammonia removal rate was relatively slower in this sample compared to the samples with lower microalgae concentrations. The results suggest that samples with a microalgae concentration of 30% MW and 20% FW demonstrated the highest ammonia removal rates. The sample with a microalgae concentration of 60% (v/v) exhibited the lowest removal rate among the tested concentrations. Therefore, based on the observed steep gradients, high coefficient rate constants, predicted NH_3 removal efficiency,

and the suitability of the first-order kinetic equation, it can be concluded that the experimental results align well with the first-order kinetic model for wastewater treatment of NH_3.

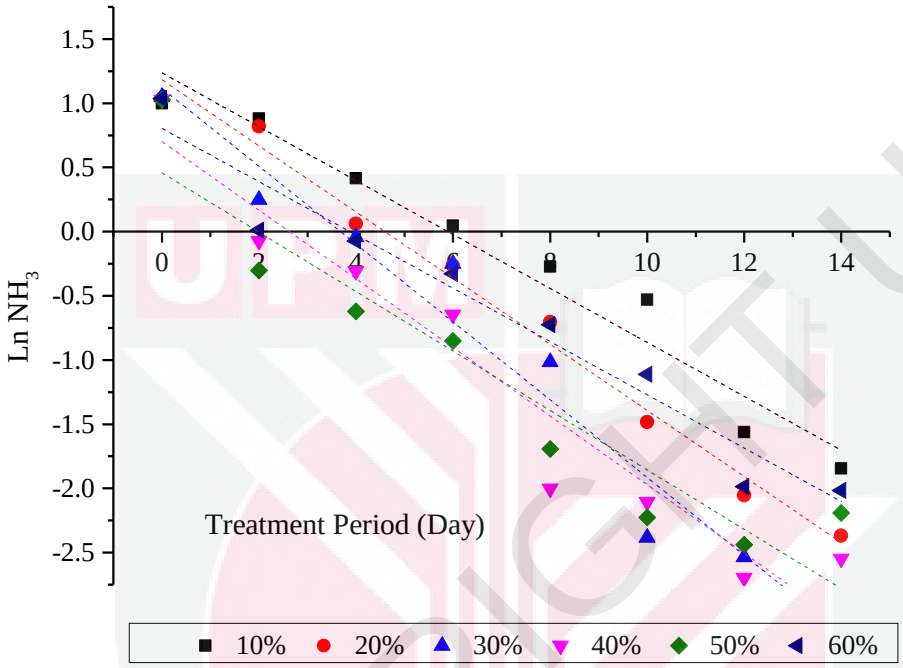

Figure 4.15 : Graph of In NH_3 Versus Treatment Period (Day) at Different Microalgae Concentrations of Marine Water Treatment

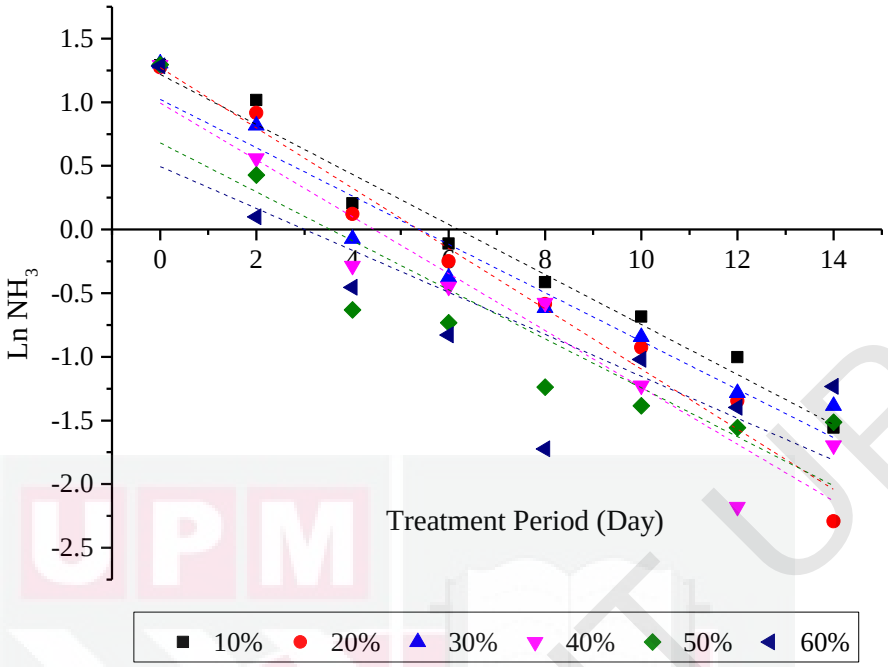

Figure 4.16 : Graph of ln NH_3 Versus Treatment Period (Day) at Different Microalgae Concentrations of Freshwater Treatment

Table 4.6 : First-Order Kinetic Equation of Ammonia, NH_3^- Removal Efficiency at Different Microalgae Concentrations for Two Types of Wastewaters

Microalgae Concentration (%, v/v)	Types of wastewater	Initial Concentration of NH_3^- (mg L^{-1})	First Order Kinetic $\ln[A] = -kt + \ln[A]_o$.	(-) k	R^2
10	MW	2.718	y=-0.21x + 1.2368	0.21	0.9608
	FW	3.635	y=-0.1965x + 1.2184	0.1965	0.9785
20	MW	2.817	y=-0.2523x + 1.1307	0.2523	0.9842
	FW	3.691	y=-0.2331x + 1.2346	0.2331	0.9775
30	MW	2.860	y=-0.2901x + 0.9854	0.2901	0.954
	FW	3.681	y=-0.1829x + 0.9527	0.1829	0.9505
40	MW	2.794	y=-0.2496x + 0.5256	0.2496	0.9389
	FW	3.688	y=-0.2135x + 0.8952	0.2135	0.925
50	MW	2.796	y=-0.2063x + 0.2064	0.2063	0.9279
	FW	3.671	y=-0.1764x + 0.52	0.1764	0.869
60	MW	2.821	y=-0.1678x + 0.4067	0.1678	0.9153
	FW	3.676	y=-0.1425 + 0.2709	0.1425	0.7218

Note: MW (Marine water), FW (Freshwater)

Figures 4.17 and 4.18 compare the predicted and experimental data of NH_3 removal in marine and freshwater aquaculture wastewater at different microalgae concentrations. The accuracy and reliability of the model's predictions can be evaluated by comparing the predicted data points with the experimental values. For marine water (MW) during the early stages of the experiment on Day 0, there was a slight deviation at 30% (v/v) with a low MAE of 0.191. However, at concentrations of 10%, 20%, 40%, and 50%, the deviations were considerably higher, with MAEs of 0.727, 0.447, 0.777, and 1.215, respectively, indicating significant differences between the predicted and experimental data at these concentrations. Similarly, the model showed larger deviations for freshwater treatment (FW) on Day 0, with MAEs ranging from 0.049 to 2.136 across different concentrations. In contrast, by Day 8, the predictions for marine and freshwater treatments improved significantly, with each concentration showing a low MAE of less than 0.1. This suggests a much closer alignment between predicted and experimental values for both types of

water, highlighting the model's enhanced accuracy as the experiment progressed. Despite these deviations, the model generally agrees with the experimental results, indicating its effectiveness in predicting NH_3 removal throughout the bioremediation process. Most differences between predicted and actual results occurred at the experiment's early stages, suggesting some initial adjustment during the early period. Therefore, the model effectively provides useful predictions for NH_3 removal.

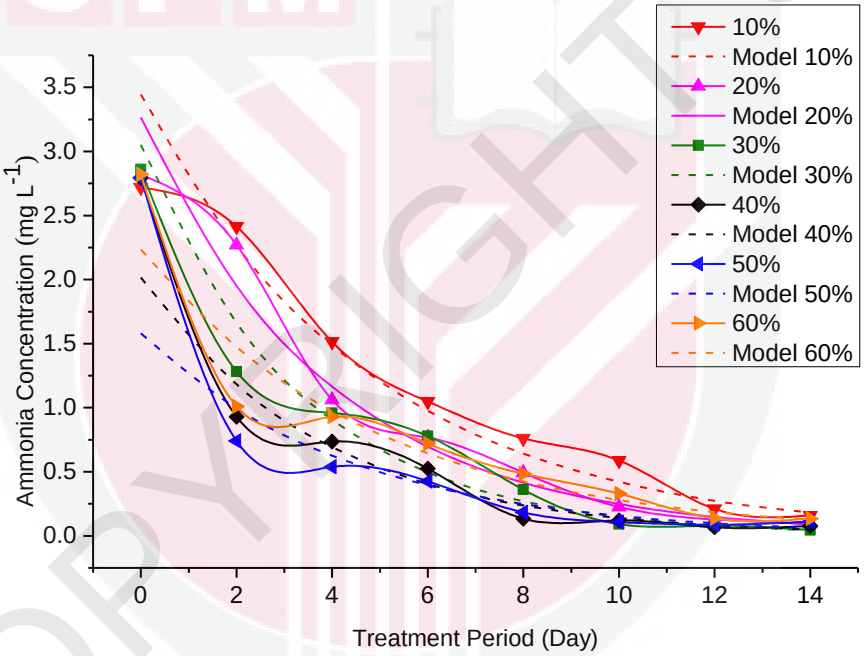

Figure 4.17 : Correlation between Predicted Data (Dash Line) and Experimental Data (Solid Line Symbol) of NH_3 Removal in Marine Aquaculture Wastewater at Different Microalgae Concentrations

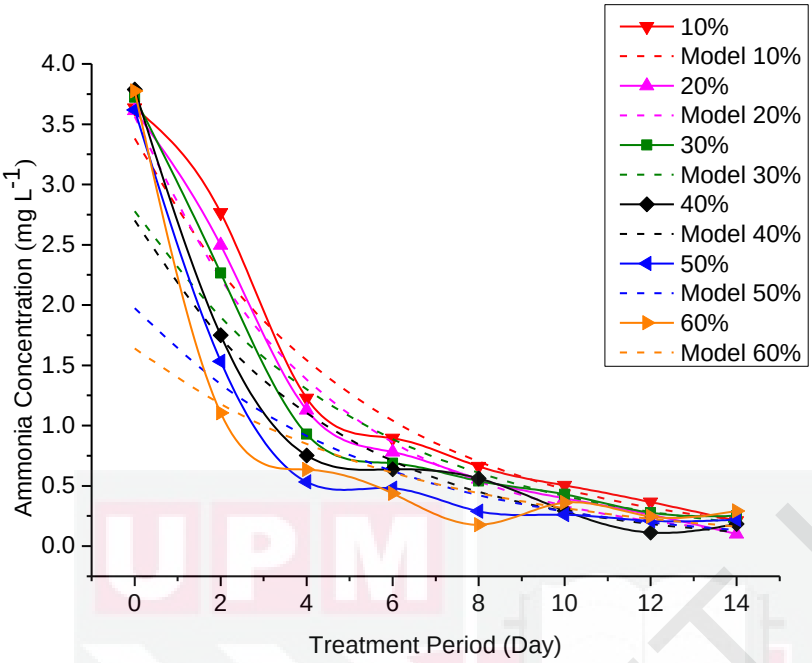

Figure 4.18 : Correlation between Predicted Data (Dash Line) and Experimental Data (Solid Line Symbol) of NH_3 Removal in Freshwater (FW) Aquaculture Wastewater at Different Microalgae Concentrations

4.4.5.2 Nitrite Removal Efficiency

Figure 4.19 and Figure 4.20 illustrate the graph of ln NO_2^- concentration versus treatment period (day), which was used to determine the first-order kinetic equation, coefficient rate constant, and coefficient of determination (R_2). The steepness of the gradient observed in the graph indicates a higher coefficient rate constant, which in turn implies a higher removal efficiency of NO_2^-. According to Table 4.7, water samples containing 40% (v/v) microalgae concentrations in both marine and freshwater exhibited the steepest gradients, measuring 0.2056 and 0.1948, respectively. The predictions for NO_2^- removal efficiency based on the development equation in marine water (MW) and freshwater (FW) samples at Day 10 yielded values lower than 85%, precisely 79.1% and 82.6%, respectively. These results suggest a slightly less effective

capability in removing NO_2^-. However, it is essential to note that as the experiment progressed until Day 12 and increased the microalgae concentration, the removal efficiency increased significantly, reaching 92%. This finding indicates that the optimum concentration is determined over an extended period, and the effectiveness of removing NO_2^- improves, resulting in higher removal efficiencies. This model highlights the importance of considering the treatment period when evaluating the efficacy of NO_2^- removal in the samples.

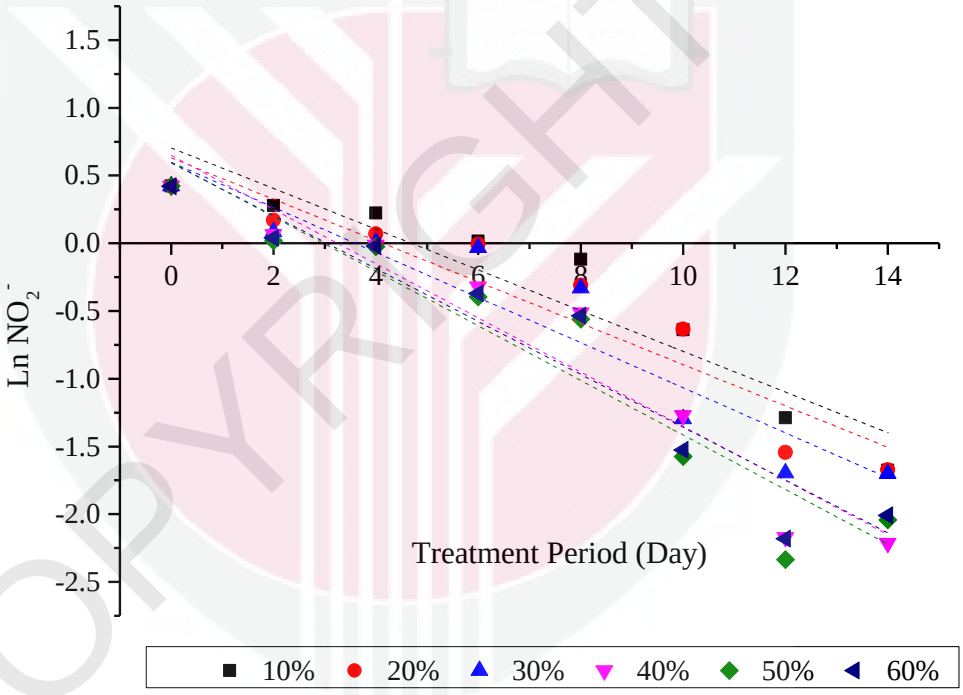

Figure 4.19 : Graph of ln NO_2^- Versus Treatment Period (Day) at Different Microalgae Concentrations of Marine Water Treatment

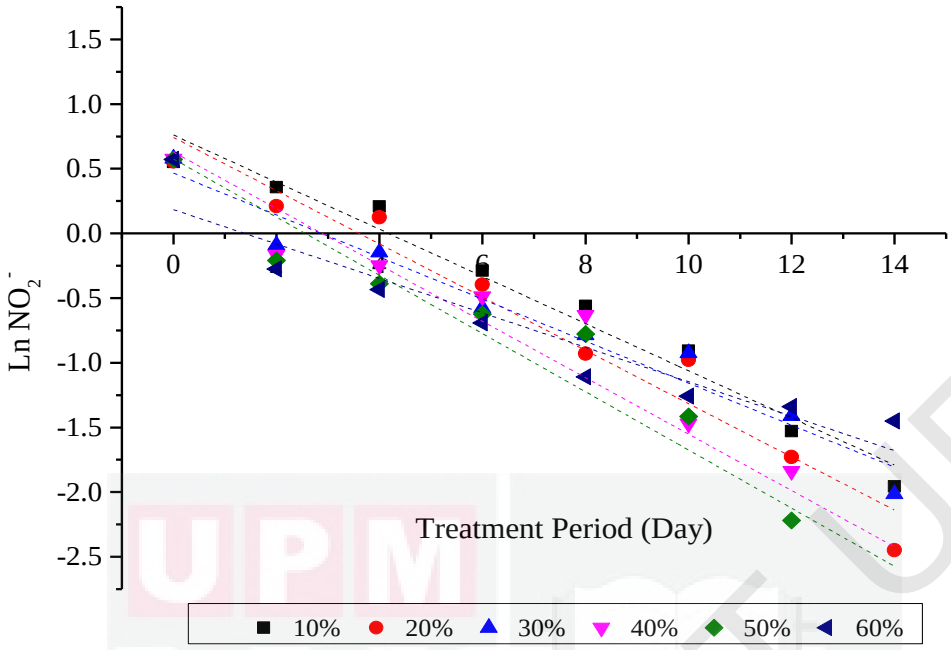

Figure 4.20 : Graph of ln NO_2^- versus Treatment Period (Day) at Different Microalgae Concentrations of Freshwater Treatment

Table 4.7 : First-Order Kinetic Equation of Nitrite, NO_2^- Removal Efficiency at Different Microalgae Concentrations for Two Types of Wastewaters

Microalgae Concentration (%, v/v)	Types of wastewater	Initial Concentration of NO_2^- (mg L^{-1})	First Order Kinetic $\ln[A] = -kt + \ln[A]_o$.	(-) k	R^2
10	MW	1.524	y=-0.1455x + 0.6558	0.1455	0.8745
	FW	1.772	y=-0.1548x + 0.3898	0.1548	0.9627
20	MW	1.525	y=-0.1435x + 0.539	0.1435	0.861
	FW	1.737	y=-0.2032x + 0.7155	0.2032	0.9536
30	MW	1.527	y=-0.1518x + 0.45	0.1518	0.8475
	FW	1.727	y=-0.1831x + 0.7684	0.1831	0.974
40	MW	1.528	y=-0.1948x + 0.596	0.1948	0.9137
	FW	1.726	y=-0.2056x + 0.5038	0.2056	0.9031
50	MW	1.527	y=-0.1923x + 0.5071	0.1923	0.889
	FW	1.754	y=-0.2053x + 0.3788	0.2053	0.9129
60	MW	1.522	y=-0.1825 + 0.4662	0.1825	0.8877
	FW	1.766	y=-0.1106x + 0.0416	0.1106	0.9653

Note: MW (Marine water), FW (Freshwater)

Figures 4.21 and 4.22 visually compare the predicted and experimental data of NO_2^- removal over time in marine water (MW) and freshwater (FW) aquaculture wastewater at various microalgae concentrations using the

developed model. During the initial phase of the experiment, slight deviations were noted between the predicted and experimental data points for all concentrations in MW. The model consistently overestimated the nitrite concentrations, with the difference between predicted and actual values ranging from 0.3 to 0.4 mg L^{-1}. This difference was calculated by subtracting the actual concentration from the predicted concentration. These deviations can be attributed to the lag phase of microbial processes, including nitrite removal, which requires time for the microalgae to acclimate and reach optimal performance. The predictive model may not be accurate for this lag phase, causing some differences between predicted and observed efficiencies at the beginning of the experiment. Therefore, despite the initial deviations, the predicted values can still be utilized effectively in the experiment's later stages (exponential, stationary, and decline).

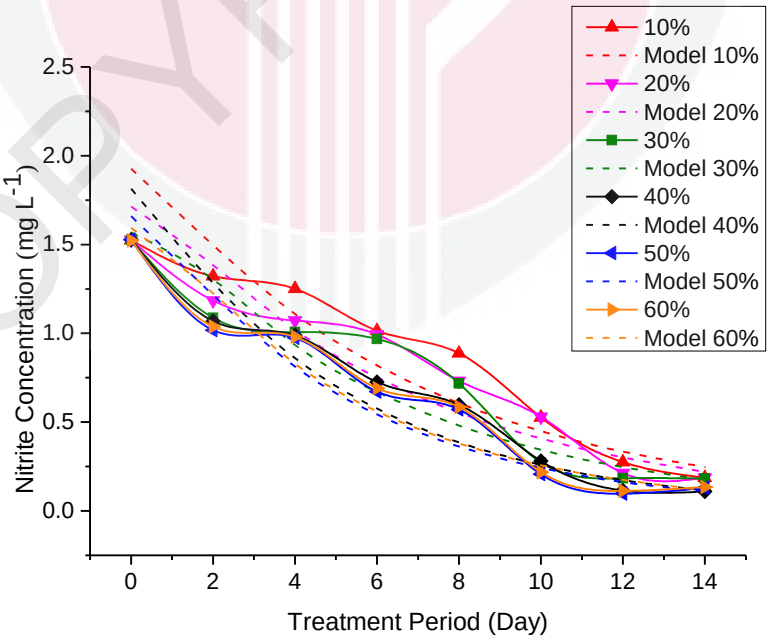

Figure 4.21 : Correlation between Predicted Data (Dash Line) and Experimental Data (Solid Line Symbol) of Removal NO_2^- in Marine Aquaculture Wastewater at Different Microalgae Concentrations

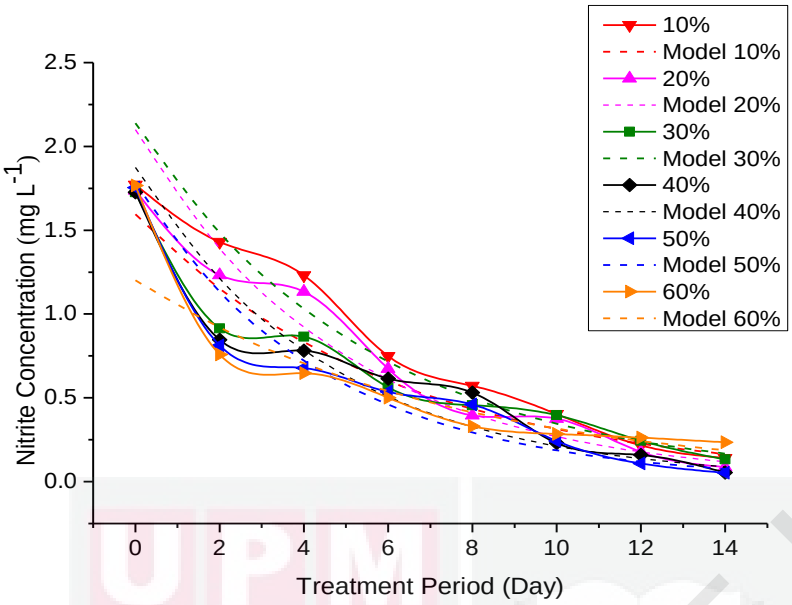

Figure 4.22 : Correlation between Predicted Data (Dash Line) and Experimental Data (Solid Line Symbol) of Reduction NO_2^- in Freshwater Aquaculture Wastewater at Different Microalgae Concentrations

4.4.5.3 Orthophosphate Removal Efficiency

Figure 4.23 and Figure 4.24 depict the relationship between the natural logarithm (ln) of PO_4^{-3} concentration and the treatment period (day). These graphs were utilized to establish the first-order kinetic equation, calculate the coefficient rate constant, and determine the coefficient of determination (R^2). The steepness of the gradient observed in the graph indicates a higher coefficient rate constant, which suggests a more rapid removal of PO_4^{-3} and, thus, higher removal efficiency of this nutrient. According to the data presented in Table 4.8, samples with a microalgae concentration of 30% v/v (MW) and 50% v/v (FW) exhibited the highest slope with 0.1372 and 0.2652, respectively. Additionally, these samples exhibited high R^2 values (>0.9), indicating a strong correlation between the ln concentration PO_4^{-3} and the treatment period (day).

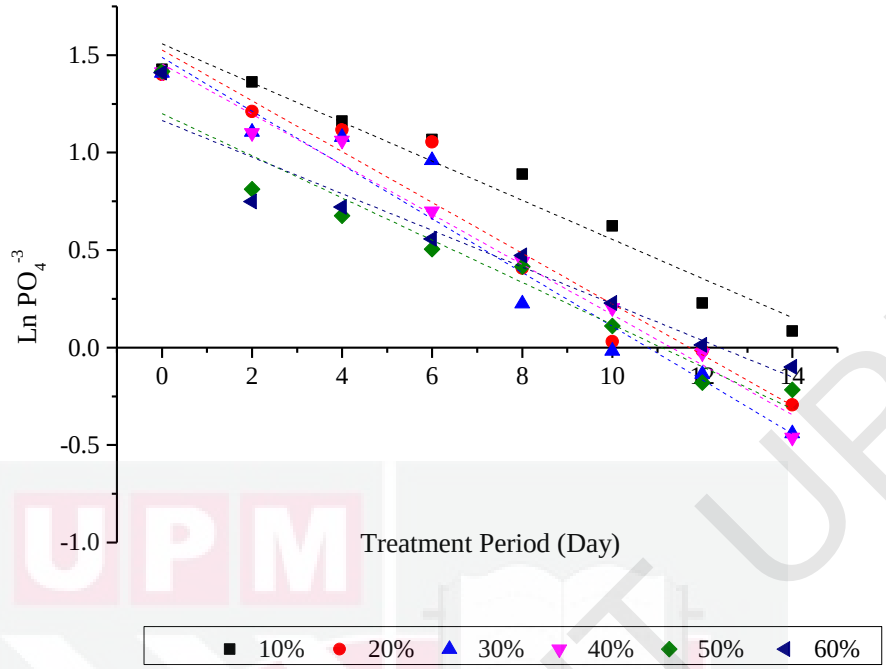

Figure 4.23 : Graph of ln PO_4^{-3} Versus Treatment Period (Day) at Different Microalgae Concentrations of Marine Water Treatment

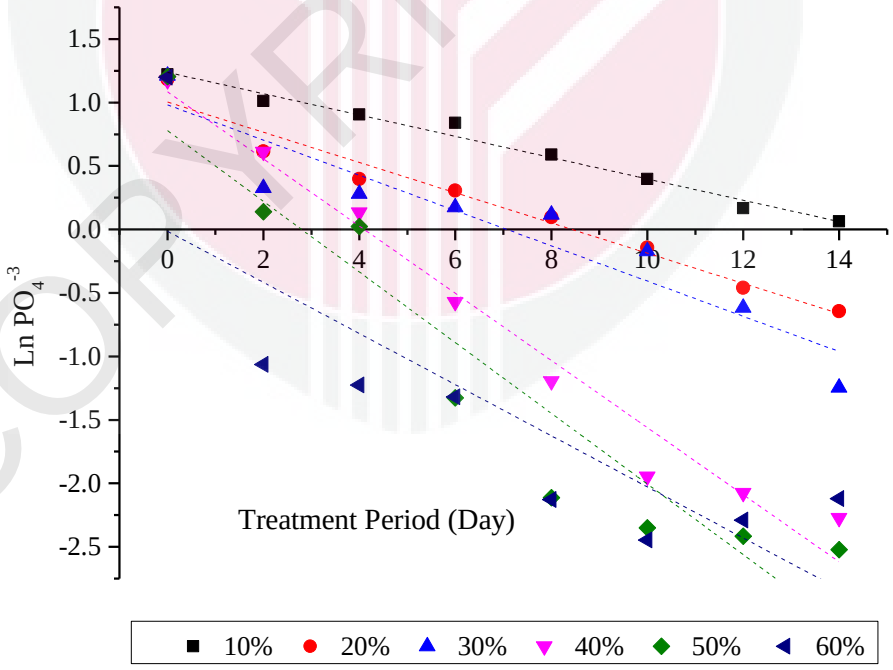

Figure 4.24 : Graph of ln PO_4^{-3} Versus Treatment Period (Day) at Different Microalgae Concentrations of Freshwater Treatment

Table 4.8 : First-Order Kinetic Equation of Orthophosphate, PO_4^{-3} Removal Efficiency at Different Microalgae Concentrations for Two Types of Wastewaters

Microalgae Concentration (%, v/v)	Types of wastewater	Initial Concentration of PO_4^{-3} (mg L^{-1})	First Order Kinetic $\ln[A] = -kt + \ln[A]_o$.	(-) k	R^2
10	MW	4.164	y=-0.1003x + 1.5578	0.1003	0.9586
	FW	3.394	y=-0.084x + 1.2373	0.084	0.9841
20	MW	4.058	y=-0.1303x + 1.5258	0.1303	0.9434
	FW	3.384	y=-0.1205x + 1.0177	0.1191	0.9642
30	MW	4.087	y=-0.1372x + 1.4814	0.1372	0.9481
	FW	3.375	y=-0.1391x + 0.9836	0.135	0.8857
40	MW	4.112	y=-0.1239x + 1.4074	0.1239	0.977
	FW	3.542	y=-0.2634x + 1.0706	0.2571	0.9683
50	MW	4.121	y=-0.1009x + 1.1263	0.1009	0.9711
	FW	3.478	y=-0.2734x + 0.7027	0.2652	0.9039
60	MW	4.094	y=-0.0833x + 1.0575	0.0833	0.969
	FW	3.466	y=-0.2032x + 0.0037	0.1833	0.6891

Note: MW (Marine water), FW (Freshwater)

Figures 4.25 and 4.26 represent the predicted and experimental data of PO_4^{-3} removal over the treatment period in marine water (MW) and freshwater (FW) aquaculture wastewater. Using the developed model, these figures visually compare the predicted and experimental values at different microalgae concentrations. The kinetic model was highly accurate in predicting orthophosphate removal from wastewater in both MW and FW, except for 60% (v/v) concentrations in FW during the early treatment period. There was a significant difference between the predicted and experimental values of 60% for FW, with the predicted value being higher by 2.452 mg L^{-1} compared to the experimental measurements. Moreover, in this study, the model's performance was comparatively lower, as indicated by the coefficient of determination (R_2) falling below 0.9. Precisely, the model's predictions for *Chlorella* sp. biomass closely matched the corresponding experimental results.

For example, the experimental concentrations of orthophosphate for freshwater (FW) on Day 6 were 1.358 mg L^{-1} for 20% (v/v) and 1.191 mg L^{-1} for 30% (v/v). These experiments aligned with the corresponding predicted concentrations of 1.334 mg L^{-1} and 1.16 mg L^{-1}, respectively. In contrast to marine water (MW), the predicted concentrations of orthophosphate for 20% (v/v) and 30% (v/v) were significantly lower compared to the experimental concentrations. The experimental concentration for 20% was 2.8713 mg L^{-1}, whereas the predicted concentration was 2.105 mg L^{-1}. Similarly, the experimental concentration for 30% was 2.6123 mg L^{-1}, while the predicted concentration was 1.936 mg L^{-1}. The obtained results for orthophosphate in aquaculture wastewater provide compelling evidence that supports the reliability and effectiveness of the kinetic model in accurately representing the growth dynamics and nutrient removal capabilities of microalgae in the specific wastewater treatment context studied.

This evidence further supports the belief that microalgae are capable of assimilating ammonia (NH_3) and phosphate (PO_4) directly for their cell growth and metabolic functions (Mohsenpour et al., 2021). The close agreement between the model predictions and the observed data for orthophosphate indicates that the model can effectively capture and predict the uptake and utilization of nutrients by microalgae in wastewater. The results suggest that microalgae significantly remove ammonia and phosphate from aquaculture wastewater, assimilating these nutrients for their growth and metabolic activities. This finding highlights the potential of microalgae as efficient bioremediation agents for nutrient removal in aquaculture systems. The kinetic

model provides valuable insights into nutrient assimilation and removal mechanisms in aquaculture wastewater treatment by understanding the interplay between microalgae, ammonia, and phosphate. These findings contribute to our knowledge of microalgae-based bioremediation processes and support their application in sustainable wastewater treatment strategies.

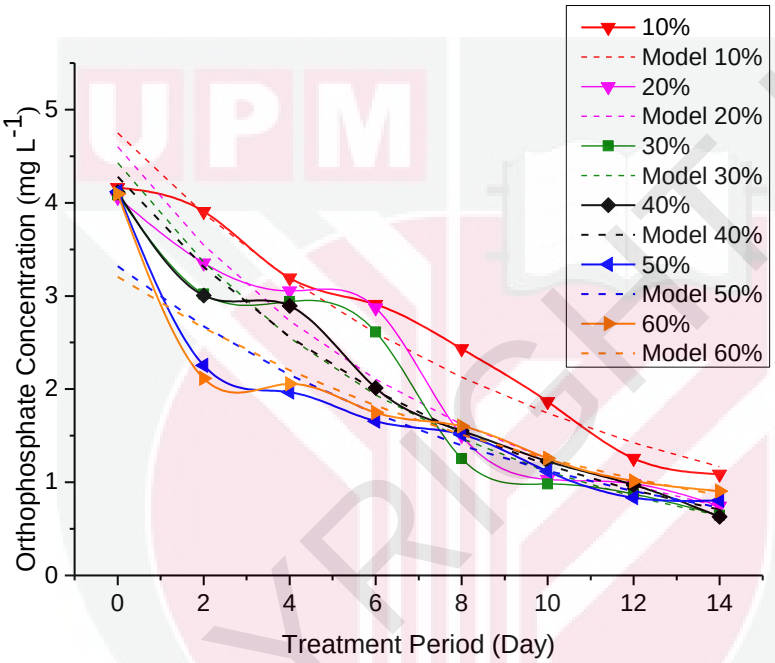

Figure 4.25 : Correlation between Predicted Data (Dash Line) and Experimental Data (Solid Line Symbol) of Removal PO_4^{-3} in Marine Aquaculture Wastewater at Different Microalgae Concentrations

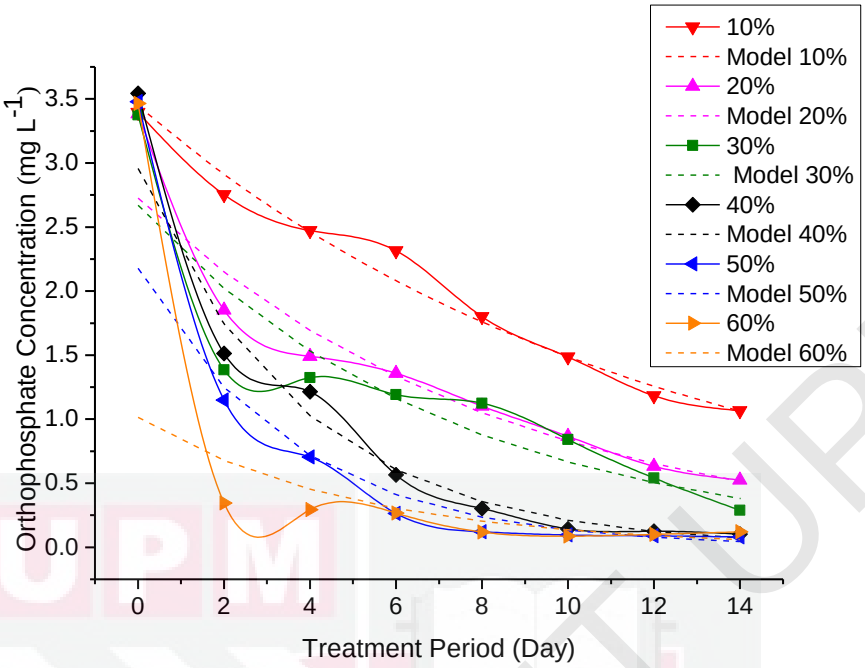

Figure 4.26 : Correlation between Predicted Data (Dash Line) and Experimental Data (Solid Line Symbol) of Removal PO_4^{-3} in Freshwater Aquaculture Wastewater at Different Microalgae Concentrations

4.5 Conclusion

In conclusion, this study presents an innovative approach to balancing aquaculture growth with environmental sustainability through bioremediation using *Chlorella* sp. in marine and freshwater conditions. The results indicate that varying dosages of *Chlorella* sp. from 10% to 60% were tested, with 30% selected for marine (MW) and 40% for freshwater (FW), based on achieving the highest nutrient removal efficiencies for ammonia, nitrite, and orthophosphate. The research also aims to achieve simultaneous wastewater treatment and nutrient removal by developing kinetic models to remove nutrients. Once calibrated with experimental data, these models can accurately predict *Chlorella* sp. cultivation performance across diverse aquaculture wastewater scenarios. Therefore, understanding the responses

of these strains to varying treatments is essential for optimizing bioremediation strategies. In addition, characterizing the effects of bioremediation on the physical and chemical properties of *Chlorella* also provides valuable insights into their effectiveness in wastewater treatment.

Building on these findings, future research should focus on critical areas to further enhance this approach. First, the kinetic model should be optimized for real-world situations. Second, exploring additional microalgae strains and their nutrient removal efficiencies can lead to more effective bioremediation. Third, studies should include continuous or semi-continuous systems. Lastly, assessing the long-term stability and economic feasibility of microalgae-based technologies in various aquaculture settings is essential for practical implementation. Addressing these factors could position microalgae technologies as a sustainable, cost-effective solution for treating aquaculture wastewater.

CHAPTER 5

OPTIMIZATION OF MICROALGAE BIO-HARVESTING USING BIO-FLOCCULANT FILAMENTOUS FUNGUS

5.1 Introduction

Microalgae are promising biorefinery biomass sources for biofuels and bio-based products due to their advantages of biodegradability and non-toxic properties over terrestrial plants (Hannon et al., 2010). Harvesting techniques, including mechanical filtration, centrifugation, and flocculation, are crucial for high efficiency (Molina Grima et al., 2003). However, harvesting microalgae presents challenges due to its low density (between 0 and 5 g L^{-1}), small size (between 3 and 30 μm diameter), and negative charges on its surfaces (Molina Grima et al., 2003). Conversely, due to the difficulties of harvesting microalgae under normal conditions, microalgae cells cannot produce flocs and self-flocculating due to negative charges on their surfaces (Madkour et al., 2020; Zhao et al., 2021). Previous studies have identified significant limitations in applying bio-flocculants, such as the flocculation activity and cultivation costs (Kurniawan et al., 2020). Nasir et al. (2015) highlighted the need for sustainable harvesting techniques to address these issues, as microalgae biomass can release absorbed nutrients, particularly ammonia, into water bodies during the declining growth phase. In water pollution, ammonia contamination is frequently found in water bodies and is widespread as an environmental issue. Therefore, sustainable harvesting techniques are required. According to our previous studies, the bio-flocculant produced by the fungus *Aspergillus niger* (*A.niger*) is efficient for the flocculation of microalgae,

Chlorella sp.

One of the promising techniques for efficient and sustainable harvesting is fungus-based harvesting, where filamentous fungi are co-cultivated with microalgae. The fungi form a network of hyphae that trap the microalgal cells, making it easier to separate the biomass from the culture medium. Optimizing the conditions for this sustainable harvesting approach is crucial to maximize harvesting efficiency. This is where Response Surface Methodology (RSM) comes into play. RSM is a statistical tool for modeling and analyzing problems where several variables influence a response. It helps understand the interactions between these variables and identify the optimal conditions for the desired outcome. Applying RSM to fungus-based microalgae harvesting can systematically vary critical factors such as pH, temperature, nutrient concentration, fungal and microalgal inoculum ratio, and agitation speed.

Through a series of well-designed experiments, RSM allows for developing a mathematical model that predicts the best conditions for maximizing harvesting efficiency. This approach saves time and resources compared to traditional optimization methods and provides valuable insights into the interactions between different variables. Consequently, it enhances the sustainability and cost-effectiveness of microalgal biomass production, contributing to the advancement of biofuel technologies and other applications. Therefore, this present study aimed to investigate the effectiveness of the *A.niger* in harvesting green microalgae, *Chlorella* sp., by determining the optimum condition. First, the harvesting process was started

by screening the variables using one-factor-at-time (OFAT). Afterwards, the significant variables for optimum harvesting efficiency were optimized by the effect of three independent variables, dosage, pH, and mixing rate, using response surface methodology (RSM) based on central composite design (CCD). RSM was used in this phase to optimize the operational conditions for the best outcomes and obtain a predictive model that adequately represents response changes based on the input variables. This research provides a solid background that can be applied in the future to microalgae harvesting techniques.

Figure 5.1 outlines the step-by-step procedure for achieving Objective 2, which is to determine the optimal conditions for harvesting green microalgae biomass using the filamentous fungus *Aspergillus niger*. The figure begins with the bio-harvesting process and progresses through the 'One-Factor-at-a-Time' (OFAT) approach, where factors such as dosage (0 – 35 g L^{-1}), pH (4 – 10), and mixing rate (0 – 150 rpm) are evaluated for their impact on harvesting efficiency. The optimal results from the OFAT analysis are then used as input for further optimization through Response Surface Methodology (RSM), employing a Central Composite Design (CCD). The RSM focuses on a narrower range of factors, including dosage (25 – 35 g L^{-1}), pH (6 – 8), and mixing rate (100 – 150 rpm), to optimize the conditions for maximizing harvesting efficiency.

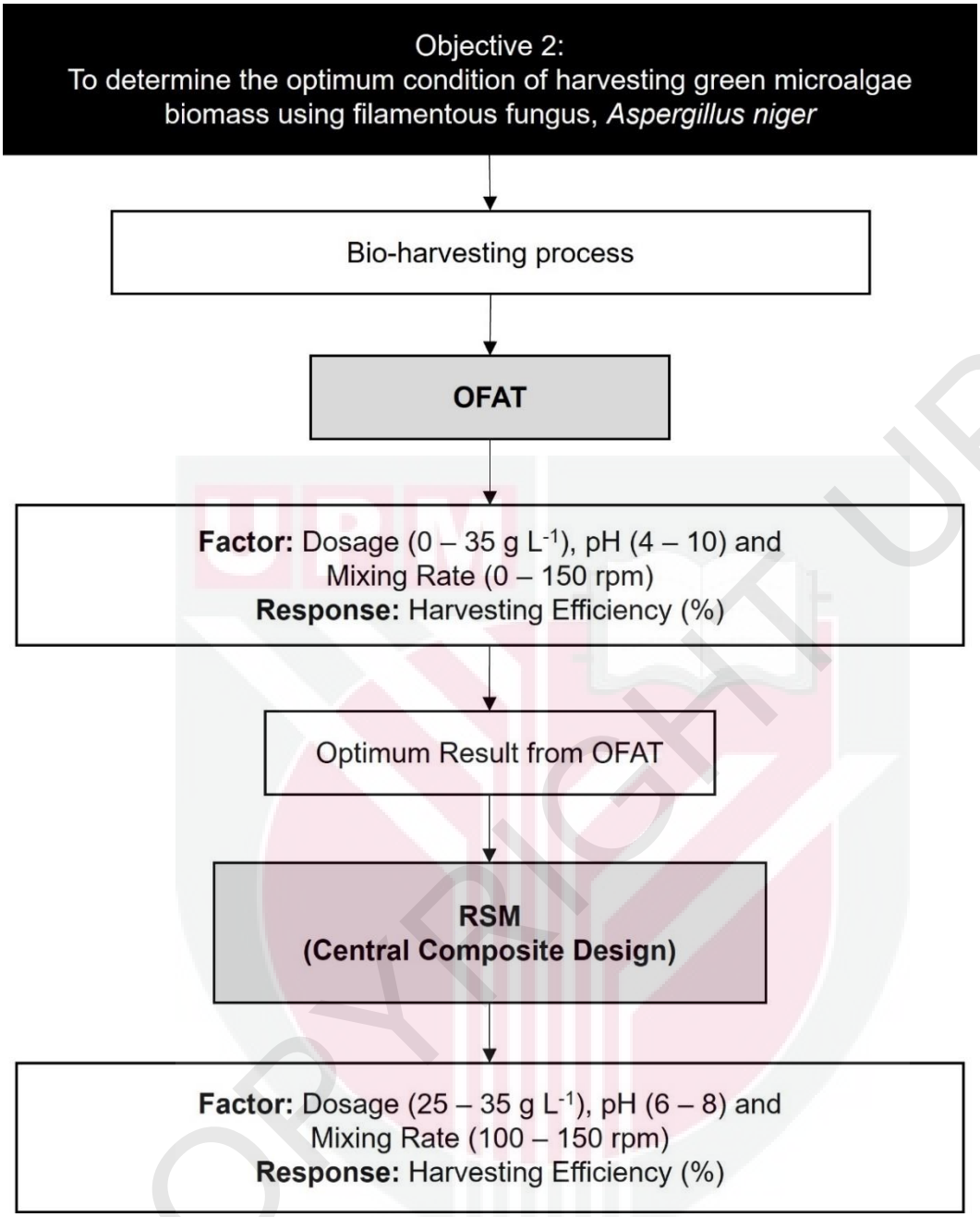

Figure 5.1 : Flow Chart of Experiments Conducted for the Optimization of Bioflocculant, *Aspergillus niger* in Harvesting Green Microalgae

5.2 Methodology

5.2.1 Experimental Design of Microalgae Harvesting

The harvesting process was conducted using water samples containing *Chlorella* sp. biomass collected from the bioremediation process on Day 10. A

detailed procedure for the harvesting process can be found in Section 3.4.3 of the study. The effects of various flocculation parameters were individually assessed before optimizing the harvesting process using response surface methodology (RSM). The initial investigation used the 'one-factor-at-a-time' (OFAT) approach to determine the optimal conditions for different parameters: bio-flocculant dosage, pH levels, and mixing rates. During OFAT, the bio-flocculant dosages were 0, 5, 10, 15, 20, 25, 30, and 35 g L^{-1}, the pH levels tested ranged from 4 to 10, and the mixing rates were 0, 25, 50, 75, 100, 125 and 150 RPM. Table 5.1 summarizes the optimal conditions and efficiency percentages for marine and freshwater wastewater treatments. The highest efficiency was achieved with a bio-flocculant dosage of 30 g L^{-1}, pH 7, and a mixing rate of 125 RPM. The OFAT results indicate that harvesting efficiency for both wastewater types exceeded 90%.

Table 5.1 : Experimental Result from Bioremediation Process for Marine Wastewater and Freshwater Wastewater

Factor	Marine water Wastewater		Freshwater Wastewater	
	Optimum	Efficiency (%)	Optimum	Efficiency (%)
Dosage (g L^{-1})	30	90.45	30	97.36
pH	7	91.0	7	96.90
Mixing Rate (rpm)	125	95.20	125	97.32

Based on the previous findings, the harvesting process was optimized using RSM. Initially, the study explored the effects of flocculation parameters on bio-flocculation efficiency. Subsequently, the harvesting process was optimized using RSM, a statistical and mathematical approach that aids in identifying the best conditions for achieving maximum efficiency.

The optimization procedure was carried out using CCD depending on the three independent factors: a dosage of bio-flocculant (X_1), pH (X_2), and mixing rate (X_3). These parameters were chosen based on a study reported by Mohd Nasir et al. (2019) as they significantly impact the microalgae biomass harvesting process. To further investigate the interaction of these factors and achieve maximum harvesting efficiency, a study was conducted under controlled conditions with a constant temperature of 27 ± 0.2 °C throughout the experiment.

5.2.2 Collection and Preparation of Water Sample for Harvesting Process

For the harvesting process, the water samples were collected in the different bioremediation aquaculture wastewater, namely freshwater and marine water wastewater. The first set of samples consisted of freshwater containing *Chlorella* sp. UMT LF1, while the second set of samples consisted of marine water with *Chlorella* sp. UMT LF2. To investigate the effect of different parameters on harvesting efficiency, the water samples were obtained based on the findings of optimum conditions (dosage of microalgae) in Chapter 4. The results indicated that the optimum condition for water samples from freshwater (FW) is 40% (v/v), while marine water (MW) is 30% (v/v).

5.2.3 Cultivation of Filamentous Fungus and Pelletization

Fungus was initially observed as creamy white spores, turning black after 4 to 6 days (Khan et al., 2003). It was grown on potato dextrose agar (PDA) and fermented in Richard's Broth. The fungus pellet, prepared as described in

Section 3.4.2, was used for harvesting *Chlorella* sp. during the harvesting process.

5.3 Data Analysis of Microalgae Harvesting

Data analysis was crucial in optimizing the microalgae harvesting process. The Design Expert® Version 13 and the Statistical Analysis System (SAS) were used for experiment design, statistical analysis, and result validation. Analysis of Variance (ANOVA) assessed the significance of factors and their interactions, with model adequacy checked through R-squared values and residual plots. Response Surface Methodology (RSM) was employed to optimize factors such as bio-flocculant dosage, pH, and mixing rate, with Central Composite Design (CCD) used to structure the experimental runs. The second-order polynomial model represented the detailed behavior of the response, while contour and 3D surface plots visualized the results. This led to identifying validated optimal conditions and contributed to advancements in sustainable harvesting techniques.

5.4 Results and Discussion

Before proceeding to the harvesting process, the optimum conditions batch experiment in our previous studies were determined using a 'one-factor-at-a-time' (OFAT) approach for microalgae harvesting with filamentous fungus (Mohd Nasir et al., 2019; Nasir et al., 2015). The OFAT results revealed that the optimal conditions were identified at conditions of 30 g L^{-1} bio-flocculant dosage, pH 7, and 125 RPM mixing rate, which were found to be most effective, and these parameters were applied to both marine and freshwater

treatments. Besides, it significantly influences the yield and quality of microalgae harvesting using *A. niger* with removal of more than 90%. Figure 5.2 shows a visual representation of the microalgae culture in a conical flask that demonstrates successful harvesting by the bio-flocculating fungus.

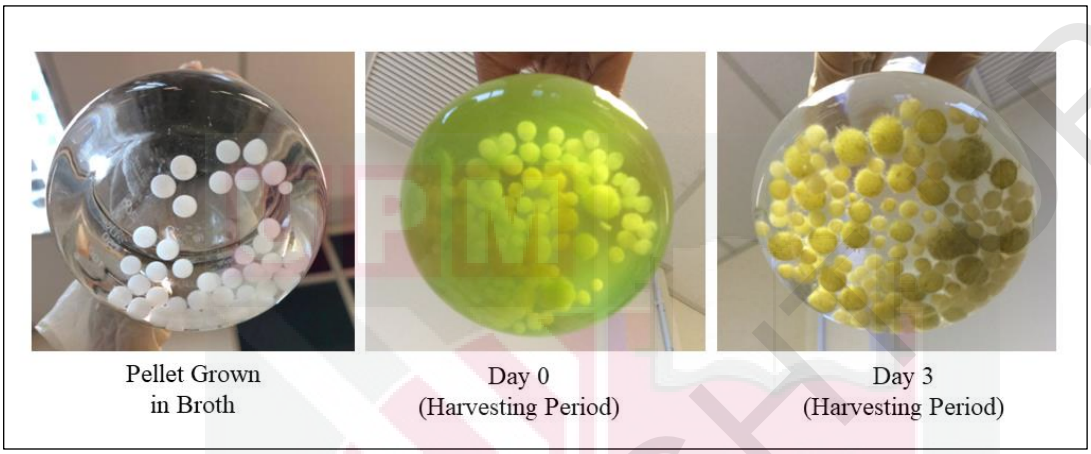

Figure 5.2 : Harvesting Process of Microalgae Using Bio Flocculant Fungus

5.4.1 Optimization Using Response Surface Methodology (RSM) of Bio-Flocculation of Microalgae

Table 5.2 compares the actual and predicted harvesting efficiency percentages of microalgae in marine and freshwater conditions across various experimental runs, with the variables considered being dosage, pH, and mixing rate. The results show a high consistency in actual values for runs with identical conditions for the optimum conditions identified using the One-Factor-At-A-Time (OFAT) approach, a dosage of 30 g L^{-1}, pH 7, and a mixing rate of 125 RPM. These conditions consistently yielded high harvesting efficiencies in marine water, ranging from 88.9% to 97.7%, and in freshwater, from 79.4% to 93.5%. The predicted values align well with the actual values, indicating that

the Response Surface Methodology (RSM) model effectively predicts harvesting efficiency, with minimal errors observed between the actual and predicted values. The data suggests that higher dosages, such as 35 g L^{-1}, do not necessarily correlate with higher harvesting efficiency, as seen in run 2, resulting in lower efficiencies than the optimum condition.

Table 5.2 : Comparison of Actual and Predicted Harvesting Efficiency of Microalgae Concentrations

Run	Dosage	pH	Mixing Rate	Marine Water Harvesting Efficiency (%)		Freshwater Harvesting Efficiency (%)	
				Actual Value	Predicted Value	Actual Value	Predicted Value
1	30	7	125	97.7	91.6	93.5	87.9
2	35	6	150	59.6	62.2	35.6	29.1
3	30	7	125	90.7	91.9	91.2	87.9
4	30	7	82.955	71.2	73.1	37.3	32.9
5	30	7	125	89.5	91.6	86.1	87.9
6	35	8	150	53.7	53.4	50.2	50.0
7	35	8	100	60.2	64.3	46.8	45.0
8	25	8	100	91.4	88.5	16.9	26.0
9	30	7	125	89.0	91.6	90.1	87.9
10	25	6	150	70.6	66.1	56.6	61.0
11	38.409	7	125	51.6	50.3	34.4	41.1
12	25	8	150	54.6	58.8	54.4	57.5
13	35	6	100	62.5	58.0	42.9	42.4
14	25	6	100	80.88	80.7	45.0	47.8
15	21.591	7	125	72.1	73.9	62.3	52.0
16	30	7	167.045	53.1	51.7	47.4	48.2
17	30	8.682	125	82.1	78.8	59.3	54.5
18	30	7	125	88.9	91.6	79.4	87.8
19	30	5.318	125	76.7	79.7	54.1	55.3
20	30	7	125	93.9	91.6	84.4	87.9

At a low concentration of *A. niger* and a high pH of 25 g L^{-1} and pH 8, the harvesting efficiency of microalgae biomass was not as significant, with yields of only 54.6% (Run 8) and 54.2% (Run 12). This suggests that the use of a low concentration of *A. niger* and a high pH may not be optimal for efficient biomass harvesting. The optimal concentration of 30 g L^{-1} aligned with the

findings of Nasir et al. (2015), who conducted their experiments in one-factor-at-time' (OFAT). In contrast, the study found that pH did not significantly impact harvesting efficiency. Therefore, a natural pH value of 7 was chosen as the optimal pH for the experiment. A previous study similarly stated that the highest harvesting rate and efficiency for microalgae using filamentous fungus White-rot fungi occurred under neutral conditions; about 99% of the microalgae were harvested within the first 24 h (Civzele & Mezule, 2022). Nevertheless, it is essential to note that aquaculture wastewater often experiences fluctuations in pH due to daily and seasonal changes (Dey et al., 2021). As a result, a reasonable inference is that in wastewater with a pH of around 7, the bio-flocculation process is expected to be most efficient. However, at pH levels significantly higher or lower than 7, achieving an equally high harvesting efficiency might require more time.

The effect of mixing rate on microalgae harvesting efficiency was investigated in the study. The range of mixing rates analyzed was from 100 rpm to 150 rpm. The results revealed that slower mixing rates did not lead to a significant improvement in harvesting efficiency. However, it was observed that at a mixing rate of 100 rpm, the microalgae began to absorb into the bio-flocculant. However, when the mixing rate was increased to 150 RPM, the microalgae were disrupted and re-dispersed. This phenomenon can be explained by the increased agitation at higher mixing rates, which caused the microalgae to become unsettled and separate from the bio-flocculant. On the other hand, at a higher mixing rate of 150 RPM, the increased agitation caused the microalgae to become unsettled and re-dispersed. The increased turbulence

and agitation may disrupt the interaction between the microalgae cells and the bio-flocculant and lead to the separation of the microalgae from the bio-flocculant. On the contrary, at a lower mixing rate, the microalgae cells have more time to encounter the bio-flocculant, allowing for better absorption and aggregation.

Harvesting efficiency tends to be slightly higher in marine water under optimal conditions than in freshwater, possibly due to differences in microalgal species' adaptability or ionic strength in marine environments, which aid in better flocculation. These findings have significant practical implications for microalgae-based bioremediation, emphasizing optimizing operational parameters for maximum efficiency. Further fine-tuning of conditions, conducting pilot-scale studies, exploring different microalgae strains, and performing a detailed cost-benefit analysis are recommended to enhance the efficacy and economic viability of the bioremediation process.

5.4.2 Fitting of Quadratic Model

The results from the optimization experiments were analyzed using standard ANOVA to examine the relationship between the response function (Y) and the independent variables (X). The central composite design was then fitted to polynomial equations. For example, a study by Elcik et al. (2023) also employed RSM. It fitted their experimental data to a quadratic model to optimize microalgae biomass harvesting using chitosan as a flocculant, achieving high biomass recovery rates. The mathematical relationship between (*X*) and (*Y*) for marine water and freshwater harvesting can be

approximated by a quadratic polynomial equation as follows:

$$Y_{marine} = 91.6 - 7.02X_1 - 0.2522X_2 - 6.35X_3 - 0.3650X_1 X_2 + 4.71X_1 X_3 - 3.77X_2 X_3 - 10.42X_1^2 - 4.36X_2^2 - 10.32 X_3^2 \quad (....5.1)$$

(R^2= 0.9597)

$$Y_{fresh} = 88.01 - 2.59X_1 + 1.30X_2 + 4.98X_3 + 4.97X_1X_2 - 7.75X_1X_3 + 1.95X_2X_3 - 15.5X_1^2 - 12.55 X_2^2 - 16.05X_3^2 \quad (....5.2)$$

(R^2 = 0.9782)

Where:

Y_{marine} is Harvesting Efficiency marine water species,

Y_{fresh} is Harvesting Efficiency Freshwater species,

X_1, X_2, and X_3 are dosages, pH, and mixing rate.

The fit of the models was evaluated using the coefficients of determination, R-squared (R_2), which were calculated to be 0.9597 and 0.9782 for Equation (5.1) and (5.2), respectively. These R-squared values indicate that these regression equations can explain approximately 96% and 98% of the variability in the response (harvesting efficiency). Since the R-squared values for both the marine and freshwater models are close to 1, it suggests that these equations provide a good fit to the data. This indicates that the models are reliable for predicting harvesting efficiency based on the specified variables.

Equations 5.1 and 5.2 include linear and quadratic terms for the independent variables. It considers the linear relationship between each variable and harvesting efficiency and allows for nonlinear relationships through the squared terms (X_1^2, X_2^2, and X_3^2). It can be seen from the coefficients in Equation 5.1 that the harvesting efficiency in marine increases with the decrease of dosage (X_1), pH (X_2), and mixing rate (X_3). Besides, the coefficient $4.71X_1X_3$ suggests a positive interaction effect between dosage (X_1) and mixing rate (X_3) on harvesting efficiency. In Equation 5.2 for freshwater, the coefficient -2.59 indicates that an X_1 (dosage) increase would decrease harvesting efficiency. In contrast, pH (X_2) and mixing rate (X_3) are variables that increase harvesting efficiency. This suggests that higher pH levels and mixing rates positively impact harvesting efficiency. Tables in Appendix G provide a comprehensive overview of how well the data aligns with different models, including linear, two-factor, quadratic, and cubic models. The statistical significance of these model equations was discussed using the F-test for ANOVA to determine the most accurate representation. This analysis revealed that a quadratic polynomial model most effectively and accurately describes the harvesting efficiency.

The *F-values* of the models were greater than 30, and their associated *P-values* ($p<0.05$) were very low, indicating that all the models were statistically significant. In other words, there was less than a 5% chance that the observed *F-values,* being of such magnitude, could be attributed to random variation or noise alone. Furthermore, the lack of fit was insignificant, indicating that the model was well-suited to represent the experimental data (Sharma et al.,

2007). This suggests that the models effectively captured the relationships between flocculation efficiency and the significant factors, as well as the concentration and significant factors. The regression models developed based on these findings are represented visually using 3-D response surface plots in Figures 5.3 and 5.4. 3-D response surface plots visually represent these relationships and help to determine the optimum levels of each variable for maximum response. These plots provide a graphical representation of these relationships, aiding in identifying optimal conditions for maximizing the desired response.

The ANOVA results for the quadratic model of harvesting efficiency are presented in Appendix G, Table G1, and Table G2. As seen in the table, the *p-values* of the coefficients are $p<0.05$, which implies that these are significant. For the marine harvesting process, the linear effect of coefficient *X1* and *X3,* dosage ($p>0.0001$), and mixing rate ($p>0.0003$) is significant, with very small p values ($p<0.05$). Similarly, the interactive effects of dosage and mixing rate ($p < 0.05$) and pH and mixing rate ($p<0.05$) are also significant. *P-values* of the quadratic coefficient, dosage (X_1^2) ($p<0.0001$), pH (X_2^2) ($p<0.0033$) and mixing rate (X_3^2) ($p<0.0001$) are significant. The other term coefficients with ($p>0.05$) were not significant. Thus, statistical data analysis shows that small variations in the values of the selected variables alter the harvesting efficiency. In this model X_1, X_3; X_1X_3, X_2X_3, X_1^2, X_2^2 and X_3^2 are significant model terms. Analysis of variance (ANOVA) for the response surface quadratic model gave an *F-value* of 26.44, R2 value of 0.9597, probability <0.0001 and coefficient of variation (CV = 5.79%), signifying that the model is highly significant, and

experiments are highly accurate and reliable.

Since the *p-values* of all the coefficients in Table 5.5 of the ANOVA results for freshwater, except for X_2 and X_2X_3, are $p<0.05$, it implies that these are significant. The linear effect of coefficients dosage X_1 ($p<0.0202$) and mixing rate X_3 ($p<0.0211$) are significant. In contrast, pH X_2 ($p<0.3027$) is insignificant, which means that the harvesting efficiency is more related to the bio flocculant dosage and mixing rate. The interactive effects of dosage and pH ($p<0.0354$), dosage and mixing rate ($p<0.019$), are significant, while pH and mixing rate ($p<0.1899$) are insignificant. *P-values* of the quadratic coefficient, dosage (X_1^2) ($p <0.0001$), pH (X_2^2) ($p<0.0033$), and mixing rate (X_3^2) ($p<0.0001$) are significant. The other term coefficients with ($p>0.05$) were not significant. Analysis of variance (ANOVA) for the response surface quadratic model gave an F-value of 49.84, R2 value of 0.9782, probability < 0.0001, and coefficient of variation (CV = 7.06%), signifying that the model is highly significant, and experiments are highly accurate and reliable.

5.4.3 Efficiency of Harvesting Microalgae Using Central Composite Design

Three-dimensional surface plots were generated to depict the relationship between the harvesting efficiency response and each factor used in the experimental design. These plots provide a visual representation of how the response changes with varying factors and assist in identifying the optimal parameter values according to Equations 5.1 and 5.2. Figures 5.2 and 5.3 display the three-dimensional response surface plots, illustrating the

interactions between the responses (harvesting efficiency) at different levels of various variables (i.e., dosages, pH and mixing rate). Figure 5.3 refers to marine water, and Figure 5.4 refers to freshwater.

The three independent factors that significantly affected the harvesting efficiency of microalgae were *Chlorella* sp., dosage, pH, and mixing rate. In Figure 5.3A and Figure 5.4A, the mixing rate was fixed at 125 rpm, and the combined effects of the bio flocculant dosage and pH were studied. The figures show that the increasing concentration of bio flocculant did not increase the harvesting efficiency, as indicated by the downward slope of the dosage curve. Furthermore, this figure also demonstrates that pH levels, whether low or high, had a relatively minor impact on harvesting efficiency as the harvesting efficiency consistently remained within the range of 80% to 85%. This observation aligns with Zhou et al. (2013), who found that fungi-algae pellets formed more rapidly in a medium with an initial pH value between 4.5 and 7.0. Results indicated that at a pH level of 4 to 5, a high harvesting efficiency (%) of 93% was achieved when 10 mg L^{-1} of glucose was added.

On the other hand, in Figure 5.3B and Figure 5.4B, pH levels were maintained at 7 while varying the dosage and mixing conditions. The figure demonstrates that higher dosages and faster mixing rates resulted in lower harvesting efficiency. This is because the mixing rate significantly impacts the neutralization of charges and the aggregation of particles, which occur because of re-stabilizing the colloidal system (Hadiyanto et al., 2022). Higher agitation rates typically result in increased shear stress within the system,

which can have various effects, both positive and negative. It can be advantageous in certain processes, such as cell disruption. However, excessively high shear stress can lead to changes in morphology and cell damage or reduced product quality, especially in sensitive biological systems (Zhou et al., 2013; Zhou et al., 2018). Finally, in Figure 5.3C and Figure 5.4C, different combinations of pH levels and mixing rates were examined while maintaining a consistent dosage of 30 g L^{-1}. According to the graph, the gently sloping curve suggests that changes in pH and mixing rate have minimal impact on the harvesting efficiency of *Chlorella* sp. The harvesting efficiency remains relatively stable, with only minor variations observed. For pH, the efficiency ranges from 80% to 90%, and the mixing rate ranges from 70% to 80%. This suggests that within the tested pH and mixing rate ranges, the harvesting process is relatively stable, and changes in these parameters do not lead to significant variations in efficiency.

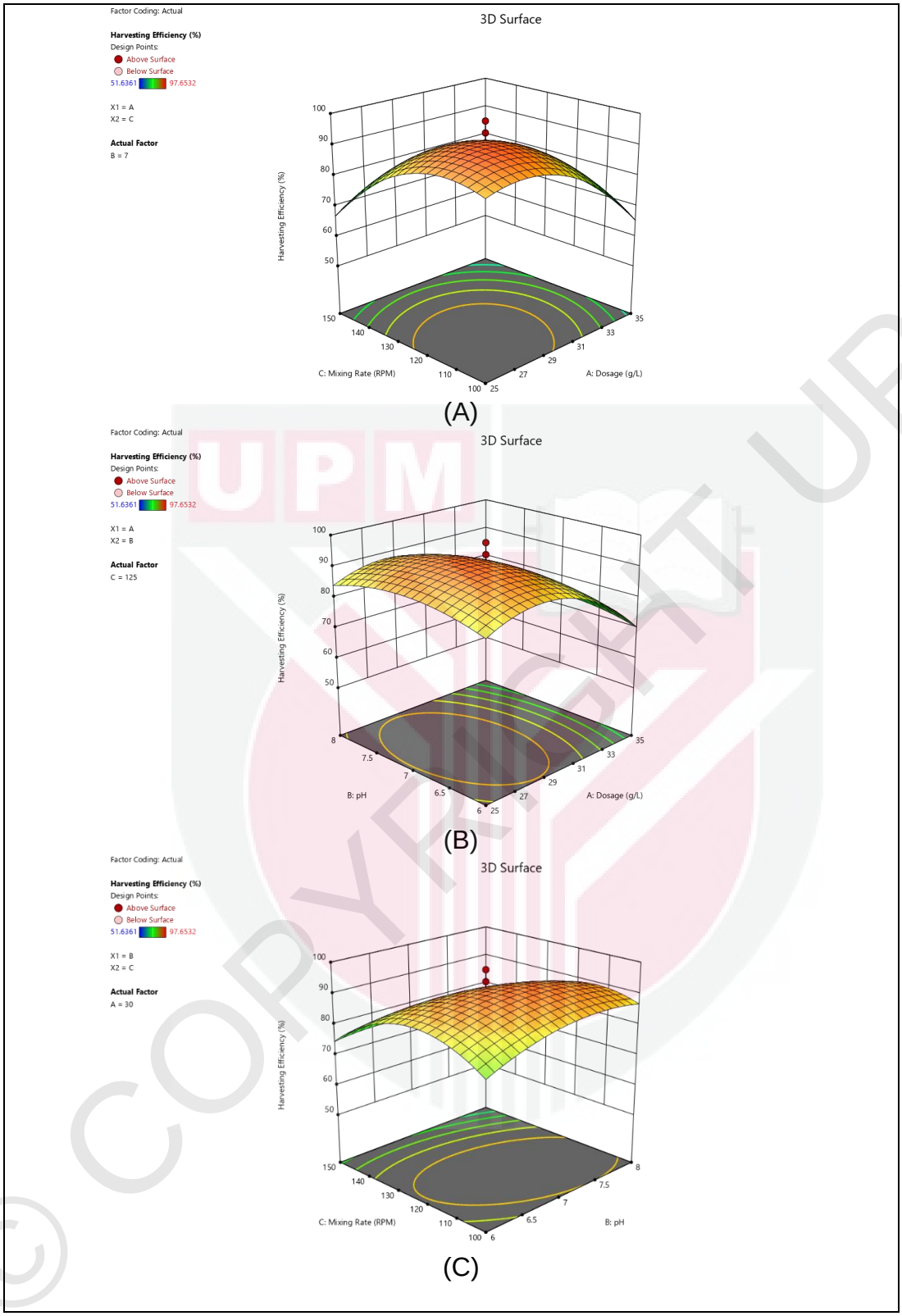

Figure 5.3 : Three–Dimensional Response Surface Plots Depicting the Effects of Three Independent Variables on Harvesting Efficiency for Marine Water Species (A) Effect of Dosage and pH (B) Effect of Dosage and Mixing Rate (C) Effect of pH and Mixing Rate

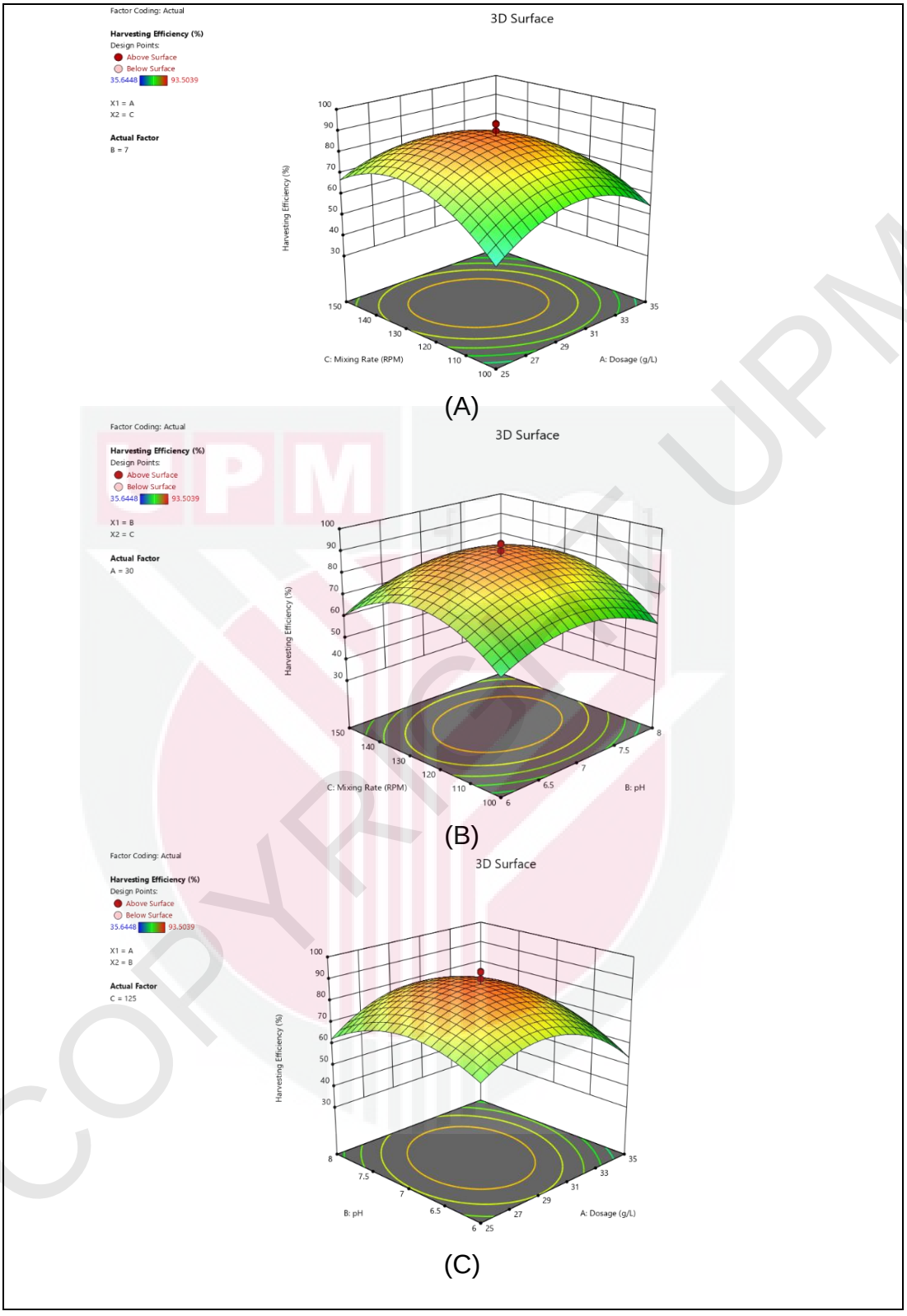

Figure 5.4 : Three–Dimensional Response Surface Plots Depicting the Effects of Three Independent Variables on Harvesting Efficiency for Freshwater Species (A) Effect of Dosage and pH (B) Effect of Dosage and Mixing Rate (C) Effect of pH and Mixing Rate

The dosage and mixing rate are crucial for harvesting efficiency. Optimizing these conditions is essential for achieving the highest efficiency and improving overall process effectiveness. Proper dosage and mixing rate optimization saves time and resources, enhances product quality, and boosts process performance. Using Response Surface Methodology (RSM) helps systematically fine-tune these variables to ensure the best possible results.

This study assessed the impact of the harvesting process on water quality, including ammonia, nitrite, and orthophosphate levels. The findings indicated that the process caused minimal changes, with percentage differences between initial and final concentrations around 0.04%. This minor change suggests that harvesting does not significantly alter water quality. However, as noted by Chu et al. (2022), there is a lack of information on whether the use of filamentous fungi affects the water quality of the harvested product for future cultivation cycles. Although the harvesting process led to only a minimal change of approximately 0.04% in water quality parameters, it is important to consider the role of extracellular polymeric substances (EPS) released by the fungal pellets. It remains uncertain whether these EPS could improve the microalgae's efficiency in utilizing remaining nutrients (Chu et al., 2022; Wang et al., 2023). Further research is needed to clarify these effects.

5.4.4 Validation of the Experimental Model

The main objective of optimization was to maximize the harvesting efficiency by recalculating all factors and applying a desirability function. Besides, the combination of CCD and desirability functions is a powerful tool for

optimization and response surface methodology that can help identify the optimal settings for input variables to achieve desired output responses. In the validation part, the potential input optimizations have five goal options: range, maximum, minimum, target, and none (for responses) that can be chosen to provide an optimized output value. In this study, the goal for response harvesting efficiency is assigned as 'maximize' and 'target' for dosage, and pH and mixing rate are assigned the same as 'minimize.' The point prediction option in the software is used to optimize the process parameters. For its validation, a triplicate experiment was performed with the optimized parameters

Table 5.3 tabulates the summary results of the comparison performance of validation runs for harvesting efficiency at optimum conditions obtained from the model. The optimal dosage, pH, and mixing rate for the marine water species are 29.3 g L^{-1}, pH 6.9, and rpm 123, respectively, at which the predicted harvesting efficiency is 92.9% (Appendix G, Figure G1). However, the actual harvesting efficiency is even higher at 97.7%, resulting in a percentage error of 4.8%. Compared to freshwater, the optimal dosage, pH, and mixing rate for achieving the highest harvesting efficiency are 29.3 g L^{-1}, pH 7, and 129 rpm, respectively (Appendix G, Figure G2). Under these optimal conditions, the predicted harvesting efficiency is 88.5%. Nevertheless, the actual harvesting efficiency achieved is even higher at 93.5%, resulting in a percentage error of 5%.

The research conducted by Ribardo & Allen (2003) stated that the maximum error obtained from the model does not exceed 20%, which is based on the Harrington function evaluation scale and is considered acceptable. Therefore, the error obtained for this study for marine and freshwater harvesting is below 20%, confirming that the model is acceptable. This indicates that the harvesting process was more effective than initially predicted, resulting in a higher yield of desired results. The results show that central composite design (CCD) incorporated with desirability functions could be successfully used to optimize the design for experiments on the microalgae harvesting process since they are closely related to the data obtained from optimization analysis using desirability functions.

Table 5.3 : Comparison of RSM Model Accuracy in Predicting Harvesting Efficiency for Marine and Fresh Water Microalgae

Type of wastewater	Findings	Harvesting Efficiency (%)
Marine water	Actual	97.7
	RSM Model	92.9
	Error (%)	4.8
Freshwater	Actual	93.5
	RSM Model	88.5
	Error (%)	5

5.5 Conclusion

In microalgae harvesting, CCD can be employed to investigate the effects of various factors on the efficiency of the harvesting process. Besides, by designing the experiment based on CCD, the desired efficiency can be successfully achieved by predicting the optimum harvesting microalgal biomass yield with the variation of harvesting conditions. In this study, a

maximum harvesting yield of 97.7% for marine water and 93.5% for freshwater was obtained using bio-flocculant concentration (dosage) of 30 g L^{-1} at pH condition of pH 7 and a mixing rate of rpm 125. The study revealed that the filamentous fungus *Aspergillus niger* could serve as a beneficial and innovative bio-flocculant in algal technology. This discovery demonstrates that the bio-flocculant is suitable for marine and freshwater microalgae harvesting and offers an alternative approach for cost-effective biodiesel production using algal lipids.

This method reduces the environmental impacts of conventional harvesting techniques. The study highlights the potential of *A. niger* as a promising solution for sustainable and economically viable biodiesel production. RSM enables the harvesting process to be optimized in less time, requiring fewer experiments than traditional methods, thereby reducing the effort needed to find optimal conditions. RSM has been successfully used to optimize parameters such as dosage, pH, and mixing rate and has been applied to various microalgae species such as *Botryococcus braunii*, *Chlorella salina*, and *Nannochloropsis salina* (Duraiarasan, 2013; Kim et al., 2013).

Looking ahead, future research could explore the scalability of these findings in industrial applications by investigating the effects of A. *niger* on other algal species and assessing the long-term sustainability of using bio-flocculants in diverse aquaculture systems. The potential for economically viable and environmentally friendly biodiesel production can be further realized and contribute to more sustainable practices in the aquaculture industry. In

conclusion, RSM presents significant advantages for optimizing microalgae harvesting, opening up opportunities for innovative strategies that address environmental challenges and the growing demand for renewable energy sources.

CHAPTER 6

DEVELOPMENT OF DATA PROFILING FOR BIOREMEDIATION AND BIO-HARVESTING PROCESS USING WAIKATO ENVIRONMENT OF KNOWLEDGE ANALYSIS (WEKA)

6.1 Introduction

In environmental science and sustainable technology, the intersection of data analysis and biotechnological processes has become increasingly crucial (Majerník et al., 2023). Decision-making frameworks play a crucial role in various processes when combined with in-depth knowledge and analysis of profiling. They can enhance the efficiency and effectiveness of decision-making. Therefore, integrating in-depth knowledge and analysis of profiling into decision-making frameworks creates a powerful combination that enhances the ability to make informed, strategic, and ethical decisions across various domains. Currently, an experimental procedure is already considered to be repetitive and time-consuming. In addition, using experimental procedures only to plan future experiments may be based on intuition and previous experience. To address this issue, Machine Learning (ML) offers a systematic and strategic approach to enhance and optimize the process while increasing efficiency. ML also can build predictive models based on existing data and help researchers make informed decisions about future experiments. The data mining environment in machine learning in this research is provided by the Waikato Environmental Knowledge Analysis (WEKA) software.

Machine Learning (ML) is one of the many branches of Artificial Intelligence (AI), which consists of a collection of data-driven algorithms (Ning et al., 2022).

The application of data mining has received much interest in various sectors, including chemical, materials, and engineering, due to its convenience and effectiveness. Similarly, many researchers have successfully applied machine learning approaches to microalgae for several purposes, such as exploring the potential of biological wastewater treatment using algae–bacteria consortia for nutrient uptake and resource recovery to improve the efficiency of microalgae classification and improving the efficiency of microalgae classification (Correa et al., 2017; Sundui et al., 2021). As for their mechanism, ML works by finding data patterns and correlating them with other variables. Summarizing the vast volume of data from a certain point of view can also efficiently predict outcomes for any future circumstance. In the decision-making procedures, several algorithms will be used interchangeably concerning the variable fed to the system. Machine learning will significantly cover the data analytics part of this research, which will help algae profiling better determine proper parameter values for biomass harvesting.

The potential of machine learning for predictive modeling and data profiling in bioremediation and bio-harvesting processes is explored using the open-source software Waikato Environment Knowledge Analysis (WEKA), building on the success of M5P models for environmental prediction (Yi et al., 2019). The data analyzed in this study were derived from previous batch experiments focusing on the bioremediation of marine aquaculture wastewater (MW) and fresh aquaculture wastewater (FW) using microalgae, Chlorella sp. The subsequent bio-harvesting process utilized a filamentous fungus *Aspergillus niger*. In bioremediation, microalgae were employed to treat aquaculture

wastewater, and their growth was monitored simultaneously. The excess microalgae growth in the water underwent bio-harvesting using filamentous fungus (flocculant). Figure 6.1 visually represents the systematic approach adopted in this study and illustrates the flow of the bioremediation and bio-harvesting processes. This flowchart depicts a systematic approach to developing data profiles for bioremediation and microalgae harvesting using WEKA. A model can be developed by analyzing the relationships between input parameters (day, dosage, pH, mixing rate) and desired outcomes (nutrient reduction, harvesting efficiency) to optimize these processes and enhance their effectiveness.

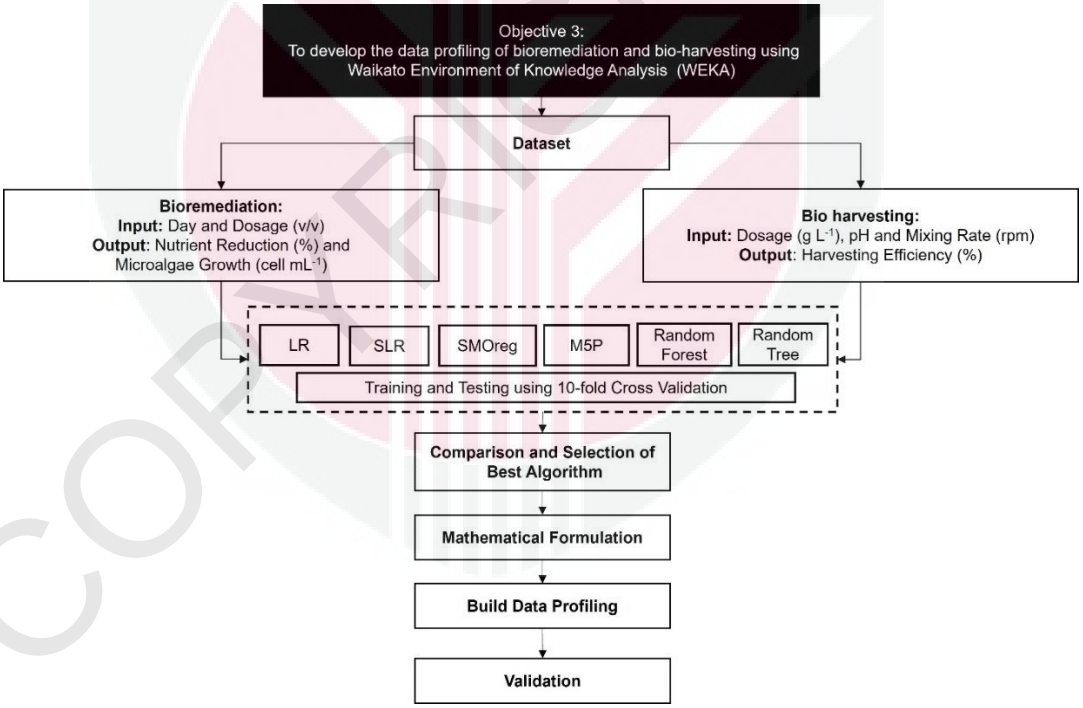

Figure 6.1 : Flowchart of Sequence for Developing Data Profiling in Bioremediation and Microalgae Harvesting Using WEKA

6.2 Green Microalgae-Based Bioremediation Profiling

6.2.1 Model Selection

To determine the suitability of algorithms for modeling bioremediation, the dataset was subjected to cross-validation across different days (Day 10, Day 12, and Day 14) and various nutrient concentrations (0% v/v to 60% v/v) using different function algorithms. These specific days were chosen because they correspond to critical phases in the microalgae growth cycle: the stationary and death phases. During this period, nutrient reduction efficiency exhibits significant variation, with the highest percentage removal observed on Day 10, providing essential data points for our analysis. The selection of the most appropriate algorithm was based on correlation coefficient analysis. The results show the performance of M5P, Random Forest, and Random Tree algorithms on different days (Day 10, 12, and 14) for predicting ammonia, nitrite, and orthophosphate removal.

This study compared the performance of M5P, Random Forest, Random Tree, LR, SLR, and SMOreg. All detailed performance comparisons are presented in Appendix H1 and H2. The results indicate that all three algorithms, M5P, Random Forest, and Random Tree, performed well in predicting the removal of ammonia, nitrite, and orthophosphate over time. The detailed results in the tables show that on Day 10, M5P achieved correlation coefficients of 0.9862, 0.9785, and 0.9875 for ammonia, nitrite, and orthophosphate, respectively. In comparison, Random Forest and Random Tree achieved correlation coefficients of 0.9964, 0.9831, and 0.9988 for the same parameters.

Table 6.1 : Correlation Coefficient of Cross-Validation Results for Different Days (Day 10, Day 12, and Day 14) and Parameters of MW Using Various Function Algorithms

Day	Algorithm	Parameters		
		Ammonia	Nitrite	Orthophosphate
10	M5P	0.9862	0.9785	0.9875
	Random Forest	0.9964	0.9831	0.9988
	Random Tree	0.9964	0.9832	0.9988
12	M5P	0.9437	0.9184	0.9685
	Random Forest	0.9549	0.9192	0.9904
	Random Tree	0.9549	0.9192	0.9904
14	M5P	0.9683	0.9618	0.9842
	Random Forest	0.9844	0.9701	0.9894
	Random Tree	0.9844	0.9701	0.9894

On Day 12, M5P showed correlation coefficients of 0.9437, 0.9184, and 0.9685, while Random Forest and Random Tree showed slightly higher values of 0.9549, 0.9192, and 0.9904. Similarly, on Day 14, M5P exhibited correlation coefficients of 0.9683, 0.9618, and 0.9842, with Random Forest and Random Tree again showing higher values of 0.9844, 0.9701, and 0.9894. Although both random forests and random trees exhibited similar highest correlation coefficients, M5P was chosen because it provides mathematical equations, offers accurate predictions, and quickly interprets decision tree models (Behnood et al., 2017). A similar trend was observed in the freshwater treatment that led to the selection of the M5P algorithm (Appendix G1). This feature is particularly advantageous when understanding the underlying relationships is crucial for comprehensive analysis and interpretation.

Appendix G2 and G3 offer a comprehensive analysis of M5P performance on Days 10, 12, and 14 by evaluating metrics such as Correlation Coefficient (CC), Mean Absolute Error (MAE), Root Mean Squared Error (RMSE), Relative Absolute Error (RAE), and Root Relative Squared Error (RRSE)

across a total of 120 instances (Shams et al., 2023). These metrics are commonly used as benchmarks to evaluate the model's performance. The assessment of whether these factors indicate a good model is contingent upon the specific context and goals of the analysis. High positive CC, close to 1, signals strong positive linear relationships between predicted and actual values, reflecting good model performance. Lower MAE and RMSE values suggest enhanced accuracy, with smaller MAE indicating better model performance. On the other hand, assessing the model over these multiple days determines how well the M5P model adapts to the changing conditions. If the model exhibits consistent performance across diverse time points, it signifies its robustness and applicability under varying conditions (McPhail et al., 2018). As the appendix shows, the M5P model displayed a consistently strong CC. The model's performance was considered highly acceptable based on its high R_2 and low error.

6.2.2 Model Development

M5P was selected for model development based on model selection due to its superior performance metrics and ability to create simple mathematical correlations. The M5P algorithm was employed to develop a user-friendly graphical interface (GUI) for algae profiling, utilizing its capability to generate linear models (LM) independently. With each run, the M5P algorithms generated an LM equation independently relating microalgae dosage (10% to 60% v/v) to four variables (cell count, ammonia, nitrite and orthophosphate). Every linear model's equation was assigned a specific concentration range that was continuously connected.

The tree output of the M5P algorithm illustrated in Figure 6.2 and tabulated equation in Table 6.3 derives from data collected during a batch bioremediation process. This combined representation provides a clear understanding of which linear model to use based on the value of the dosage variable. Each linear model is associated with a specific range of dosage values, ensuring appropriate predictions of ammonia concentration across different dosage levels. The linear model (LM) symbol represents the branch denoting distinct linear equations used for output estimation of nutrient removal. For example:

LM1 is applicable when the dosage is less than or equal to 25% v/v.

LM2 is applicable when the dosage is greater than 25% and less than or equal to 35% v/v.

LM3 is applicable when the dosage is greater than 35% and less than or equal to 55% v/v.

LM4 is applicable when the dosage is greater than 55% v/v.

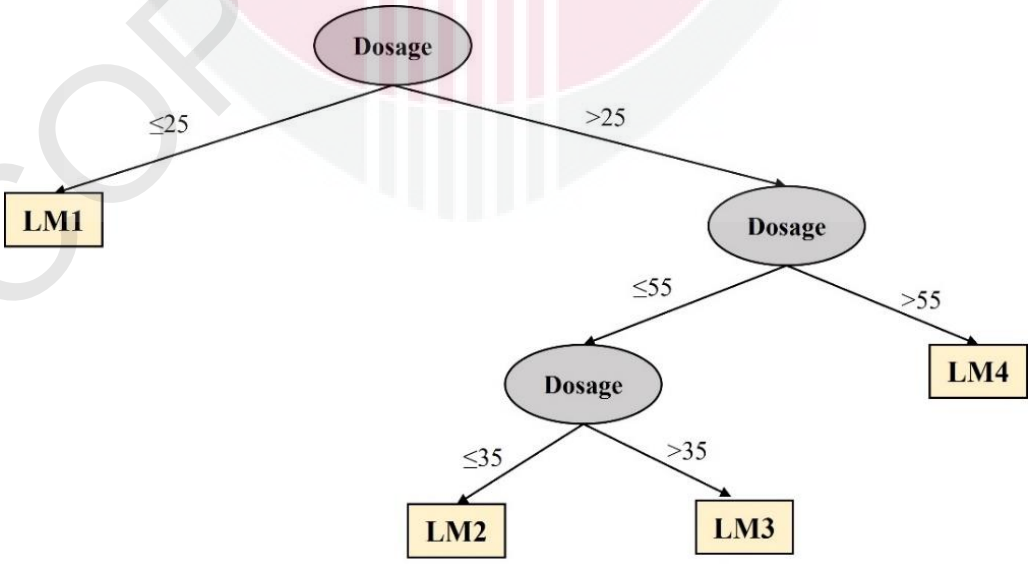

Figure 6.2 : M5P Tree Output for Ammonia on Day 10 (MW)

Table 6.2 : Linear Equation for Ammonia on Day 10 (MW)

LM num: 1	LM num: 2	LM num: 3	LM num: 4
Ammonia =	Ammonia =	Ammonia =	Ammonia =
-0.028 * Dosage	0.0006 * Dosage	0.0006 * Dosage	0.0018 * Dosage
+ 0.8118	+ 0.0976	+ 0.1096	+ 0.1695

Hence, as part of the novelty approach, the equation was manipulated, which involves inverting the equation. The function of inverting an equation is to rearrange it so that the dependent variable becomes the independent variable and vice versa. This process is often done to facilitate analysis or solve for a different variable. In creating an interface, inverting an equation may be necessary to make it more user-friendly or applicable to specific scenarios.

For this study, the inverted mathematical model, as presented in Table 6.4 for marine and Table 6.5 for freshwater on Day 10, optimizes water quality in aquaculture systems. This inversion, which transforms the equation to make 'Dosage' the dependent variable (y), is particularly valuable for comprehending the impact of variations in nutrient levels. In each case, concentrations such as "Ammonia, nitrite, and orthophosphate" represent the system's actual or specific concentration values. "Dosage" represents the amount of microalgae concentration to be applied. The dosage is calculated using a formula where "Concentration" is subtracted by a constant, and the result is divided by another constant. The conditions associated with each statement define the ranges of ammonia concentrations and corresponding dosage limits. The M5P output model is a practical tool that helps users decide when and how much treatment is needed based on the nutrient levels in the water.

Table 6.3 : Inverted Equation Model of M5P Day 10 Marine Wastewater (MW) Treatment

Nutrients	Limit Range Parameters	Equation	Limit Range (Dosage)
Cell Count	If, cell count < 128284369.2	$\text{Dosage} = \frac{\text{Cell Count - 126842351.0148}}{96134.5464}$	≤15
	If, 131721341.5 < cell count < 136379211.7	$\text{Dosage} = \frac{\text{Cell Count - 128186977.6963}}{234063.8293}$	>15 and ≤35
	if 132604077.6 < cell count < 132886592.7	$\text{Dosage} = \frac{\text{Cell Count - 131602433.1782}}{28536.8774}$	>35 and ≤45
	If cell count ≤ 137535839.4	$\text{Dosage} = \frac{\text{Cell Count - 135138340.5773}}{53159.6193}$	>45
Ammonia	If, Ammonia >0.1118	$\text{Dosage} = \frac{\text{Ammonia - 0.8118}}{0.028}$	≤25
	If, 0.1127 < Ammonia < 0.1186	$\text{Dosage} = \frac{\text{Ammonia - 0.0976}}{0.006}$	>25 and ≤35
	If, 0.1307 < Ammonia < 0.1426	$\text{Dosage} = \frac{\text{Ammonia - 0.1096}}{0.0006}$	>35 and ≤55
	If, Ammonia < 0.2687	$\text{Dosage} = \frac{\text{Ammonia - 0.1695}}{0.0018}$	>55
Nitrite	If, Nitrite >0.4969	$\text{Dosage} = \frac{\text{Nitrite - 0.5469}}{-0.002}$	≤25
	If, 0.2986 < Nitrite < 0.2648	$\text{Dosage} = \frac{\text{Nitrite - 0.3413}}{-0.0017}$	>25 and ≤45
	If, Nitrite < 0.2216	$\text{Dosage} = \frac{\text{Nitrite - 0.2712}}{-0.0011}$	>45
Orthophosphate	If, Orthophosphate > 0.8072	$\text{Dosage} = \frac{\text{Orthophosphate - 2.3747}}{-0.0627}$	≤25
	If, 1.0426 < Orthophosphate < 1.055	$\text{Dosage} = \frac{\text{Orthophosphate - 1.01}}{0.0013}$	>25 and ≤35
	If, 1.2230 < Orthophosphate < 1.1195	$\text{Dosage} = \frac{\text{Orthophosphate - 1.0455}}{-0.0052}$	>35 and ≤55
	If, Orthophosphate ≥ 1.2043	$\text{Dosage} = \frac{\text{Orthophosphate - 1.2043}}{}$	>55

Table 6.4 : Inverted Equation Model of M5P Day 10 Fresh Wastewater (FW) Treatment

Nutrients	Limit Range Parameters	Equation	Limit Range (Dosage)
Cell Count	If, cell count < 117964044.1	$\text{Dosage} = \frac{\text{Cell count - 80458421.4064}}{\text{- 1500224.9058}}$	≤25
	If, 121532086.8 > cell count < 148390266.4	$\text{Dosage} = \frac{\text{Cell count - 87655689.4364}}{\text{- 1349657.2656}}$	>25 and ≤45
	If, 129885715.5 > cell count < 129483809.7	$\text{Dosage} = \frac{\text{Cell count - 131716619.5929}}{\text{- 40596.5428}}$	>45 and ≤55
	If, Cell count > 117200266	$\text{Dosage} = \frac{\text{Cell count - 126988163.7183}}{\text{- 177638.797}}$	>55
Ammonia	If, Ammonia > 0.4764	$\text{Dosage} = \frac{\text{Ammonia - 0.5049}}{\text{- 0.0019}}$	≤15
	If, 0.4056 < Ammonia < 0.4235	$\text{Dosage} = \frac{\text{Ammonia - 0.392}}{\text{0.009}}$	>15 and ≤35
	If, 0.2848 < Ammonia < 0.3127	$\text{Dosage} = \frac{\text{Ammonia - 0.3618}}{\text{- 0.0014}}$	>35 and ≤55
	If, Ammonia > 0.3395	$\text{Dosage} = \frac{\text{Ammonia - 0.3175}}{\text{0.0004}}$	>55
Nitrite	If, Nitrite < 0.3956	$\text{Dosage} = \frac{\text{Nitrite - 0.4046}}{\text{- 0.0006}}$	≤15
	If, 0.3728 < Nitrite < 0.3847	$\text{Dosage} = \frac{\text{Nitrite - 0.3637}}{\text{0.0006}}$	>15 and ≤35
	If, 0.2499 < Nitrite < 0.2519	$\text{Dosage} = \frac{\text{Nitrite - 0.2554}}{\text{- 0.0001}}$	>35 and ≤55
	If, Nitrite > 0.2745	$\text{Dosage} = \frac{\text{Nitrite - 0.2634}}{\text{0.0002}}$	>55
Orthophosphate	If, Orthophosphate > 1.3287	$\text{Dosage} = \frac{\text{Orthophosphate - 1.5807}}{\text{- 0.0168}}$	≤15
	If, 0.7327 < Orthophosphate < 0.9874	$\text{Dosage} = \frac{\text{Orthophosphate - 1.1807}}{\text{- 0.0128}}$	>15 and ≤35
	If, 0.1692 < Orthophosphate < 0.2355	$\text{Dosage} = \frac{\text{Orthophosphate - 0.4707}}{\text{- 0.0067}}$	>35 and ≤45
	If, Orthophosphate < 0.1408	$\text{Dosage} = \frac{\text{Orthophosphate - 0.4249}}{\text{- 0.0063}}$	>45

6.2.3 Model Validation

In the final stages of model profiling, model validation is essential to continuously monitor its performance and make any required adjustments based on new information that becomes available. So, for this study, regular monitoring and fine-tuning of the model are vital to ensure its effectiveness in predicting water quality parameters and assessing its performance in real-world conditions. The dataset was derived from a batch test of the bioremediation process, allocating 80% for training and 20% for testing (validation).

In the validation process, LM equations obtained from WEKA are utilized, with each equation's dosage variable value replaced by the corresponding dosage value from the testing set. This substitution allows for calculating predicted values and compares them with the actual observed values of relevant parameters, such as ammonia concentration. By repeating this process for each LM equation and testing the value sample, the accuracy and overall performance of the models can be thoroughly evaluated. For example, the LM equation 6.1 for ammonia in marine wastewater (MW) on Day 10:

$$\text{Ammonia} = -0.028 * \text{Dosage} + 0.8118 \quad (6.1)$$

and have a testing with a dosage value of 30 % (v/v), substitute 30 for "Dosage" in the equation 6.2:

$$\text{Ammonia} = -0.028 * 30 + 0.8118 \quad (6.2)$$

Then, calculate the predicted value of ammonia using this equation. This predicted value can be compared with the actual observed value of ammonia in the testing set to evaluate the accuracy of the LM equation. Repeat this process for each LM equation and each testing instance to assess the overall performance of the models. On the other hand, the percentage difference needs to be calculated to determine how close the predictions are to the actual values. This information is essential for assessing model performance and identifying improvement gaps. Calculating the percentage difference also helps ensure the reliability and validity of predictive models.

Figure 6.3 depicts an example of a validation graph for the M5P Algorithm predicting ammonia levels for marine wastewater (MW) on Day 10. The predicted values line closely follows the actual values line, suggesting good model performance. The predictions are generally close to the actual observations, with a Mean Absolute Error (MAE) of 0.00045. While the model performs well on Day 10, further validation with data from other days is recommended. Table 6.6 tabulates the detailed data for the other day.

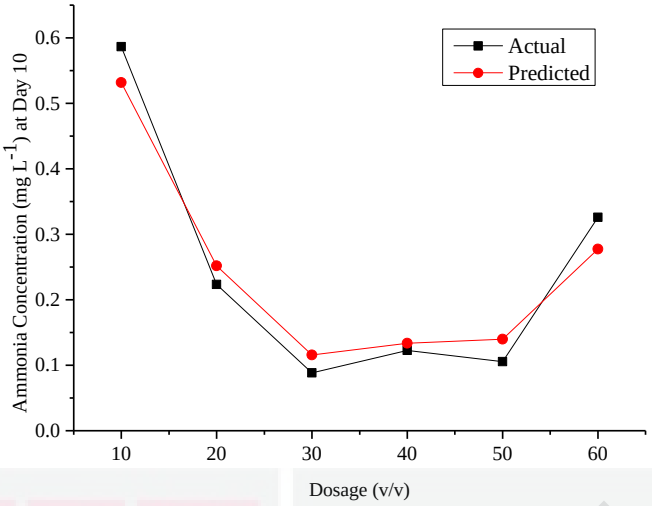

Figure 6.3 : Validation Graph for Ammonia Day 10

Table 6.5 presents the average differences between the predicted values generated by equations derived from the WEKA software and the actual values obtained from the original dataset. These differences are calculated across days (Day 10, Day 12, and Day 14) and various parameters, including cell count, ammonia concentration, nitrite concentration, and orthophosphate concentration in MW.

Table 6.5 : Comparison Value between WEKA Predictions with the Actual Dataset for Validation Analysis MW

Average percentage difference (%) of the generated equation from WEKA with 20% original dataset				
Day	Cell Count	Ammonia	Nitrite	Orthophosphate
10	2.126	2.941	2.764	7.396
12	2.630	0.486	0.678	2.572
14	2.297	0.866	1.260	3.362

The differences between predicted and actual values indicate how accurate the models generated by WEKA. The result shows that orthophosphate consistently shows higher differences than cell count, ammonia, and nitrite.

For instance, on Day 10, orthophosphate exhibits a significantly higher average difference of 7.396, indicating a considerable gap between predicted and actual values. On the contrary, parameters such as cell count, ammonia, and nitrite demonstrate lower average differences, suggesting a closer alignment between predicted and actual values for these variables. Predictions might show higher deviations during the late exponential growth phase of microalgae (Day 10). The cell density and some activities were rapid changes.

Microalgae typically absorb nutrients for growth during the exponential phase. They may release some of those nutrients into the surrounding water during the stationary and death phases due to cell death or excretion. This nutrient release can affect the models' accuracy, leading to differences in the predicted and actual values. The decrease in the difference observed during Days 12 and 14 compared to Day 10, especially ammonia, Day 12 is 0.486, and Day 14 is 0.866 could be attributed to various factors. During Days 12 and 14, which correspond to the early death phase of microalgae, the dynamics of nutrient release and environmental interactions may differ compared to Day 10. As microalgae enter the early death phase, changes in metabolic activity and nutrient cycling within the system could influence the performance of the predictive models. During this phase, microalgae may release nutrients back into the water, contributing to a more balanced nutrient profile and reduced variability in water quality parameters. These changes may result in a closer alignment between the predicted and actual values, leading to a lower difference in the performance of the predictive models during Days 12 and 14.

In conclusion, model validation results highlight the importance of verifying the accuracy of predictive models before developing any interface or application. Any discrepancies or inaccuracies in the model's performance can be identified by comparing the actual and predicted values (Decostere et al., 2016; Manhaeghe et al., 2020). This process is also crucial for ensuring that the predictive models provide reliable and trustworthy results when integrated into interfaces or systems for practical use. Without thorough validation, there is a risk of relying on inaccurate predictions, leading to incorrect decisions or outcomes in real-world scenarios. Therefore, model validation is a necessary step in the development process to enhance the reliability and effectiveness of predictive models before their implementation in practical applications.

6.3 Filamentous Fungus-Based Bioharvesting

6.3.1 Model Selection

When selecting a model for bio-harvesting using WEKA, it is important to consider the specific characteristics of the data, such as the number of attributes and sample size (Merlini & Rossini, 2021). This study examined the interactions among three variables: dosage, pH, and mixing rate for the bio-harvesting of green microalgae. The data for this study originated from previous batch experiments, and bio-harvesting is a subsequent study following the bioremediation process. After the bioremediation of wastewater, excess microalgae biomass remained in the water. To address this, bio-harvesting using filamentous fungus is employed. The filamentous fungus acts as a bio-flocculant, aggregating and settling the excess microalgae.

Various machine learning models, such as linear regression (LR), SMO Reg, M5P, and Random Forest, were applied to optimize the experimental dataset. Table 6.6 compares algorithm models for cross-validating harvesting performance on Days 1, 2, and 3. This analysis helps determine the most suitable algorithm for efficient bio-harvesting.

Table 6.6 : Comparison of Algorithm Models for Cross-Validation: Harvesting Performance between Dosage and Day for Marine Water Treatment (MW)

Day	Factors	Algorithms			
		LR	SMOreg	M5P	Random Forest
1	CC	0.9036	0.9024	0.99	0.992
	MAE	4720919.5	4505289.05	1453985.01	1195085.23
	RMSE	5891386.47	5958999.09	1953921.48	1736706.89
2	CC	0.9393	0.949	0.9947	0.995
	MAE	5180583.81	5059053.47	1398243.36	1299199.51
	RMSE	5667497.75	5864662.90	1862301.33	1791495.26
3	CC	0.9658	0.9657	0.9946	0.995
	MAE	4421369.03	4174286.50	1349270.78	1149116.93
	RMSE	4861827.10	5344615.62	1952900.27	1869988.21

The results indicate that the M5P and Random Forest algorithms consistently outperform Linear Regression (LR) and SMOreg. On Day 1, M5P and Random Forest show the highest correlation coefficients (0.99 and 0.992) and the lowest MAE and RMSE values. This trend continues in Days 2 and 3, with M5P and Random Forest maintaining high accuracy and low error metrics. The analysis across different days highlights the superiority of the M5P and Random Forest algorithms in accurately predicting bio-harvesting performance. The lower error metrics (MAE and RMSE) and higher correlation coefficients demonstrate their suitability for handling the complex relationships between dosage, pH, mixing rate, and harvesting performance. Results for

additional days and parameters, which further support these findings, are provided in Appendix G4.

6.3.2 Model Development

Using WEKA for bio-harvesting profiling with filamentous fungus (flocculant) in microalgae harvesting presents a promising pathway for optimizing harvesting processes. In this study, based on model selection, the M5P algorithm was selected for bio-harvesting profiling due to its high correlation coefficient compared to other algorithms. Its capacity to provide accurate predictions and create easily interpretable decision tree models significantly enhances the understanding and optimization of bio-harvesting processes. Hence, the M5P algorithm produced both the decision tree and linear model (LM) equation used throughout this study.

The equation presented in Table 6.7 appears to be a mathematical model generated from the M5P that describes the relationship between the cell density of microalgae and the parameter (dosage) that influenced the harvesting process using a fungus. The equation suggests that the dosage of a substance influences the value of cell density. The coefficients indicate the strength and direction of these influences. The negative coefficients suggest that higher levels of these factors are associated with lower cell density, while the positive coefficient suggests increased cell density over time. The equation provides a quantitative way to understand how these parameters contribute to harvesting and impact microalgae cell density.

Table 6.7 : M5P Linear Equation of Cross-Validation for Determination of Cell Density vs Dosage for Marine Water Harvesting on Day 1

	Equation	Dosage Range
LM1	Cell density = -437227.77 * Dosage + 49936572.89	**Dosage** ≤22.5
LM2	Cell density = - 314337.77* Dosage + 35302612.74	>22.5 **Dosage** ≤27.5
LM3	Cell density = 824804.91* Dosage - 11396530.85	**Dosage** >27.5

Notes: Dosage refers to the initial concentration of flocculant utilized in the harvesting process (g mL^{-1})

However, this study focuses on identifying the most effective day, dosage, and mixing rate based on a specific cell density. In practical applications, the cell density is often a known parameter. Therefore, the goal is to find the optimal combination of factors leading to the desired cell density for effective harvesting. To achieve this goal, the provided equation needs to be inverted, enabling the determination of the appropriate dosage, day, and mixing rate required to reach the target cell density. This inversion process is essential for guiding the decision-making process and ensuring the successful harvesting of microorganisms at the desired density. Table 6.8 displays the inverted equation for marine water on Day 1, with dosage represented on the y-axis as a function of cell density (CD).

Table 6.8 : Inverted M5P Linear Equation of Cross-Validation for Determination of Cell Density vs Dosage for Marine Water Harvesting on Day 1

	Equation	Cell Density Range
LM1	$\text{Dosage} = \frac{\text{Cell Density} - 49936572.89}{437227.77}$	**CD** ≤ 40098947.9
LM2	$\text{Dosage} = \frac{\text{Cell Density} - 35302612.74}{314337.77}$	7573982.05 < **CD** ≤ 11285604.1
LM3	$\text{Dosage} = \frac{\text{Cell Density} + 11396530.85}{824804.91}$	**CD** > 11698006.6

Notes: CD refers to the cell density of microalgae in a water sample

6.3.3 Model Validation

For the validation part, the similar method utilized in the bioremediation process was duplicated for the bio-harvesting process. This involved substituting the actual values of the parameters into the equations obtained from WEKA to calculate the predicted cell density for each instance in your dataset. Then, compare the predicted cell density values obtained from the equations with actual cell density values in your dataset. Calculate the accuracy of the predictions by determining the percentage of instances where the predicted cell density matches the actual cell density. This will provide information on the performance of the M5P algorithm in accurately predicting cell density. A comprehensive performance evaluation of the model was achieved by splitting a dataset obtained from a bio-harvesting batch test into an 80/20 split for training and validation, respectively.

Table 6.9 shows the average difference between the predicted cell density reduction values generated by a WEKA model trained using the M5P algorithm and the actual cell density reduction values obtained in the experiments. This difference is calculated for the reduction in cell density (a measure of

harvesting efficiency) on three different days (Day 1, Day 2, and Day 3) and various parameters (initial concentrations of microalgae measured in cells per millilitre (cell mL^{-1}). The mixing rate is measured in rotations per minute (rpm).

Table 6.9 : M5P Model Performance in Predicting Harvesting Efficiency (Average Difference): Dosage (a) and Mixing Rate (b)

	Average difference of generated equation from WEKA with 20% original dataset							
Day/Dosage ($g\ L^{-1}$)	0	5	10	15	20	25	30	35
1	0.724	1.689	2.986	4.035	4.379	5.654	8.772	3.548
2	0.498	2.492	1.611	2.570	7.603	11.463	21.248	18.346
3	0.303	3.562	3.428	8.987	5.947	6.532	46.865	42.801

(a)

	Average difference of generated equation from WEKA with 20% original dataset						
Day/Mixing rate (rpm)	0	25	50	75	100	125	150
1	2.487	3.201	4.989	5.906	12.362	6.098	4.872
2	4.682	11.011	4.649	14.526	7.993	13.105	14.288
3	4.522	7.328	5.290	13.253	15.622	16.234	12.932

(b)

The table shows the average difference between the model's predicted cell density reduction and experimental values. The average differences varied depending on the day and parameters. Smaller average differences indicate better agreement between the model and the experiments. The model exhibited greater accuracy for varying dosages, with lower differences observed on Day 1 and the following days, particularly at lower dosage levels. Similarly, the model demonstrated a comparable trend regarding mixing rates, achieving higher accuracy on Day 1 across all mixing rates. In contrast, on the following days, accuracy was higher for lower mixing rates.

This trend suggests that the M5P model in WEKA achieved an acceptable average difference between predicted and actual cell density reduction across various initial microalgae concentrations, mixing rates, and days. However, the model demonstrates improved performance in predicting cell density reduction during the early stage of the process (Day 1), particularly when lower dosage levels (below 20 g L^{-1}) and mixing rates (below 75 RPM) are applied. Hence, further exploration could focus on alternative algorithms better suited for non-linear relationships and utilizing larger training datasets that improve model accuracy across different conditions.

In addition, the absence of existing research on harvesting microalgae using specific parameters has motivated the creation of synthetic data using Monte Carlo simulations (MCS). While generating extra data (data augmentation) might be helpful when you have limited data, it's important to remember that these new data points might not perfectly represent what happens in the real world. This can lead to the model making inaccurate predictions, which might be reflected in larger differences between predicted and actual values.

6.4 Development of User-Friendly Interface

Treating aquaculture wastewater is a significant challenge in environmental sustainability (Al-Jabri et al., 2021; Bhatt et al., 2022). Microalgae-based bioremediation and fungal bio-harvesting offer promising solutions, but optimizing these processes requires user-friendly interfaces. This study focuses on developing an interface to enhance monitoring and decision-making. The interface is designed to improve the effectiveness of wastewater

treatment and biomass harvesting in aquaculture.

6.4.1 Interface Development

The next part of this chapter is to develop a framework interface using machine learning to identify optimal conditions and effective parameters for treating nutrients in wastewater using microalgae. This will be accomplished by applying machine learning techniques, enabling a systematic and data-driven approach to enhance the efficiency of nutrient removal processes. The study aims to improve aquaculture practices using machine learning to optimize microalgae use in wastewater treatment, control algal blooms, and improve nutrient management. A framework with many parameters is first built, then the prepared data is fed into the model.

As an integral part of the interface development for bioremediation of aquaculture wastewater using microalgae, the IF function in Excel plays a crucial role. The IF function facilitates dynamic decision-making within the Excel interface, contributing to the optimization of data analysis and enhancing the efficiency of the bioremediation process. This function allows one to perform a logical test and return one value if the test is true and another if the test is false. Equation 6.3 shows the structured formula and how to use the IF function:

$$= \text{IF (logical\_test, value\_if\_true, value\_if\_false)} \quad (6.3)$$

Where:

logical_test is the condition or test to evaluate. It can be a comparison, a logical

expression, or any statement that results in either true or false.

value_if_true is the value that the formula returns if the logical test evaluates to true.

value_if_false is the value that the formula returns if the logical test evaluates to false.

Figure 6.4 shows that the interface in the Excel sheet is designed to operate seamlessly without requiring any user input, and its functionality is achieved through the effective utilization of the IF function. The instructions for using the interface are provided in this figure. Users input specific nutrient concentrations in their wastewater, allowing customized treatment plans. The interface incorporates valid nutrient ranges to ensure safe and effective treatment. Based on the entered data, the system utilizes algorithms to calculate the recommended amount of *Chlorella* sp. culture to add on different days, optimizing nutrient removal and water quality improvement throughout the treatment process. Finally, users can easily interpret the results to determine the precise amount of culture to add daily to their wastewater. Therefore, Figure 6.5 illustrates the interface with user input.

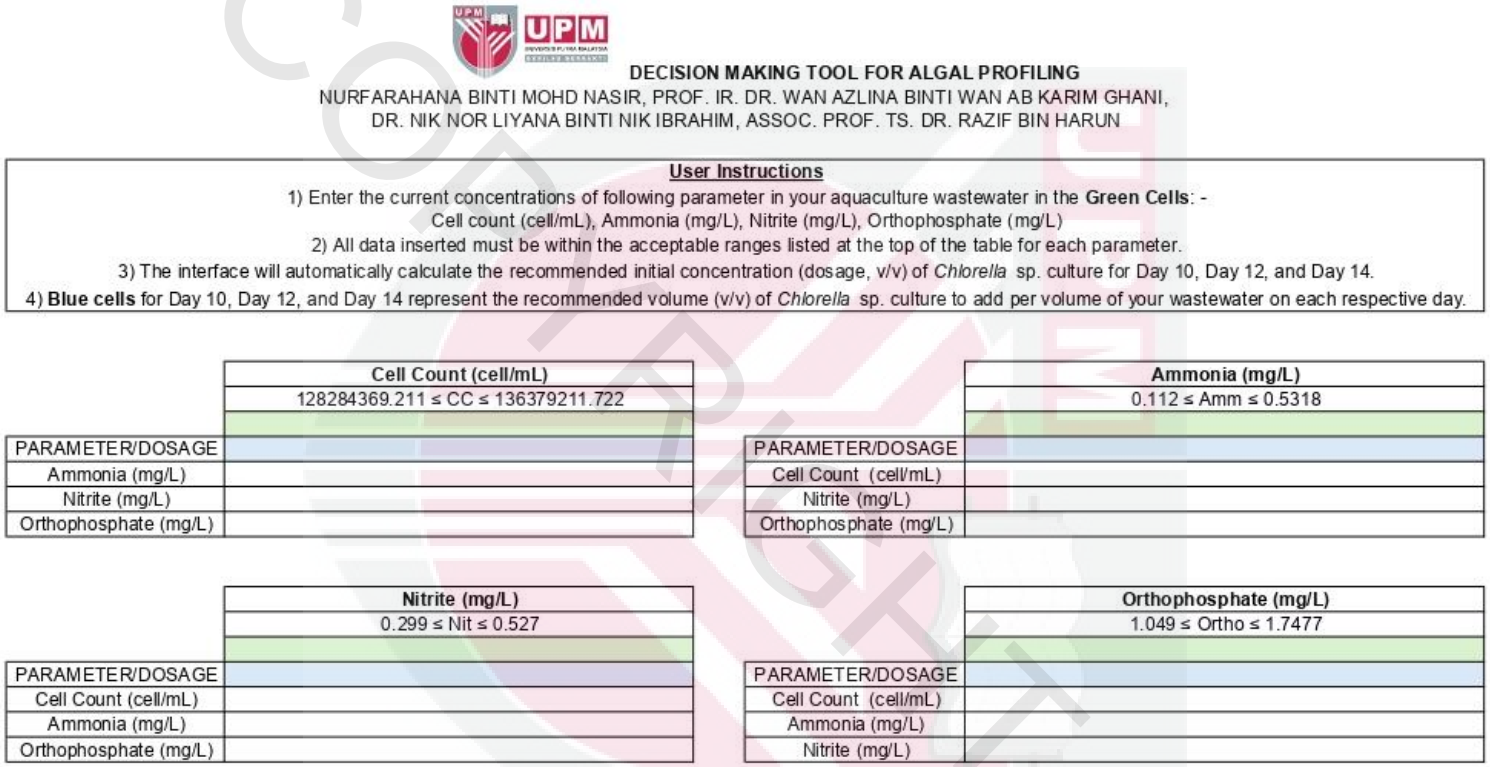

DECISION MAKING TOOL FOR ALGAL PROFILING

NURFARAHANA BINTI MOHD NASIR, PROF. IR. DR. WAN AZLINA BINTI WAN AB KARIM GHANI,
DR. NIK NOR LIYANA BINTI NIK IBRAHIM, ASSOC. PROF. TS. DR. RAZIF BIN HARUN

User Instructions

1) Enter the current concentrations of following parameter in your aquaculture wastewater in the **Green Cells**: -
Cell count (cell/mL), Ammonia (mg/L), Nitrite (mg/L), Orthophosphate (mg/L)
2) All data inserted must be within the acceptable ranges listed at the top of the table for each parameter.
3) The interface will automatically calculate the recommended initial concentration (dosage, v/v) of *Chlorella* sp. culture for Day 10, Day 12, and Day 14.
4) **Blue cells** for Day 10, Day 12, and Day 14 represent the recommended volume (v/v) of *Chlorella* sp. culture to add per volume of your wastewater on each respective day.

	Cell Count (cell/mL)
	128284369.211 ≤ CC ≤ 136379211.722
PARAMETER/DOSAGE	
Ammonia (mg/L)	
Nitrite (mg/L)	
Orthophosphate (mg/L)	

	Ammonia (mg/L)
	0.112 ≤ Amm ≤ 0.5318
PARAMETER/DOSAGE	
Cell Count (cell/mL)	
Nitrite (mg/L)	
Orthophosphate (mg/L)	

	Nitrite (mg/L)
	0.299 ≤ Nit ≤ 0.527
PARAMETER/DOSAGE	
Cell Count (cell/mL)	
Ammonia (mg/L)	
Orthophosphate (mg/L)	

	Orthophosphate (mg/L)
	1.049 ≤ Ortho ≤ 1.7477
PARAMETER/DOSAGE	
Cell Count (cell/mL)	
Ammonia (mg/L)	
Nitrite (mg/L)	

Figure 6.4 : Interface without User Input

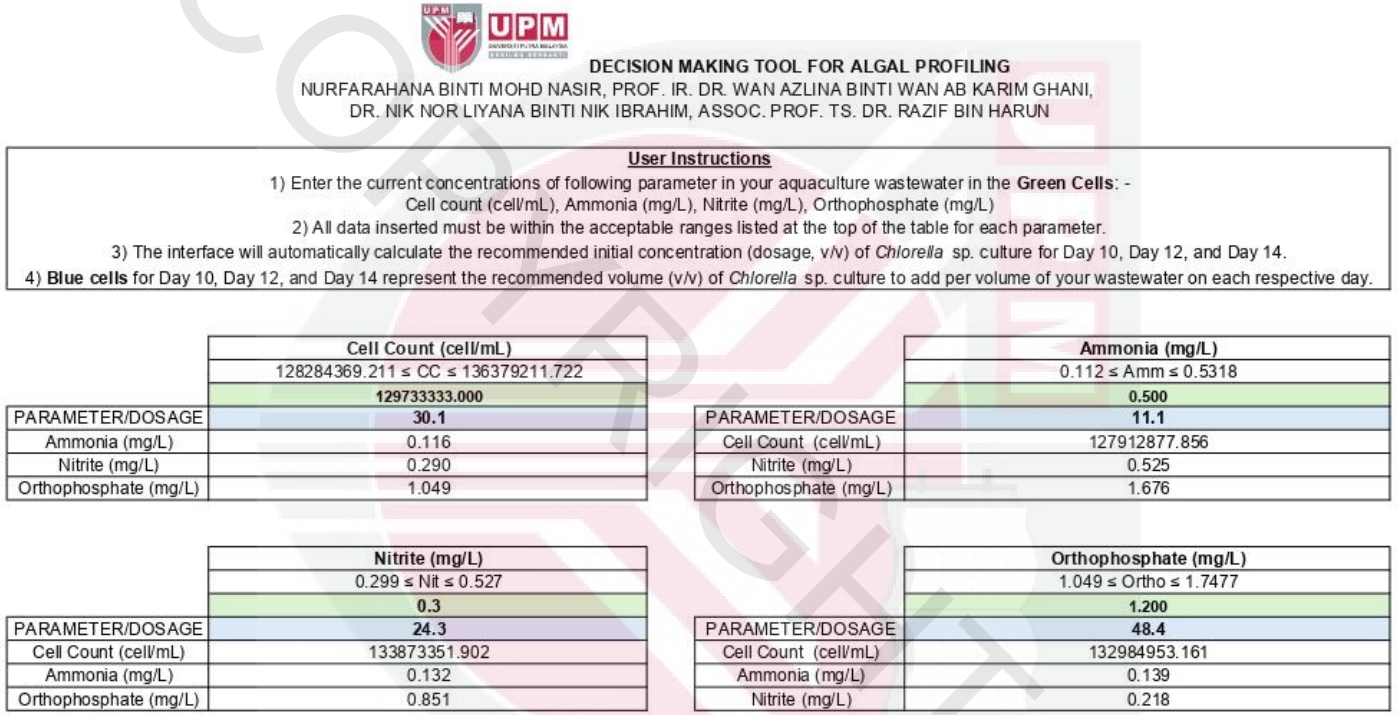

DECISION MAKING TOOL FOR ALGAL PROFILING

NURFARAHANA BINTI MOHD NASIR, PROF. IR. DR. WAN AZLINA BINTI WAN AB KARIM GHANI,
DR. NIK NOR LIYANA BINTI NIK IBRAHIM, ASSOC. PROF. TS. DR. RAZIF BIN HARUN

User Instructions

1) Enter the current concentrations of following parameter in your aquaculture wastewater in the **Green Cells**: -
Cell count (cell/mL), Ammonia (mg/L), Nitrite (mg/L), Orthophosphate (mg/L)
2) All data inserted must be within the acceptable ranges listed at the top of the table for each parameter.
3) The interface will automatically calculate the recommended initial concentration (dosage, v/v) of *Chlorella* sp. culture for Day 10, Day 12, and Day 14.
4) **Blue cells** for Day 10, Day 12, and Day 14 represent the recommended volume (v/v) of *Chlorella* sp. culture to add per volume of your wastewater on each respective day.

	Cell Count (cell/mL)
	128284369.211 ≤ CC ≤ 136379211.722
	129733333.000
PARAMETER/DOSAGE	**30.1**
Ammonia (mg/L)	0.116
Nitrite (mg/L)	0.290
Orthophosphate (mg/L)	1.049

	Ammonia (mg/L)
	0.112 ≤ Amm ≤ 0.5318
	0.500
PARAMETER/DOSAGE	**11.1**
Cell Count (cell/mL)	127912877.856
Nitrite (mg/L)	0.525
Orthophosphate (mg/L)	1.676

	Nitrite (mg/L)
	0.299 ≤ Nit ≤ 0.527
	0.3
PARAMETER/DOSAGE	**24.3**
Cell Count (cell/mL)	133873351.902
Ammonia (mg/L)	0.132
Orthophosphate (mg/L)	0.851

	Orthophosphate (mg/L)
	1.049 ≤ Ortho ≤ 1.7477
	1.200
PARAMETER/DOSAGE	**48.4**
Cell Count (cell/mL)	132984953.161
Ammonia (mg/L)	0.139
Nitrite (mg/L)	0.218

Figure 6.5 : Interface with User Input

6.4.2 Interface Testing and Validation

Internal testing and validation were employed to ensure the functionality and accuracy of the Excel-based interface. This involved entering various input parameters for initial concentrations of nutrients and other relevant factors. The interface was verified to retrieve corresponding predicted efficiency values for bioremediation and biomass harvesting from the pre-defined data sheets. Furthermore, consistency checks were performed to confirm data validation rules, ensure consistent unit usage throughout the interface, and maintain information accuracy, as demonstrated in Table 6.10.

Table 6.10 : Validation of Experimental and Predicted Values Using Interface with Percentage Error

Parameters	Concentration	Experimental (%, v/v)	Predicted Interface (%, v/v)	Error (%)
Cell density (Cell mL^{-1})	128611430.6	20	18	10
	135033553	30	29.3	2.3
	131571319.5	40	49.2	23
Ammonia ($mg\ L^{-1}$)	0.53	10	10.1	1
	0.24	20	20.4	2
	0.118	40	34.6	13.5
Nitrite ($mg\ L^{-1}$)	0.51	20	18.5	7.5
	0.28	30	38.1	27
	0.49	30	28.5	5
Orthophosphate ($mg\ L^{-1}$)	1.63	10	11.9	19
	1.04	20	21.3	6.5
	1.2	40	48.4	21

The table presents significant differences between predicted and experimental values, especially for higher concentrations. For example, at 40% (v/v), the error for cell density is 23%, ammonia shows an error of 13.5%, and orthophosphate records a significant 21% error. These larger deviations highlight the challenges in accurately predicting performance at higher

concentrations. However, lower concentration levels generally show smaller errors, with the smallest error observed for cell density at 30% (v/v) (2.3%) and ammonia at 10% v/v (1%), indicating more reliable predictions. This suggests the model performs better at lower concentrations but requires further refinement at higher levels.

However, users should be mindful of the limitations of the M5P model, as its predictions are solely based on the training data. For experimental validation, it's recommended to perform small-scale trials to confirm the predicted efficiencies across various dosages before large-scale implementation.

6.5 Development of New Framework

As the final part of the study, developing a new framework for bioremediation of aquaculture wastewater using microalgae and bio-harvesting using fungus represents a significant advancement in sustainable wastewater treatment methodologies. Integrating machine learning algorithms such as M5P into the framework has enhanced our ability to predict and optimize bioremediation processes, leading to more efficient and environmentally friendly wastewater treatment systems.

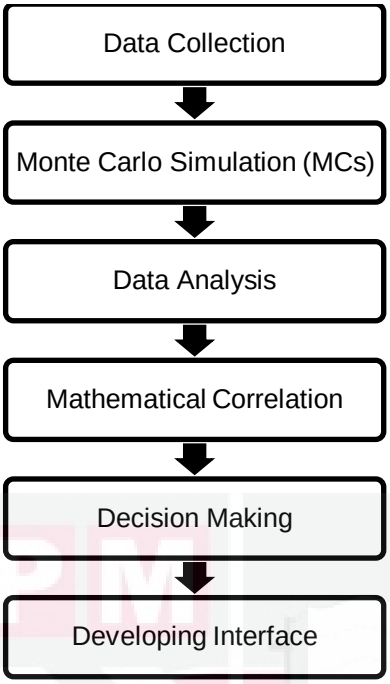

Figure 6.6 : Flow of the Proposed Framework

Figure 6.6 presents an overview of the machine learning framework employed in the research. The typical data mining process involves data collection, analysis, and decision-making. However, three additional steps were incorporated to address specific challenges and limitations encountered in the study: Monte Carlo Simulation, mathematical correlation, and interface development. These supplementary steps were introduced to improve the model's efficacy and mitigate the encountered issues.

Data collection is a fundamental stage in any data mining study and is placed as the first in the framework. It can be obtained through a new experimental procedure, but most industries nowadays save time by utilizing previous data. This research's data was sourced from earlier studies, as outlined in Chapters 4 and 5. Subsequently, due to the limited data sources and time constraints, Monte Carlo Simulation was employed as the second step of the process. In

Monte Carlo simulation, mean and standard deviation are crucial parameters as they define the central tendency and variability of the input variables. It ensures the generation of representative data samples for accurate modeling of uncertain systems. Following data collection and simulation, data analysis was performed. This step involved preprocessing the data to remove outliers and preparing it for analysis using machine learning algorithms. WEKA software was used to classify and analyze the data, producing metrics such as the correlation coefficient (CC), mean absolute error (MAE), and root mean square error (RMSE), which were thoroughly examined. Mathematical correlation was then used to establish the relationships between key variables, ensuring the modeled results aligned with expected outcomes. This helped refine the predictions and improve the accuracy of the overall model.

The next step, decision-making, involved utilizing the results of the data analysis to make informed decisions that optimized both the bioremediation and biomass harvesting processes. Finally, the framework included interface development to create a user-friendly tool for applying the optimized model. This interface addressed issues identified during the study and allowed for future improvements or adaptations. Ultimately, this framework aims to optimize bioremediation processes and enhance bio-harvesting techniques in aquaculture systems.

6.6 Conclusion

Incorporating machine learning into decision-making frameworks significantly advances environmental science and sustainable technology. By integrating

comprehensive data analysis and profiling, these frameworks can amplify the efficiency and efficacy of decision-making processes. Machine learning offers an approach to constructing predictive models and informing future experiments based on existing data. In this study, the utilization of the Waikato Environment Knowledge Analysis (WEKA) tool, specifically using the M5P algorithm, facilitated the analysis of data derived from batch experiments focusing on marine and freshwater aquaculture wastewater bioremediation using microalgae alongside the subsequent bio-harvesting process employing filamentous fungus.

The M5P algorithm enabled the generation of predictive equations for both bioremediation and bio-harvesting, providing a valuable understanding of the relationships between operational parameters and process outcomes. The algorithm produced an equation for bioremediation that accurately predicts nutrient removal efficiency based on variables such as microalgae concentration, nutrient levels, and environmental conditions. Similarly, for bio-harvesting, the generated equation offers predictions on the efficiency of microalgae separation using filamentous fungus, considering factors such as dosage, mixing rate, and pH.

This framework offers a general approach to wastewater treatment by harnessing the unique capabilities of microalgae and fungus in nutrient removal and bio-harvesting, respectively. Machine learning algorithms enable real-time monitoring, adaptive control, and continuous optimization of the treatment processes. The framework's performance can be continuously

refined and improved by incorporating feedback mechanisms and model validation techniques to adapt to changing conditions and evolving research needs. In general, developing this new framework represents a significant step towards sustainable aquaculture practices, offering a cost-effective, energy-efficient, and eco-friendly solution for wastewater management in aquaculture facilities. Through further research, collaboration, and implementation, the full potential of this framework can be realized, contributing to the preservation and protection of aquatic ecosystems worldwide.

CHAPTER 7

SUMMARY, GENERAL CONCLUSION AND RECOMMENDATIONS FOR FUTURE RESEARCH

7.1 Summary and General Conclusion

The study aimed to assess how effectively microalgae can treat shrimp aquaculture wastewater by removing nitrogen and phosphorus pollutants. *Chlorella* sp. UMT LF1 and UMT LF2, isolated from shrimp cultures, were tested at different concentrations to identify the optimal level for pollutant removal, with nutrient uptake rates analyzed using kinetic models. The results showed that the optimum nutrient removal occurred at 40% (v/v) for *Chlorella* sp. UMT LF1 and 30% (v/v) for UMT LF2 with more than 90% removal efficiency. The study also explored using a bioflocculant to harvest the excess microalgae biomass from the bioremediation process. The bio flocculant, tested at specific conditions (30 g L^{-1}, pH 7, 125 rpm), achieved over 90% efficiency in separating microalgae biomass from the water. This finding suggests that the bio flocculant is an effective and practical biomass recovery and wastewater purification method. Finally, the study focused on predicting the results of bioremediation and bio-harvesting processes using machine learning, specifically through the Waikato Environment of Knowledge Analysis (WEKA) software. The goal was to develop predictive models with WEKA that could estimate how effectively microalgae would remove pollutants from shrimp aquaculture wastewater and how efficiently the biomass could be harvested. In conclusion, these findings provide a strong foundation for future research and practical applications focused on improving water quality and

sustainability in the shrimp aquaculture industry

7.2 Recommendations for Future Research

This study has raised some questions that need further investigation to produce high-quality microalgae biomass and harness harvesting techniques for the potential of microalgae. The following considerations should be considered:

1) Optimize growth conditions: Temperature, light intensity and duration, pH, and nutrient availability can significantly influence microalgae growth.

2) Determine the optimal harvesting time: Harvesting microalgae biomass at the right time is essential for achieving the desired quality.

3) Extension to Other Aquatic Environments: While the study focuses on aquaculture wastewater, future research could explore the application of microalgae-based bioremediation in diverse aquatic environments, such as natural water bodies facing eutrophication challenges

4) Optimization of Machine Learning Models: The study utilises machine learning, specifically the M5P algorithm, to model bioremediation and bioharvesting processes. Future research could focus on further optimizing and validating machine learning models using larger datasets and considering additional factors that may influence the efficiency of these processes.

REFERENCES

Abdelfattah, A., Ali, S. S., Ramadan, H., El-Aswar, E. I., Eltawab, R., Ho, S. H., Elsamahy, T., Li, S., El-Sheekh, M. M., Schagerl, M., Kornaros, M., & Sun, J. (2023). Microalgae-based wastewater treatment: Mechanisms, challenges, recent advances, and future prospects. *Environmental Science and Ecotechnology*, 13: 100205.

Abdel-Raouf, N., Al-Homaidan, A. A., & Ibraheem, I. B. M. (2012). Microalgae and wastewater treatment. *Saudi Journal of Biological Sciences*, 19(3): 257–275.

Abdul Hamid, S. H., Lananan, F., Din, W. N. S., Lam, S. S., Khatoon, H., Endut, A., & Jusoh, A. (2014). Harvesting microalgae, *Chlorella* sp. by bio-flocculation of *Moringa oleifera* seed derivatives from aquaculture wastewater phytoremediation. *International Biodeterioration and Biodegradation*, 95*:* 270–275.

Aditya, L., Mahlia, T. M. I., Nguyen, L. N., Vu, H. P., & Nghiem, L. D. (2022). Microalgae-bacteria consortium for wastewater treatment and biomass production. *Science of The Total Environment*, 838: 155871.

Ahmad, A. L., Mat Yasin, N. H., Derek, C. J. C., & Lim, J. K. (2011). Optimization of microalgae coagulation process using chitosan. *Chemical Engineering Journal*, 173(3): 879–882.

Ahmad, A., Sheikh Abdullah, S. R., Hasan, H. A., Othman, A. R., & Ismail, N. ‘Izzati. (2021). Aquaculture industry: Supply and demand, best practices, effluent and its current issues and treatment technology. *Journal of Environmental Management*, 287: 112271.

Alazaiza, M. Y. D., He, S., Su, D., Abu Amr, S. S., Toh, P. Y., & Bashir, M. J. K. (2023). Sewage Water Treatment Using *Chlorella vulgaris* Microalgae for Simultaneous Nutrient Separation and Biomass Production. *Separations*, 10(4): 229

Alishah Aratboni, H., Rafiei, N., Garcia-Granados, R., Alemzadeh, A., & Morones-Ramírez, J. R. (2019). Biomass and lipid induction strategies in microalgae for biofuel production and other applications. *Microbial Cell Factories*, 18(1): 1–17.

Al-Jabri, H., Das, P., Khan, S., Thaher, M., & Abdulquadir, M. (2021). Treatment of wastewaters by microalgae and the potential applications of the produced biomass—a review. *Water*, 13(1): 27.

Aljuboori, A. H. R., Uemura, Y., & Thanh, N. T. (2016). Flocculation and mechanism of self-flocculating lipid producer microalga *Scenedesmus quadricauda* for biomass harvesting. *Biomass and Bioenergy*, 93: 38–42.

Amorim, C. A., & Moura, A. do N. (2021). Ecological impacts of freshwater algal blooms on water quality, plankton biodiversity, structure, and ecosystem functioning. *Science of The Total Environment*, 758: 143605.

Ansari, F. A., Singh, P., Guldhe, A., & Bux, F. (2017). Microalgal cultivation using aquaculture wastewater: Integrated biomass generation and nutrient remediation. *Algal Research*, 21: 169–177.

Aragão, C., Gonçalves, A. T., Costas, B., Azeredo, R., Xavier, M. J., & Engrola, S. (2022). Alternative Proteins for Fish Diets: Implications beyond Growth. *Animals*, 12(9): 1211.

Aslan, S., & Kapdan, I. K. (2006). Batch kinetics of nitrogen and phosphorus removal from synthetic wastewater by algae. *Ecological Engineering*, 28(1): 64–70.

Babiak, W., & Krzemińska, I. (2021). Extracellular polymeric substances (EPS) as microalgal bioproducts: A review of factors affecting EPS synthesis and application in flocculation processes. *Energies*, 14(13): 4007.

Bahiram, V. K., Waskar, D. P., & Khandare, V. S. (2020). Effect of Pretreatments on Dehydration and Quality of Spine Gourd (Momordica dioica Roxb.) Slices. *Journal of Agriculture Research and Technology*, 45(1).

Bajwa, K., Bishnoi, N. R., Kirrolia, A., Gupta, S., & Tamil Selvan, S. (2019). Response surface methodology as a statistical tool for optimization of physio-biochemical cellular components of microalgae *Chlorella pyrenoidosa* for biodiesel production. *Applied Water Science*, 9(5): 1–16.

Baker, L. A., & Newman, R. M. (2013). 4.4 Managing the Biological, Economic, and Social Aspects of Sustainability of Lake Ecosystems. In *Comprehensive Water Quality and Purification* (pp. 76–86). Elsevier.

Behnood, A., Behnood, V., Modiri Gharehveran, M., & Alyamac, K. E. (2017). Prediction of the compressive strength of normal and high-performance concretes using M5P model tree algorithm. *Construction and Building Materials*, 142: 199–207.

Bhatt, P., Bhandari, G., Turco, R. F., Aminikhoei, Z., Bhatt, K., & Simsek, H. (2022). Algae in wastewater treatment, mechanism, and application of biomass for production of value-added product. *Environmental Pollution*, *309*, 119688.

Bhatt, P., Huang, J.-Y., Brown, P., Shivaram, K. B., Yakamercan, E., & Simsek, H. (2023). Electrochemical treatment of aquaculture wastewater effluent and optimization of the parameters using response surface methodology. *Environmental Pollution,* 331: 121864.

Bhattacharya, A., Mathur, M., Kumar, P., Prajapati, S. K., & Malik, A. (2017). A rapid method for fungal assisted algal flocculation: Critical parameters & mechanism insights. *Algal Research*, 21: 42–51.

Braimah, M. N., Anozie, A. N., & Odejobi, O. J. (2016). Utilization of Response Surface Methodology (RSM) in the Optimization of Crude Oil Refinery Process, New Port-Harcourt Refinery, Nigeria. *Journal of Multidisciplinary Engineering Science and Technology (JMEST)*, 3(3).

Calicioglu, O., Sengul, M. Y., Femeena, P. V., & Brennan, R. A. (2021). Duckweed growth model for large-scale applications: Optimizing harvesting regime and intrinsic growth rate via machine learning to maximize biomass yields. *Journal of Cleaner Production*, 324: 129120.

Cardoso, L. G., Duarte, J. H., Andrade, B. B., Lemos, P. V. F., Costa, J. A. V., Druzian, J. I., & Chinalia, F. A. (2020). Spirulina sp. LEB 18 cultivation in outdoor pilot scale using aquaculture wastewater: High biomass, carotenoid, lipid and carbohydrate production. *Aquaculture*, 525: 735272.

Chia, W. Y., Ying Tang, D. Y., Khoo, K. S., Kay Lup, A. N., & Chew, K. W. (2020). Nature's fight against plastic pollution: Algae for plastic biodegradation and bioplastics production. *Environmental Science and Ecotechnology*, 4: 100065.

Choi, Y. N., Cho, H. U., Utomo, J. C., Shin, D. Y., Kim, H. K., & Park, J. M. (2016). Efficient harvesting of Synechocystis sp. PCC 6803 with filamentous fungal pellets. *Journal of Applied Phycology*, 28(4): 2225–2231.

Chowdhury, A., Talib, A., & Yahya, K. (2013). A review on marine shrimp aquaculture production trend and sustainability in Malaysia and the world perspective. *Proceedings of the Conference: International Fisheries Symposium*, 6–8.

Chu, F., Cheng, J., Zhang, X., Ye, Q., & Zhou, J. (2019). Enhancing lipid production in microalgae *Chlorella* PY-ZU1 with phosphorus excess and nitrogen starvation under 15% CO_2 in a continuous two-step cultivation process. *Chemical Engineering Journal*, 375: 121912.

Chu, R., Hu, D., Zhu, L., Li, S., Yin, Z., & Yu, Y. (2022). Recycling spent water from microalgae harvesting by fungal pellets to re-cultivate *Chlorella vulgaris* under different nutrient loads for biodiesel production. *Bioresource Technology*, 344: 126227.

Civzele, A., & Mezule, L. (2022). Microalgae Harvesting after Tertiary Wastewater Treatment with White-Rot Fungi. *Journal of Fungi*, 8(11): 1232.

Correa, I., Drews, P., Botelho, S., De Souza, M. S., & Tavano, V. M. (2017). Deep learning for microalgae classification. *Proceedings - 16th IEEE International Conference on Machine Learning and Applications, ICMLA 2017*, *2017-December*, 20–25.

De Farias Silva, C. E., De Oliveira Cerqueira, R. B., De Lima Neto, C. F., De Andrade, F. P., De Oliveira Carvalho, F., & Tonholo, J. (2020). Developing a kinetic model to describe wastewater treatment by microalgae based on simultaneous carbon, nitrogen and phosphorous removal. *Journal of Environmental Chemical Engineering*, 8(3): 103792.

de Morais, E. G., Sampaio, I. C. F., Gonzalez-Flo, E., Ferrer, I., Uggetti, E., & García, J. (2023). Microalgae harvesting for wastewater treatment and resources recovery: A review. *New Biotechnology*, 78: 84–94.

Dean, A. P., Sigee, D. C., Estrada, B., & Pittman, J. K. (2010). Using FTIR spectroscopy for rapid determination of lipid accumulation in response to nitrogen limitation in freshwater microalgae. *Bioresource Technology*, 101(12): 4499–4507.

Decostere, B., De Craene, J., Van Hoey, S., Vervaeren, H., Nopens, I., & Van Hulle, S. W. H. (2016). Validation of a microalgal growth model accounting with inorganic carbon and nutrient kinetics for wastewater treatment. *Chemical Engineering Journal*, 285: 189–197.

Delgadillo-Mirquez, L., Lopes, F., Taidi, B., & Pareau, D. (2016). Nitrogen and phosphate removal from wastewater with a mixed microalgae and bacteria culture. *Biotechnology Reports*, 11: 18–26.

Department of Fisheries Malaysia. (2020). *Annual Report 2019*.

Desai, K. M., Survase, S. A., Saudagar, P. S., Lele, S. S., & Singhal, R. S. (2008). Comparison of artificial neural network (ANN) and response surface methodology (RSM) in fermentation media optimization: Case study of fermentative production of scleroglucan. *Biochemical Engineering Journal*, 41(3): 266–273.

Dey, S., Botta, S., Kallam, R., Angadala, R., & Andugala, J. (2021). Seasonal variation in water quality parameters of Gudlavalleru Engineering College pond. *Current Research in Green and Sustainable Chemistry*, 4: 100058.

Do, C. V. T., Pham, M. H. T., Pham, T. Y. T., Dinh, C. T., Bui, T. U. T., Tran, T. D., & Nguyen, V. T. (2022). Microalgae and bioremediation of domestic wastewater. *Current Opinion in Green and Sustainable Chemistry*, 34: 100595.

Dong, J., Huang, G., Wu, L., Liu, F., Li, S., Cui, Y., Wang, Y., Leng, M., Wu, J., & Wu, S. (2022). Modelling Soil Temperature by Tree-Based Machine Learning Methods in Different Climatic Regions of China.

Applied Sciences, 12(10): 5088.

Dou, Y., & Meng, W. (2023). Comparative analysis of weka-based classification algorithms on medical diagnosis datasets. *Technology and Health Care*, 31(S1): 397–408.

Douglas, H. W., Collins, A. E., & Parkinson, D. (1959). Electric charge and other surface properties of some fungal spores. *Biochimica et Biophysica Acta*, 33(2): 535–538.

Duraiarasan, S. (2013). Influence of bioflocculation parameters on harvesting Chlorella salina and its optimization using response surface methodology. *Journal of Environmental Chemical Engineering*, 1: 1051–1056.

Duygu, D. (Yalcin), Udoh, A. U., Ozer, T. (Baykal), Akbulut, A., Erkaya, I. (Acikgoz), Yildiz, K., & Guler, D. (2012). Fourier transform infrared (FTIR) spectroscopy for identification of *Chlorella vulgaris* Beijerinck 1890 and *Scenedesmus obliquus* (Turpin) Kützing 1833. *Journal African of Biotechnology*, 11(16): 3817–3824.

Egede, E. J., Jones, H., Cook, B., Purchase, D., & Mouradov, Aidyn. (2016). Application of microalgae and fungal-microalgal associations for wastewater treatment. *Fungal Applications in Sustainable Environmental Biotechnology*, 143–181.

Eixler, S., Karsten, U., & Selig, U. (2006). Phosphorus storage in *Chlorella vulgaris* (Trebouxiophyceae, Chlorophyta) cells and its dependence on phosphate supply. *Phycologia*, 45(1): 53–60.

Elcik, H., Karadag, D., Kara, A. I., & Cakmakci, M. (2023). Microalgae Biomass Harvesting Using Chitosan Flocculant: Optimization of Operating Parameters by Response Surface Methodology. *Separations*, 10(9): 507.

Elieh-Ali-Komi, D., Hamblin, M. R., & Daniel, E.-A.-K. (2016). Chitin and Chitosan: Production and Application of Versatile Biomedical Nanomaterials HHS Public Access. *International Journal of Advanced Research*, 4(3): 411–427.

FAO. (2018). *The state of world fisheries and aquaculture 2018: meeting the sustainable development goals.*

FAO. (2020). The State of World Fisheries and Aquaculture. Sustainability in Action. In *FAO*.

FAO. (2022). *The State of World Fisheries and Aquaculture: Towards Blue Transformation*.

Fathi, S., Harun, A. N., Rambat, S., & Tukiran, N. A. (2018). Current Issues in Aquaculture: Lessons from Malaysia. *Advanced Science Letters*, 24(1):

503–505.

Felsenstein J. (1985). Confidence limits on phylogenies: An approach using the bootstrap. *Evolution*, 39(4): 783–791.

Ferreira, A. F., Soares Dias, A. P., Silva, C. M., & Costa, M. (2015). Evaluation of thermochemical properties of raw and extracted microalgae. *Energy*, 92: 365–372.

Ferrer Llagostera, P., Kallas, Z., Reig, L., & Amores de Gea, D. (2019). The use of insect meal as a sustainable feeding alternative in aquaculture: Current situation, Spanish consumers' perceptions and willingness to pay. *Journal of Cleaner Production*, 229: 10–21.

Gakii, C., & Jepkoech, J. (2019). A classification model for water quality analysis using decision tree. *European Journal of Computer Science and Information Technology*, 7(3): 1–8.

Ganeson, Y., Paramasivam, P., Palanisamy, K. M., Govindan, N., & Maniam, G. P. (2024). LCMS and FTIR profiling of microalga *Chlorella* sp. for cosmetics and skin care applications. *Cleaner Water*, 2: 100028.

Gao, F., Li, C., Yang, Z. H., Zeng, G. M., Feng, L. J., Liu, J. zhi, Liu, M., & Cai, H. wen. (2016). Continuous microalgae cultivation in aquaculture wastewater by a membrane photobioreactor for biomass production and nutrients removal. *Ecological Engineering*, 92: 55–61.

Ghee-Thean, L. , Islam, G. M. N., & Ismail, M. M. (2016). Malaysian white shrimp (*P. vannamei*) aquaculture- an application of stochastic frontier analysis on technical efficiency. *International Food Research Journal*, 23(2): 638–645.

Ghiassi, M., & Lee, S. (2018). A domain transferable lexicon set for Twitter sentiment analysis using a supervised machine learning approach. *Expert Systems with Applications*, 106: 197–216.

Ghosh, D., & Hallenbeck, P. C. (2010). Response surface methodology for process parameter optimization of hydrogen yield by the metabolically engineered strain *Escherichia coli* DJT135. *Bioresource Technology*, 101(6): 1820–1825.

Goh, P. S., Lau, W. J., Ismail, A. F., Samawati, Z., Liang, Y. Y., & Kanakaraju, D. (2023). Microalgae-Enabled Wastewater Treatment: A Sustainable Strategy for Bioremediation of Pesticides. *Water*, 15(1): 70.

Granados, M. R., Acién, F. G., Gómez, C., Fernández-Sevilla, J. M., & Molina Grima, E. (2012). Evaluation of flocculants for the recovery of freshwater microalgae. *Bioresource Technology*, 118: 102–110.

Gultom, S. O., & Hu, B. (2013). Review of Microalgae Harvesting via Co-Pelletization with Filamentous Fungus. *Energies*, 6(11): 5921–5939.

Guo, H. N., Wu, S. B., Tian, Y. J., Zhang, J., & Liu, H. T. (2021). Application of machine learning methods for the prediction of organic solid waste treatment and recycling processes: A review. *Bioresource Technology*, 319.

Guo, Z., Liu, Y., Guo, H., Yan, S., & Mu, J. (2013). Microalgae cultivation using an aquaculture wastewater as growth medium for biomass and biofuel production. *Journal of Environmental Sciences*, 25(S1): S85–S88

Gupta, A. (2021). *Steps to Complete a Machine Learning Project*.

Hadiyanto, H., Widayat, W., Christwardana, M., & Pratiwi, M. E. (2022). The flocculation process of *Chlorella* sp. using chitosan as a bio-flocculant: Optimization of operating conditions by response surface methodology. *Current Research in Green and Sustainable Chemistry*, *5*, 100291.

Hall, B. G. (2013). Building phylogenetic trees from molecular data with MEGA. *Molecular Biology and Evolution*, 30(5: 1229–1235.

Han, P., Lu, Q., Fan, L., & Zhou, W. (2019). A review on the use of microalgae for sustainable aquaculture. *Applied Sciences*, 9(11): 2377.

Han, W., Mao, Y., Wei, Y., Shang, P., & Zhou, X. (2020). Bioremediation of aquaculture wastewater with algal-bacterial biofilm combined with the production of selenium rich biofertilizer. *Water*, 12(7): 2071.

Hannon, M., Gimpel, J., Tran, M., Rasala, B., & Mayfield, S. (2010). Biofuels from algae: challenges and potential. *Biofuels*, 1(5): 763–784.

Heasman, M., Diemar, J., O'connor, W., Sushames, T., & Foulkes, L. (2000). Development of extended shelf-life microalgae concentrate diets harvested by centrifugation for bivalve molluscs - a summary. *Aquaculture Research*, 31(8–9): 637–659.

Heidari, M., Kariminia, H. R., & Shayegan, J. (2016). Effect of culture age and initial inoculum size on lipid accumulation and productivity in a hybrid cultivation system of *Chlorella vulgaris*. *Process Safety and Environmental Protection*, 104: 111–122.

Hing, G. B. (2022, April 26). Salvaging Malaysia's shrimp industry reputation. *Monash University Malaysia*.

Hom-Diaz, A., Passos, F., Ferrer, I., Vicent, T., & Blánquez, P. (2016). Enzymatic pretreatment of microalgae using fungal broth from Trametes versicolor and commercial laccase for improved biogas production. *Algal Research*, 19: 184–188.

Hossain, N., Hasan, M. H., Mahlia, T. M. I., Shamsuddin, A. H., & Silitonga, A. S. (2020). Feasibility of microalgae as feedstock for alternative fuel in Malaysia: A review. *Energy Strategy Reviews*, 32, 100536.

Huang, C., Luo, Y., Zeng, G., Zhang, P., Peng, R., Jiang, X., & Jiang, M. (2022). Effect of adding microalgae to whiteleg shrimp culture on water quality, shrimp development and yield. *Aquaculture Reports*, 22: 100916.

Iasimone, F., De Felice, V., Panico, A., & Pirozzi, F. (2017). Experimental study for the reduction of CO2 emissions in wastewater treatment plant using microalgal cultivation. *Journal of CO2 Utilization*, 22: 1–8.

Iber, B. T., & Kasan, N. A. (2021). Recent advances in Shrimp aquaculture wastewater management. *Heliyon*, 7(11): 08283

Icke, O., Van Es, D. M., De Koning, M. F., Wuister, J. J. G., Ng, J., Phua, K. M., Koh, Y. K. K., Chan, W. J., & Tao, G. (2020). Performance improvement of wastewater treatment processes by application of machine learning. *Water Science and Technology*, 82(12): 2671–2680.

Isa, S. H., Ramlee, M. N. A., Lola, M. S., Ikhwanuddin, M., Azra, M. N., Abdullah, M. T., Zakaria, S., & Ibrahim, Y. (2021). A system dynamics model for analysing the eco-aquaculture system of integrated aquaculture park in Malaysia with policy recommendations. *Environment, Development and Sustainability*, 23(1): 511–533.

Isaac Abiodun, O., Jantan, A., Esther Omolara, A., Victoria Dada, K., AbdElatif Mohamed, N., & Arshad, H. (2018). State-of-the-art in artificial neural network applications: A survey. *Heliyon*, 4: 938.

Ismail, N. H., Ahmad, F., & Aziz, A. A. (2013). Implementing WEKA as a Data Mining Tool to Analyze Students' Academic Performances Using Naïve Bayes Classifier. *Conference: UniSZA Postgraduate Research*.

Jegatheesan, V., Shu, L., & Visvanathan, C. (2011). Aquaculture Effluent: Impacts and Remedies for Protecting the Environment and Human Health. *Encyclopedia of Environmental Health*, 1–5: 123–135.

Jin, F. J., Hu, S., Wang, B. T., & Jin, L. (2021). Advances in Genetic Engineering Technology and Its Application in the Industrial Fungus *Aspergillus oryzae*. *Frontiers in Microbiology*, 12: 644404.

Jumatli, A., & Ismail, M. S. (2021). Promotion of Sustainable Aquaculture in Malaysia. *Proceedings of the International Workshop on the Promotion of Sustainable Aquaculture, Aquatic Animal Health, and Resource Enhancement in Southeast Asia*, 31–40.

Kalil, S. J., Maugeri, F., & Rodrigues, M. I. (2000). Response surface analysis and simulation as a tool for bioprocess design and optimization. *Process Biochemistry*, 35(6): 539–550.

Kanchanatip, E., Su, B. R., Tulaphol, S., Den, W., Grisdanurak, N., & Kuo, C. C. (2016). Fouling characterization and control for harvesting microalgae *Arthrospira* (*Spirulina*) maxima using a submerged, disc-

type ultrafiltration membrane. *Bioresource Technology*, 209: 23–30.

Kasan, N. A., Dagang, A. N., & Abdullah, M. I. (2018). Application of biofloc technology (BFT) in shrimp aquaculture industry. *IOP Conference Series: Earth and Environmental Science*, 196(1): 012043.

Kassim, M. A., Hashim, N. H. F., Jaafar, M. H., & Lalung, J. (2022). Chapter 2: Microalgae biotechnology for bioremediation applications. In *Algal Biotechnology* (pp. 33–46). Elsevier.

Khan, M. I., Shin, in H., & Kim, J. D. (2018). The promising future of microalgae: current status, challenges, and optimization of a sustainable and renewable industry for biofuels, feed, and other products. *Microbial Cell Factories*, 17(1): 36.

Khatoon, H., Banerjee, S., Syakir Syahiran, M., Mat Noordin, N. Bt., Munafi Ambok Bolong, A., & Endut, A. (2016). Re-use of aquaculture wastewater in cultivating microalgae as live feed for aquaculture organisms. *Desalination and Water Treatment*, 57(60): 29295–29302.

Kholssi, R., Riouchi, O., Douhri, H., & Debdoubi, A. (2023). Microalgae as a sustainable energy source: Growth and lipids production of *Nitzschia* sp., *Nannochloropsis* sp., and *Tetraselmis* sp. from Mediterranean seawater. *Biocatalysis and Agricultural Biotechnology*, 50: 102720.

Khoo, K. S., Ahmad, I., Chew, K. W., Iwamoto, K., Bhatnagar, A., & Show, P. L. (2023). Enhanced microalgal lipid production for biofuel using different strategies including genetic modification of microalgae: A review. *Progress in Energy and Combustion Science*, 96: 101071.

Kim, D. G., Oh, H. M., Park, Y. H., Kim, H. S., Lee, H. G., & Ahn, C. Y. (2013). Optimization of flocculation conditions for *Botryococcus braunii* using response surface methodology. *Journal of Applied Phycology*, 25(3): 875–882.

Kuo, C. M., Jian, J. F., Lin, T. H., Chang, Y. Bin, Wan, X. H., Lai, J. T., Chang, J. S., & Lin, C. S. (2016). Simultaneous microalgal biomass production and CO_2 fixation by cultivating *Chlorella* sp. GD with aquaculture wastewater and boiler flue gas. *Bioresource Technology*, 221: 241–250.

Kurniawan, S. B., Abdullah, S. R. S., Imron, M. F., Ahmad, A., Mohd Said, N. S., Mohd Rahim, N. F., Mohammad Alnawajha, M., Abu Hasan, H., Othman, A. R., & Purwanti, I. F. (2021). Potential of valuable materials recovery from aquaculture wastewater: An introduction to resource reclamation. *Aquaculture Research*, 52(7): 2954–2962.

Kurniawan, S. B., Abdullah, S. R. S., Imron, M. F., Said, N. S. M., Ismail, N. ‘Izzati, Hasan, H. A., Othman, A. R., & Purwanti, I. F. (2020). Challenges and opportunities of biocoagulant/bioflocculant application for drinking water and wastewater treatment and its potential for sludge

recovery. *International Journal of Environmental Research and Public Health*, 17(24): 1–33.

Kurniawan, S. B., Ahmad, A., Rahim, N. F. M., Said, N. S. M., Alnawajha, M. M., Imron, M. F., Abdullah, S. R. S., Othman, A. R., Ismail, N. 'Izzati, & Hasan, H. A. (2021). Aquaculture in Malaysia: Water-related environmental challenges and opportunities for cleaner production. *Environmental Technology & Innovation*, 24: 101913.

Kusumaningrum, H. P., Zainuri, M., Marhaendrajaya, I., & Subagio, A. (2018). Nanosilver microalgae biosynthesis: Cell appearance based on SEM and EDX methods. *Journal of Physics: Conference Series*, 1025(1): 012084.

Laamanen, C. A., Ross, G. M., & Scott, J. A. (2016). Flotation harvesting of microalgae. *Renewable and Sustainable Energy Reviews*, 58: 75–86.

Laezza, C., Salbitani, G., & Carfagna, S. (2022). Fungal Contamination in Microalgal Cultivation: Biological and Biotechnological Aspects of Fungi-Microalgae Interaction. *Journal of Fungi*, 8(10): 1099.

Lananan, F., Abdul Hamid, S. H., Din, W. N. S., Ali, N., Khatoon, H., Jusoh, A., & Endut, A. (2014). Symbiotic bioremediation of aquaculture wastewater in reducing ammonia and phosphorus utilizing Effective Microorganism (EM-1) and microalgae (*Chlorella* sp.). *International Biodeterioration & Biodegradation*, 95(PA): 127–134.

Lananan, F., Mohd Yunos, F. H., Mohd Nasir, N., Abu Bakar, N. S., Lam, S. S., & Jusoh, A. (2016). Optimization of biomass harvesting of microalgae, *Chlorella* sp. utilizing auto-flocculating microalgae, *Ankistrodesmus* sp. as bio-flocculant. *International Biodeterioration and Biodegradation*, 113: 391–396.

Li, T., Lu, J., Wu, J., Zhang, Z., & Chen, L. (2022). Predicting Aquaculture Water Quality Using Machine Learning Approaches. *Water*, 14(18): 2836.

Li, Y., Xu, Y., Liu, L., Li, P., Yan, Y., Chen, T., Zheng, T., & Wang, H. (2017). Flocculation mechanism of *Aspergillus niger* on harvesting of *Chlorella vulgaris* biomass. *Algal Research*, 25: 402–412.

Liu, C., Sun, D., Liu, J., Zhu, J., & Liu, W. (2021). Recent advances and perspectives in efforts to reduce the production and application cost of microbial flocculants. *Bioresources and Bioprocessing*, 8(1): 51.

Madkour, A. G. M. E., Ibrahim, H. A. H., El-Sayed, W. M. M., & El-Moselhy, K. M. (2020). Bioflocculation technique for microalgal harvesting and wastewater nutrient recovery. *Iranian Journal of Fisheries Sciences*, 19(4): 1780–1794.

Mahesh, B. (2018). Machine Learning Algorithms-A Review. *International Journal of Science and Research*, 9(1): 381–386.

Mahlangu, D., Mphahlele, K., De Paola, F., & Mthombeni, N. H. (2024). Microalgae-Mediated Biosorption for Effective Heavy Metals Removal from Wastewater: A Review. *Water*, 16(5): 718.

Majerník, M., Chovancová, J., Drábik, P., & Štofková, Z. (2023). Environmental Technological Innovations and the Sustainability of their Development. *Ecological Engineering and Environmental Technology*, 24(4): 245–252.

Manhaeghe, D., Blomme, T., Van Hulle, S. W. H., & Rousseau, D. P. L. (2020). Experimental assessment and mathematical modelling of the growth of Chlorella vulgaris under photoautotrophic, heterotrophic and mixotrophic conditions. *Water Research*, 184: 116152.

Manyangadze, M., Chikuruwo, N. H. M., Narsaiah, T. B., Chakra, C. S., Radhakumari, M., & Danha, G. (2020). Enhancing adsorption capacity of nano-adsorbents via surface modification: A review. *South African Journal of Chemical Engineering* 31: 25–32.

Martin, Marcel. (2011). Cutadapt Removes Adapter Sequences from High-Throughput Sequencing Reads. *EMBnet.Journal*, 17(1): 10–12.

Masojídek, J., & Torzillo, G. (2008). Mass Cultivation of Freshwater Microalgae. In *Encyclopedia of Ecology* (pp. 2226–2235).

McPhail, C., Maier, H. R., Kwakkel, J. H., Giuliani, M., Castelletti, A., & Westra, S. (2018). Robustness Metrics: How Are They Calculated, When Should They Be Used and Why Do They Give Different Results? *Earth's Future*, 6(2): 169–191.

Merlini, D., & Rossini, M. (2021). Text categorization with WEKA: A survey. *Machine Learning with Applications*, 4: 100033.

Miao, H., Sun, L., Tian, Q., Wang, S., & Wang, J. (2012). Study on the Effect of Monochromatic Light on the Growth of the Red Tide Diatom Skeletonema Costatum. *Optics and Photonics Journal*, 2(3): 152–156.

Mishra, P., Pandey, C. M., Singh, U., Gupta, A., Sahu, C., & Keshri, A. (2019). Descriptive statistics and normality tests for statistical data. *Annals of Cardiac Anaesthesia*, 22(1): 67–72.

Mitchell, D. A., Von Meien, O. F., Krieger, N., & Dalsenter, F. D. H. (2004). A review of recent developments in modeling of microbial growth kinetics and intraparticle phenomena in solid-state fermentation. *Biochemical Engineering Journal*, 17(1): 15–26.

Mohd Nasir, N., Mohd Yunos, F. H., Wan Jusoh, H. H., Mohammad, A., Lam, S. S., & Jusoh, A. (2019). Subtopic: Advances in water and wastewater

treatment harvesting of *Chlorella* sp. microalgae using *Aspergillus niger* as bio-flocculant for aquaculture wastewater treatment. *Journal of Environmental Management*, 249: 109373.

Mohd Yunos, F. H., Nasir, N. M., Wan Jusoh, H. H., Khatoon, H., Lam, S. S., & Jusoh, A. (2017). Harvesting of microalgae (*Chlorella* sp.) from aquaculture bioflocs using an environmental-friendly chitosan-based bio-coagulant. *International Biodeterioration and Biodegradation*, 124: 243–249.

Mohsenpour, S. F., Hennige, S., Willoughby, N., Adeloye, A., & Gutierrez, T. (2021). Integrating micro-algae into wastewater treatment: A review. *Science of the Total Environment*, 752: 142168.

Mohyedin, A. S. M., Mahadi, B., Awang, S. R., Kohar, U. H. A., & Talib, N. B. A. (2019). Exploring management and monitoring of harmful algal bloom events in Malaysia: government sector. *Asian Journal of Research in Business and Management*, 1(1): 1–8.

Molina Grima, E., Belarbi, E. H., Acién Fernández, F. G., Robles Medina, A., & Chisti, Y. (2003). Recovery of microalgal biomass and metabolites: process options and economics. *Biotechnology Advances*, 20(7–8): 491–515.

Mundi, G., Zytner, R. G., Warriner, K., Bonakdari, H., & Gharabaghi, B. (2021). Machine learning models for predicting water quality of treated fruit and vegetable wastewater. *Water*, 13(18): 2485.

Muradov, N., Taha, M., Miranda, A. F., Wrede, D., Kadali, K., Gujar, A., Stevenson, T., Ball, A. S., & Mouradov, A. (2015). Fungal-assisted algal flocculation: Application in wastewater treatment and biofuel production. *Biotechnology for Biofuels*, 8(1).

Mustafa, S., Bhatti, H. N., Maqbool, M., & Iqbal, M. (2021). Microalgae biosorption, bioaccumulation and biodegradation efficiency for the remediation of wastewater and carbon dioxide mitigation: Prospects, challenges and opportunities. *Journal of Water Process Engineering*, 41: 102009.

Najjar, Y. S. H., & Abu-Shamleh, A. (2020). Harvesting of microalgae by centrifugation for biodiesel production: A review. *Algal Research*, *51*, 102046.

Narayanan, M., Prabhakaran, M., Natarajan, D., Kandasamy, S., Raja, R., Carvalho, I. S., Ashokkumar, V., Chinnathambi, A., Alharbi, S. A., Devarayan, K., & Pugazhendhi, A. (2021). Phycoremediation potential of *Chlorella* sp. on the polluted Thirumanimutharu river water. *Chemosphere*, 277: 130246.

Nasir, N. M., Bakar, N. S. A., Lananan, F., Abdul Hamid, S. H., Lam, S. S., & Jusoh, A. (2015). Treatment of African catfish, *Clarias gariepinus*

wastewater utilizing phytoremediation of microalgae, *Chlorella* sp. with *Aspergillus niger* bio-harvesting. *Bioresource Technology*, 190: 492–498.

Nazari, M. T., Freitag, J. F., Cavanhi, V. A. F., & Colla, L. M. (2020). Microalgae harvesting by fungal-assisted bioflocculation. *Reviews in Environmental Science and Bio/Technology*, 19(2): 369–388.

Nazari, M. T., Rigueto, C. V. T., Rempel, A., & Colla, L. M. (2021). Harvesting of *Spirulina platensis* using an eco-friendly fungal bioflocculant produced from agro-industrial by-products. *Bioresource Technology*, 322: 124525.

Nguyen, N. T., Tran-Nguyen, P. L., & Vo, T. T. B. C. (2024). Advances in aeration and wastewater treatment in shrimp farming: emerging trends, current challenges, and future perspectives. *Aqua Water Infrastructure, Ecosystems and Society,* 73(5): 902–916.

Ni, B. J., Pan, Y., Guo, J., Virdis, B., Hu, S., Chen, X., & Yuan, Z. (2017). Chapter 16: Denitrification Processes for Wastewater Treatment. In *RSC Metallobiology* (Vols. 2017-January, Issue 9, pp. 368–418). Royal Society of Chemistry.

Nie, J., Sun, Y., Zhou, Y., Kumar, M., Usman, M., Li, J., Shao, J., Wang, L., & Tsang, D. C. W. (2020). Bioremediation of water containing pesticides by microalgae: Mechanisms, methods, and prospects for future research. *Science of The Total Environment*, 707: 136080.

Ning, H., Li, R., & Zhou, T. (2022). Machine learning for microalgae detection and utilization. *Frontiers in Marine Science*, 9: 947394.

Nowak, A., Kutyła, M., Kaczmarek, J., Jaroszuk-Ściseł, J., & Jędryczka, M. (2023). Differences in the Production of Extracellular Polymeric Substances (EPS) and Other Metabolites of *Plenodomus* (*Leptosphaeria*) Infecting Winter Oilseed Rape (Brassica napus L.). *Metabolites*, 13(6): 759.

Oberacker, P., Stepper, P., Bond, D. M., Höhn, S., Focken, J., Meyer, V., Schelle, L., Sugrue, V. J., Jeunen, G. J., Moser, T., Hore, S. R., von Meyenn, F., Hipp, K., Hore, T. A., & Jurkowski, T. P. (2019). Bio-On-Magnetic-Beads (BOMB): Open platform for high-throughput nucleic acid extraction and manipulation. *PLoS Biology*, 17(1): e3000107.

Olguín, E. J. (2003). Phycoremediation: key issues for cost-effective nutrient removal processes. *Biotechnology Advances*, 22(1–2): 81–91.

Oliveira, H. R., Bassin, I. D., & Cammarota, M. C. (2019). Bioflocculation of cyanobacteria with pellets of *Aspergillus niger*: Effects of carbon supplementation, pellet diameter, and other factors in biomass densification. *Bioresource Technology*, 294: 122167.

Oruganti, R. K., Biji, A. P., Lanuyanger, T., Show, P. L., Sriariyanun, M., Upadhyayula, V. K. K., Gadhamshetty, V., & Bhattacharyya, D. (2023). Artificial intelligence and machine learning tools for high-performance microalgal wastewater treatment and algal biorefinery: A critical review. *Science of the Total Environment*, 876: 162797.

Ozili, P. K. (2022). The Acceptable R-Square in Empirical Modelling for Social Science Research. *SSRN Electronic Journal*.

Pel, H. J., De Winde, J. H., Archer, D. B., Dyer, P. S., Hofmann, G., Schaap, P. J., Turner, G., De Vries, R. P., Albang, R., Albermann, K., Andersen, M. R., Bendtsen, J. D., Benen, J. A. E., Van Den Berg, M., Breestraat, S., Caddick, M. X., Contreras, R., Cornell, M., Coutinho, P. M., … Stam, H. (2007). Genome sequencing and analysis of the versatile cell factory *Aspergillus niger* CBS 513.88. *Nature Biotechnology*, 25(2): 221–231.

Phu, D. H., Ngoc, L. T., Tu, L. N. Q., Hieu, D. T. M., Long, N. Q., & Le, M.-V. (2021). Simultaneous recovery of phosphorus and nitrogen from inorganic fertilizer wastewater. *Journal of Applied Science and Engineering*, 25(4): 673–684.

Picos-Benítez, A. R., Martínez-Vargas, B. L., Duron-Torres, S. M., Brillas, E., & Peralta-Hernández, J. M. (2020). The use of artificial intelligence models in the prediction of optimum operational conditions for the treatment of dye wastewaters with similar structural characteristics. *Process Safety and Environmental Protection*, 143: 36–44.

Prajapati, S. K., Bhattacharya, A., Kumar, P., Malik, A., & Vijay, V. K. (2016). A method for simultaneous bioflocculation and pretreatment of algal biomass targeting improved methane production. *Green Chemistry*, 18(19): 5230–5238.

Prepas, E. E., & Charette, T. (2003). Worldwide Eutrophication of Water Bodies: Causes, Concerns, Controls. *Treatise on Geochemistry*, 9–9: 311–331.

Rajasulochana, P., & Preethy, V. (2016). Comparison on efficiency of various techniques in treatment of waste and sewage water – A comprehensive review. *Resource-Efficient Technologies*, 2(4): 175–184.

Rasoul-Amini, S., Montazeri-Najafabady, N., Shaker, S., Safari, A., Kazemi, A., Mousavi, P., Mobasher, M. A., & Ghasemi, Y. (2014). Removal of nitrogen and phosphorus from wastewater using microalgae free cells in bath culture system. *Biocatalysis and Agricultural Biotechnology*, 3(2): 126–131.

Ratomski, P., & Hawrot-Paw, M. (2021). Production of *Chlorella vulgaris* biomass in tubular photobioreactors during different culture conditions. *Applied Sciences*, 11(7): 3106.

Rawat, I., Ranjith Kumar, R., Mutanda, T., & Bux, F. (2011). Dual role of microalgae: Phycoremediation of domestic wastewater and biomass production for sustainable biofuels production. *Applied Energy*, 88(10): 3411–3424.

Ribardo, C., & Allen, T. T. (2003). An alternative desirability function for achieving “six sigma” quality. *Quality and Reliability Engineering International*, 19(3): 227–240.

Roopashri, A. N., & Savitha, J. (2022). Screening of freshwater microalgae species for occurrence of lectins and their carbohydrate-binding specificity. *Journal of Applied Biological Sciences* , 16(1): 24–34.

Roy, D., Hassan, K., & Boopathy, R. (2010). Effect of carbon to nitrogen (C:N) ratio on nitrogen removal from shrimp production waste water using sequencing batch reactor. *Journal of Industrial Microbiology and Biotechnology*, 37(10): 1105–1110.

Ruban, A. V. (2015). Evolution under the sun: Optimizing light harvesting in photosynthesis. *Journal of Experimental Botany*, 66(1): 7–23.

Sacristán de Alva, M., Luna Pabello, V. M., Orta Ledesma, M. T., & Cruz Gómez, M. J. (2018). Carbon, nitrogen, and phosphorus removal, and lipid production by three saline microalgae grown in synthetic wastewater irradiated with different photon fluxes. *Algal Research*, 34: 97–103.

Safarpour, M., Safikhani, A., & Vatanpour, V. (2021). Polyvinyl chloride-based membranes: A review on fabrication techniques, applications and future perspectives. *Separation and Purification Technology*, 279.

Saitou, N., & Nei, M. (1987). The Neighbor-joining Method: A New Method for Reconstructing Phylogenetic Trees. *Molecular Biology and Evolution*, 4: 406–425.

Salbitani, G., & Carfagna, S. (2021). *Ammonium Utilization in Microalgae: A Sustainable Method for Wastewater Treatment*.

Salim, S., Bosma, R., Vermuë, M. H., & Wijffels, R. H. (2011). Harvesting of microalgae by bio-flocculation. *Journal of Applied Phycology*, 23(5): 849–855.

Sánchez-Bayo, A., Morales, V., Rodríguez, R., Vicente, G., & Bautista, L. F. (2020). Cultivation of Microalgae and Cyanobacteria: Effect of Operating Conditions on Growth and Biomass Composition. *Molecules*, 25(12): 2834.

Santos, F. M., Gonçalves, A. L., & Pires, J. C. M. (2019). Chapter 1: Negative emission technologies. In *Bioenergy with Carbon Capture and Storage: Using Natural Resources for Sustainable Development* (pp. 1–13). Academic Press.

Schagerl, M., Siedler, R., Konopáčová, E., & Ali, S. S. (2022). Estimating Biomass and Vitality of Microalgae for Monitoring Cultures: A Roadmap for Reliable Measurements. *Cells*, 11(15): 2455.

Serediak, N. A., Prepas, E. E., & Putz, G. J. (2013). Eutrophication of Freshwater Systems. *Treatise on Geochemistry: Second Edition*, 11: 305–323.

Shams, M. Y., Elshewey, A. M., El-kenawy, E. S. M., Ibrahim, A., Talaat, F. M., & Tarek, Z. (2023). Water quality prediction using machine learning models based on grid search method. *Multimedia Tools and Applications*, 83: 35307–35334.

Sharma, S., Agarwal, L., & Saxena, R. K. (2007). Statistical optimization for tannase production from *Aspergillus niger* under submerged fermentation. *Indian Journal of Microbiology*, 47: 132–138.

Shoener, B. D., Schramm, S. M., Béline, F., Bernard, O., Martínez, C., Plósz, B. G., Snowling, S., Steyer, J. P., Valverde-Pérez, B., Wágner, D., & Guest, J. S. (2019). Microalgae and cyanobacteria modeling in water resource recovery facilities: A critical review. *Water Research X*, 2: 100024.

Silva, V., Pereira, P., Aranha Martins, M., Lorenzo, M., Cella, H., Lopes, R., Derner, R., Magallón-Servin, P., & do Nascimento Vieira, F. (2022). Effects of Microalgae Addition and Fish Feed Supplementation in the Integrated Rearing of Pacific White Shrimp and Nile Tilapia Using Biofloc Technology. *Animals*, 2022: 1–15.

Singh, R. S., Thakur, S. R., & Bansal, P. (2015). Algal lectins as promising biomolecules for biomedical research. *Critical Reviews in Microbiology*, 41(1): 77–88.

Singh, V., & Mishra, V. (2021). Exploring the effects of different combinations of predictor variables for the treatment of wastewater by microalgae and biomass production. *Biochemical Engineering Journal*, 174: 108129.

Singh, V., & Mishra, V. (2022). Evaluation of the effects of input variables on the growth of two microalgae classes during wastewater treatment. *Water Research*, 213: 118165.

Singhal, M., Jadhav, S., Sonone, S. S., Sankhla, M. S., & Kumar, R. (2021). Microalgae Based Sustainable Bioremediation of Water Contaminated by Pesticides. *Biointerface Research in Applied Chemistry*, 12(1): 149–169.

Song, H., Gi, I., Ryu, J., Kwon, Y., & Jeong, J. (2023). Production Planning Forecasting System Based on M5P Algorithms and Master Data in Manufacturing Processes. *Applied Sciences*, 13(13): 7829.

Sousa, C. A., Sousa, H., Vale, F., & Simões, M. (2021). Microalgae-based bioremediation of wastewaters - Influencing parameters and mathematical growth modelling. *Chemical Engineering Journal*, 425: 131412.

Spain, O., & Funk, C. (2022). Detailed Characterization of the Cell Wall Structure and Composition of Nordic Green Microalgae. *Journal of Agricultural and Food Chemistry*, 70(31): 9711–9721.

Sultana, N., Hossain, S. M. Z., Mohammed, M. E., Irfan, M. F., Haq, B., Faruque, M. O., Razzak, S. A., & Hossain, M. M. (2020). Experimental study and parameters optimization of microalgae based heavy metals removal process using a hybrid response surface methodology-crow search algorithm. *Scientific Reports*, 10(1): 15068.

Sundui, B., Ramirez Calderon, O. A., Abdeldayem, O. M., Lázaro-Gil, J., Rene, E. R., & Sambuu, U. (2021). Applications of machine learning algorithms for biological wastewater treatment: Updates and perspectives. *Clean Technologies and Environmental Policy*, 23(1): 127–143.

Suparmaniam, U., Shaik, N. B., Lam, M. K., Lim, J. W., Uemura, Y., Shuit, S. H., Show, P. L., Tan, I. S., & Lee, K. T. (2022). Valorization of fish bone waste as novel bioflocculant for rapid microalgae harvesting: Experimental evaluation and modelling using back propagation artificial neural network. *Journal of Water Process Engineering*, 47.

Sutherland, D. L., & Ralph, P. J. (2019). Microalgal bioremediation of emerging contaminants - Opportunities and challenges. *Water Research*, 164: 7829.

Tamura, K., Nei, M., & Kumar, S. (2004). Prospects for inferring very large phylogenies by using the neighbor-joining method. *Proceedings of the National Academy of Sciences*, 101(30): 11030–11035.

Tan, S.-Y., Sethupathi, S., Leong, K.-H., & Ahmad, T. (2024). Challenges and opportunities in sustaining aquaculture industry in Malaysia. *Aquaculture International*, 32(1): 489–519.

Tang, D., Han, W., Li, P., Miao, X., & Zhong, J. (2011). CO_2 biofixation and fatty acid composition of Scenedesmus obliquus and *Chlorella pyrenoidosa* in response to different CO2 levels. *Bioresource Technology*, 102(3): 3071–3076.

Tejido-Nuñez, Y., Aymerich, E., Sancho, L., & Refardt, D. (2019). Treatment of aquaculture effluent with *Chlorella vulgaris* and *Tetradesmus obliquus*: The effect of pretreatment on microalgae growth and nutrient removal efficiency. *Ecological Engineering*, 136: 1–9.

Thakur, I. S., & Medhi, K. (2019). Nitrification and denitrification processes for mitigation of nitrous oxide from waste water treatment plants for

biovalorization: Challenges and opportunities. *Bioresource Technology*, 282: 502–513.

Thamer, B. M., Aldalbahi, A., Meera Moydeen, A., Rahaman, M., & El-Newehy, M. H. (2021). Modified electrospun polymeric nanofibers and their nanocomposites as nanoadsorbents for toxic dye removal from contaminated waters: A review. *Polymers*, 23(2): 1–37

Thiviyanathan, V. A., Ker, P. J., Amin, E. P. P., Tang, S. G. H., Yee, W., & Jamaludin, M. Z. (2023). Quantifying Microalgae Growth by the Optical Detection of Glucose in the NIR Waveband. *Molecules*, 28(3): 1318.

Turcios, A., & Papenbrock, J. (2014). Sustainable Treatment of Aquaculture Effluents—What Can We Learn from the Past for the Future? *Sustainability*, 6(2): 836–856.

Ugonabo, V. I., Ovuoraye, P. E., Chowdhury, A., & Fetahi, E. (2022). Machine learning model for the optimization and kinetics of petroleum industry effluent treatment using aluminum sulfate. *Journal of Engineering and Applied Science*, 69(1): 108.

Vaser, R., Sović, I., & Nagarajan, N. (2017). Fast and Accurate de Novo Genome Assembly from Long Uncorrected Reads. *Genome Research*, 27(5): 737–746.

Veiter, L., Rajamanickam, V., & Herwig, C. (2018). The filamentous fungal pellet—relationship between morphology and productivity. *Applied Microbiology and Biotechnology*, 102(7): 2997–3006.

Wagner, H., Dunker, S., Liu, Z., & Wilhelm, C. (2013). Subcommunity FTIR-spectroscopy to determine physiological cell states. *Current Opinion in Biotechnology*, 24(1): 88–94.

Wan Mahari, W. A., Waiho, K., Fazhan, H., Azwar, E., Shu-Chien, A. C., Hersi, M. A., Kasan, N. A., Foo, S. S., Wong, K. Y., Draman, A. S., Ma, N. L., Chang, J.-S., Dong, C.-D., & Lam, S. S. (2024). Emerging paradigms in sustainable shellfish aquaculture: Microalgae and biofloc technologies for wastewater treatment. *Aquaculture*, 587: 740835.

Wang, C., Zou, S., Fei, C., Wang, C., Gao, Z., Bao, Y., & He, M. (2016). How DNA barcoding can be more effective in microalgae identification: A case of cryptic diversity revelation in *Scenedesmus* (Chlorophyceae). *Scientific Reports*, 6: 36822.

Wang, D., Thunéll, S., Lindberg, U., Jiang, L., Trygg, J., Tysklind, M., & Souihi, N. (2021). A machine learning framework to improve effluent quality control in wastewater treatment plants. *Science of the Total Environment*, 784.

Wang, M., Kuo-Dahab, W. C., Dolan, S., & Park, C. (2014). Kinetics of nutrient removal and expression of extracellular polymeric substances of the

microalgae, *Chlorella* sp. and *Micractinium* sp., in wastewater treatment. *Bioresource Technology*, 154: 131–137.

Wang, Q. R., Hong, Y., & Li, L. H. (2023). Insights into differences between spore-assisted and pellet-assisted microalgae harvesting using a highly efficient fungus: Efficiency, high-value substances, and mechanisms. *Science of the Total Environment*, 877: 162945.

Windarti, M., & Prasetyaninrum, P. T. (2020). Prediction Analysis Student Graduate Using Multilayer Perceptron. *Proceedings of the International Conference on Online and Blended Learning 2019 (ICOBL 2019)*, 53–57.

Witten, I. H., Frank, E., & Hall, M. A. (2017). *Data Mining: Practical Machine Learning Tools and Techniques: Vol. Forth Edition* (4th ed.). Elsevier Science.

Wrede, D., Taha, M., Miranda, A. F., Kadali, K., Stevenson, T., Ball, A. S., & Mouradov, A. (2014). Co-cultivation of fungal and microalgal cells as an efficient system for harvesting microalgal cells, lipid production and wastewater treatment. *PLoS ONE*, 9(11): e113497.

Wurtsbaugh, W. A., Paerl, H. W., & Dodds, W. K. (2019). Nutrients, eutrophication and harmful algal blooms along the freshwater to marine continuum. *Wiley Interdisciplinary Reviews: Water*, 6(5): 1373.

Xiong, J. Q., Kurade, M. B., & Jeon, B. H. (2017). Biodegradation of levofloxacin by an acclimated freshwater microalga, *Chlorella vulgaris*. *Chemical Engineering Journal*, 313: 1251–1257.

Xu, J., Du, Y., Qiu, T., Zhou, L., Li, Y., Chen, F., & Sun, J. (2021). Application of hybrid electrocoagulation–filtration methods in the pretreatment of marine aquaculture wastewater. *Water Science and Technology*, 83(6): 1315–1326.

Xu, K., Zou, X., Chang, W., Qu, Y., & Li, Y. (2021). Microalgae harvesting technique using ballasted flotation: A review. *Separation and Purification Technology*, 276: 119439.

Xu, M., Xue, Z., Liu, J., Sun, S., Zhao, Y., & Zhang, H. (2022). Observation of few GR24 induced fungal-microalgal pellets performance for higher pollutants removal and biogas quality improvement. *Energy*, 244(Part B): 123171.

Xu, N., Zhang, X., Fan, X., Han, L., Zeng, C., & Tseng, C. K. (2001). Effects of nitrogen source and concentration on growth rate and fatty acid composition of *Ellipsoidion sp.* (*Eustigmatophyta*). *Journal of Applied Phycology*, 13: 463–469.

Xu, Y., Zhou, Y., Sekula, P., & Ding, L. (2021). Machine learning in construction: From shallow to deep learning. *Developments in the Built*

Environment, 6: 100045.

Yaakob, M. A., Mohamed, R. M. S. R., Al-Gheethi, A., Ravishankar, G. A., & Ambati, R. R. (2021). Influence of nitrogen and phosphorus on microalgal growth, biomass, lipid, and fatty acid production: An overview. *Cells*, 10(2): 1–19.

Yan, C., Song, X., Yu, M., Tong, Y., & Zhang, W. (2019). Determining the effects of polyaluminum chloride alkalinities and dosage treatments on various microalgal growth phases for the treatment of microalgae-laden water. *Separation and Purification Technology*, 209: 202–210.

Yang, L., Li, H., & Wang, Q. (2019). A novel one-step method for oil-rich biomass production and harvesting by co-cultivating microalgae with filamentous fungi in molasses wastewater. *Bioresource Technology*, 275: 35–43.

Yang, L., Wang, L., Zhang, H., Li, C., Zhang, X., & Hu, Q. (2018). A novel low cost microalgal harvesting technique with coagulant recovery and recycling. *Bioresource Technology*, 266: 343–348.

Yao, B., Xi, B., Hu, C., Huo, S., Su, J., & Liu, H. (2011). A model and experimental study of phosphate uptake kinetics in algae: Considering surface adsorption and P-stress. *Journal of Environmental Sciences*, 23(2): 189–198.

Yi, H. S., Lee, B., Park, S., Kwak, K. C., & An, K. G. (2019). Prediction of short-term algal bloom using the M5P model-tree and extreme learning machine. *Environmental Engineering Research*, 24(3): 404–411.

Yolmeh, M., & Jafari, S. M. (2017). Applications of Response Surface Methodology in the Food Industry Processes. *Food and Bioprocess Technology*, 10(3): 413–433.

Yousif, Y. I. D., Mohamed, E. S., & El-Gendy, A. S. (2022). Using *Chlorella vulgaris* for nutrient removal from hydroponic wastewater: experimental investigation and economic assessment. *Water Science and Technology*, 85(11): 3240–3258.

Zenooz, M. A., Ashtiani, F. Z., Ranjbar, R., Nikbakht, F., & Bolouri, O. (2017). Comparison of Different Artificial Neural Network (ANN) Architectures in Modeling of *Chlorella* sp. Flocculation. *Preparative Biochemistry and Biotechnology*, 47(6): 570–577.

Zerrouki, D., & Henni, A. (2019). Outdoor Microalgae Cultivation for Wastewater Treatment. In *Application of Microalgae in Wastewater Treatment* (pp. 81–99). Springer International Publishing.

Zhang, H., & Zhang, X. (2019). Microalgal harvesting using foam flotation: A critical review. *Biomass and Bioenergy*, 120: 176–188.

Zhao, P., Huang, J., Wang, X. H., Song, X. L., Yang, C. H., Zhang, X. G., & Wang, G. C. (2012). The application of bioflocs technology in high-intensive, zero exchange farming systems of *Marsupenaeus japonicus*. *Aquaculture*, 354–355: 97–106.

Zhao, S., Zhang, S., Liu, J., Wang, H., Zhu, J., Li, D., & Zhao, R. (2021). Application of machine learning in intelligent fish aquaculture: A review. *Aquaculture*, 540: 736724.

Zhao, Z., Liu, B., Ilyas, A., Vanierschot, M., Muylaert, K., & Vankelecom, I. F. J. (2021). Harvesting microalgae using vibrating, negatively charged, patterned polysulfone membranes. *Journal of Membrane Science*, 618: 118617.

Zheng, H., Gao, Z., Yin, J., Tang, X., Ji, X., & Huang, H. (2012). Harvesting of microalgae by flocculation with poly (γ-glutamic acid). *Bioresource Technology*, 112: 212–220.

Zheng, Y., Chu, Q., Ji, Q., Peng, S., & Liu, X. (2020). Effect of nitrogen and phosphorus removal by two species of Chlorella in allelochemical EMA condition. *IOP Conference Series: Earth and Environmental Science*, 467.

Zhou, W., Li, Y., Min, M., Hu, B., Zhang, H., Ma, X., Li, L., Cheng, Y., Chen, P., & Ruan, R. (2012). Growing wastewater-born microalga *Auxenochlorella protothecoides UMN280* on concentrated municipal wastewater for simultaneous nutrient removal and energy feedstock production. *Applied Energy*, 98: 433–440.

Zhou, W., Min, M., Hu, B., Ma, X., Liu, Y., Wang, Q., Shi, J., Chen, P., & Ruan, R. (2013). Filamentous fungi assisted bio-flocculation: A novel alternative technique for harvesting heterotrophic and autotrophic microalgal cells. *Separation and Purification Technology*, 107: 158–165.

Zhou, Y., Han, L. R., He, H. W., Sang, B., Yu, D. L., Feng, J. T., & Zhang, X. (2018). Effects of agitation, aeration and temperature on production of a novel glycoprotein gp-1 by *Streptomyces kanasenisi* zx01 and scale-up based on volumetric oxygen transfer coefficient. *Molecules*, 23(1): 125.

APPENDICES

Appendix A

Growth Curve for Determination of Microalgae Cell

Appendix A: Dry Weight

Appendix B

Appendix B1

Standard Curve for Water Quality Determination

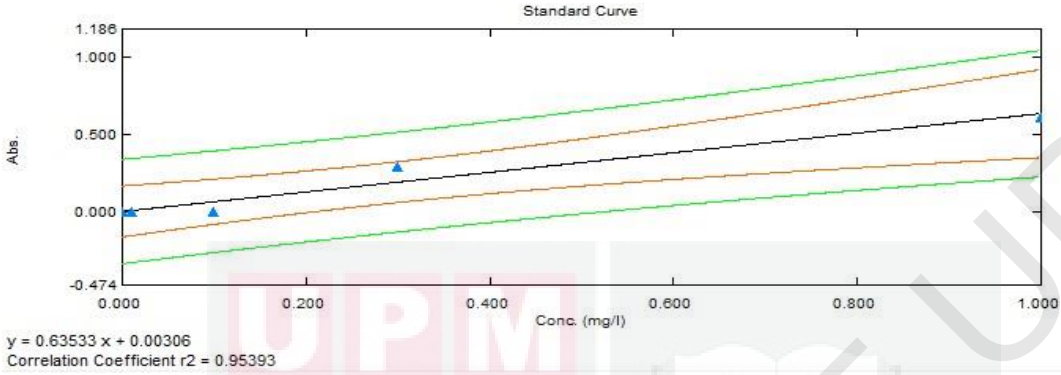

Appendix B: Standard Calibration Curve of Phenate Method for Ammonia Determination

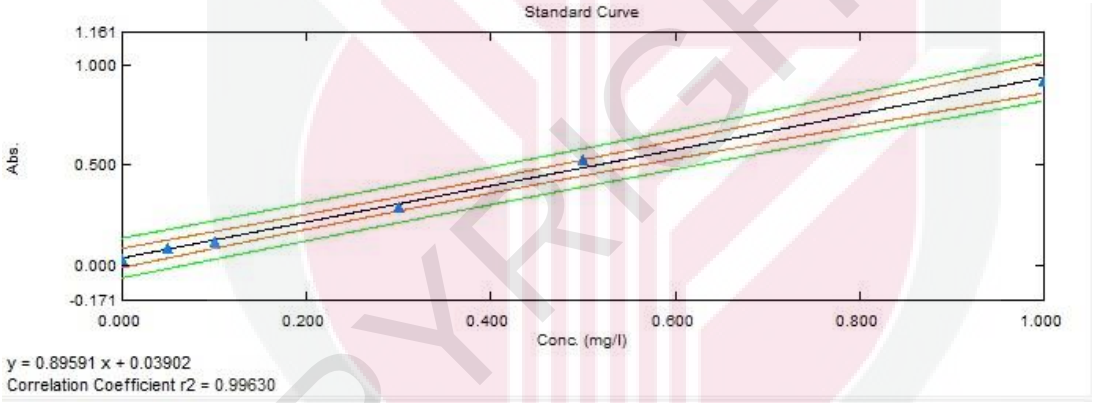

Appendix B: Standard Calibration Curve of Colorimetric Method for Nitrite Determination

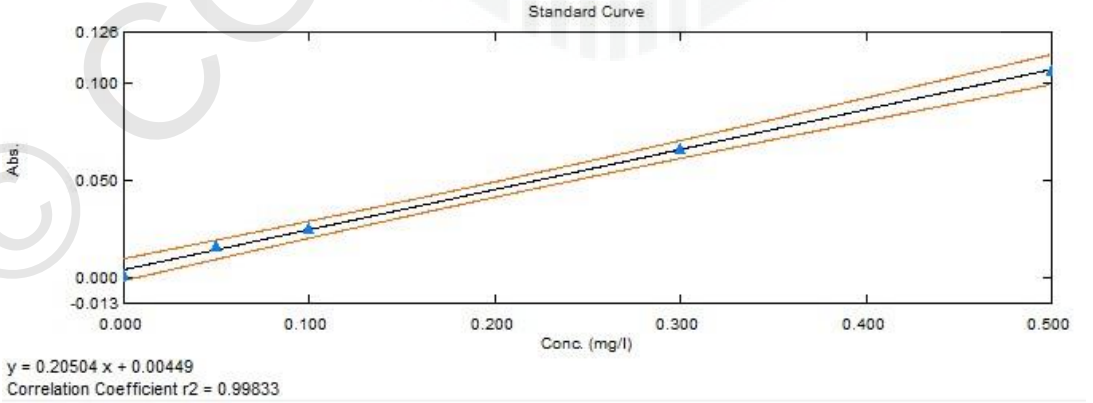

Appendix B: Standard Calibration Curve of Ascorbic Acid Method for Orthophosphate Determination

Appendix B2

Water Quality Analysis Using Standard Apha

Ammonia (NH_3-N) Determination

1. Phenol Solution:
   - Mix 11.1 mL of liquefied phenol (≥ 89%) with 95% (v/v) ethyl alcohol.
   - Dilute to a final volume of 100 mL with ethyl alcohol.
   - Prepare weekly to maintain activity.

2. Sodium Nitroprusside Solution:
   - Dissolve 0.5 g of sodium nitroprusside in 100 mL of distilled water.
   - Store in an amber bottle to protect from light degradation.
   - Stable for up to one month.

3. Alkaline Citrate Solution:
   - Dissolve 200 g of trisodium citrate and 10 g of sodium hydroxide in distilled water.
   - Dilute to a final volume of 1000 mL.

4. Sodium Hypochlorite Solution:
   - Use 5% (v/v) sodium hypochlorite solution from a commercial source.
   - Replace every two months after opening.

5. Oxidizing Solution:
   - Mix 100 mL of alkaline citrate solution with 25 mL of sodium hypochlorite solution.

6. Stock Ammonium Chloride Solution:
   - Dissolve 3.819 g of anhydrous NH4Cl in distilled water to a final volume of 1000 mL.

7. Standard Ammonium Chloride Solutions:
   - Dilute stock NH4Cl solution with distilled water to prepare standard solutions ranging from 0.2 to 1.6 mg NH3 L-1.

Nitrite (NO_2^-) Determination

1. Sulfanilamide Solution:
   - Dissolve 1.0 g of sulfanilamide in 10 mL of absolute hydrochloric acid (37% w/w).
   - Dilute with additional HCl to a final volume of 100 mL.
   - Store in an amber bottle for up to one month.

2. N-(1-Naphthyl) Ethylenediamine Dihydrochloride (NED) Solution:
   - Dissolve 0.1 g of NED in 100 mL of distilled water.
   - Store in an amber bottle for up to one month.

3. Stock Sodium Nitrite Solution:
   - Dissolve 1.5 g of $NaNO_2$ in distilled water to a final volume of 1000 mL.

4. Standard Sodium Nitrite Solutions:
   - Dilute stock $NaNO_2$ solution to prepare standard solutions ranging from 0.1 to 1.0 mg NO_2 L^{-1}.

Orthophosphate (PO_4^{3-}) Determination

1. Ammonium Paramolybdate Solution:
   - Dissolve 4.0 g of ammonium paramolybdate in 100 mL of distilled water.
   - Stable for up to one month.

2. Sulfuric Acid Solution:
   - Add 140 mL of absolute sulfuric acid to 500 mL of distilled water.
   - Cool and dilute to a final volume of 1000 mL.

3. Ascorbic Acid Solution:
   - Dissolve 1.76 g of ascorbic acid in 100 mL of distilled water.
   - Prepare fresh daily.

4. Potassium Antimonyl Tartrate Solution:
   - Dissolve 1.357 g of potassium antimonyl tartrate in 500 mL of distilled water.

5. Mixed Reagents:
   - In a 500 mL volumetric flask, mix 75 mL of ammonium paramolybdate solution, 250 mL of sulfuric acid solution, 150 mL of ascorbic acid solution, and 25 mL of potassium antimonyl tartrate solution.

Appendix C

Bio-Harvesting Process

Appendix C: Richard's Synthetic Agar is Used for Isolation and Cultivation of Fungi from Soil Samples

Ingredients	Grams / Litre
Potassium nitrate	10
Monopotassium dihydrogen phosphate	5
Magnesium sulphate	2.5
Ferric Chloride	0.02
Sucrose	50
Agar	15

Appendix D

Appendix D1: Normality Test Spss

Tests of Normality

		Kolmogorov-Smirnov[a]			Shapiro-Wilk		
	Treatment	Statistic	df	Sig.	Statistic	df	Sig.
Ammonia_Day10	0%	.350	3	.	.828	3	.184
	10%	.178	3	.	1.000	3	.958
	20%	.219	3	.	.987	3	.780
	30%	.292	3	.	.923	3	.463
	40%	.253	3	.	.964	3	.637
	50%	.314	3	.	.893	3	.363
	60%	.202	3	.	.994	3	.853

a. Lilliefors Significance Correction

Appendix D2: One-Way Anova for Nutrients on Day 10

ANOVA

Ammonia_Day10

	Sum of Squares	df	Mean Square	F	Sig.
Between Groups	17.250	6	2.875	972.699	<.001
Within Groups	.041	14	.003		
Total	17.291	20			

ANOVA

Nitrite_Day10

	Sum of Squares	df	Mean Square	F	Sig.
Between Groups	3.812	6	.635	8942.534	<.001
Within Groups	.001	14	.000		
Total	3.813	20			

ANOVA

Phosphate_Day10

	Sum of Squares	df	Mean Square	F	Sig.
Between Groups	22.290	6	3.715	5458.371	<.001
Within Groups	.010	14	.001		
Total	22.300	20			

Appendix D3: Freshwater Specific Growth Rate (Sgr)

Multiple Comparisons

Dependent Variable: Dosage

	(I) Treatment	(J) Treatment	Mean Difference (I-J)	Std. Error	Sig.	95% Confidence Interval	
						Lower Bound	Upper Bound
Tukey HSD	10%	20%	.07701*	.00345	.000	.0654	.0886
		30%	.06198*	.00345	.000	.0504	.0736
		40%	.04132*	.00345	.000	.0297	.0529
		50%	.02902*	.00345	.000	.0174	.0406
		60%	.05433*	.00345	.000	.0427	.0659
	20%	10%	-.07701*	.00345	.000	-.0886	-.0654
		30%	-.01503*	.00345	.009	-.0266	-.0034
		40%	-.03570*	.00345	.000	-.0473	-.0241
		50%	-.04800*	.00345	.000	-.0596	-.0364
		60%	-.02268*	.00345	.000	-.0343	-.0111
	30%	10%	-.06198*	.00345	.000	-.0736	-.0504
		20%	.01503*	.00345	.009	.0034	.0266
		40%	-.02066*	.00345	.001	-.0323	-.0091
		50%	-.03296*	.00345	.000	-.0446	-.0214
		60%	-.00765	.00345	.298	-.0192	.0039
	40%	10%	-.04132*	.00345	.000	-.0529	-.0297
		20%	.03570*	.00345	.000	.0241	.0473
		30%	.02066*	.00345	.001	.0091	.0323
		50%	-.01230*	.00345	.035	-.0239	-.0007
		60%	.01302*	.00345	.025	.0014	.0246
	50%	10%	-.02902*	.00345	.000	-.0406	-.0174
		20%	.04800*	.00345	.000	.0364	.0596
		30%	.03296*	.00345	.000	.0214	.0446
		40%	.01230*	.00345	.035	.0007	.0239
		60%	.02532*	.00345	.000	.0137	.0369
	60%	10%	-.05433*	.00345	.000	-.0659	-.0427
		20%	.02268*	.00345	.000	.0111	.0343
		30%	.00765	.00345	.298	-.0039	.0192
		40%	-.01302*	.00345	.025	-.0246	-.0014
		50%	-.02532*	.00345	.000	-.0369	-.0137

*. The mean difference is significant at the 0.05 level.

Appendix D4: Marinewater Specific Growth Rate (Sgr)

Multiple Comparisons

Dependent Variable: Dosage

	(I) Treatment	(J) Treatment	Mean Difference (I-J)	Std. Error	Sig.	95% Confidence Interval	
						Lower Bound	Upper Bound
Tukey HSD	10%	20%	.02961*	.00336	.000	.0183	.0409
		30%	.04297*	.00336	.000	.0317	.0543
		40%	.05156*	.00336	.000	.0403	.0629
		50%	.07142*	.00336	.000	.0601	.0827
		60%	.08955*	.00336	.000	.0782	.1008
	20%	10%	-.02961*	.00336	.000	-.0409	-.0183
		30%	.01336*	.00336	.018	.0021	.0247
		40%	.02195*	.00336	.000	.0106	.0333
		50%	.04181*	.00336	.000	.0305	.0531
		60%	.05993*	.00336	.000	.0486	.0712
	30%	10%	-.04297*	.00336	.000	-.0543	-.0317
		20%	-.01336*	.00336	.018	-.0247	-.0021
		40%	.00859	.00336	.183	-.0027	.0199
		50%	.02845*	.00336	.000	.0171	.0397
		60%	.04657*	.00336	.000	.0353	.0579
	40%	10%	-.05156*	.00336	.000	-.0629	-.0403
		20%	-.02195*	.00336	.000	-.0333	-.0106
		30%	-.00859	.00336	.183	-.0199	.0027
		50%	.01986*	.00336	.001	.0086	.0312
		60%	.03798*	.00336	.000	.0267	.0493
	50%	10%	-.07142*	.00336	.000	-.0827	-.0601
		20%	-.04181*	.00336	.000	-.0531	-.0305
		30%	-.02845*	.00336	.000	-.0397	-.0171
		40%	-.01986*	.00336	.001	-.0312	-.0086
		60%	.01813*	.00336	.002	.0068	.0294
	60%	10%	-.08955*	.00336	.000	-.1008	-.0782
		20%	-.05993*	.00336	.000	-.0712	-.0486
		30%	-.04657*	.00336	.000	-.0579	-.0353
		40%	-.03798*	.00336	.000	-.0493	-.0267
		50%	-.01813*	.00336	.002	-.0294	-.0068

*. The mean difference is significant at the 0.05 level.

Appendix E

Identification of Microalgae Species (Phylogenetic Tree)

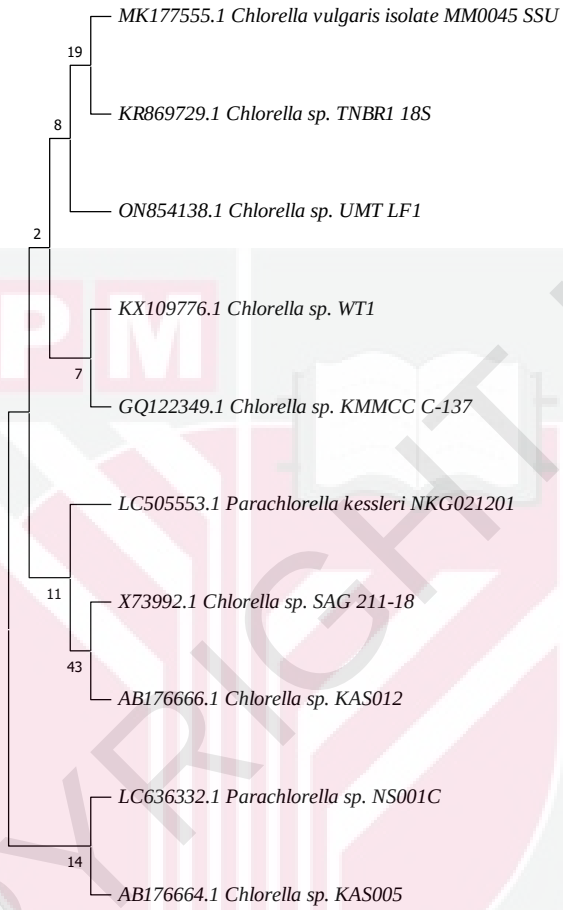

Appendix E1: Neighbour Joining Tree Showing the Phylogenetic Relations among 18S rDNA Sequences from Marine Microalgae, *Chlorella* sp. UMT LF1 Used in This Study and Those Obtained from NCBI GenBank Database

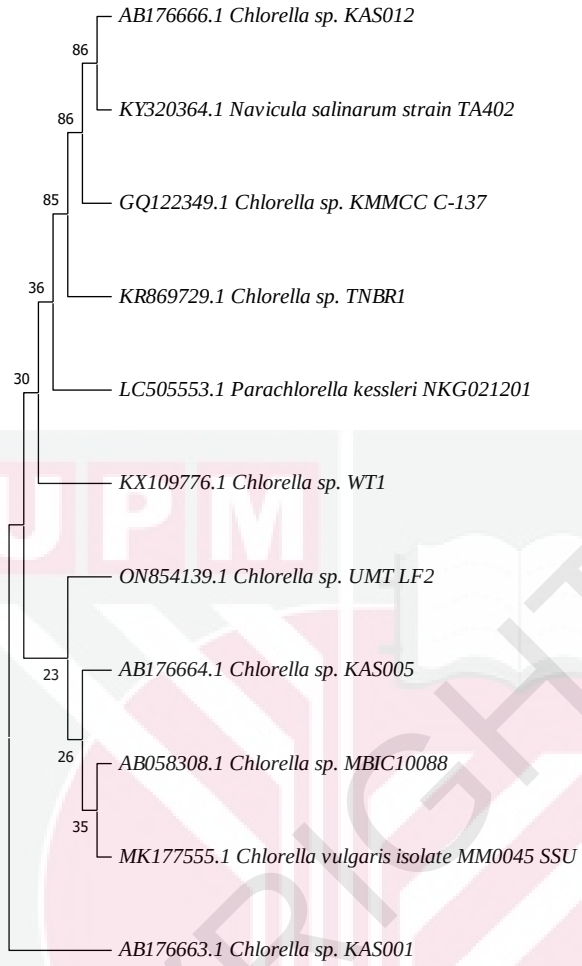

Appendix E2: Neighbour Joining Tree Showing the Phylogenetic Relations among 18S rDNA Sequences from Marine Microalgae, *Chlorella* sp. UMT LF2 Used in This Study and Those Obtained from NCBI GenBank Database

Appendix F

Detailed Result of Removal Efficiency Generated from First-Order Kinetic Model

Appendix F1 : Removal Efficiency of Ammonia (Experimental Data)

Dosage	Day 0		Day 2		Day 4		Day 6		Day 8		Day 10		Day 12		Day 14	
	MW	FW	MW	FW	MW	FW	MW	FW	MW	FW	MW	FW	MW	FW	MW	FW
0%	0	0	6.31	0.39	5.55	-0.77	6.27	-0.98	4.91	1.15	0.77	-2.10	6.59	-3.96	7.09	1.15
10%	0	0	11.22	23.92	44.28	66.22	61.43	75.39	72.00	81.82	78.36	86.14	92.27	89.92	94.19	94.21
20%	0	0	8.63	23.90	57.22	65.56	69.10	76.22	80.11	83.03	90.86	87.94	94.85	92.06	96.23	96.92
30%	0	0	38.78	27.48	54.16	70.28	62.80	78.02	82.70	82.73	95.59	86.23	96.21	91.14	97.90	91.99
40%	0	0	49.24	39.11	59.84	73.82	71.36	77.81	92.63	80.43	93.36	89.77	96.32	96.05	95.72	93.60
50%	0	0	51.66	38.30	64.86	78.59	72.12	80.63	87.97	88.32	92.94	89.91	94.29	91.50	92.7	91.13
60%	0	0	7.05	47.65	14.59	69.90	33.69	79.29	55.46	91.55	87.97	82.90	87.37	88.29	87.77	86.18

Appendix F2 : Removal Efficiency Ammonia (Predicted Data)

Dosage	Day 0		Day 2		Day 4		Day 6		Day 8		Day 10		Day 12		Day 14	
	MW	FW	MW	FW	MW	FW	MW	FW	MW	FW	MW	FW	MW	FW	MW	FW
0%	0	0	0	0	0	0	0	0	0	0	0	0	0	0	0	0
10%	0	0	34.30	32.5	56.83	54.43	71.63	69.24	81.36	79.24	87.75	85.98	92.07	90.54	94.71	93.61
20%	0	0	40.26	37.71	64.31	61.20	78.68	75.83	87.26	84.95	92.39	90.62	95.46	94.16	97.29	96.36
30%	0	0	45.46	31.6	70.25	53.21	83.77	68.0	91.15	78.11	95.17	85.03	97.37	89.76	98.56	93.0
40%	0	0	41.41	36.03	65.67	59.08	79.89	73.83	88.22	83.26	93.10	89.29	95.95	93.15	97.63	95.62
50%	0	0	37.05	31.94	6.37	53.68	75.05	68.48	84.30	78.54	90.11	85.40	93.78	90.06	96.08	93.4
60%	0	0	33.97	28.09	56.40	48.29	71.21	62.82	80.99	73.27	87.44	80.78	91.71	86.18	94.53	90.0

Appendix F3 : Removal Efficiency Nitrite Experimental Data

Dosage	Day 0		Day 2		Day 4		Day 6		Day 8		Day 10		Day 12		Day 14	
	MW	FW	MW	FW	MW	FW	MW	FW	MW	FW	MW	FW	MW	FW	MW	FW
0%	0	0	-0.07	1.39	-0.09	1.77	0.13	2.96	0.26	1.17	-0.11	1.72	0.22	1.39	0.09	-0.85
10%	0	0	2.65	19.25	7.86	30.4	25.26	57.70	34.59	67.75	61.16	77.23	79.72	87.77	86.23	92.02
20%	0	0	3.35	24.69	12.49	30.80	18.91	58.90	40.21	75.88	56.72	77.04	82.56	89.17	84.68	94.73
30%	0	0	1.72	38.42	7.24	41.70	10.77	62.14	33.86	69.24	74.80	73.26	83.09	83.53	83.21	91.01
40%	0	0	20.53	35.88	26.55	40.78	46.03	53.44	55.50	59.68	79.13	82.59	91.52	87.92	91.87	95.91
50%	0	0	17.01	26.48	20.52	38.65	45.19	51.51	553.42	58.36	83.10	78.02	92.12	90.16	89.43	95.17
60%	0	0	7.46	26.50	12.54	37.35	38.44	51.48	47.80	68.04	80.63	72.47	89.93	74.6	88.06	77.31

Appendix F4 : Removal Efficiency Nitrite (Predicted Data)

Dosage	Day 0		Day 2		Day 4		Day 6		Day 8		Day 10		Day 12		Day 14	
	MW	FW	MW	FW	MW	FW	MW	FW	MW	FW	MW	FW	MW	FW	MW	FW
0%	0	0	0	0	0	0	0	0	0	0	0	0	0	0	0	0
10%	0	0	25.96	27.75	45.18	47.80	59.42	62.28	69.95	72.75	77.75	80.31	83.53	85.77	87.81	89.72
20%	0	0	26.32	33.74	45.71	56.19	60.0	70.91	70.52	80.73	78.28	87.23	84.0	91.54	88.21	94.39
30%	0	0	28.32	30.55	48.62	51.77	63.18	66.51	73.61	76.74	81.08	83.85	86.4	99.78	90.28	92.21
40%	0	0	32.98	35.34	55.09	58.19	69.9	72.96	79.83	82.52	86.48	88.7	90.94	92.68	93.93	95.27
50%	0	0	33.16	36.24	55.32	59.34	70.13	74.08	80.04	84.37	86.65	89.46	91.08	93.28	94.04	95.71
60%	0	0	32.32	23.37	54.20	41.28	69	55.0	79.02	65.52	85.30	73.58	90.39	79.75	93.5	84.49

Appendix F5 : Removal Efficiency of Orthophosphate (Experimental Data)

Dosage	Day 0		Day 2		Day 4		Day 6		Day 8		Day 10		Day 12		Day 14	
	MW	FW	MW	FW	MW	FW	MW	FW	MW	FW	MW	FW	MW	FW	MW	FW
0%	0	0	-1.85	2.08	-0.85	7.06	0.69	10.27	-0.18	9.01	-0.01	4.28	-0.63	7.84	0.11	5.32
10%	0	0	6.20	18.90	23.31	27.16	30.15	31.78	41.54	46.93	55.19	56.19	69.82	65.16	73.88	68.58
20%	0	0	17.29	43.34	24.70	54.41	29.18	58.44	62.91	66.26	74.57	73.49	75.71	80.65	81.63	83.93
30%	0	0	24.85	54.68	26.85	56.68	35.03	61.04	68.85	63.25	75.57	72.47	78.30	83.35	83.97	90.58
40%	0	0	18.21	31.76	21.25	57.71	45.22	79.12	57.7	88.83	66.65	94.73	73.56	95.36	82.82	96.19
50%	0	0	34.74	52.82	43.05	57.94	52.03	89.10	56.14	95.03	67.66	96.08	75.91	96.33	76.69	96.70
60%	0	0	33.06	83.95	34.95	86.35	44.75	87.54	49.29	94.46	60.25	95.97	67.97	95.28	71.35	94.42

Appendix F6 : Removal Efficiency of Orthophosphate (Predicted Data)

Dosage	Day 0		Day 2		Day 4		Day 6		Day 8		Day 10		Day 12		Day 14	
	MW	FW	MW	FW	MW	FW	MW	FW	MW	FW	MW	FW	MW	FW	MW	FW
0%	0	0	0	0	0	0	0	0	0	0	0	0	0	0	0	0
10%	0	0	18.18	15.46	33.05	28.54	45.2	39.59	55.17	48.93	63.32	56.83	69.99	63.51	75.44	69.15
20%	0	0	22.94	21.2	40.62	37.9	54.24	51.06	64.64	61.43	72.83	69.61	79.09	76.05	83.87	81.13
30%	0	0	24.10	40.45	42.40	54.89	56.28	65.83	66.82	74.12	74.82	80.40	80.89	85.15	85.49	88.75
40%	0	0	22.68	41.09	40.21	65.3	53.77	79.56	64.26	87.96	72.36	92.91	78.63	95.82	83.48	97.54
50%	0	0	19.46	42.68	35.13	67.15	47.75	81.17	57.92	89.12	66.11	93.81	72.7	96.45	78.01	97.97
60%	0	0	17.16	33.16	31.37	55.32	43.14	70.13	52.9	80.04	60.98	86.65	67.67	91.08	73.22	94.04

Appendix G

Table G1 : ANOVA Test for Response Function Y_{marine}

Source	Sum of Sq	Df	Mean Square	F-value	P-value	
Model	4427.29	9	491.92	26.44	<0.0001	Significant
X_1-Dosage	672.90	1	672.90	36.17	0.0001	
X_2-pH	0.8687	1	0.8687	0.0467	0.8333	
X_3-Mixing rate	551.37	1	551.37	29.64	0.0003	
$X_1 X_2$	1.07	1	1.07	0.0573	0.8157	
$X_1 X_3$	177.49	1	1177.49	9.54	0.0115	
$X_2 X_3$	113.79	1	113.79	6.12	0.0329	
X_1^2	1563.65	1	1563.65	84.05	<0.0001	
X_2^2	274.03	1	274.03	14.73	0.0033	
X_3^2	1535.27	1	1535.27	82.53	<0.0001	
Residual	186.03	10	18.60			
Lack of Fit	125.10	5	25.02	2.05	0.2243	Not significant
Pure Error	60.94	5	12.19			
Cor Total	4613.32	19				

R-squared = 0.9597; adjusted R-squared = 0.9234;
predicted R-squared = 0.7527; adequate precision = 13.5308.

Table G2 : ANOVA Test for Response Function Y_{fresh}

Source	Sum of Sq	df	Mean Square	F-value	P-value	
Model	7828.55	9	869.84	49.84	<0.0001	Significant
X_1-Dosage	132.69	1	132.69	7.60	0.0202	
X_2-pH	20.61	1	20.61	1.18	0.3027	
X_3-Mixing rate	130.35	1	130.35	7.47	0.0211	
$X_1 X_2$	103.16	1	103.16	5.91	0.0354	
$X_1 X_3$	136.27	1	136.27	7.81	0.0190	
$X_2 X_3$	34.52	1	34.52	1.98	0.1899	
X_1^2	3270.06	1	3270.06	187.36	<0.0001	
X_2^2	1704.80	1	1704.80	97.68	<0.0001	
X_3^2	3669.89	1	3669.89	210.27	<0.0001	
Residual	174.53	10	17.45			
Lack of Fit	21.41	5	4.28	0.1399	0.9750	Not significant
Pure Error	153.21	5	30.62			
Cor Total	8003.09	19				

R-squared = 0.9782; adjusted R-squared = 0.9586;
predicted R-squared = 0.9516; adequate precision = 17.924.

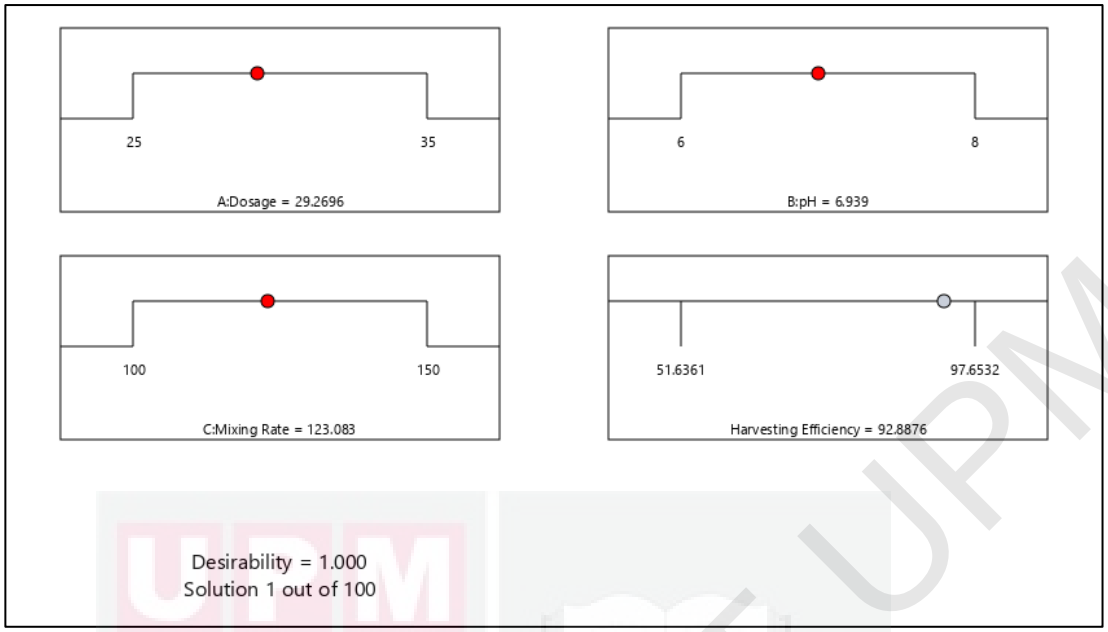

Figure G1 : Desirability Ramp for Optimization of Marine Water Species

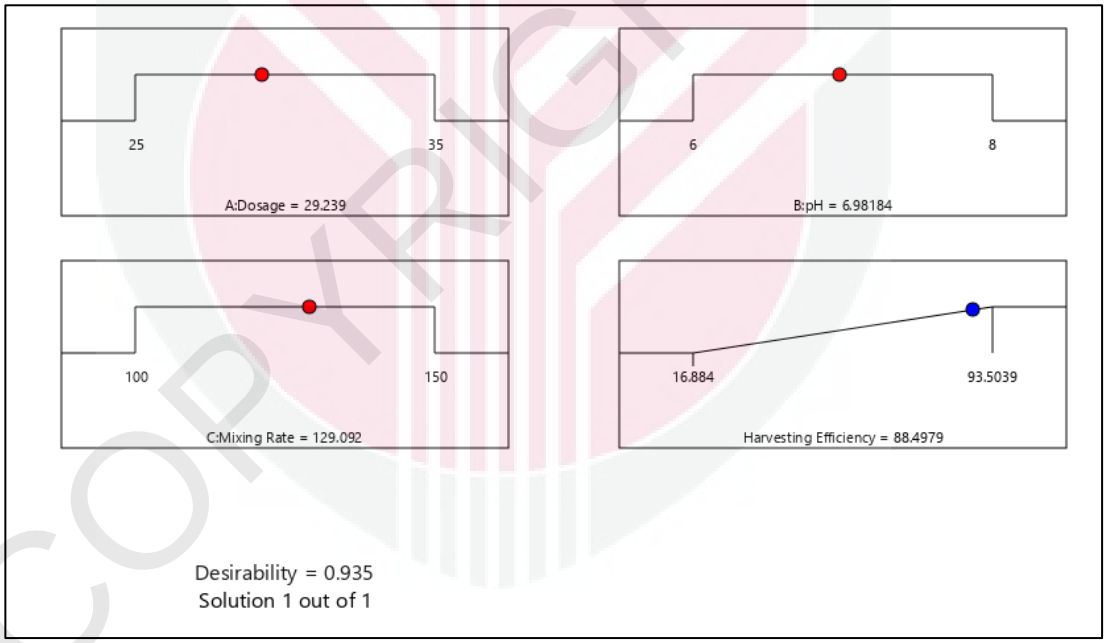

Figure G2 : Desirability Ramp for Optimization of Freshwater Species

Appendix H

Appendix H1: Correlation Coefficient of Cross-Validation Results for Different Days (Day 10, Day 12, and Day 14) and Different Nutrient Concentrations (MW) Using Various Function Algorithms

Day	Algorithm	Parameter		
		Ammonia	Nitrite	Orthophosphate
10	LR	0.432	0.878	0.402
	SLR	0.432	0.878	0.402
	SMOreg	0.45	0.881	0.448
	M5P	0.986	0.979	0.988
	Random Forest	0.996	0.983	0.999
	Random Tree	0.996	0.983	0.999
12	LR	0.424	0.865	0.54
	SLR	0.424	0.865	0.54
	SMOreg	0.445	0.864	0.498
	M5P	0.944	0.918	0.969
	Random Forest	0.955	0.919	0.990
	Random Tree	0.955	0.919	0.990
14	LR	0.224	0.771	0.143
	SLR	0.224	0.771	0.143
	SMOreg	0.056	0.767	0.201
	M5P	0.968	0.962	0.984
	Random Forest	0.984	0.970	0.99
	Random Tree	0.984	0.970	0.99

Appendix H2: Correlation Coefficient of Cross-Validation Results for Different Days (Day 10, Day 12, and Day 14) and Different Nutrient Concentrations (FW) Using Various Function Algorithms

Day	Algorithm	Parameter		
		Ammonia	Nitrite	Orthophosphate
10	LR	0.961	0.768	0.93
	SLR	0.961	0.768	0.93
	SMOreg	0.701	0.711	0.927
	M5P	0.942	0.976	0.992
	Random Forest	0.961	0.985	0.998
	Random Tree	0.961	0.985	0.998
12	LR	0.563	0.342	0.920
	SLR	0.563	0.342	0.920
	SMOreg	0.556	0.148	0.92
	M5P	0.978	0.963	0.992
	Random Forest	0.992	0.982	0.999
	Random Tree	0.992	0.982	0.999
14	LR	0.55	0.209	0.868
	SLR	0.55	0.209	0.868
	SMOreg	0.527	0.303	0.871
	M5P	0.954	0.972	0.990
	Random Forest	0.982	0.987	0.998
	Random Tree	0.982	0.987	0.998

Appendix H3: Performance Algorithm Models for Cross-Validation of Bioremediation Process for Marine Water Treatment (MW)

Factors	Nutrients	Day		
		10	12	14
CC	Cell Count	0.7279	0.7364	0.9268
MAE		2961468.0	3132312.44	6310252.91
RMSE		3848001.67	4086301.52	8515253.94
CC	Ammonia	0.9862	0.9437	0.9683
MAE		0.0382	0.012	0.0101
RMSE		0.0455	0.0176	0.0137
CC	Nitrite	0.9785	0.9184	0.9618
MAE		0.0194	0.0124	0.0071
RMSE		0.0296	0.0232	0.0093
CC	Orthophosphate	0.9875	0.9685	0.9842
MAE		0.0663	0.0372	0.0402
RMSE		0.0793	0.0416	0.0484

Appendix H4: Performance Algorithm Models for Cross-Validation of Bioremediation Process for freshwater Treatment (FW)

Factors	Nutrients	Day		
		10	12	14
CC	Cell Count	0.957	0.9801	0.9947
MAE		5267858.19	13497053.31	12203742.43
RMSE		7044641.48	15619241.58	16193777.27
CC	Ammonia	0.9415	0.9781	0.9542
MAE		0.0233	0.0168	0.0186
RMSE		0.0283	0.0204	0.0219
CC	Nitrite	0.9756	0.9629	0.972
MAE		0.0124	0.0184	0.0191
RMSE		0.0164	0.0235	0.0225
CC	Orthophosphate	0.9923	0.9922	0.9903
MAE		0.0566	0.0419	0.0437
RMSE		0.067	0.0508	0.0516

LIST OF PUBLICATIONS

Nasir, N. M., Jusoh, A., Harun, R., Ibrahim, N. N. L. N., Rasit, N., Ghani, W. A. W. A. K., & Kurniawan, S. B. (2023). Nutrient consumption of green microalgae, *Chlorella* sp. during the bioremediation of shrimp aquaculture wastewater. *Algal Research*, *72*. https://doi.org/10.1016/j.algal.2023.103110

Nasir, N. M., Jusoh, A., Manan, H., Kasan, N. A., Kamaruzzan, A. S., Wan Abdul Karim Ghani, W. A., Kurniawan, S. B., & Lananan, F. (2023). Utilization of microalgae, *Chlorella* sp. UMT LF2 for bioremediation of *Litopenaeus vannamei* culture system and harvesting using bio-flocculant, *Aspergillus niger*. *Biocatalysis and Agricultural Biotechnology*, *47*. https://doi.org/10.1016/j.bcab.2022.102596

Nasir, N. M., Razif Harun, A. J., Nik Ibrahim, N. N. L., & Abdul Karim Ghani, W. A. W. (2021). Optimization of aquaculture wastewater bioremediation and harvesting utilizing response surface methodology (RSM). *Chemical Engineering Transactions*, *83*, 151 – 156. https://doi.org/10.3303/CET218302